Heterogeneity of tumour response to hypoxia: Carbonic anhydrase IX induction defines a subpopulation of hypoxic cells with stem cell properties and drug resistance



Thesis submitted by

Ioanna Ledaki

St Hugh's College

For the degree of

Doctor of Philosophy

Trinity Term 2013

ABSTRACT

Carbonic anhydrase IX (CA9) is strongly induced by hypoxia and its overexpression is associated with poor therapeutic outcome in cancer. The function of CAIX is to catalyze the reversible hydration of CO_2 to bicarbonate and a proton. This helps hypoxic tumours to maintain a more neutral intracellular pH (pH_i) promoting survival, but produces a more acidic extracellular ($pH_{e)}$ which promotes invasion and metastasis. Recent evidence has expanded on the role of hypoxia and CAIX by relating them to stem cell niches. In this study, taking advantage of the transmembrane location of CAIX, we show for the first time, a direct marked heterogeneity in response to hypoxia within each tumour cell population studied, associated with major biological differences. Based on CAIX expression pattern under hypoxic conditions, we identify, isolate and characterize two distinct populations of tumour cells, one that express CAIX and the other that does not. Interestingly, we discover that the CAIX positive population is enriched with cells expressing cancer stem cell markers. These include ALDHA1, IGF1, LIN28 and genes involved in epithelial-mesenchymal transition (EMT) and multi-drug resistance (i.e. WNT2, TWIST1, and ABCC2). Accordingly, CAIX+ve cells show higher self-renewal capacity and form tumours significantly faster compared to the CAIX-ve population. Importantly, functional suppression of CAIX *in vitro* and *in vivo*, in two breast cancer cell lines resulted in the downregulation of breast cancer stem cell signatures, suggesting that CAIX is not just a marker of stemness but also a regulator of stemness.

The molecular mechanism underlying the differential expression of CAIX in the two populations is not HIF-1α-dependent, but instead driven by hypoxia-induced reorganization of chromatin structure. In line with this, we provide experimental evidence showing that the genomic locus encoding *CA9* has a more “open” and transcriptionally active chromatin structure in CAIX+ve cells, and a condense and transcriptionally silent chromatin structure in the CAIX-ve cells. Given that HIF induces the transcription of *CA9* by binding to hypoxia response elements (HREs) in

its promoter we show a significant reduction in binding of HIF to the *CA9* promoter of the negative population. We suggest that the reduce HIF binding is a result of the compact chromatin structure of *CA9* promoter of the negative cells.

Analysis of the transcriptome of the positive and negative populations suggests a symbiotic relationship between these two subpopulations and their environment, likely required to promote tumour growth. This is based on the following observations: Firstly, we identified that CAIX-ve cells express high levels of cytokines and based on this, we suggest that the cytokines secreted by CAIX-ve cells may transmit paracrine signals that regulate the CAIX+ve cells, thus providing a wider hypoxia tolerant microenvironment to protect the stem cell population. Secondly, we identified a metabolic heterogeneity between the CAIX+ve and CAIX-ve cells. The CAIX+ve cells show an upregulation of genes implicated in oxidative phosphorylation, TCA cycle and fatty acid synthesis. Whereas in CAIX-ve cells there is an upregulation of genes implicated in autophagy and mitophagy. Given the above together with the upregulation of oxidative phosphorylation and TCA cycle in the CAIX+ve cells, we proposed the existence of a metabolic symbiosis between the CAIX+ve and CAIX-ve cells. We postulate that the catabolic process such as autophagy and mitophagy in the CAIX-ve cells may results in the overproduction of high-energy metabolites such as lactate, glutamine and ketone bodies which in turns they are been utilized by CAIX+ve cells to fuel mitochondria respiration.

Finally, we also demonstrated that in the CAIX+ve cells mTORC1 signaling is upregulated, and contributes to the regulation of CAIX expression. Given the role of mTORC1 in stem cell maintenance and EMT as well as the interdependence of mTORC1 and CAIX expression in the CAIX+ve cells we suggest that mTORC1 signaling may be the critical factor by which CAIX regulates stemness. Interestingly, the subpopulations show a differential sensitivity to HDAC inhibitors, NaBu and SAHA as treatment of MCF7 breast cancer cell line and HCT116 colon cancer cell line leads to elimination of the CAIX+ve population. This is not driven by the downregulation of HIF-1α, the major transcriptional regulator of CAIX. In contrast,

we demonstrate that SAHA causes downregulation mTORC1. This suggests that SAHA-induced downregulation of CAIX expression could be due to its effect on mTORC1 pathway.

Of wider significance, our findings show that tumours are not homogenous in their response to hypoxia, and distinct signal transduction networks regulate different populations of cells within the tumour. This highlights the need for the utilization of biomarkers, which reveal distinct functional hypoxia profiles of human cancers, and permit the stratification of tumours. Furthermore, the identification of epigenetic regulation of the histones in response to hypoxia for highly selective gene regulation, provides a connection between the epigenetic mechanisms under environmental stress and cancer progression, and is model for development of novel epigenetic cancer therapeutic drugs.

DEDICATION

To my Dad, Achilleus Ledakis, whose life showed me that you do not need shoes to walk successfully in life, hard work and a honorable and courageous character is only what you need.

AKNOWLEDGEMENTS

I am extremely grateful to Professor Adrian Harris for giving me this opportunity to work in his laboratory. His support, guidance and passion for research have made all of this possible.

I would also like to thank all the members of Growth Factor Laboratory: Helen Sheldon, Simon Lord, Andrew Lomas, Harriet Gee, Chern Ein Oon, Robert McCormick, Luke Pike, Richard Sainson, Joh Williams, Ulrike Harjes, Christos Zois, Karim Bensaad, Dean Singlenton, Helen Turley, Ester Bridges for providing me invaluable advice and support but most important making the lab such a welcome and enjoyable place to work.

I am really thankful to Alan McIntyre and Simon Wigfield for their supervision, guidance and support for the last 3 years.

I would also like to thank Francesca Buffa and Laura Winchester for analysing the RNA-seq and microarray data.

Manuela Milani, Elena Favaro, Ana Ramachandran and Andri Tzortzi for their lovely friendship and support through my difficult times.

A big thank you to my “Best” friend that he shared his nice and tough times with me and he was by my side the last 3 years. I want to thank him also for helping me putting this document together.

Last but not least, I would like to thank my parents, my brother and sister for their love and support over the years. Thank you for always being there for me.

TABLE OF CONTENTS

List of Figures xiii

List of Tables xvi

List of Abbreviations xvii

1 Chapter One 21

***Introduction* 21**

1.1 Cancer 22

1.2 Hypoxia 23

1.2.1 The HIF-1 pathway 24

1.3 Activation of Hypoxia Inducible Factor 25

1.3.1 Hypoxia dependent HIF activation 25

1.3.2 Hypoxia-independent HIF activation in cancer cells 25

1.4 Hypoxia regulated pathways 27

1.4.1 Proliferation 27

1.4.2 Angiogenesis 27

1.4.3 Glycolysis 28

1.4.4 pH regulation 29

1.5 Cancer stem cells 30

1.5.1 Cancer stem cell markers 30

1.6 Stem cell signaling pathways 32

1.6.1 Wnt signaling 33

1.6.2 Hedgehog signaling 35

1.6.3 ABC transporters 37

1.6.4 mTORC1 signaling 39

1.6.5 mTORC1 and Cancer Stem Cells 41

1.7 Hypoxia and cancer stem cells 42

1.8 Tumour Microenvironment 44

1.8.1 Tumour associated macrophages 44

1.8.2 Extracellular Matrix 45

1.8.3 ECM serves as stem cell niche 47

1.8.4 Inflammation and Cancer 48

1.8.5 Inflammation and Cancer stem cells 51

1.9 Tumour Metabolism 52

1.9.1 Metabolic Symbiosis 54

1.9.2 Autophagy 55

1.10 Carbonic anhydrase IX 56

1.10.1 Identification and Structure of CAIX 57

1.10.2 Regulation of CAIX 59

1.10.3 CAIX in tumours 62

1.10.4 pH regulation 62

1.10.5 Cell adhesion 64

1.10.6 Cell proliferation 65

1.11 Inhibition of CAIX as therapeutic target 66

1.11.1 Monoclonal antibody therapy 66

1.11.2 CAIX small molecules inhibitors 68

1.12 Aims 70

2 Chapter Two 71

***Materials and Methods* 71**

2.1 Cell Culture....72

2.2 Hypoxic Incubators....72

2.3 Cell Lines....72

2.4 Counting Cells....73

2.5 Preparation and Recovery of cell stocks (cryo-preserved cells)....73

2.6 Gene silencing by RNA Interference....74

2.7 Spheroid culture....74

2.8 Embedding and Processing of spheroids....75

2.9 Immunostaining of paraffin – embedded tissue sections....75

2.10 Generation of Mammospheres....76

2.11 Soft Agar Assay for Colony Formation....77

2.12 Clonogenic Assay....77

2.13 Chromatin analysis of CAIX using Epiq Chromatin Analysis kit....77

2.14 Chromatin immunoprecipitation assay for HIF-1 beta....**79**

2.14.1 Day One....79

2.14.2 Second Day....79

2.14.3 Third Day....80

2.15 Chromatin immunoprecipitation assay for trimethylated H3K9....81

2.16 Immunoblotting....82

2.16.1 Protein Extraction....82

2.16.2 Protein Polyacrylamide Electrophoresis....82

2.16.3 Antibody Incubation....83

2.17 Real-time PCR (qPCR)....83

2.17.1 RNA extraction and cDNA synthesis 83

2.17.2 Real Time Quantitative PCR 84

2.18 Flow cytometry 85

2.19 Aldefluor Assay 86

2.20 RNA-sequencing analysis 86

2.21 Microarrays analysis **....87**

2.21.1 Pathway Analysis 88

2.22 Xenograft studies 88

2.23 HRE Transfection 89

2.24 Oxygen consumption assays 89

2.25 Statistical analyses 90

2.26 Buffers and Solutions **....90**

3 Chapter Three 93

***Differential expression of CAIX* 93**

3.1 Introduction 94

3.1.1 Tumour heterogeneity 94

3.1.2 Hypoxic Microenvironmental Heterogeneity 97

3.1.3 Changes in gene expression 97

3.1.4 Epigenetic regulation of gene expression 98

3.1.5 Mutational load of hypoxic cells 100

3.1.6 CAIX as Hypoxic Tumour Biomarker 101

3.2 Results 103

3.3 Carbonic anhydrase expression under hypoxic conditions 103

3.3.1 Differential expression of CAIX 107

3.3.2 Generation of CAIX positive and CAIX negative cell lines 112

3.3.3 Molecular Mechanisms of CAIX silencing 117

3.4 Discussion.....127

4 Chapter Four 131

Genes and pathways expressed from RNA-seq analysis 131

4.1 Introduction.....132

4.1.1 CAIX and stem cells.....132

4.1.2 RNA sequencing.....133

4.2 Results.....135

4.2.1 Genes upregulated in CAIX positive cells versus CAIX negative cells…135

4.2.2 The two subpopulations showed similar hypoxia core responses 136

4.2.3 KEGG and IPA Pathway Analysis 140

4.2.4 CAIX positive cells upregulate stem cells genes.....146

4.2.5 CAIX positive cells display an upregulation of mTORC1 pathway.....150

4.2.6 Genes and pathways upregulated in CAIX negative cells.....153

4.3 Discussion.....157

5 Chapter Five 163

CAIX+ve cells show functional properties of stem cells and differential sensitivity to HDAC inhibitors 163

5.1 Introduction.....164

5.1.1 *In vitro* stem cells assays: Anchorage independent cell growth and colony forming ability 164

5.1.2 *In Vivo* assays: Tumour Xenografts.....165

5.1.3 Histone Deacetylases inhibitors.....165

5.2 Results.....168

5.2.1 The CAIX+ve cells are ALDH positive and have the ability to recapitulate the original expression pattern of unsorted MCF7 cells. 168

5.2.2 The CAIX+ve cells have stem cell properties and shows increased clonogenic and mammosphere forming activity. 170

5.2.3 CAIX+ve cells form faster growing tumours in NSG mice 174

5.2.4 CAIX+ve and CAIX-ve cells show differential sensitivity to HDAC inhibitors 176

5.2.5 Effects of SAHA treatment on survival of CAIX+ve and CAIX-ve cell lines. 181

5.2.6 Effects of SAHA on cell survival are CAIX dependent. 183

5.3 Discussion....185

6 Chapter Six 189

Metabolic Heterogeneity revealed by Microarray analysis 189

6.1 Introduction....190

6.2 Results....192

6.2.1 Microarray analysis: Genes upregulated in CAIX+ve population versus CAIX negative populations....192

6.2.2 Pathways and genes upregulated in the CAIX+ve populations....197

6.2.3 Validation of the expression of genes implicated in Fatty Acid synthesis and pyruvate metabolism in CAIX+ve cells....200

6.2.4 Pathways and genes upregulated in CAIX-ve cells....206

9 Chapter Seven 219

***Final Discussion* 219**

9.1 CAIX expression and Hypoxic Heterogeneity 220

9.2 The CAIX positive population is enriched with hypoxic cancer stem cells....222

9.3 A symbiotic relationship between CAIX+ve and CAIX-ve cells....225

9.4 Concluding Remarks and Future Prospects 227

9.5 Future Experimental Work 231

10 Appendix One 233

Top 100 genes upregulated in CAIX+ve and CAIX-ve populations (RNA – Seq analysis) 233

Top 100 genes upregulated in CAIX+ve and CAIX-ve population (Microarray analysis) 243

11 Appendix Two 243

12 Appendix Three 250

Genes and pathways upregulated in CAIX+ve and CAIX-ve population (RNA-seq analysis) 250

13 Appendix Four 257

Genes and pathways upregulated in CAIX+ve and CAIX-ve cells (Microarray analysis) 257

14 Appendix Five 270

Common genes between microarray gene lists and RNA-seq gene lists 270

15 Appendix Six 275

List of publications arising from thesis 275

16 BIBLIOGRAPHY 276

LIST OF FIGURES

Figure 1.1 Regulation of HIF-1 activity.. 29

Figure 1.2 Wnt signaling. 35

Figure 1.3 Hedgehog signaling pathway. 36

Figure 1.4 Domain composition of CAIX protein.. 59

Figure 2.1 Justification of 15 reads threshold. 87

Figure 3.1 Expression of CAIX in MCF7 breast cancer cell line. 105

Figure 3.2 Pimonidazole and CAIX expression in HCT116 spheroids 106

Figure 3.3 Hypoxic subpopulations of CAIX expression. 109

Figure 3.4 The percentage of CAIX+ve cells in breast and colorectal cancer cell lines.. 110

Figure 3.5 Sorted CAIX positive and CAIX negative cells. 111

Figure 3.6 FACS analysis of sorted cells in culture.....113

Figure 3.7 Expression profile of CAIX+ve and CAIX-ve sorted cells cultured for 3 weeks.....115

Figure 3.8 Long-term culture of CAIX+ve and CAIX-ve cells. 116

Figure 3.9 Epigenetic regulation of *CA9* expression.. 126

Figure 4.1 Percentage overlap between genes up-regulated under hypoxia in the unsorted population and genes differentially regulated between the two CAIX subpopulations.. 138

Figure 4.2 Relationship between CAIX transcriptional regulation and hypoxia. 139

Figure 4.3 Treatment of unsorted MCF7 cells with verapamil. 143

Figure 4.4 mRNA expression profiles of the CAIX+ve and CAIX-ve sorted MCF-7 cells. 147

Figure 4.5 q-PCR analysis of genes implicated in stem cell maintenance in CAIX+ve cells transfected with Scr RNAi or CAIX RNAi. 149

Figure 4.6 Expression of mTORC1 components in CAIX+ve and CAIX-ve cell lines.. 152

Figure 4.7 Examples of HCT116 EV and FLCA9, HT29 EV and sh CA9 xenografts stained for F4/80 antibody 156

Figure 5.1 Representative FACS analysis of CAIX positive and CAIX negative cell lines for ALDH activity (ALDEFLUOR kit).....169

Figure 5.2 Generation of mammospheres and 3D spheroids. 172

Figure 5.3 Anchorage independent growth of CAIX+ve and CAIX-ve cell lines.. ..173

Figure 5.4 Analysis of CAIX positive and CAIX negative cell lines on ability to promote tumour growth in vivo. 175

Figure 5.5 Treatment of unsorted HCT116 cells with sodium butyrate.. 177

Figure 5.6 Treatment of HCT116 spheroids with sodium butyrate. 178

Figure 5.7 Treatment of MCF7 cells with SAHA.....180

Figure 5.8 Effects of SAHA treatment on colony formation of CAIX+ve and CAIX-ve MCF-7 cell lines.....182

Figure 5.9 Effects of SAHA treatment on cell growth of CAIX+ve, CAIX-ve cells cell lines and CAIX knockdown cells.. 184

Figure 6.1 Comparison of microarrays and RNA-seq gene lists. 194

Figure 6.2 Comparison of microarrays and RNA-seq gene lists of upregulated and downregulated genes 195

Figure 6.3 Comparison of CAIX+ve and CAIX-ve gene signatures with a conserved core hypoxia signatures. 196

Figure 6.4 Expression of genes implicated in fatty acid synthesis. 203

Figure 6.5 LDHB mRNA expression levels in CAIX+ve and CAIX-ve cells and oxygen consumption measurements for CAIX+ve and CAIX-ve cell lines.....205

Figure 6.6 Expression of autophagy genes.. 210

Figure 6.7 mRNA expression levels of LC3B, BNIP3 and LAMP1. LC3B 212

Figure 7.1 Schematic representation of CAIX+ve and CAIX-ve regulation.....229

LIST OF TABLES

Table 2.1 Immunostaining Antibodies 78

Table 2.2 The sequences of the primers used 86

Table 2.3 Number of (un)mapped reads in each dataset 89

Table 4.1: KEGG pathway analysis for CAIX+ve cells 143

Table 4.2: Ingenuity pathway analysis for CAIX+ve cells 143

Table 4.3 KEGG pathway analysis for CAIX-ve cells 157

Table 4.4 Ingenuity pathway analysis for CAIX-ve cells 157

Table 6.1: KEGG pathway analysis for CAIX+ve cells 200

Table 6.2: Ingenuity pathway analysis for CAIX+ve cells 200

Table 6.3: Upregulated genes in CAIX+ve population 200

Table 6.4: KEGG pathway analysis for CAIX-ve cells 210

Table 6.5: Ingenuity pathway analysis for CAIX-ve cells 210

Table 6.6: Upregulated genes in CAIX-ve population 211

Table1: 100 genes upregulated in CAIX+ve populations (RNA – Seq) 236

Table 2:Top 100 genes upregulated in CAIX-ve populations (RNA – Seq) 239

Table 1: Common upregulated genes between the CAIX+ve microarray gene list and CAIX+ve RNA-seq gene list 273

Table 2: Common upregulated genes between the CAIX-ve microarray gene list and CAIX-gene list 275

LIST OF ABBREVIATIONS

FDG	2-[18F]-fluoro-2-deoxy-D-glucose
5-aza-dC	5-aza-20–deoxycytidin
ATZ	Acetazolamide
APC	Adenomatous Polyposis Coli protein
AMPK	AMP-activated protein kinase
ADCC	Antibody-mediated cell cytotoxicity
ARNT	Aryl hydrocarbon receptor nuclear translocator
ABC	ATP binding cassette
ATG5	Autophagy-related 5
BRAC1	Breast cancer 1
IC	C-terminal intracellular tail
CTC	Cancer stem cells
CA	Carbonic anhydrase
cDNA	Complementary DNA
CRE	CREB-binding protein
°C	Degrees celcius
ΔΔCT	Delta delta cycle threshold
DNA	Deoxyribonucleic acid
(Dhh	Desert hedgehog
DMSO	Dimethylsulphoxide
ES	Embryonic stem cells
EMT	Epithelial-mesenchymal transition
EMT	Epithelial–mesenchymal transition
ER	Estrogen receptor
4EBP1	Eukaryotic initiation factor 4E–binding protein 1
ECM	Extracellular matrix
ERK	Extracellular signal-regulated
FIH1	Factor inhibiting HIF-1

FASN	Fatty acid synthase
FA	Fatty acids
FCS	Foetal calf serum
FC	Fold Change
GSK3	Glycogen synthase kinase 3
HP1	Heterochromatin protein 1
HAT	Histone acetyltransferases
HDAC	Histone deacetylases
HER2	Human epidermal factor receptor 2
HIF-1	Hypoxia inducible transcription factor 1
HRE	Hypoxia-response elements
Ihh	Indian Hedgehog
IGF	Insulin growth factor
IGF1	Insulin-like growth factor
IFNs	Interferons
IL	Interleukins
pHi	Intracellular pH
JmjC	Jumonji C
kDa	kiloDaltons
LDHA	Lactate dehydrogenase-A
L	Litre
LPR	Low density lipoprotein receptor related protein
MDCK	Madin-Darby canine kidney
MMP	Matrix metalloproteinases
mRNA	Messenger RNA (Ribonucleic acid)
µg	Micrograms
µl	Microlitres
µm	Micrometres
µM	Micromolar
LC31B	Microtubule-associated protein 1 light

	chain 3β
ml	Millilitres
mM	Millimolar
MAPK	Mitogen activated protein kinase pathway
M	Molar
MCT	Monocarboxylate transporter
mAb	Monoclonal antibodies
MMAE	Monomethyl auristatin E
mTORC	mTOR complex
MDR	Multidrug resistance
NSAIDs	Non-steroidal anti-inflammatory drugs
NF-κB	Nuclear factor κB
Oct	Octamer-binding transcription factor
ODDDs	Oxygen dependent degradation domains
%	Percent
PPARγ	Peroxisome proliferator-activated receptor-γ
PTEN	Phosphatase and tensin homolog deleted on Chromosome 10
PBS	Phosphate-buffered saline
PI3K	Phosphatidylinositol 3-OH kinase
PDGF	Platelet-derived growth factor
PCR	Polymerase chain reaction
pH	Power of hydrogen (in solution)
PHDs	Prolyl hydroxylase
PR	Protective regions
PG	Proteoglycan
PDK	Pyruvate dehydrogenase kinase
ROS	Reactive oxygen species
RNA	Ribonucleic acid
scr	Scramble control
SP	Side populations
SP	Single peptide

siRNA	Small interfering RNA
Smo	Smoothened
NaBu	Sodium butyrate
SDS	Sodium dodecyl sulfate
Shh	Sonic hedgehog
SREBPs	Sterol-regulatory-element-binding proteins
Tcf	T-cell factor
bHLH	Basic helix-loop-helix
TOR	Target of Rapamycin
TGF β	Transforming growth factor β
TNFα	Tumor necrosis factor α
TAMs	Tumour associated macrophages
VEGF	Vascular endothelial growth factor
VHL	Von Hippel Lindau

Chapter One

Introduction

1.1 Cancer

Cancer is a disease that has been affecting people for centuries. The oldest documented evidence of cancer cases come from ancient Egypt at around 1500 B.C, where bone tumours were found in human mummies, and a description of eight cases of breast tumours was documented in the Ancient Egyptian textbook on trauma surgery (Zimmerman, 1977). Over two thousand year later, the Greek physician, Hippocrates (460-370 BC), who is known as the "Father of Medicine" described cancer in detail and used the term *carcinos*, which means crab in Greek (Society, 2009). This description derives from the finger-like spreading projections of tumours mimicking the shape of the craw of a crab. Nowadays we know that this appearance of cancer is driven by the hyperproliferation of cells that gives tumours an abnormal and irregular border, infiltrating surrounding normal tissues with a finger-like projections.

Cancer is one of the most common diseases in the world and it is estimated that every two minutes someone in UK will be diagnosed, and four in 10 British people will develop cancer at some point in their lifetimes. While, the number of people dying from the most common cancers has been declining since 1971, still out of the nearly 12.7 million new cases diagnosed every year, around 7.5 million people will go on to die from cancer (Ferlay et al., 2010).

Research has provided a better understanding of the genetic factors underlying cancer resulting in the development of new diagnostic tools, therapies and preventive measures. However, there is still a lot to be done as in some way cancer has the Laernea Hydra's characteristics. Current therapies such as surgery, radiotherapy, and chemotherapy seem to cut off the head of cancer, but over time more heads grow back

and patients develop resistance to therapies, cancer recurrence and metastasis. Therefore, better understanding of the molecular mechanisms that govern these processes will enable us to find the "Achilles heel" of cancer, and eventually a cure.

1.2 Hypoxia

The microenvironment of solid tumours is substantially different from normal tissue (Liotta and Rao, 1985). Most solid tumours are characterized by an insufficient and defective vascularization that are incapable of supplying enough oxygen and nutrients to the growing tumour mass (Harris, 2002). Therefore, most human tumours are heterogeneously oxygenated developing hypoxic areas. Tissue hypoxia is defined as an oxygen concentration of less than 1% and is associated with a variety of cellular responses (Harris, 2002). These hypoxic regions are characterized by low nutrient availability and a reduction of ATP production (Wilson et al., 1977). Hypoxia is believed to be one of the factors that drive cells to acquire a more resistant and invasive phenotype (Harris, 2002; Maxwell et al., 2001). Classically, two types of hypoxia are recognized: diffusion-related (chronic) hypoxia and perfusion (acute) hypoxia. Chronic hypoxia was first demonstrated by Thomlinson and Gray in 1955 (Thomlinson and Gray, 1955). They showed that cells that were located more than 180μm away from blood vessels were becoming necrotic (Thomlinson and Gray, 1955). Now it is being recognised that the uncontrolled tumour growth results in an inadequate O_2 supply for cells distant (>70 μm) from vasculature. This limit in oxygen diffusion is termed "chronic hypoxia" (Harris, 2002). The second type of hypoxia- "perfusion" or "acute" hypoxia arises when aberrant blood vessels are shutting down, limiting perfusion (Brown and Giaccia, 1998). However, closed vessels can be reopened leading to reoxygenation of the hypoxic areas (Harris, 2002).

Exposure to low oxygen levels under acute hypoxia lasts for a duration of only minutes to few hours. A consequence of the fluctuating levels of oxygen is an increase in free radicals, tissue damage and activation of stress–response genes, a phenomenon called reoxygenation injury (Prabhakar, 2001).

1.2.1 The HIF-1 pathway

Cellular responses and adaptation to hypoxia are mediated partly through activation of hypoxia inducible transcription factor 1 (HIF-1). HIF-1 is a heterodimer consisting of two subunits, a hypoxia inducible-expressed HIF-1α and a constitutively-expressed HIF-1-beta subunit, also known as aryl hydrocarbon receptor nuclear translocator (ARNT) (Jiang et al., 1996). Both subunits belong to the PER-ARNT-SIM (PAS) subfamily of the basic helix-loop-helix (bHLH) family of transcription factors (Jiang et al., 1996). Their structures are similar and both contain the following domains: a N-terminus bHLH domain for DNA binding, a central region with a Per-ARNT-Sim (PAS) domain that facilitates heterodimerization and a C-terminus responsible for the recruitment of transcriptional co-regulatory proteins (Zhulin et al., 1997) (Yang et al., 2005). Two other isoforms of HIF exist, named HIF2α and HIF3α. HIF2α has a similar structure to HIF-1α and it is restricted in its expression to endothelial cells, glial cells, kidney, hepatocytes and the interstitial cells of the pancreas and duodenum (Wiesener et al., 2003). The role of HIF3α is not well understood, but it has been shown to act as a dominant–negative regulator of HIF (Makino et al., 2001).

1.3 Activation of Hypoxia Inducible Factor

1.3.1 Hypoxia dependent HIF activation

Under normal oxygen HIF-1α is hydroxylated on two proline amino acids residues (P402 and P564) located in the oxygen dependent degradation domains (ODDDs) by prolyl hydroxylase (PHDs) (Yee Koh et al., 2008). The prolyl hydroxylation results in ubiquitination of HIF-1α by the von Hippel Lindau (VHL) protein and subsequent proteasomal degradation. In addition, one asparagine (Asp803) residue in the C terminal transactivation domain is also hydroxylated by an asparaginyl hydroxylase termed factor inhibiting HIF-1 (FIH1). FIH1 hydroxylation prevents binding of HIF-1 to p300 resulting in inhibition of HIF mediated transcription. Under hypoxic conditions HIF-1α is stabilized and it translocates to the nucleus, where it dimerizes with the HIF-1β and associates with co-activators, such as CREB-binding protein (CBP)/p300 (Yamashita et al., 2001). The HIF-1 heterodimer induces the transcription of many hypoxia-response genes, involved in angiogenesis e.g. vascular endothelial growth factor (*VEGF*), pH regulation e.g. carbonic anhydrase 9 (*CA9*), and alterations in cellular metabolism e.g. lactate dehydrogenase-A (*LDHA*) by binding to hypoxia-response elements (HRE) in their promoters (Forsythe et al., 1996).

1.3.2 Hypoxia-independent HIF activation in cancer cells

Apart from the hypoxia dependent regulation of HIF-1α, other hypoxia independent oncogenic pathways are able of inducing activation of HIF-1α. These include growth factor signaling pathways and loss of tumour suppressor genes (Bardos and Ashcroft, 2005).

The growth factors such as insulin growth factor (IGF) and epidermal growth factor (EGF) activate signaling cascades that result in an increase HIF-1α expression (Semenza, 2003). For example, activation of the mitogen activated protein kinase pathway (MAPK) induces HIF-1α protein synthesis (Semenza, 2003). Additionally, it has been shown that MAPK pathway stimulates HIF-1α transactivation domain function (Richard et al., 1999). Moreover, HIF-1α expression can be elevated by the activation of PI3K/mTOR (Zundel et al., 2000). In support of this, it has been shown that treatment of MCF7 breast cancer cell line with rapamycin, a mTOR inhibitor, causes reduction of HIF-1α synthesis (Laughner et al., 2001). Therefore, inhibition of the oncogenes that activate these signaling pathways may block protein synthesis of HIF-1α.

Further to this, the loss of tumour suppressor genes, von Hippel Lindau (VHL), phosphatase and tensin homolog deleted on chromosome 10 (PTEN), and p53 can amplify HIF-1α expression. The loss of function of VHL has been well documented in clear cell carcinomas and cereberal haemangiomas (Maxwell et al., 1999; Zhong et al., 1999). This in turn affects VHL-dependent ubiquitylation and proteasome degradation of HIF-1α and HIF2α, which results in a marked increase in HIF-1 activity under normoxic conditions (Semenza, 2003). Whereas the loss of PTEN results in an increase of HIF-1α in non hypoxic conditions due to loss of the antagonistic effect of on the PI3K pathway (Zundel et al., 2000). Lastly loss of p53 facilitates HIF-1α expression by promoting the MDM2–mediated ubiquitination of HIF-1α (Feki and Irminger-Finger, 2004). This is important as mutation of p53 has been observed in approximately 50% of breast tumours, and is associated with cancer progression and metastasis (Feki and Irminger-Finger, 2004).

The upregulation of HIF-1α by hypoxia differs in two important ways from its upregulation in response to growth factor. Firstly, hypoxia dependent activation of HIF-1α occurs in all cell types, whereas the growth factors stimulation induces HIF-1α in a cell type specific manner. Secondly, hypoxia is associated with decreased degradation of HIF-1α, whereas growth factors induce HIF-1α protein synthesis through activation of the signaling pathway described above.

1.4 Hypoxia regulated pathways

1.4.1 Proliferation

Hypoxia activates various pathways that transduce proliferative and survival signals from growth factors and growth factor receptors that promote cell proliferation. Among those growth factors upregulated in response to hypoxia are the transforming growth factor β (TGF β), and platelet-derived growth factor (PDGF) (Harris, 2002). Additionally, hypoxia increases the activity of phosphatidylinositol 3-OH kinase (PI3K), which is involved in the regulation of cell proliferation and suppression of apoptosis (Zundel et al., 2000) (Harris, 2002).

1.4.2 Angiogenesis

In the presence of prolonged hypoxia and the absence of vascular support, tumours become necrotic or even apoptotic (Holmgren et al., 1995). Therefore, in order to avoid this and to ensure cancer progression, cancer cells have co-opted mechanisms that promote the formation of new blood vessels, a process called angiogenesis. This process involves the migration, growth and differentiation of endothelial cells, which line the inside of blood vessels. Hypoxia is a key regulator of angiogenesis and

induces the expression of growth factors that regulate endothelial cell proliferation and blood vessels. The angiogenic factor vascular endothelial growth factor *(*VEGF) and its receptors, VEGF receptor 1 (VEGFR1) which are key regulators of angiogenesis are activated under hypoxic conditions by HIF-1α. Under hypoxia, VEGF is released by cancer cells and normal cells. The circulating VEGF then binds to the VEGFR1 and VEGFR2 on endothelial cells and activates proteins that transmit a signal to the nucleus of the endothelial cell. This signal activates a group of genes responsible for the production of new blood vessels. Hypoxia also upregulates other pro-angiogenic factors including, angiopoietin-2 and transforming growth factors β3 (TGF β3) (Pugh and Ratcliffe, 2003).

1.4.3 Glycolysis

Under hypoxia cells switch their methods of glucose metabolism from oxidative phosphorylation to glycolysis in order to meet the energy requirements necessary for their survival. Despite the fact that oxidative phosphorylation generates more energy, i.e. 36 molecules of ATP per molecule of glucose compared to glycolysis, which yields only 2 ATP molecules per molecule of glucose, hypoxic cells use glycolysis as the primary mechanism of ATP production (Dang and Semenza, 1999; Seagroves et al., 2001). HIF-1α is responsible for the upregulation of all the genes that are involved in the glycolytic pathway (Cantor and Sabatini, 2012). These include lactate dehydrogenase A (LDHA), which is responsible for the conversion of pyruvate to lactate and pyruvate dehydrogenase kinase-1 (PDK-1), which inhibits the entrance of pyruvate into mitochondria metabolism (Cantor and Sabatini, 2012). Furthermore, HIF-1 upregulates the expression of the glucose transporters GLUT1 and GLUT3, which mediate cellular glucose uptake (Chen et al., 2001).

1.4.4 pH regulation

Tumours have been shown to grow at more acidic pH compared to normal tissues. This is partly due to increased activity of cancer cells, and especially glycolysis, which produces lactic acid. Tumour acidification is associated with increased invasion and metastatic potential. Carbonic anhydrase (CA) IX and XII, which are strongly induced by hypoxia in a range of tumour cell lines, and reversibly convert carbon dioxide and water to carbonic acid are also implicated in this process (Harris, 2002).

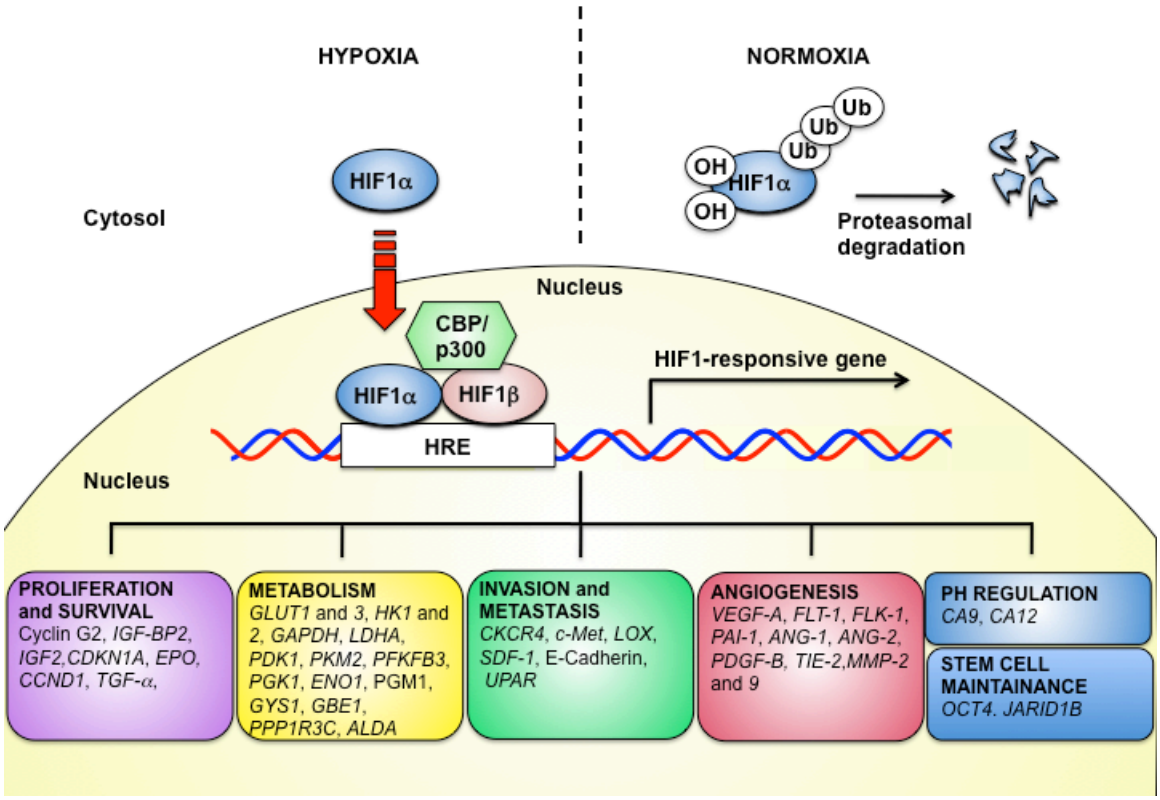


Figure 1.1 Regulation of HIF-1 activity. Under normal oxygen HIF-1α is hydroxylated on two proline amino acids residues (P402 and P564) by prolyl hydroxylase (PHDs). The prolyl hydroxylation results in ubiquitination of HIF-1α by the von Hippel Lindau (VHL) protein and subsequent proteasomal degradation. Under hypoxic conditions HIF-1α is stabilized and it translocates to the nucleus, where it dimerizes with the HIF-1β and associates with co-activators, such as CREB-binding

protein (CBP)/p300. The HIF-1 heterodimer induces the transcription of many hypoxia-response genes, involved in proliferation, survival, metabolism, angiogenesis, invasion, and metastasis, pH regulation, and stem cell maintenance by binding to hypoxia-response elements (HRE) in their promoters (Favaro et al., 2011).

1.5 Cancer stem cells

The tumour stem cell hierarchy states that only a small subpopulation of cells, named cancer stem cells (CSCs) are capable of generating the bulk mass of heterogeneous and differentiated cancer cells within tumours (Section 3.1). It is believed that cancer stem cells are the main cause of cancer progression, metastases, resistance to current cancer therapies and disease relapse ((Ma et al., 2011; Mimeault et al., 2007; Mimeault et al., 2012). The cancer stem cell model has been proposed to explain tumour heterogeneity. According to this model, tumour heterogeneity is generated by differences between tissue-resident stem cell types at the origin of particular cancer subtypes as well as progressive changes in the number and phenotypes of these immature cancer cells and their differentiated progenies and their local microenvironment during disease progression and after treatment initiation (Blazek et al., 2007; Mimeault and Batra, 2010, 2013). Thus identification of the molecular mechanisms and pathways that regulate cancer stem cells will help to improve current therapies and to prevent relapse.

1.5.1 Cancer stem cell markers

Cancer stem cells are typically recognized by the expression of cell surface markers such as CD133, CD44, CD24, ABCG2 and cellular activities like the efflux of

Hoechst dye or aldehyde dehydrogenase activity. Identification of these cancer stem cell markers has enabled the isolation of CSCs from primary malignant tumours such as leukemia (Al-Hajj et al., 2003b; Bonnet and Dick, 1997; Lapidot et al., 1994), breast (Al-Hajj et al., 2003b), colon (Cammareri et al., 2008; Dou and Gu, 2010) and brain (Singh et al., 2003).

Isolation of cancer stem cells in solid tumours was achieved for the first time in breast tumours in 2003, when Al-Hajj demonstrated that a lineage of estrogen receptor (ER) negative breast cancer cells with $CD44^{+HIGH}/CD24^{-LOW}$ cell surface phenotype had greater *in vivo* tumour forming ability compared with the remaining bulk cells of these tumours (Al-Hajj et al., 2003a). The following studies showed that this subpopulation of breast cancer stem cells have also other functional characteristics of mammary stem cells, such as the ability to self renew and to recapitulate the original tumour heterogeneity (Ponti et al., 2005; Sheridan et al., 2006). Interestingly, it has been shown that breast tumours with a high proportion of $CD44^{+HIGH}/CD24^{-LOW}$ cells are associated with poor patient survival and increased distant metastasis (Balic et al., 2006).

Recently it has been shown that ALDH1 can be used as a complementary marker for the identification of normal human breast and cancer stem cells (Ginestier et al., 2007). Moreover, ALDH1 has been recently recognized as a surrogate marker for the identification of stem cells populations in other cancer types, including human multiple myeloma, acute myeloid leukemia (AML) (Pearce et al., 2005), pancreatic (Feldmann et al., 2007) and colon (Li et al., 2010). ALDH1 is a detoxifying enzyme that oxidizes intracellular aldehydes (Dylla et al., 2008; Magni et al., 1996; Sophos and Vasiliou, 2003; Yoshida et al., 1998) and it may also have a role in early

differentiation of stem cells through its role in oxidizing retinol to retinoic acid (Chute et al., 2006). Ginestier *et al.* showed that the breast cancer $ALDH^{+}$ cells displayed high self-renewal capacity *in vivo* and *vitro* as well as high tumour forming capability in NOD/SCID xenografts (Ginestier et al., 2007). Subsequent studies showed that knockdown of ALDH1 inhibited CSC growth and sensitized CSCs to chemotherapies in various types of human cancers including breast (Marcato et al., 2011b), colon (Carpentino et al., 2009) and pancreatic (Marcato et al., 2011a) cancers. Additionally, a higher proportion of $ALDH^{+high}$ cells in breast tumours have been associated with poor clinical outcome (Ginestier et al., 2007; Morimoto et al., 2009).

Interestingly however, it has been shown that the overlap between the $CD44^{+HIGH}$ /$CD24^{-LOW}$ and the $ALDH^{+high}$ cells was very small (Ricardo et al., 2011). Nevertheless, the combination of $CD44^{+HIGH}$/$CD24^{-LOW}$ markers with ALDH resulted in the isolation of a highly tumourigenic stem cell population capable to form tumours from as few as 20 cells (Ricardo et al., 2011).

1.6 Stem cell signaling pathways

Several signaling pathways have been identified as playing a role in stem cell survival and maintenance. Among them Wnt, Hedgehog and ABC transporters signaling network have been shown to be implicated in the maintenance of tissue homeostasis by regulating self-renewal of normal stem cells as well as proliferation or differentiation of progenitor (transit-amplifying) cells (Katoh, 2007). Aberrant activation of these stem cell associated signaling pathways correlates with development of breast cancer and/or other types of cancer, suggesting that deregulation of stem /progenitor cell functionality may be involved in carcinogenesis (Wicha et al., 2006).

1.6.1 Wnt signaling

The Wnt signaling pathway is a network of proteins best known for their roles in embryogenesis and cancer, but also involved in physiological processes in adult animals (Lie et al., 2005). In a canonical pathway, Wnt signaling is initiated by the binding of Wnt ligand to the low density lipoprotein receptor related protein (LPR5) or LPR6, and to seven transmembrane receptors of the Frizzled proteins. This results in an increase in the cytosolic β catenin, which then translocates to the nucleus and binds to the transcription factors of the T-cell factor (Tcf) family and activates transcription of Wnt target genes, such as c-myc (He et al., 1998), MMP7 (Barker et al., 2007; Brabletz et al., 1999) and Lgr5 (Barker et al., 2007). In the absence of Wnt signals, the cytosolic pool of β catenin is continuously degraded by the proteasome as a results of its phosphorylation by a multi-protein complex (composed of Adenomatous Polyposis Coli protein (APC), axin, and kinases CK1 and GSK3), which marks it for ubiquitination.

Wnt signaling plays a critical role in the development of the normal mammary gland. The formation of embryonic mammary gland is under the tight control of several Wnt components such as the Wnt ligands (Wnt1, Wnt2, Wnt3, Wnt3a, Wnt5a, Wnt5b, Wnt6, Wnt7b, Wnt10a, Wnt10b, Wnt11), Wnt associated receptors (*i.e.*, Fzd1-9, Lrp5, Lrp6), and downstream DNA-binding proteins (*i.e.*, Tcf1, 3, and 4 and Lef1) (Chu et al., 2004). The development of breast cancer is associated with deregulation of Wnt signaling. Interestingly, several studies have shown that Wnt/β-catenin is a key regulator of breast cancer stem cell survival and maintenance (Ling et al., 2009). Evidence for this comes from reports showing that β-catenin upregulates the

expression of breast cancer stem cell markers CD44 and CD24 (Shulewitz et al., 2006). Additionally, it has been shown that the metastatic ability of triple negative breast cancers is associated with the upregulation of the LRP6 receptor (DiMeo et al., 2009; Liu et al., 2010a). Moreover basal and triple negative breast cancers show an abnormal regulation of β catenin, which is also associated with poor clinical outcome (Geyer et al., 2011). Furthermore Teissedre *et. al.* demonstrated that the transgenic Wnt1 overexpression activates Wnt signaling only in distinct progenitor compartments in the mouse mammary tumours (Teissedre et al., 2009).

Previous reports have shown that the radioresistance of cancer stem cells isolated from breast cancer cell lines is in part due to an aberrant activation of Wnt signaling (Chen et al., 2007; Debeb et al., 2009; Woodward et al., 2007). Additionally, a recent study has demonstrated that radioresistant mouse mammary stem cells isolated from p53 null mice had altered DNA repair in response to radiation, and increased AKT and β-catenin activation (Zhang et al., 2010). In line with this, inhibition of Akt and β catenin resulted in radiosensitization of these cells (Zhang et al., 2010). Therefore, all these results support a role of Wnt signaling and its downstream targets in maintaining and regulating breast cancer stem cells. It follows that better understanding of Wnt signaling in breast cancer may help the development of more effective cancer therapies.

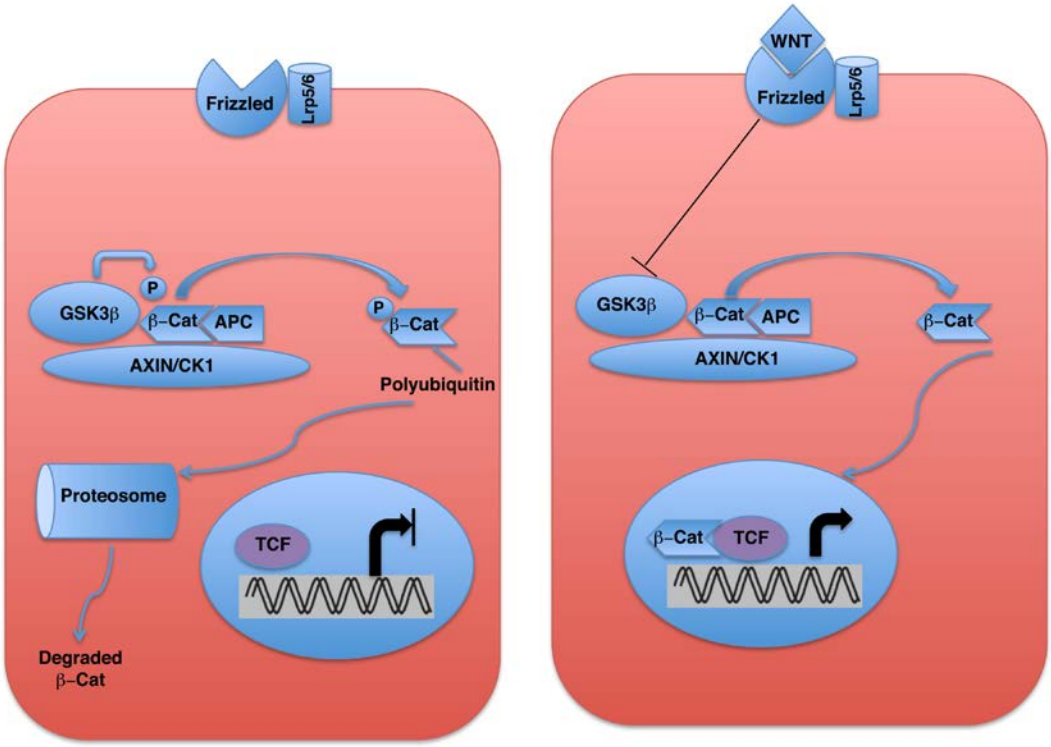


Figure 1.2 Wnt signaling. In the absence of Wnt signals, the cytosolic pool of □ catenin is continuously degraded by the proteasome as a results of its phosphorylation by a multi-protein complex (composed of Adenomatous Polyposis Coli protein (APC), axin, and kinases CK1 and GSK3), which then becomes degraded. In the presence of Wnt ligand, the formation of the destruction complex is inhibited, increasing the intracellular pool of β-catenin, which then translocates to the nucleus and binds to the transcription factors of the T-cell factor (Tcf) family and activates transcription of Wnt target genes. Adopted from Inke Näthke (Nathke, 2006).

1.6.2Hedgehog signaling

Hedgehog signaling consists of three lipid-modified ligands, Sonic hedgehog (Shh), Desert hedgehog (Dhh), and Indian Hedgehog (Ihh). In the absence of Hh ligands, the Patched (Ptch1), a 12-pass transmembrane-spanning receptor, constitutively represses the activity of the co-receptor Smoothened (Smo), by preventing its localization to the primary cilium (Merchant and Matsui, 2010). Activation of Hh signaling is initiated

by the binding of one of the three Hh ligands to the Ptch1. Hh ligand binding to Ptch1 relieves a Ptch1-mediated repression of Smo, which leads to the phosphorylation and cleavage of the Gli zinc-finger transcription factors, Gli2 and Gli3. Gli2 and Gli3 act as transcription repressors, whereas when Hh signaling is active, Gli2 and Gli3 function as transcription activators for Hh target genes (Sasaki et al., 1999).

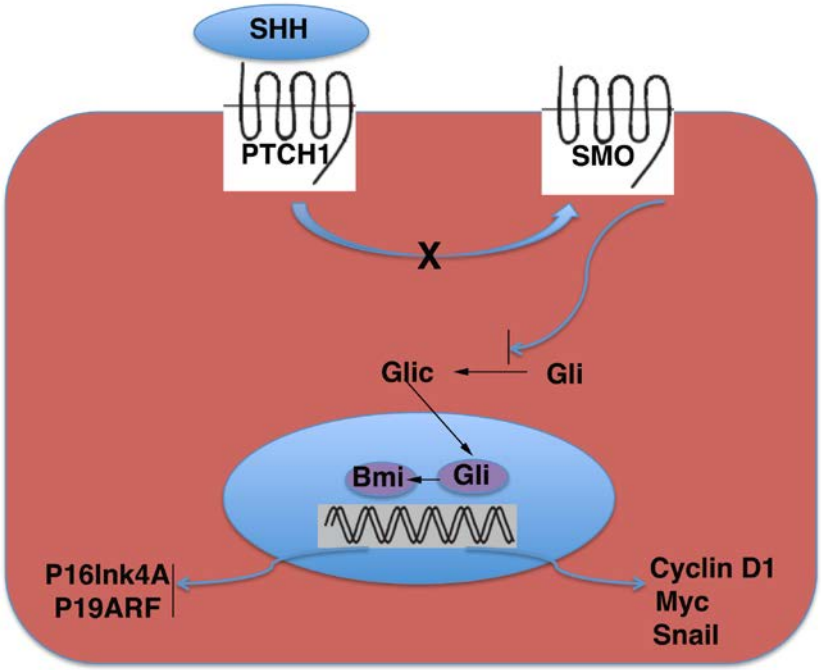


Figure 1.3 Hedgehog signaling pathway. In the absence of Hh ligands, the Patched (Ptch1), constitutively represses the activity of the co-receptor Smoothened (Smo), by preventing its localization to the primary cilium. Activation of Hh signaling is initiated by the binding of one of the three Hh ligands to the Ptch1. Hh ligand binding to Ptch1 relieves a Ptch1-mediated repression of Smo, which leads to the phosphorylation and cleavage of the Gli zinc-finger transcription factors. Gli2 and Gli3 function as transcription activators for Hh target genes.

Several studies have shown that the Hedgehog signaling pathway regulates

glioblastoma, colon and breast cancer stem cells as well as multiple myeloma and chronic myeloid leukemia cancer stem cells (Bar et al., 2007; Dierks et al., 2008; Liu et al., 2006).

In breast cancer stem cells PTCH, Gli1 and Gli2 transcripts are upregulated relative to the bulk of the tumour (Varnat et al., 2009). In line with this finding, activation of the Hh pathway, by adding Shh or overexpressing Gli1, Gli2 or SmoM2 leads to an increase in mammosphere formation (Kasper et al., 2009; Moraes et al., 2007). Additionally, aberrant expression of Hh ligands and Gli1 and Gli2 expression alters the expression of BMI-1 (Liu et al., 2006). Bmi-1 is a transcription repressor involved in the maintenance of neuronal, hematopoietic and mammary gland stem cells (Kasper et al., 2009; Liu et al., 2006; Molofsky et al., 2003). Moreover breast tumours derived from Gli transgenic mouse exhibit basal epithelial phenotype, with a basal keratin expression profile (Fiaschi et al., 2009). Inhibition of Hh signaling with antibodies, pharmacologic SMO antagonists, or small interfering RNA (siRNA) results in tumour growth inhibition (Merchant and Matsui, 2010). In addition, cyclopamine, a SMO inhibitor, reduces the proliferation of cancer stem cells and abrogates metastasis (Liu et al., 2006; Mimeault and Batra, 2006). Taken together these data indicate the involvement of Hh in regulating breast CSCs cells.

1.6.3 ABC transporters

Cancer cell resistance to chemotherapy is a major problem that limits the success of many anticancer agents. Cancer cells have evolved mechanisms that allow them to pump chemotherapeutic agents out of the cells, leading to the reduction of intracellular drug levels and consequent drug insensitivity. The increased expression of members of the ATP binding cassette (ABC) transporter superfamily plays a

crucial role in the development of multidrug resistance (MDR). Accordingly, increased expression of ABC transporters correlated with a reduction in overall survival (Wind and Holen, 2011). Moreover, their role in drug resistance has drawn attention to them as potential cancer therapy targets.

Normal and cancer stem cells express high levels of ABC transporters (Zhou et al., 2001). For example hematopoietic stem cells express high levels of ABCG2 and ABCB1, and they lose the expression of these genes upon differentiation into mature blood cells (Scharenberg et al., 2002). The high drug efflux property of stem cells related to ABC transporters expression was used as an early method for their isolation. For example, so-called "side populations" (SP), with stem cell characteristics and high drug efflux property were isolated using the fluorescence dye Hoechst 33342.

Previous reports have shown that the SP from MCF7 breast cancer cell line had increased expression of stem cell markers and displayed functional properties of cancer stem cells, such as a high capacity to form mammospheres. They are also more tumourigenic when transplanted into immunodeficient mice (Engelmann et al., 2008; Steiniger et al., 2008; Zhou et al., 2009). Additionally, it has been shown that the MCF7 SP is more radioresistant and chemoresistant to agents, including mitoxantrone and carboplatin (Woodward et al., 2007). Further to this, treatment with ABCG2 with ABCG2 inhibitors resulted in the elimination of the SP in MCF7 cells (Yin et al., 2008).

Almost all chemotherapeutic drugs are known to be substrate for ABC transporters, thus increasing the possibility of developing multidrug resistance tumours. Therefore, combinatorial treatment with chemotherapy and ABC transporter inhibitors may be

able to eliminate the cancer stem cell populations as well as the cells making up the bulk of the tumour.

1.6.4 mTORC1 signaling

In all eukaryotes, the target of Rapamycin (TOR), is a highly conserved Ser/Thr kinase that regulates cell growth, metabolism, survival and proliferation in response to growth factors, nutrients, energy, and environmental conditions (Wullschleger et al., 2006). The fact that mTOR dysregulation is associated with cancer development highlights its importance in the regulation of cellular growth and homeostasis. mTOR inhibitors such as rapamycin and its analogues have been successfully developed and are currently used clinically, as FDA-approved chemotherapeutic drugs, for the treatment of cancer, including breast cancer (Lock et al., 2012; Vignot et al., 2005).

mTOR forms two multi protein complexes, mTOR complex 1 (mTORC1) and mTOR complex 2 (mTORC2). The mTOR-containing complexes have different sensitivities to rapamycin as well as upstream inputs and downstream outputs (Laplante and Sabatini, 2012). mTORC1 is the primary effector for the nutrient-sensitive functions of TOR, whereas mTORC2 has been implicated in cytoskeletal reorganization, cell survival and metabolism (Russell et al., 2011).

The best-described upstream regulators of mTORC1 are growth factors, energy status, oxygen, nutrients, and amino acids. Additionally, it has been shown that inflammation, Wnt signalling and phosphatidic acid contribute to the activation of mTORC1(Laplante and Sabatini, 2009).

Growth factors such as insulin and insulin-like growth factor 1 (IGF1) stimulate the PI3K and Ras pathways, an event that results in the activation of AKT (a

serine/threonine protein kinase). Active AKT promotes mTORC1 activation by phosphorylating and inhibiting the TSC1/TSC2 complex (Miron et al., 2003; Russell et al., 2011). AKT also signals to mTORC1 in a TSC1/2-independent fashion by phosphorylating, and causing the dissociation from raptor of PRAS40, an mTORC1 inhibitor (Kovacina et al., 2003; Vander Haar et al., 2007).

Cellular stresses such as low energy, oxygen levels or DNA damage, restrain the activation of mTORC1. In response to these cellular stresses, ATP generation decreases and AMP levels rise leading to the activation of the AMP-activated protein kinase (AMPK) (Inoki et al., 2003). AMPK halts mTOR signaling by phosphorylation of raptor and TSC2 (Gwinn et al., 2008; Inoki et al., 2003).

Additionally, Wnt signaling has been also shown to regulate the mTORC1 pathway. Wnt activation increases mTORC1 signaling through the inhibition of glycogen synthase kinase 3 (GSK3), a kinase that phosphorylates TSC2 (Inoki et al., 2006).

The cellular events occurring downstream of mTORC1 are key regulators of protein synthesis. Activated mTORC1 directly phosphorylates two translator regulators, the eukaryotic initiation factor 4E–binding protein 1 (4EBP1) and ribosomal protein S6 kinase 1(Hara et al., 1998; Laplante and Sabatini, 2012). Under a nutrient limited environment, the binding of 4EBP1 to the eukaryotic initiation factor (eIF4F) inhibits the assembly of the translation initiation complex (De Benedetti and Graff, 2004). In a nutrient rich environment mTORC1 is activated and directly phosphorylates 4EBP1, which results in its release from the eIF4F, enabling it to participate in the formation of the translation initiation complex (De Benedetti and Graff, 2004). These events promote the initiation of the cap-dependent translation of a set of proteins involved in G1-S-phase progression, including cyclin D and MYC (Hashemolhosseini et al.,

1998; West et al., 1998). Phosphorylation of S6K1 results in the phosphorylation of multiple substrates involved in translation initiation, such as the 40S ribosomal protein S6 and the regulatory subunit (eIF4B) of RNA helicase (eIF4A).

mTOR is not only a key regulator of protein translation but it is also implicated in the regulation of other major process. For example, mTORC1 promotes lipid biosynthesis through the sterol-regulatory-element-binding proteins (SREBPs) and peroxisome proliferator-activated receptor-γ (PPARγ), two transcription factors that control the expression of genes encoding proteins involved in lipid and cholesterol homeostasis (Kim and Spiegelman, 1996; Kim et al., 1998). Additionally, mTORC1 has been shown to control mitochondrial metabolism and biogenesis (Chen et al., 2008; Cunningham et al., 2007). For instance, mTORC1 activation increases the number of copies of mitochondrial DNA and the expression of genes that encode proteins regulating mitochondrial metabolism (Chen et al., 2008; Cunningham et al., 2007).

1.6.5 mTORC1 and Cancer Stem Cells

Several studies have implicated the mTORC1 pathway in the regulation of cancer stem cells, including breast cancer stem cells (Korkaya et al., 2009). Accordingly, the PTEN/PI3K/AKT/mTOR signaling pathway plays a crucial role in the survival and proliferation of cancer stem cells (Korkaya et al., 2009). In tumours, hyperactivation of the PTEN/PI3K/AKT/mTOR/ pathway may occur by activation of upstream growth factor receptors, overexpression or amplification of AKT, or inactivation of phosphatase and tensin homolog (PTEN) (Jiang and Liu, 2008). PTEN usually functions as a negative regulator of the PI3K/mTOR pathway (Song et al., 2012). It has been shown that the *PTEN* knock-out mice display an increase in the number of hematopoietic cancer stem cells and have an increased risk of developing leukemia

(Magee et al., 2012). Interestingly, rapamycin treatment prevented the development of leukemia in these mice (Guo et al., 2011b).

Moreover, recent studies have shown that mTOR also plays an important role in the regulation of breast cancer stem cells and epithelial-mesenchymal transition **(**EMT) (Korkaya et al., 2009,(Zhou et al., 2007a). In line with this, inhibition of the mTOR pathway with shRNA or rapamycin in MCF7 cells resulted in a decrease in the stem cell pool coupled with reduced colony formation and *in vivo* tumourgenicity (Lock et al., 2012). Further to this, EMT and metastasis is inhibited upon mTORC1 inhibition in colon cancer cell lines (Gulhati et al., 2011).

Given the above, it is not surprising that key regulators of signaling pathways, such as mTOR, are upregulated in cancer stem cells helping them survive and maintain their stem cell phenotype. Therefore, gaining better understanding of the molecular mechanisms linking mTOR with cancer stem cell survival will help in the development of new therapies targeting the CSC compartment.

1.7 Hypoxia and cancer stem cells

It has been suggested that hypoxic regions serve as a stem cell niche providing a microenvironment that is crucial for stem cell survival and maintenance. In line with this it has been shown that hypoxia is a key regulator of fetal development and stem cell differentiation (Simon and Keith, 2008) and also that it inhibits the differentiation of adipocytes, chondrocytes and myocytes (Malladi et al., 2006; Yun et al., 2005; Yun et al., 2002).

Recent evidence has expanded on the role of hypoxia, and a role for hypoxia has been suggested in regulating cancer stem cells. Consistent with this notion, it has been

demonstrated that HIF-1α and HIF2α are upregulated in cancer stem cells during cancer progression and metastasis (Mimeault and Batra, 2013). The upregulation of HIF-1α and HIF-2α results in the activation of stem cell associated pathways and genes that are important for their survival (Kaelin, 2004; Ma et al., 2011; Mathieu et al., 2011; Mimeault and Batra, 2013; Stoeltzing et al., 2003). Among the upregulated stem cell associated pathways are regulators of pluripotency such as the octamer-binding transcription factor Oct-3/4, SOX2, Nanog, genes that are involved in the epithelial mesenchymal transition (EMT) such as EGFR, CXCR4, snail and twist, metabolic enzymes such as glucose transporters (GLUT-1/2) and glycolytic enzymes and drug resistance genes such as the ATP binding transporters (Kaelin, 2004; Ma et al., 2011; Mathieu et al., 2011; Mimeault and Batra, 2013; Stoeltzing et al., 2003).

Moreover, breast cancer stem cells overexpress HIFs and regulators of EMT (Conley et al., 2012; Mayer et al., 2012; Quail et al., 2011). For example, recent analysis of 253 samples of breast ductal carcinoma showed a strong localization of HIF-1α in the breast cancer stem cell compartment, defined by the $CD44^{+}/CD24^{-}$ phenotype (Oliveira-Costa et al., 2011). Additionally, it has been observed that hypoxic breast cancer stem cells are overexpressing markers of mesenchymal phenotype such as N-cadherin and vimentin (Conley et al., 2012; Han et al., 2012b; Quail et al., 2011). Moreover the stem cell associated signaling pathways WNT/β catenin and PI3K/AKT are upregulated in these cells and also display stem cell functional properties such as high clonogenic and mammosphere-forming capacity and tumourigenicity (Conley et al., 2012; Han et al., 2012b; Quail et al., 2011). Consistent with this, cycling hypoxia causes an increase in the stem pool of the metastatic MDA-MB-231 and BCM2 breast cancer cells (Louie et al., 2010). Interestingly, these cancer stem cells displayed

higher mammosphere-forming ability, tumourigenicity and metastatic potential to lungs compared to the parental breast cancer cell lines (Louie et al., 2010).

1.8 Tumour Microenvironment

The survival and growth of normal cells is controlled by signals that derived from their microenvironment. For example, specific cell surface receptors such as integrins, link the cells to the extracellular matric (ECM) and pass information from the ECM to the cells (Lee and Juliano, 2004). This activates signaling pathways that influence cell responses. Detachment of normal cells from the ECM results in programmed cell death, a process called anoikis (Frisch and Ruoslahti, 1997). This prevents the seeding of cells in inappropriate sites, which could lead to dysplastic growth. Additionally, secretion of cytokines and growth factors influence the rate of cell proliferation. Several studies have expanded on the role of tumour microenvironment by relating it to tumour progression. The tumour microenvironment is comprised of the extracellular matrix, activated fibroblasts, adipocytes, epithelial cells, endothelial cells, and inflammatory cells such as macrophages, neutrophils, mast cells and lymphocytes (Castells et al., 2012). Dysregulated signals and interactions of these components with tumour cells play an important role in tumour infiltration, progression, metastasis and ultimately, the clinical outcome.

1.8.1 Tumour associated macrophages

Tumour associated macrophages (TAMs) play an important role in tumour development by promoting tumour survival, metastasis, migration and angiogenesis. Additionally, it has been shown that increased infiltration of macrophages is associated with poor patient outcome (Bingle et al., 2002; Kamangar et al., 2006;

Leek et al., 1996). The release of cytokines from tumour cells, such as CSF-1, results in the recruitment of the macrophages to the tumour periphery (Korkaya et al., 2011). Macrophages can be differentiated into pro-inflammatory M1 macrophages or anti-inflammatory M2 macrophages (Solinas et al., 2009). The release of these cytokines and chemokines enhance the development and differentiation of Th1, Th17, and NK cells, which have proinflammatory functions (Mantovani et al., 2002). Hypoxic areas of advanced tumours attract the M2 macrophages, which in turn release specific sets of cytokines such as CCL17, CCL22, CCLL2 which results in the recruitment and differentiation of T cells (Hall, 2006). In turn, T cells produces TGFβ and IL10 inhibiting the anticancer immunity. In support of this, inhibition of CSF-1 significantly decreased the infiltration of macrophages at the tumour sites, which was accompanied by a reduced formation of metastasis and slower tumour growth (Aharinejad et al., 2004; Lin et al., 2001).

1.8.2 Extracellular Matrix

Extracellular (ECM) matrix is a non-cellular component of the tumour environmental niche, and the interaction of cells with the ECM plays an important role in normal organogenesis and morphogenesis (Lu et al., 2012). ECM controls many aspects of cell biology such as gene expression, differentiation and proliferation as well as an invasive/metastatic phenotype of tumour cells (Iseri et al., 2010). The regulatory mechanisms between cells and the ECM is important as it allows cells and tissues to swiftly adapt to their environment (Lu et al., 2012; Samuel et al., 2011). These macromolecules structure the basement membrane and the interstitial matrix (Jarvelainen et al., 2009; Schaefer and Schaefer, 2010). The basement membrane separates the epithelium or endothelium from stroma cells, and is rich in type IV

collagen, fibronectin, and laminins (Jarvelainen et al., 2009). Whereas the composition of the interstitial matrix, which is predominantly made up from fibrillar collages, proteoglycans, and various glycoproteins is responsible for the flexibility of the ECM (Frantz et al., 2010; Jarvelainen et al., 2009).

Recent evidence has expanded on the role of ECM by relating it to cancer progression (Erler et al., 2009; Erler et al., 2006; Levental et al., 2009). For example, a stiffer ECM compared to normal tissues and an increased deposition of collagens characterizes tumours (Levental et al., 2009). ECM stiffness results in a mechanically weaker and less elastic but also more rigid ECM. This severely compromises ECM organization, and alters epithelial function that can lead to the promotion of tumourigenesis. Part of the increase in ECM stiffness is induced by ECM deposition and remodeling by ECM-associated fibroblasts and by increased contractility of the transformed epithelium (Butcher et al., 2009; Levental et al., 2009). This results in the upregulation of integrin signaling, which contributes to cell survival and proliferation of tumour cells (Paszek et al., 2005; Wozniak et al., 2003). Additionally, the secretion of growth factors such as transforming growth factor-β (TGF-β) and cytokines acts as stimuli for the proliferation and trans-differentiation of infiltrated fibroblast to myofibroblasts, which further promote tissue desmoplasia (De Wever et al., 2008). Moreover, recent studies suggest that the ECM is an essential component of the metastatic niche. In support of this, it has been shown that cells expressing the CD44, a component of the ECM, have a survival advantage during invasion compared to the metastatic cells that do not express it (Yu et al., 1997). In addition, tumours display an increased expression of lysyl oxidase (LOX), which cross-links collagen fibers and other ECM components and contributes to the stiffness of ECM (Barker et al., 2011). Previous studies have also shown that overexpression of LOX increases metastatatic

potential and tumour growth (Erler et al., 2009). The upregulation of LOX enzymes has been observed in many tumours including breast cancer and head and neck cancer and is associated with poor patient prognosis (Barker et al., 2011; Le et al., 2009). Further to this, increased expression of the ECM proteins matrix metalloproteinases (MMPs), which are proteins present in the ECM, by tumour cells and myofibroblasts also contribute to the remodeling of ECM (Egeblad et al., 2010b). Activated MMPs release ECM-embedded growth factors such as vascular endothelial growth factor (VEGF), and in this way promote the formation and growth of new blood vessels contributing to the induction of angiogenesis (Hiratsuka et al., 2002).

1.8.3 ECM serves as stem cell niche

A growing body of evidences supports the notion that the ECM can serve as a niche for stem cells, and is also essential for the maintenance and regulation of stemness. In support of this, it has been shown that stem cells can be isolated using as surface markers various ECM receptors such as α6 or β1 integrin chains (Shen et al., 2008) Additionally, functional suppression of ECM receptors (O'Reilly et al., 2008; Tanentzapf et al., 2007) and reduction of ECM components (Frye et al., 2003) results in reduction of the stem cell pool. The ECM produces multiple secreted signals and therefore the anchorage of stem cells into the ECM plays a key role in the regulation of stem cell maintenance and proliferation (Li and Xie, 2005). For example, the maintenance of stem cell polarity, the orientation of their mitotic spindles and the regulation of asymmetric division are tightly dependent on the attachment of stem cells to the ECM (Lambert and Nagy, 2002; Lu et al., 2012; Yamashita and Fuller, 2008). In support of this, suppression of components that regulate cell polarity such as Numbl and Lgr disrupt asymmetric cell division and increase the number of neural

stem cells, leading to brain tumour development (Klezovitch et al., 2004; Li et al., 2003b; Lu et al., 2012).

The structure of the ECM is also important for the survival and differentiation of stem cells by providing them with structural support (Lu et al., 2012). This is supported by studies demonstrating that when mesenchymal stem cells are grown in different condition they differentiate into specific cell lineages. For example, mesenchymal stem cells grown on polymer gels, which are mimicking the elasticity of brain microenvironment, express neuronal markers, whereas when they are grown on gels that resemble the skeletal muscle tissue they express bone proteins (Engler et al., 2006; McBeath et al., 2004).

1.8.4 Inflammation and Cancer

It has been suggested that tumours are “wounds that do not heal”. In 1863 Rudolf Virchow, a German pathologist, made a connection between chronic inflammation and cancer (Balkwill and Mantovani, 2001). He suggested that sites of chronic inflammation promote tumour development, postulating that immune cells release factors that stimulate cell proliferation (Balkwill and Mantovani, 2001). Since then, multiple studies have substantiated this showing that chronic inflammatory diseases are associated with high predisposition to cancer development (Balkwill and Mantovani, 2001; Coussens and Werb, 2002; Philip et al., 2004). For example, recent epidemiological studies have shown that over 25% of all cancers are related to chronic inflammation and it is estimated that 15% of all cancers are associated with inflammation (Kuper et al., 2000; Ramos-Nino, 2013; Vendramini-Costa and Carvalho, 2012). Accumulated data have demonstrated that chronic inflammation can influences processes that contribute to cancer progression such as DNA damage,

DNA replication, apoptosis evasion, angiogenesis, and metastasis (Kamp et al., 2011). Extrinsic factors such as chronic infections, autoimmune diseases, chronic exposure to tobacco or asbestos as well as intrinsic factors caused by genetic alterations within the cancer cells are potential inducers of chronic inflammation (Heinrich et al., 2012).

The inflammatory tumour microenvironment is characterized by the infiltration of immune cells such as tumour-associated macrophages (TAM), mast cells, dendritic cells, natural killer (NK) cells, neutrophils, eosinophils and lymphocytes (Vendramini-Costa and Carvalho, 2012). Cancer cells release cytokines and chemokines that lure the immune cells to infiltrate the tumour sites and facilitate cancer progression (Coussens and Werb, 2002). In support of this, it has been shown that high serum concentrations of proinflammatory cytokines such as TNFα, IL-6, or inflammasome-related IL-1β/IL-18 correlate with advanced malignancies, and are associated with reduced survival (Coussens et al., 2013). Tumour associated neutrophils and macrophages generate high amounts of reactive oxygen species (ROS) and nitrogen species leading to increased mutation rate, as they can directly induce damage DNA, and/or alter the function of proteins involved in DNA repair, cell cycle control and apoptosis through covalent modifications of these macromolecules (Antsiferova and Werner, 2012). Additionally, it has been proposed that mitochondrial dysfunction of epithelia cells due to activation of RAS, MYC and p53 produces ROS, which act as the central endogenous carcinogens that activate cancer-promoting signaling pathways important in inflammation-associated cancer (Kamp et al., 2011). In line with this, recent studies have shown that an inflammatory tumour microenvironment inhibits the proliferation of normal cells, and in turns provide a survival advantage to mutated cells, which are resistant to ROS-induced stress (Blagosklonny, 2002; Marusyk and DeGregori, 2008; Polyak et al., 2009).

Further to this, ROS and nitrogen species induce epigenetic changes in stromal cells and epithelial cells, which further promote tumour growth and progression (Egeblad et al., 2010a). Additionally, the tumour associated immune cells contribute to cancer development through the secretion of tumour necrosis factor α (TNFα), interleukins (IL-1, IL-6, IL-8), interferons (IFNs) and enzymes such as cyclooxygenase-2 (COX-2), lipooxygenase-5 (LOX-5) and phospholipase A2 (PLA2), which activate or are activated by transcription factors. In addition, nuclear factor κB (NF-κB) and signal transducers and activators of transcription-3 (STAT3) further contribute to tumour development (Vendramini-Costa and Carvalho, 2012). For example, it has been shown that the expression of IL-10 and prostaglandin E_2 by tumour associated macrophages suppresses their antitumour response (Elgert et al., 1998). In addition, TAMs release angiogenic factors such as VEGF and endothelin-2 which promote formation of new blood vessels, and induce angiogenesis (Bando and Toi, 2000; Pollard, 2004). The tumour associated immune cells also secrete diverse classes of proteolytic enzymes such as matrix metalloproteinases (MMP-2 and MMP-9), which degrade the extracellular matrix and modify its function, promoting cell invasion and metastasis (Coussens et al., 1999; Pollard, 2004).

Given the association of inflammation and cancer recent studies have shown that the inhibition of inflammatory mediators with anti-inflammatory drugs decreases cancer incidence and progression (Cerhan et al., 2003; Lee et al., 2012; Shebl et al., 2012). These inhibitors are specific, non-steroidal anti-inflammatory drugs (NSAIDs) such as aspirin and COX2 inhibitors. Additionally, an anti-IL6 therapy is under development for the treatment of multiple myeloma (Kamp et al., 2011). Given the above it has become clear that blocking inflammation will play a big role in cancer prevention and treatment in the future.

1.8.5 Inflammation and Cancer stem cells

Recent studies have shown that cytokines generated within the tumour microenvironment stimulate cancer stem cell self-renewal (Sansone et al., 2007b). In support of this, it has been shown that the release of IL-8 from endothelial and stroma cells controls the proliferation and self-renewal of mammary stem cells and is important for the communication between stem cells and microenvironment (Bussard and Smith, 2011). Moreover, previous studies have shown that breast cancer stem cells and lung cancer stem cells express high levels of the IL-8 receptor CXCR1 and blockage of CXCR1 with either a CXCR1-specific blocking antibody or repertaxin, a small-molecule CXCR1 inhibitor, significantly reduced the stem cell population (Ginestier et al., 2010b). Further to this, IL-6 and its receptors have been shown to play an important role in the breast cancer stem cells (Sansone et al., 2007b; Schafer and Brugge, 2007). Accordingly, self renewal of breast cancer stem cells is regulated by IL-6 through activation of STAT3 signaling (Iliopoulos et al., 2009). STAT3 plays an important role in stem cells reprogramming and stem cell renewal (Chen and Tuan, 2008). Activation of STAT3 results in the activation of NF-kB and its downstream targets Lin28 and microRNAlet7 (Korkaya et al., 2011a). Interestingly, both Lin28 and let7 are implicated in the self renewal of embryonic stem cells (Iliopoulos et al., 2009). Elevated levels of proinflammatory cytokines such as TGFβ, TNFα and IL-1, have been also linked to NF-kB activation. For example, IL-1 TNF-α, and IL-6 upregulate MMP expression, invasiveness, and metastasis via NF-κB and STAT3 signaling. Currently, a NF-κB inhibitor called parthenolide, has shown positive results *in vitro* and in early clinical studies in suppressing tumour growth (Hassane et al., 2010). Additionally, xenograft experiments have demonstrated that mesenchymal

stem cells are attracted to breast tumour sites by gradients of IL-6 (Liu et al., 2011a). Also, activation of Jagged/Notch 1 signaling by IL-6 promotes breast cancer bone metastasis (Sethi et al., 2011).

Overall, it is clear that there is a link between inflammation (as well as growth factors and cytokines produced by inflammation) and the acquisition of a stem like phenotype in cancer cells. Elucidation of the role(s) of these pathways in these processes may provide new targets for therapeutic intervention.

1.9 Tumour Metabolism

Uncontrolled cell proliferation is one of the hallmarks of cancer cells. Highly energetic metabolic processes are required in order to sustain cellular growth and the synthesis of biomass in tumours. In the 1920s, Otto Warburg, showed that the metabolism of cancer cells differs from normal cells. He demonstrated that tumour cells use preferentially use glycolysis, instead of mitochondrial oxidative phosphorylation in order to meet their energy demands. He identified that this was regardless of whether the cells were well-oxygenated or not (Warburg, 1956). Glycolysis results in the conversion of glucose to pyruvate, and then to the "waste" product lactic acid. Indeed, it has been shown that cancer cells display glycolytic rates up to 200 times higher than normal cells (Warburg, 1956). In addition to this, carbon labeling studies have shown that 90% of the glucose is converted to lactate in cancer cells (DeBerardinis et al., 2007). The high aerobic glycolysis of tumour has lead to the development of 2-[18F]-fluoro-2-deoxy-D-glucose (FDG) probe for positron emission tomography (PET), which is currently used clinically to diagnose and monitor treatment responses of cancers.

In most normal cells, glucose enters the cytosol through specific transporters (the GLUT family) and is metabolized into two molecules of pyruvate (Bricker et al., 2012). The pyruvate is directed into the mitochondria but it can be diverted on two different pathways. In one of them, pyruvate is carboxylated to form oxaloacetate, which can be used for gluconeogenesis. In the second pathway, pyruvate is decarboxylated into acetyl–CoA, and it is cycled through the tricarboxylic acid where it is either used as a substrate for oxidative phosphorylation or it is converted to citrate to use as a substrate for fatty acid synthesis.

In contrast, in cancer cells the majority of pyruvate is converted to lactate via LDHA, and is secreted into the extracellular environment. This is achieved by the upregulation of pyruvate dehydrogenase kinase, isoenzyme 1 (PDK1), a Ser/Thr kinase which phosphorylates and activates the mitochondrial pyruvate dehydrogenase (PDH). Given the fact that PDH is an enzyme responsible for the conversion of pyruvate to acetyl–CoA, its inhibition by PDK1 is believed to be a key regulatory step of the Warburg effect (Kim and Dang, 2006).

Oxidative phosphorylation generates more energy, 36 molecules of ATP per molecule of glucose, than glycolysis which yields only 2 ATP molecules per molecule of glucose (Tennant et al., 2010). The reason why cancer cells switch to a less energy efficient pathway to generate ATP is still unclear. However it is postulated that upregulation of glycolysis is likely to be adaptation to hypoxia, acquisition of resistance to mitochondria-mediated apoptosis and acidification of the tumour microenvironment by lactate from cancer cells, which leads to tumour invasion or metastasis (Fujiwara et al., 2013; Garber, 2010).

1.9.1 Metabolic Symbiosis

While the Warburg effect has been widely accepted, recent studies have shown that tumour metabolism appears to be more complex. It has been proposed that tumours display a metabolic symbiosis. According to this, there is a metabolic cooperativity between cancer populations and supporting host cells (stroma, adipocyte, fibroblasts, muscle, and endothelial cells), where one population's end product of glycolysis, lactate, is consumed by the second population to "fuel" mitochodrial oxidative metabolism (Martinez-Outschoorn et al., 2011a). In addition to this, cancer cells induce autophagy and mitophagy to the surrounding host cells which produce high energy metabolites such as L-lactate, ketone bodies, glutamine and free fatty acids (Capparelli et al., 2012). Cancer cells then take up these metabolites for the production of ATP through oxidative phosphorylation (Salem et al., 2012).

Further to this, variability of FDG uptake in cancers gives more evidence that tumour cells may use sources other than glucose to generate energy (Avril et al., 2001; Schmidt et al., 2009). For example, it has been shown that HeLa cells are use glutamine and pyruvate almost exclusively to generate ATP (Rossignol et al., 2004). Additionally, prostate cancer, which is characterized by slow glycolysis and poor FDG uptake, uses fatty acids as a source of energy despite the presence of abundant glucose (Liu, 2006; Liu et al., 2010b). Interestingly, [11 C] acetoacetate (a ketone body related to 3-hydroxy-butyrate) is currently being developed as an imaging agent for PET-scanning for the early detection of tumours (Authier et al., 2008; Prenen et al., 1990).

1.9.2 Autophagy

Autophagy is an evolutionary conserved cellular process in which unwanted or dysfunctional proteins and cellular components are sequestered in double-membrane vacuoles called autophagosomes and delivered to lysosomes for degradation. Cancer cells induce autophagy as a survival mechanism in response to hypoxia, metabolic stress and starvation and to resist radiotherapy (Rouschop et al., 2010; Rzymski and Harris, 2007; Rzymski et al., 2010). The degradation of cellular components provides an alternative metabolic pathway for the production of energy and structural building blocks in a nutrient limited environment. During autophagy amino acids and other nutrients are exported from the autophagolysosomes into the cytosol where they are recycled as biosynthetic precursors or as substrates and are oxidized to support bioenergetics (Yang and Klionsky, 2010). For example, previous studies have shown that pancreatic cancer cells display high levels of basal autophagy in order to sustain increased oxidative phosphorylation, a phenomenon termed autophagy addiction (Guo et al., 2011a; Yang et al., 2011).

A key negative regulator of autophagy is mTORC1 signalling. In mammals, the autophagy initiation complex consists of the ULK1, ATG13, FIP200 and ATG101 proteins. In a nutrient rich environment, where mTORC1 is active, it phosphorylates and inhibits the ULK1 complex, and the mammalian Atg13 and represses the induction of autophagy (Onodera and Ohsumi, 2006). In addition, a negative ULK-1 dependent feedback loop inhibits mTORC1 during nutrient limitation (Dunlop et al., 2011).

Under hypoxic conditions LC31B (microtubule-associated protein 1 light chain 3β) and ATG5 (autophagy-related 5) two key autophagy genes are upregulated through

the activity of ATF4 and CHOP [C/EBP (CCAAT/enhancer-binding protein)-homologous protein], respectively (Pike et al., 2013). During autophagy, LC3I is cleaved and lipidated and is converted to LC3II. This conversion is important as it allows the association of LC3II with the autophagosomes, an event important for autophagosome's formation. At present, LC3 is the most reliable cellular marker for autophagy activation.

In addition, intracellular environmental conditions can turn the mitochondria into harmful organelles, as they can produce reactive oxygen and also release pro death proteins, which leads to the disruption of ATP synthesis and cell death (Kubli and Gustafsson, 2012). For this reason, cells have developed a selective autophagy process called mitophagy, whereby damaged mitochondria are degraded into the autophagolysosomes. A key regulator of mitophagy is the mitochondrial protein BNIP3, a conserved member of the BH3-only sub-group of the Bcl-2 family of cell death regulators. Previous reports have shown that BNIP3 is responsible for mitochondrial fragmentation and mitophagy through interactions with OPA-1 and LC-3, respectively (Landes et al., 2010; Rikka et al., 2011). Moreover, it has been shown that BNIP3 does not affect the mitochondrial number but instead BNIP3 reduces both nuclear- and mitochondria-encoded proteins involved in oxidative metabolism (Thomas et al., 2011).

1.10 Carbonic anhydrase IX

The high rate of glycolysis of cancer cells leads to the production and export of acidic metabolites such as lactic acid and carbonic acids to the extracellular space. This creates an acidic extracellular microenvironment and provide a selective advantage for tumour cells that can survive these harsh conditions (McDonald et al., 2012). The

acidic microenvironment affects the survival of non-tumour cells and also causes increased degradation of the extracellular matrix, thus promoting by this way the proliferation and invasion of acid resistant cancer cells. The tumour cells that are resistant to acid microenvironment are able to survive by maintaining their intracellular pH (pHi) within physiological limits by extruding lactate and protons.

The maintenance of pH homeostasis is regulated by various proteins and buffer systems that ensures the preservation of an alkaline intracellular pH (pHi), and the generation of an extracellular environment (Neri and Supuran, 2011; Parks et al., 2011). Carbonic anhydrases (CAs) are a family of 16 distinct, but related, zinc metalloenzymes that catalyse the reversible conversion of CO_2 to bicarbonate and protons. They are key pH regulators but they are also involved in the regulation of respiration, bone restoration and calcification, and biosynthetic processes (Supuran, 2008). The CA that has been most strongly associated with cancer, and thus most widely studied is CAIX (Neri and Supuran, 2011; Opavsky et al., 1996).

1.10.1 Identification and Structure of CAIX

CAIX was initially identified as a transmembrane protein of the cervival carcinoma human cell line, HeLa, and was initially named MN (Opavsky et al., 1996). The initial studies showed that confluent cultures as well as cells infected with the MaTu quasi-viral agent, which is derived from a human mammary tumour, were expressing the MN protein. MaTu was found to be a two-component system, having an exogenous transmissible component, MX, and an endogenous cellular component, MN. Using monoclonal antibodies it was shown that MN formed a twin band of 54 and 58 kiloDaltons (kDa), and associated with virions of vesicular stomatitis virus reproduced in MaTu infected HeLa cells. The MX was found to be the 58 kDa protein

that turned out to be a nucleoprotein of lymphocytic choriomeningitis virus (Reiserova et al., 1999). Sequence analysis of the MN cDNA identified the presence of a 257 AA long extracellular carbonic anhydrase domain. Due to its homology with CAs and the fact that it was the ninth CA to be identified by that time, the MN was renamed as CAIX (Opavsky et al., 1996; Pastorek et al., 1994).

CAIX is a dimeric protein and one of the most active CAs for the CO_2 hydration reaction (De Simone and Supuran, 2010; Hilvo et al., 2008). The extracellular domain contains a single peptide (SP), a proteoglycan (PG) –like domain and catalytic domain (De Simone and Supuran, 2010; Innocenti et al., 2009). Its catalytic domain is responsible for the efficient function of CAIX at acidic pH values (De Simone and Supuran, 2010; Innocenti et al., 2009). An N-terminal extracellular part links the transmembrane TM region to the C-terminal intracellular tail (IC), which is involved in regulation of CAIX's enzymatic activity (Ditte et al., 2011). The CAIX mRNA is processed into two transmembrane proteins of 54kDa and 58kDa. However, the functional consequences of this remain unclear. Interestingly the IC domain of the CAIX contains three putative phosphorylation sites (Thr433, Ser448, and Tyr448). In line with this, previous studies have shown that the epidermal factor dependent phosphorylation of Tyr448 is implicated in signal transduction via PI3K/Akt pathway (Morgan et al., 2007). The full-length protein has not been crystallised, however the crystal structure of the catalytic domain has been solved recently (Alterio et al., 2009).

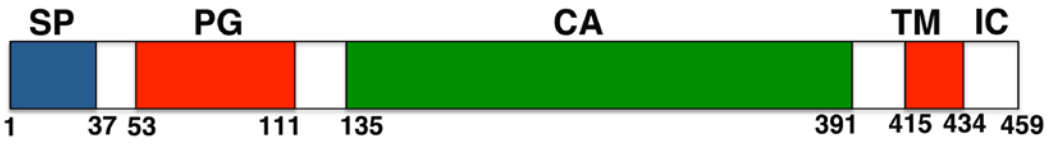


Figure 1.4 Domain composition of CAIX protein. Amino acid positions indicate boundaries of domains. SP, signal peptide; PG proteoglycan–like domain; CA, carbonic anhydrase domain; TM, transmembrane anchor; IC, intracellular tail.

1.10.2 Regulation of CAIX

CAIX is strongly induced by HIF-1 under hypoxic conditions, whereas its expression in normoxia is very low. The only cells expressing CAIX under normoxic conditions are those with a mutant or epigenetically silenced *von Hippel-Lindau* gene. The CAIX promoter contains a hypoxia responsive element that is located immediately upstream of the transcription start site (-3-10) where HIF-1α binds (Kaluz et al., 2009b). This is also the most critical regulatory element within the CAIX promoter. Accordingly, mutations within the HRE site inactivate the CAIX promoter and also, no promoter activity was observed in HIF-1α deficient cells (Kaluz et al., 2009b). Thus, HIF-1α is a key regulator of CAIX expression and CAIX is the most strongly upregulated gene in response to hypoxia.

Additionally, the CAIX promoter also contains transcription factor binding sites that appear to coordinate with the HRE to promote or amplify the HIF-1 response. Five transcription factor binding sites have been identified, which are called protective regions (PR1-5) (Kaluzova et al., 2001). The PR4 has been shown to repress CAIX's transcriptional activity, whereas the remaining four PRs are positive cis elements (Kaluz et al., 2009b). At the PR1/PR5 the binding factors SP1/SP3 are binding and

their constitutive binding to PR1/PR5 together with the HIF-1α activity is crucial for CAIX transcription. In line with this, it has been shown that treatment with mithramycin, an inhibitor of SP1/SP3 binding, effectively prevents CAIX expression (Kaluz et al., 1999; Kaluzova et al., 2001) The PR2 (-71-56) was identified as a AP1-binding site (Kaluz et al., 1999). Hypoxic induction of AP-1 is facilitated by the extracellular signal-regulated (ERK) and Jun N-terminal kinase/stress-activated protein kinases of the MAP kinase family and the phosphatidylinositol 3-kinase (PI3-K) pathway (Kaluz et al., 1999; Kaluzova et al., 2001). Therefore, the activation of AP-1 *via* these signaling pathways and its binding to the PR2 intensify the transcription level of CAIX. The functional importance of PR3 is not yet well understood but it has been suggested to bind proteins from nuclear extracts (Kaluz et al., 1999). Moreover, deletion and/or mutations within the negative regulatory element PR4 result in an increased activity of CAIX promoter, conferring its role as repressor of CAIX's transcriptional activity (Kaluz et al., 2009b). However, the presumed repressor protein binding PR4 has not been yet identified.

Acidification of glioblastoma cells growth media under normoxia results in an increased activity of CAIX promoter and an upregulation of CAIX expression. It was suggested that this upregulation is due to HIF-1 stabilization and activation of ERK kinase (Ihnatko et al., 2006). However, subsequent studies showed that acidification of the extracellular pH did not increase CAIX expression in HeLa cells suggesting that this effect could be cell type specific (Rafajova et al., 2004).

In high cell density cultures there is a pericellular hypoxia, which is associated with the activation of various signaling pathway, and especially PI3K pathway (Kaluz et al., 2002; Zavada et al., 1993). In line with this, it has been shown that the PI3K

pathway is activated in most cells grown in confluent cultures (Kaluz et al., 2002; Zavada et al., 1993). Additionally, treatment with PI3K inhibitors caused reduction of the cell density and induced CAIX expression (Kaluz et al., 2002; Kopacek et al., 2005). Interestingly, activation of the PI3K pathway in confluent cultures did not induce HIF-1α but in contrast, it was shown that the upregulation of CAIX in high cell density culture was due to the activation of HIF-1α by PI3K. Therefore, it was suggested that CAIX expression is driven solely by the increased transcriptional activity of HIF-1α, which could be due to combination of mild hypoxia and activation of PI3K, without apparent stabilization of HIF-1α.

Beside PI3K activation in dense cell culture, it has been observed that RAS-MAPK signaling pathway is also induced under this condition, and it is required for the cell density mediated HIF-1 induction of HRE activity (Kaluz et al., 2006; Kopacek et al., 2005). In support of this, it has been observed that HIF-1α protein is upregulated in high cell density cultures of LNCaP, a human prostate cancer cell line (Sheta et al., 2001). This upregulation was associated with an induction of HRE activity, which could be inhibited by gentle shaking, suggesting the need for an oxygen gradient. Interestingly, treatment with UO126, an inhibitor of MAP/ERK kinase causes downregulation of CAIX protein expression and promoter activity (Kaluz et al., 2006; Kopacek et al., 2005). It has been also observed that UO126 inhibits the HRE, SP1/SP3 binding to PR1, and the activity of p300, which is a transcriptional co activator of HIF-1 (Kaluz et al., 2006).

1.10.3 CAIX in tumours

CAIX is expressed in the majority of solid tumours. It is commonly upregulated in area of hypoxia in malignancies, including carcinomas of the cervix (Liao et al., 1994), the renal clear cell carcinoma (Liao et al., 1997), breast cancer (Chia et al., 2001), head and neck (Beasley et al., 2001), lung (Giatromanolaki et al., 2001) and tumours of the brain (Proescholdt et al., 2005). The expression of CAIX is also associated with poor survival in most cancers, such as breast cancer (Chia et al., 2001), non-small cell lung (Giatromanolaki et al., 2001) and head and neck (Jonathan et al., 2006).

In addition, CAIX expression has been associated with specific cancer subtypes. In support of this, it has been shown that CAIX is overexpressed in the basal-like or triple negative breast cancers, which is a breast cancer subtype associated with poor prognosis and resistance to therapies (Lou et al., 2011; Tan et al., 2009). Additionally, in lung cancer the squamous cell carcinoma subtype is associated with high CAIX expression (Ilie et al., 2010).

Furthermore, clinical studies have demonstrated that CAIX expression is correlated with metastatic disease. This is supported by recent findings showing that in breast cancer CAIX is an independent biomarker of poor prognosis for distant metastasis (Lou et al., 2011). Additionally, a high level of CAIX is associated with greater lymph node metastasis (Lee et al., 2007; Woelber et al., 2011).

1.10.4 pH regulation

It is well established that the extracellular pH (pHe) in tumours is lower (pH 6.2-6.3) compared to normal tissues (pH 7.2-7.4) (Gillies et al., 2002). This is a consequence

of the increased rate of glycolysis, an associated characteristic of tumour cells, which results in the export of acidic metabolites, such as lactic acid and carbonic acids (McDonald et al., 2012). Interestingly however, cancer cells maintain a more alkaline intracellular pH compared to non tumour cells, despite their acidic environment (Gillies et al., 2002). The regulation of intracellular pH is crucial for cancer cells in order to prevent disruption of basic cell functions such as membrane permeability, enzyme activity, cellular metabolism, ATP maintenance, cell proliferation and apoptotic mechanisms (Parks et al., 2011).

It has been shown that CAIX controls the pH dynamics by participating in the extracellular acidification and regulation of the intracellular pH (Parks et al., 2011; Swietach et al., 2010). CAIX enables the transmembrane removal of CO_2 (a weak base acid), by hydrating extracellular CO_2 to H^+ and HCO_3^-. The CAIX catalytic domain, which has one of the highest rates of catalytic activity amongst the CAs, is oriented toward the extracellular milleu and contributes to the acidification of tumour microenvironment in hypoxia (Hilvo et al., 2008). It has been shown that the proteoglycan domain of CAIX enables the hydration of CO_2 to occur at low pH levels (Innocenti et al., 2009). Additionally, the bicarbonate generated by CAIX may be subsequently transported by different bicarbonate transporters, such as sodium bicarbonate co-transporters, into cancer cells helping to neutralize the intracellular pH (Chiche et al., 2010; Lou et al., 2011). Therefore, CAIX has a dual function, first it produces and maintains an alkaline intracellular pH, which enables cells to grow and survive in acidic environments. Secondly, it participates in the acidification of tumour microenvironment, thus promoting cell invasiveness.

Supporting evidence of the role of CAIX in the regulation of intracellular pH comes from studies showing that overexpression of CAIX in Madin-Darby canine kidney (MDCK) epithelial cells decreased the pH of the culture media under hypoxia. In contrast treatment with CAIX-selective sulphonamide inhibitors reduced the medium acidity by inhibiting the catalytic activity of the enzyme (Svastova et al., 2004). Further to this, it has been shown that an acidic (6.8) pH culture medium increased the invasiveness of human melanoma cells compared to the a normal pH (7.4) medium (Martinez-Zaguilan et al., 1996). A separate study has shown that treatment with acetazolamide (ATZ), a CA inhibitor suppressed the invasiveness of renal cancer cells (Kivela et al., 2000).

1.10.5 Cell adhesion

The proteoglycan domain of CAIX has been shown to be implicated in cell adhesion (Svastova et al., 2003). In support of this, in CAIX-null MDCK cells the CAIX protein was detected in cell-cell junctions and was co localizing with E-cadherin, a key adhesion molecule (Svastova et al., 2003). Interestingly, reoxygenation of hypoxia cultured cells caused relocalization of CAIX and E-cadherin from the membrane to the cytoplasm, and this reversed again upon re-exposure to hypoxia (McDonald et al., 2012; Svastova et al., 2003). Moreover, overexpression of CAIX in MDCK cells reduced cell-cell adhesion, by reducing the binding of E-cadherin to β-catenin (Svastova et al., 2003). β-Catenin plays a role in the formation of adherent junctions between epithelial cells by connecting E-cadherin to α-catenin and thereby to the cytoskeleton (Svastova et al., 2003). It was suggested that, CAIX might modulate E-cadherin-mediated cell adhesion by competing with E-cadherin for binding to β-catenin (Svastova et al., 2003). Moreover, gene expression profiling of

cervical carcinoma cells overexpressing exogenous human CAIX identified that the gene signature of these cells was enriched for pathways associated with cell growth, cell adhesion and cytoskeletal organization (Shin et al., 2011). Additionally, they displayed a weakened cell-cell adhesion and an increased cell motility as well as an increased EMT (Shin et al., 2011).

A soluble form of CAIX was detected in the tissue culture medium of CAIX expressing cells, and in the blood and urine of RCC patients (Zavada et al., 2003). This form of CAIX has a shorter extracellular domain compared to the cell associated protein (Zavada et al., 2003). It has been suggested that this is a result of proteolytic cleavage of the extracellular domain mediated by matrix metalloproteinase dependent process (Zatovicova et al., 2005).

1.10.6 Cell proliferation

Several studies have shown that CAIX plays a role in cell proliferation and inhibition of its expression results in reduction in tumour growth (Cianchi et al., 2010; Dubois et al., 2011; Morris et al., 2011). Accordingly, the hypoxia-induced expression of CAIX is essential for the regulation of tumour growth in breast and colon cancer xenografts (Chiche et al., 2009; Lou et al., 2011). In line with this, our laboratory has shown that overexpression of CAIX in HCT116 colon cancer cell line increased xenograft tumour growth, whereas CAIX knockdown in the colon cancer cell line HT29 reduced xenograft tumour growth (McIntyre et al., 2012). CAIX expression also increased the protein levels of Ki67, a marker of cell proliferation (McIntyre et al., 2012). Furthermore, treatment with TR1 and GA15, which are two newly synthesized aromatic sulfonamides with high inhibitory affinity of CAIX, caused reduction of cell proliferation and induction of apoptosis in CAIX-positive HeLa and 786-O cells

(Cianchi et al., 2010). Similar results were observed with the treatment of S-glycosides that are small molecule inhibitors of CAIX (Morris et al., 2011).

Although CAIX is overexpressed in most solid tumours, in normal tissues its expression is very restricted. In the intestine, CAIX is limited to the epithelial cells at the bottom of the crypts of Lieberkuhn (Saarnio et al., 1998). The cells within the crypts of Lieberkuhn are characterized by a high proliferate rate, which further supports the role of CAIX in cell proliferation (Saarnio et al., 1998). Additionally CAIX expression has been detected during mice embryogenesis. Its expression is evident by days E11.5-E12.5 and CAIX is detected in high levels in the brain, lung, liver and pancreas, whereas kidney and stomach cells express low levels of CAIX (Hilvo et al., 2004; Kallio et al., 2006).

1.11 Inhibition of CAIX as therapeutic target

Given its important function in tumour progression CAIX is a promising target for anticancer therapy. This is further underscored by its highly restricted expression in normal tissues providing a wider therapeutic window. Two major therapeutic approaches are currently under development as pharmacological inhibitors of CAIX for cancer therapy, this includes a monoclonal antibody and small molecule inhibitors.

1.11.1 Monoclonal antibody therapy

The transmembrane localisation of CAIX is advantageous for development of specific CAIX monoclonal antibodies (mAb). These monoclonal antibodies can target CAIX through three main mechanisms. First, the direct binding of mAb to CAIX can activate an effector cell of the immune system to lyse the target cell, a process that is called antibody-mediated cell cytotoxicity (ADCC). Secondly, coupling the CAIX

specific mAb to cytotoxins and radionuclides permits greater control of drug pharmacokinetics and significantly improves drug delivery. Lastly, mAb that specifically inhibits the active site of CAIX can block CAIX function (McDonald et al., 2012).

Currently there have been developed two CAIX specific antibodies, M75 (Zavada et al., 1993) and G250 (Oosterwijk et al., 1986). M75 recognizes the PG-like domain of the CAIX, and currently it is the only one used for immunodetection of CAIX in human tissue and cancer cell lines. A derivative of the M75 has been developed for imaging CAIX in hypoxic tumours preclinically (Chrastina et al., 2003a; Chrastina et al., 2003b).

The monoclonal antibody G250 (mAb G250) recognizes a determinant on CAIX. A chimeric (murine Fv and human Fc) form of G250, necessary to reduce the immunogenicity, has been constructed and used as an anticancer immunotherapy agent (Surfus et al., 1996). G250 exerts its anticancer effects by antibody-mediated cell cytotoxicity or complement-dependent cytotoxicity (Surfus et al., 1996). Its antitumoural activity can be improved by modification to a bispecific antibody and combination with cytokine therapy. Phase I and II clinical trials have been completed and demonstrated that cG250 is safe, with low toxicity and increased survival either alone or in combination with interferon treatment (IFN-α) (Davis et al., 2007; Siebels et al., 2011). A phase III clinical trial, named ARISER is currently ongoing to test the efficacy of cG250 antibody as an adjuvant therapy in combination with interleukin 2 or IFN-α in RCC surgically-treated renal cell carcinoma (RCC) patients and metastasic RCC (Siebels et al., 2011).

Development of CAIX monoclonal antibodies that target its catalytic domain are underway. These mAb are aiming to target CAIX's functions such as pH regulation, which have been shown to be important for cancer progression. Phage display libraries have identified CAIX antibodies and epitopes of some of those have been mapped to the catalytic site. Currently these antibodies have been tested only in *in vitro* experimemts (Ahlskog et al., 2009b). These experiments have shown that treatment with the mAb resulted in CAIX inhibition in cell cultures and spheroid models. Additionally, a separate mAb also targeting the catalytic domain of CAIX has been generated using hydridoma technology (Zatovicova et al., 2010). This mAb has been tested *in vitro* and it shows promising results only when the treatment starts before the establishment of tumour (Zatovicova et al., 2010). Recently, a CAIX mAb has been coupled to monomethyl auristatin E (MMAE) and its effect was tested in various *in vitro* tumour models. The results showed that this possesses a potent antitumour efficacy and in some models led to partial or even complete tumour shrinkage following a single dose treatment (Petrul et al., 2012).

1.11.2 CAIX small molecules inhibitors

Targeting the function of CAIX with small molecule inhibitors is another therapeutic option. The first molecules used for CAIX inhibition were based on acetazolamide conjugated with albumin binding moieties or charged fluorophores (Ahlskog et al., 2009a). These inhibitors bind directly to the Zn(II) ion within the active site. *In vitro* experiments showed that treatement with these inhibitors was sufficient to cause reduction in tumour growth rate (Ahlskog et al., 2009). Currently the best described small molecule inhibitor of CAIX is FITC labelled fluorescent sulphonamide (Supuran, 2008). This inhibitor binds the extracellular CAs with great affinity

(Supuran, 2008). Additionally, *in vitro* experiments showed that it binds specifically to the active CAIX in hypoxia and inhibits the CAIX-mediated acidification of extracellular microenviroment (Dubois et al., 2007; Lou et al., 2011). TR1 and GA15, two aromatic sulfonamides have also been reported to inhibit CAIX function, and their use resulted in the reduction of intracellular pH as well as reduction in cell proliferation only in CAIX posistive cells, but not in the CAIX negative population (Cianchi et al., 2010). More recently, another molecule called indanesulfonamide has been demonstrated to inhibit CAIX (Dubois et al., 2011), and treatment with this inhibitor resulted in reduced tumour growth. Its anti-tumoural effect was further increased when it was used in combination with radiotherapy (Dubois et al., 2011). Interestingly, it has been observed that the sulfonamide and coumarin inhibitors of CAIX can cause reduction of metastasis. Supportive evidences of this come from findings from two separate studies showing that the treatment of experimental models of breast cancer metastasis with novel ureido sulfonamides resulted in a significant decrease in lung metastases (Lou et al., 2011; Touisni et al., 2011).

1.12 Aims

1. To investigate CAIX heterogeneity in cancer cell lines and to examine if the hypoxia response in a cell population is uniform.
2. To investigate the differential gene expression profiles and pathways of the two CAIX subpopulations with a particular interest in stem cell phenotype and drug resistance.
3. To investigate the in vivo properties of the two CAIX subpopulations.
4. To investigate the biological mechanisms for the differential CAIX expression.

Chapter Two

Materials and Methods

2.1Cell Culture

Cell were grown in a tissue culture incubator in a humidified atmosphere of 5% CO_2 and 95% filtered atmospheric air, and maintained at a temperature of 37 ° C, unless otherwise indicated. Cells were passaged by aspirating medium, washing the cells with PBS, and then adding 1 x trypsin-EDTA (Invitrogen) until they detached. The trypsin was neutralized by adding equal amount of DMEM supplemented with 10% (v/v) FBS. The cells then were centrifuged for 5 minutes at 1000 rpm to generate a pellet from which the supernatant was aspirated. The pellet was then split 1:10 and reseeded. This process was carried out every 6-7 days. Cells were cultured on sterile, tissue culture grade, non-pyrogenic plasticware (Corning). Cells were treated with the HDAC inhibitor SAHA (Sigma) at 2 μM for 72h, and sodium butyrate (NaBu) (Sigma) at 5 mM for 72h. The demethylating agent 5-aza-2′-deoxycytidine (5-aza-dC) (Sigma) was used at 10 μM for 72h. The mTOR inhibitor, Rapamycin (Sigma-Aldrich) was used at 20 μM for 72h.

2.2Hypoxic Incubators

Hypoxic incubations (0.1% O_2, 5% CO_2,) were performed using an INVIVO$_2$ 400 hypoxic workstation (Pro-Lab Diagnostics). All cells were allowed 6 hours to attach and recover after being plated in final densities before being exposed to hypoxia.

2.3Cell Lines

MCF-7, MDA-MB-231 and SW1222 cells were maintained in DMEM supplemented with 10% (v/v) FBS, penicillin (100 U/ml), streptomycin (100mg/ml) (Life Technologies). HCT116 were maintained in McCoys 5A supplemented with 10% (v/v) FBS, penicillin (100 U/ml), streptomycin (100mg/ml) (Life Technologies). The

medium was changed every two to three days. All cell lines were obtained from Cancer Research UK Cell Production Laboratories (Clare Hall, Hertfoshire, UK). All cells were free from mycoplasma contamination. All media obtained from Cancer Research UK Central Services (Clare Hall, Hertfordshire, UK).

2.4 Counting Cells

Where a specific number of cells were required for an experiment they were detached, centrifuged, and resuspended, in an appropriate volume of medium. Cells then were counted using the Coulter Particle Counter Z2 (Beckman Coutler) according to maufacturer's instructions. Briefly, 400 μL of cell suspension were diluted with 19.6 μL of isoton buffer and a particle count take in the range of 9-27 μM. The machine was calibrated to calculate the number of cells/ ml

2.5 Preparation and Recovery of cell stocks (cryo-preserved cells)

Only cells in the log phase of growth were used for cryopreservation. Cells were detached as described previously. The cell pellet was then resuspended in freezing medium and divided between rounded bottomed cryo-vials (Corning). Freezing medium was prepared with dimethylsulphoxide (DMSO), foetal calf serum (FCS), and culture medium at a ratio of 1:3:6, respectively. Vials were frozen down to 1° C per minute to -80 ° C in an isopropanol-bath freezing container (MrFrosty;Nalgene). Within one week, cell vials were transferred to liquid nitrogen for long term storage. To recover the cells from storage, cryovials were rapidly defrosted to 37 °C and transferred to pre-warmed media.

2.6 Gene silencing by RNA Interference

Cells were plated on 10cm^2 dishes at 8 x 10^5 per dish and left overnight to adhere. siRNA duplexes were transfected into cells at 20nM using Oligofectamine^{TM} and then cultured in Optimen^{TM} for 4 hours prior to the addition of serum for overnight recovery (8mL siRNA, 120mL Oligofectamine^{TM}, 7.872 mL Optimem^{TM}, 2 mL FCS). Next day, the cells were reseeded as appropriate.

Transfections of siRNA duplexes targeting CAIX or a scrambled control (scr) (ON-TARGETplus SMARTpool) at a final concentration of 20 nM, were performed in Optimem (Invitrogen), using Oligofectamine reagent (Invitrogen). The sequences of siRNA used to target CAIX were 118898, 9567 and 9473 (Invitrogen). Reduction in CAIX protein expression, measured by Western blot analysis, was used to indicate gene silencing.

2.7 Spheroid culture

Aggregation of cells into spheroids was initiated by plating 4 x 10^6 cells containing 250 mL of standard growth medium in 1 L spinner flask (Techne MCS, UK) and spinning at 40 rpm for 7d. HCT116 spheroids were treated with 5mM sodium butyrate (5mM) for 3d. MCF-7 spheroids were generated following the method described by Ivascu *et. al* (Ivascu and Kubbies, 2007). Briefly, 200 μL of a 2.5x10^4/mL cell suspension was added to each well of a round bottom 96-well plate. For MCF-7 cells, Matrigel (BD Biosciences) was added at a final concentration of 2.5%. Plates were centrifuged at 1000 x g for 10 min and then incubated under standard cell culture conditions. Microscope pictures were taken with an inverted light microscope (Axiovert) and volumes were measured at day 7. After the final time

point, the spheroids were fixed in formalin, embedded in wax, and sliced and mounted onto slides for immunohistochemical analysis.

2.8 Embedding and Processing of spheroids

HCT116 and MCF7 spheroids harvested either from spinning flasks or from 96-well plates were placed into a 15 ml conical tube and allowed to rest in the bottom by gravity. The medium was carefully aspirated. The spheroids then were fixed in formalin (VWR International) overnight. Next day the spheroids were embedded into agarose –formalin gel and placed in a pre-labelled tissue cassette. The sealed cassete was processed through an automatic tissue processor for paraffin infiltration of tissues in the Histopathology Laboratory at the John Radcliffe Hospital, Oxford. Following processing the paraffin-infiltrated lens was embedded into a paraffin block. Four micrometre sections were cut by H. Turley using Leica RM2135 microtome and adhered onto slides. The sections were racked and air-dried.

2.9 Immunostaining of paraffin – embedded tissue sections

Staining of formalin-fixed paraffin-embedded spheroids for Pimonidazole and CAIX was performed according to the following description. Slides were heated at 65 ° C for 10 min to melt the wax and help the sections adhere. They were then dewaxed and immersed in Citroclear (HD, Supplies, UK) for 5 min twice and rehydrated in graded in graded Industrial Methylated Spirit solutions (100% twice followed by 50% once for 5min in each) before rinsing in tap water followed by a PBS wash. Antigen retrieval was performed in a decloaking chamber (Biocare Medical, USA) set at 2min, high pressure, in EDTA pH 8.0 buffer for pimonidazole and Tris EDTA pH 9.0 buffer for CAIX. After cooling slides were placed in PBS. To minimize non specific antibody binding, the slides were blocked with 10% normal horse serum (Vector

Laboratories, UK). In the next step, primary antibody was applied to the slides and incubated at room temperature for 1 hour. Both antibodies were diluted in RPM1 (Lonza) with 10% bovine serum (Sigma-Aldrich). After 1 hour incubation, the slides were washed three times with PBS, and then they were incubated with the anti-mouse secondary antibody for 50 minutes at room temperature. The slides were then washed with PBS for three times, and DAB was applied to the sections for 5-8 min. The reaction was stopped by washing the slides with tap water. In the final step the slides were counterstained and immersed in heamatoxylin solution (Gill No3) for 20 s, rinsed in tap water and mounted with Aquamount. Slides were visualized on a BX51 microscope (Olympus) attached to a DP70 digital camera (Olympus) and images were captured using the DP manager and DP Contoller software (Olympus).

Table 2.4 Immunostaining Antibodies

Antibody	Antibody name/catalogue number	Species	Clonality	Source	Primary antibody dilution
CAIX	M75	Mouse	Monoclonal	Gift from J.Pastorek , Institute of Virology, Batislava, Slovak Republic	1:50
Hypoxy-prode-1 (pimonidazole)	HP1-1000	Mouse	Monoclonal	Chemicon International, USA	1:50

2.10 Generation of Mammospheres

MCF-7 cells were detached, washed and plated in a 6 well low attachment plate (Corning), filled with 3mL MammoCult Basal Medium and supplemented with MammoCult proliferation Supplements, 4 μg/mL Heparin, 0.48 μg/mL Hydrocortisol and penicillin (100 U/mL), streptomycin (100mg/mL). MCF-7 mammospheres started forming after day 4-6 and were processed at day 10. Secondary generation mammospheres were generated by incubating the primary mammospheres with 1 X Trypsin EDTA solution (PAA Laboratories) for 2-3 min and resuspended in the above

medium and plated again in the low attachment plates. After 7 days the capacity of cells to generate secondary mammospheres were tested by visualizing the cells with the inverted light microscope (Axiovert).

2.11 Soft Agar Assay for Colony Formation

Each well of a six well plate (Corning) was covered with 0.6% noble agar (Sigma). Cells were detached and 10^3 cells mixed with 0.3% noble agar were plated in each well. Cells were incubated for 3 weeks and fed every 2 weeks. Colonies were stained with 0.005% crystal violet for 1h. Stained colonies were counted using Image J software.

2.12 Clonogenic Assay

CAIX+ve and CAIX-ve cells were seeded at a density of 10^3 cells per 6 cm dish in triplicates and treated with 2 μM SAHA for 72h under hypoxic conditions, untreated control cells were also included in the experiment. After 72h the dishes incubated in hypoxia (0.1 % O_2) were returned to normoxia for 10 days, washed three times with fresh medium and allowed to form colonies. Cell colonies were washed with PBS and fixed and stained with Coomassie blue for 1 h. The dishes were washed with distilled water and allowed to air dry. Visible colonies were counted using a ColCount automated colony counter (Optronix).

2.13 Chromatin analysis of CAIX using Epiq Chromatin Analysis kit

The quantitative assessment of chromatin states of CAIX+ve and CAIX-ve cells was performed using the Epiq Chromatin analysis kit according to the manufacturer's instructions (BioRad). Accordingly, the CAIX+ve cell line and CAIX-ve cell line

were plated in 48 well culture plate to 80-95% confluent and exposed for 72hrs in 0.1% O_2 or they were maintained under normoxic conditions. Three wells remained undigested and the other 3 wells were digested with 2□l of DNase nuclease I for 1 hour at 37°C. After 1 hour the 25ml of Epiq stop buffer was added to each well followed by 10 minutes incubation at 37 °C. Cell lysates were then transferred to 1.5 ml tube and 375□l of DNA lysis solution was added in each sample. Samples were mixed and centrifuged for 5 seconds. In each sample 100 □l of 100% ethanol was added to each tube. Following extraction and purification of DNA, samples were transferred to mini column and spun for 1minute at 12,000rpm for 1min. The flowthrough was discarded and 650 □l of DNA low stringency wash solution was added in each sample. Cells were spun for 1 minute at 12,000 rpm. The flowthrough was discarded and 650 □l of DNA high stringency wash solution was added to each sample. Cells were spun for 1 minute at 12,000 rpm. The flowthrough was discarded and 650 □l of DNA low stringency wash solution was added again to each sample. Cells were spun for 1 minute at 12,000 rpm. The flowthrough was discarded and the cells were spun for 3 minutes at 12,0000 rpm. Each column was transferred into a new capped tube. At the end, 52 □l of DNA elution solution was added to each sample and cells were spun for 2 minutes at 12,000rpm. This step was repeated twice and both elutions were collected. DNA was quantified using the nanodrop and each sample was diluted to 1ng/ml. The nuclease sensitivity was assessed by qPCR (with primers as shown in Table 2.1). The data were analysed using EpiQ Chromatin Kit Data Analysis Tool (www.bio-rad.com/epiq) and normalized against the *RHO* (Rhodopsin) gene in the undigested sample as a negative reference. The GAPDH region was used as a positive reference gene region for an open chromatin.

2.14 Chromatin immunoprecipitation assay for HIF-1 beta

2.14.1 Day One

Immunoprecipitation assays for HIF-1β were performed using the Upstate EZ ChIP Kit Reagents and chromatin immunoprecipitation (ChIP) assay. 10^6 CAIX+ve and CAIX-ve cells were exposed to hypoxia for 72h or grown to normoxia. After 72 h cells were cross-linked with formaldehyde (final concentration of 1%) and then unreached formaldehyde was quenched using 125 mM glycine for 10 minutes on ice. After extensive PBS washing, the cells were lysed with 1mL of 1% SDS lysis buffer in the presence of a protease inhibitor cocktail. The cells then were sonicated in 15s on/off pulses for a total of 15 min (Diagenode Bioruptor water bath sonicator). In each IP 60 µl Protein G Agarose beads were added followed by 1h incubation at 4°C with rotation. The agarose beads were spun for 1minute and 10 µl of the supernatant was kept as input control. The rest of the supernatant was collected and was dispensed in 1mL aliquots into fresh microfuge tubes. Immunoprecipitating antibodies were added to the supernatant fraction. For positive control, 10 µl of ant-RNA Polymerase (Upstate) antibody per sample was added, for negative control 10 µl of Normal Mouse IgG per tube were added and 10 µl of the rabbit polyclonal antisera to HIF-1β (Novus NB-100-110) were added and incubated overnight at 4C with rotation.

2.14.2 Second Day

Next day, 60 µl of Protein Agarose was added to each IP 60 µl followed by 1 h incubation at 4°C with rotation. This helps to collect the antibody/antigen/DNA complex. The tubes were spun for 1 minute at 5000 x g and the supernatant fraction was collected. The Protein G Agarose- antibody/chromatin complexes were washed by adding 1 mL of the cold buffers in the order listed below and incubating for 3-5

minutes on a rotating platform followed by brief centrifugation (5000 x g for 1 minute): 1) Low Salt Immune Complex Wash Buffer, 2) High Salt Immune Complex Wash Buffer 3) LiCl Immune Complex Wash Buffer 4) TE Buffer. After the washes, in each IP tube was added 100 μl of Elution Buffer followed by 15 minutes incubation at room temperature. The tubes then were spun at 5,000 x g for 1 minute and the supernatant was collected into new centrifuged tubes. This was repeated twice and the eluates were combined. The next step involved the crosslinking of Protein/DNA complexes in order to free DNA. For this reason 8 μl of 5M NaCl was added to each IP and incubated overnight at 65° C.

2.14.3 Third Day

Next day 1 μl of RNase A was added to all tubes and incubated for 37 °C for 30 minutes. After 30 minutes 4μl 0.5M EDTA, 8μl of 1M Tris-HCl, and 1 μl Proteinase K was added in each tube 4μl 0.5M EDTA, 8μl of 1M Tris-HCl, and 1 μl Proteinase K followed by 2 hours incubation. The next step involved the purification of DNA using spin Columns. To each IP and input tubes, which were collected at day one, was added 1ml of bind reagent A. The mixture was transferred then to spin filter collection tube and spun for 30 seconds at 13,000 rpm. The flowthrough was discarded and 500 μl of Wash Reagent B was added to each spin filter collection tube. The tubes then were centrifuged for 30 seconds at 13, 000 rpm. The flowthrough was discarded and the spin filter was placed in a new clean collection tube. Then 50 μl of Elution Buffer was added to each tube followed by spin of the tubes for 30 seconds at 13,000 rpm. DNA isolated from ChIP was quantified by qPCR. The *CA9* promoter primers used are listed in **Table 2.1**. The data was normalized against promoter sequence of the housekeeping gene UBC gene.

2.15 Chromatin immunoprecipitation assay for trimethylated H3K9

Immunoprecipitation assays for for trimethylated H3K9 was done using the EpiQuik Tri-Methyl-Histone H3K9 ChIP Kit (Epigentek, Brooklyn, NY) according to manufacturer's instructions. 10^6 CAIX+ve and CAIX-ve cells were exposed to hypoxia for 72h or grown to normoxia. After 72 h, cells were cross-linked with formaldehyde (final concentration of 1%) and then untreated formaldehyde was quenched using 125 mM glycine for 10 minutes on ice. After extensive PBS washing, the cells were lysed with 1mL of 1% SDS lysis buffer in the presence of a protease inhibitor cocktail. The cells then were sonicated in 15s on/off pulses for a total of 15 min (Diagenode Bioruptor water bath sonicator). In order to remove cell dedris, cells were spun for 10 minutes at 14,000 rpm. The supernatant then was then transferred to a new 1.5 ml vial and it was diluted by adding equal volume of CP4. Then 5 μL of diluted supernatant was removed and stored as input DNA. Next 100 μL of the rest of the diluted supernatant was transferred to microwell immobilized with the antibody, followed by an hour incubation on a rocking platform. After an hour supernatant was removed, and the wells were washed six times with 150 μL of CP1 wash buffer and once with 1x TE buffer. The next step involved the crosslinking of Protein/DNA complexes in order to free DNA. For this reason 1 μL of Proteinase K was added to each 40 μL of CP5 DNA Release buffer and then the mix were added to each well and to the input DNA vials and they were then incubated for 15 minutes at 65 °C. After 15 minutes 40 μL of CP6 Reverse buffer was added to all wells and all input DNA vials and incubated for 90 minutes at 65 °C. After this step the DNA was

purified. For this reason, 150 μL of CP7 Binding buffer was added to each well and input DNA vial and the contents of the wells and the input vials were transferred to a spin filter column and spun for 20 seconds at 12, 000 rpm. Then it was added 70 % of ethanol to each filter column and spun for 15 seconds at 12,000 rpm. After the centrifugation, the flowthrough was discarded. 90% of Ethanol was added to each column and spun for 20 seconds at 12,000 rpm. This was followed by the addition of another 90% of ethanol to each column and then they spun for 35 seconds at 12, 000 rpm. To elute the DNA, the spin column was transferred to a new and clean collection tube and 20 μL of CP8 Elution buffer was added to each well. The *CA9* promoter primers used are listed in **Table 2.2.** The data were normalized against the promoter sequence of the housekeeping gene UBC gene.

2.16 Immunoblotting

2.16.1Protein Extraction

Cells were washed in ice cold PBS and lysed in 2 x sample buffer (125mmol/L Tris [pH 6.8], 4% sodium dodecyl sulfate, 0.01% bromophenol blue, 10% β-mercaptoethanol, 10% glycerol).

2.16.2 Protein Polyacrylamide Electrophoresis

The required volume of 6x SDS-PAGE sample buffer (72mM Tris pH 6.8, 20% glycerol, 4.5 % SDS, 10% β-mercaptoethanol and 0.015% bromophenol blue) was added and samples were heated to 95 °C for 10 minutes. Whole cell lysates were resolved on SDS-PAGE followed by electroblotting onto polyvinylidene difluoride membrane (Millipore).

2.16.3 Antibody Incubation

Membranes were incubated overnight with an appropriate concentration of primary antibody in PBS containing 5% milk powder and 0.1% Tween-20. Membranes were incubated with Horseradish peroxidase – conjugated anti-rabbit or anti-mouse antibodies (DAKO Inc). Immunoreactivity was detected using CL system (Amersham Biosciences). The following antibodies were used, mouse anti-HIF-1α, (BD Transduction Laboratories, USA), mouse anti-CAIX (Gift from J. Pastrorek, Institute of Virology, Slovak Republic), goat anti-LDHA (Santa-Cruz), goat anti-PDK1 (Santa-Cruz), goat anti-AK4 (Santa-Cruz), mouse anti-ALDH (BD Biosciences), mouse anti- β actin (Sigma), rabbit anti-ULK1 (Cell Signaling), rabbit anti-pS6K$^{SER235/236}$ (Cell Signaling), anti-rabbit 4E-BP1 (Cell Signaling), anti-mouse CHOP/GADD153 (santa-cruz). Blots were quantified with image analysis in Image J.

2.17 Real-time PCR (qPCR)

2.17.1 RNA extraction and cDNA synthesis

Cells were lysed in Tri Reagent (Sigma-Aldrich), and extracted using ethanol precipitation. RNA quality and quantity were confirmed using the NanoDrop ND-1000 spectrophotometer (Wilmington). cDNA was synthesized by reverse transcribing RNA using the High Capacity cDNA Archive Kit (Applied Biosynthesis). Briefly, a 2x mastermix was prepared by adding 10 μL reverse transcription buffer, 4ml 25X dNTPs, 10 μL of 10X random primers, 5μL of reverse transcriptase and 21μL of nuclease free H_2O and was mixed with 50 μL of RNA. The reverse transcription was then performed on a thermal cycler (PTC-2000, MJ Systems) for 10 minutes at 25 followed by 120 minutes at 37 °C.

2.17.2 Real Time Quantitative PCR

Real-time PCR (qPCR) reactions were performed in biological triplicate using the Corbett Research Rotor Gene RG-300 (Sydney, Australia). Each reaction was performed in an individual tube and made up to 25 μl containing 10 μL cDNA, 12.5μL SYBRgreen PCR Master Mix (Applied Biosystems), 1 μL of forward and reverse primer and 0.2 μL H_2O. Conditions of the PCR reaction were 2 min at 50°C, 10 min at 95 °C and then 40 cycles, each containing of 15 s at 95 °C, and 1 min at 60 °C. β-Actin was used as a reference gene.

Table 5.2 The sequences of the primers used

Gene Name	Forward Primer	Reverse Primer
CA9	CTTGGAAGAAATCGCTGAGG;	TGGAAGTAGCGGCTGAAGTC
LDHA	CAGAAGGCTCGAGAAGGTATATTGCTGTTGACAGTGAGCG	CCTAAAGTAGCCCCTTGAATTCCGAGGCAGTAGGCA
PDK1	CTGGGTAATGAGGATTTGACTGT	AAGTCTGTCAATTTTCCTCAAAGG
ALDH1	CGGGAAAAGCAATCTGAAGAGGG	GATGCGGCTATACAACACTGGC
WNT2	AGGATGCCAGAGCCCTGATGAA	AGCCAGCATGTCCTGAGAGTAC
TWIST1	GCCAGGTACATCGACTTCCTCT	TCCATCCTCCAGACCGAGAAGG
LIN28	CCAGTGGATGTCTTTGTGCACC	GTGACACGGATGGATTCCAGA;
ABCC2	GCCAACTTGTGGCTGTGATAGG	ATCCAGGACTGCTGTGGGACAT
IGF1	CTCTTCAGTTCGTGTGTGGAGAC	CAGCCTCCTTAGATCACAGCTC
SOX2	GCTACAGCATGATGCAGGACCA	TCTGCGAGCTGGTCATGGAGTT
CHOP	AAGGCACTGAGGGTATCATGT	TGAAGATACACTTCCTTCTTGAACA
LDHB	AACACCTGCCACATTCACAC	GATGGATTTTGGGGGAACAT
AK4	AATGATGTCCGAGTTGGAGAA	TCGGCTTGTCCTAATGTCCT
ULK1	GCACAGAGACCGTGGGCAA	CCACGCAGGTGCAGAACTA
β-Actin	CCCAGCACAATGAAGATCAA	CGATCCACACGGAGTACTTG
CA9 HREs	GTCCATGGCCCCGATAACCTTCTG	GGGGCAACCTCTGGGGATGGAC
GAPDH	CGCACGTAGCTCAGGCCTCAAGACC	GGCTGACTGTCGAACAGGAGGAGCA
RHO	GGCTGACTGTCGAACAGGAGGAGCA	CCTTGGCCCCTCTTAGAAGCCAATT

Relative quantitation of gene expression was performed using the method described by Pfaffi (Pfaffl, 2001). In brief, comparisons were made between the number of cycles required for the fluorescence of a sample to reach a predetermined threshold

that lay within the exponential phase and above the non-specific background. The relative ration of gene expression was calculated as follows

$$\text{Relative ratio} = \frac{(Etarget)^{\Delta Ct\ TARGET(mean\ comparator - mean\ sample)}}{(Eref)^{\Delta Ct\ REF(mean\ comparator - mean\ sample)}}$$

Etarget=reaction efficiency of the gene of interest, Eref=reaction efficiency of the reference gene, ΔCt=the cycle difference between the comparator and the sample. All calculations are based on the mean value of PCRs performed in triplicate.

2.18 Flow cytometry

Cells were exposed for 72hrs in 0.1% O_2 or they were maintained under normoxic conditions and they were stained with a FITC conjugated CAIX or isotype IgG antibody (R&D systems, USA). Briefly the cells were detached washed with PBS and resuspended on ice in 100μL of PBS + 10% FBS, at a concentration of 2 x 10^6 cells. The FITC conjugated CAIX antibody or isotype IgG antibody was added and incubated for 1 hour at 4°C. Cells were washed with PBS and resuspended in PBS + 10% FBS. Samples were analyzed using a DakoCytomation Cyan machine, or sorted using a MoFlo cell sorter (Beckman Coulter). The bottom 10% of CAIX negative subpopulation and the top 10% of CAIX positive subpopulation was collected for further experiments. Analysis of the results were performed using the Summit Software. Relative fluorescence was assessed and mean fluorescence intensity was recorded. The same protocol was used for the staining of the cells with the APC conjugated CD133 antibody (Miltenyi Biotec) and APC conjugated CD44 antibody (BD Biosciences) and PE conjugated CD24 antibody (BD Biosciences).

2.19 Aldefluor Assay

To detect ALDH activity in cells, we used the ALDEFLUOR kit from Stem Cell Technologies. Briefly, cells were trypsinized and $1x10^6$ cells were taken up into 1 mL of assay buffer provided in the kit. This was the sample tube. In the negative control tube 5 μL of the DEAB solution; an inhibitor of ALDH enzyme was added. In the sample tube 5μL of the ALDEFLUOR substrate was added, mixed and then 500 μL of sample solution was transferred to the negative control tube containing the DEAB. Both sample and control tubes were incubated at 37°C for 50 minutes. Cell were resuspended in assay buffer and analyzed in the DakoCytomation Cyan machine. Control samples were used to set a gate for ALDH positivity, after which the test sample was analysed. MCF-7 cells were exposed for 72hrs in 0.1% O_2 and stained for ALDH as mentioned above.

2.20 RNA-sequencing analysis

RNA was extracted as described above. The RNA-seq was performed according to the sample preparation guide (Illumina, TruSeq RNA). TopHat (Langmead et al., 2009) was used to align RNA-Seq reads to the human genome build 37.1. Bedtools (Quinlan and Hall, 2010) was used to summarize the number of reads per exon per transcript. Threshold for transcript presence was set to 15 reads. In the low reads region there are some artificially high fold changes and a high variability, so you cannot trust the fold changes in that region are not reliable. This is the reason for filtering out low reads (in our case <15) (**Figure 2.1**). Samples were then normalized using the total number of mapped reads. Table 2.3 describes the number of unmapped and mapped reads in each dataset. The logarithm base 2 of the ratio of counts between conditions was estimated and a filter was applied to select genes with an absolute

logarithm greater than 1; this is equivalent to one fold change up- or down-regulation between conditions.

Figure 2.1 Justification of 15 reads threshold.

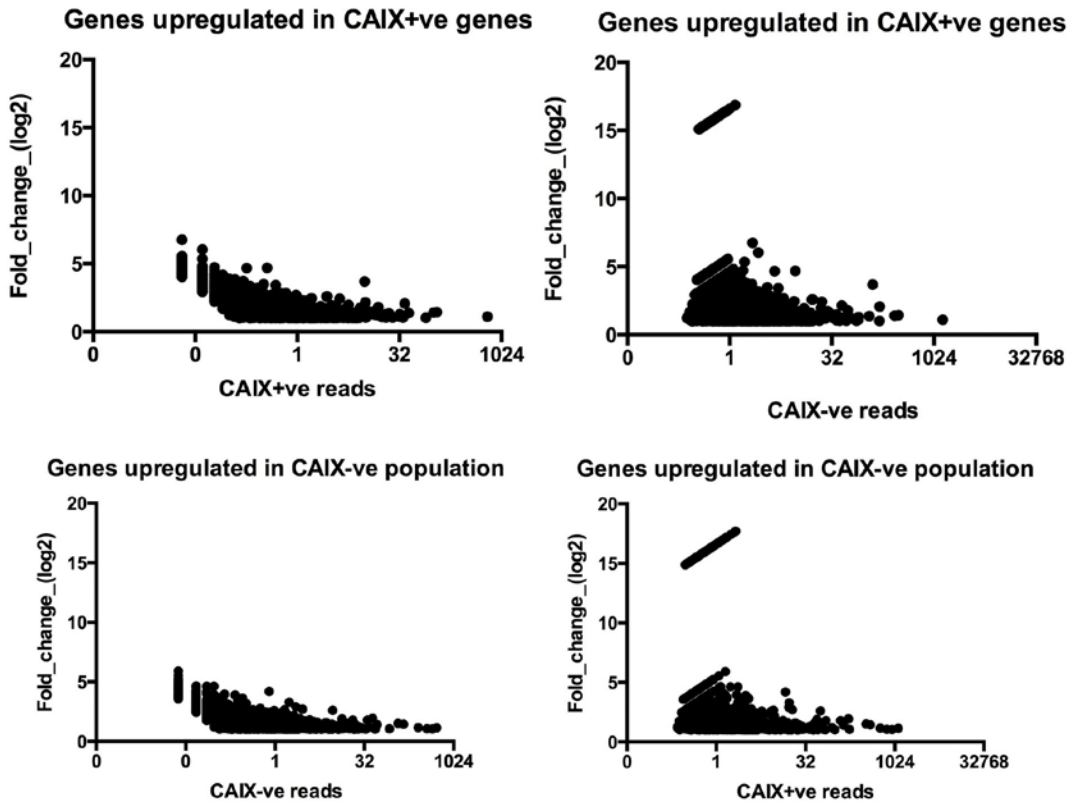


Table 2.6 Number of (un)mapped reads in each dataset

Name of populations	Mapped Reads	Total Reads
CAIX+ve population	42548582	54584512
CAIX-ve population	50139590	62659956

2.21 Microarrays analysis

Arrays, quantile normalized using the lumi Bioconductor (http://www.bioconductor.org/) package and log2 transformed. Quality control was satisfactory, specifically Illumina internal probes passed for all samples, no batch effect was observed and replicate runs showed a high correlation (r=0.98 to r=0.99). The limma and samr Bioconductor packages were used to study differential

expression. Genes with false discovery rate lower than 5% were considered significantly differentially expressed. GOStats was used for pathway analysis of significant genes.

2.21.1 Pathway Analysis

Enrichment for KEGG pathways (http://www.genome.jp/kegg/) was performed using Genecodis 2.0 (Carmona-Saez et al., 2007; Nogales-Cadenas et al., 2009); and Ingenuity® Variant Analysis™ software (www.ingenuity.com/variants) from Ingenuity Systems. Ensembl IDs (GRCh37 assembly) were used as reference, hypergeometric test was used and false discovery rate threshold was set to 0.05.

2.22 Xenograft studies

Mice were housed at BMS, University of Oxford, UK, and procedures were carried out under a Home Office licence. SW1222 cells were exposed in hypoxia for 72h and then were sorted in CAIX+ve and CAIX-ve population. 1000 CAIX+ve and CAIX-ve sorted cells and 200 CAIX+ve and CAIX-ve sorted cells were washed twice in serum-free medium prior to inoculation in mice. Six to seven-week old male NSG triple negative mice were injected subcutaneously in the lower flank with 100μL Matrigel (BD Bioscience) and cells suspended in 100μl of serum-free medium. Tumour growth was monitored three times per week measuring the length (L), width (W) and height (H) of each tumour using calipers. Volumes were calculated from the formula 1/6 x π x L x W x H. When tumours reached 1.44 cm^3 the mice were sacrificed by cervical dislocation. Ninety minutes prior to sacrifice, mice were injected intravenously with 2 μg of pimonidazole (Hypoxyprobe-1; Chemicon International, USA) as described previously (Zhang et al., 2007).

2.23 HRE Transfection

GFP tagged HRE vector (pPUR.EpoE.SV40p.GFP) was kindly provided by Peter J Ratcliffe (Oxford University, UK). HCT116 cells were transected with this vector using Lipofectamine 2000 (Invitrogen, Mo, USA) according to manufacture instructions. Cells were seeded at a density 4 x 10^5 per well of a 6-well plate. The following day the cells were 50-80% confluent and they were transfected using the Lipofectamin 2000 (Invitrogen, Mo, USA). For a transfection of 4 μg of DNA per well of a 6-well plate, 250μL of Opti-MEM Reduced Serum Medium with GlutaMAX (Invitrogen) was added to a sterile 1.5 μL microcentrifuge tube (Tube 1). Next 250μL of Opti-MEM was mixed with 10μL of Oligofectamine in a 1.5 μL microcentrifuge tube (Tube 2). Both tubes containing the complexes were incubated for 5 minutes at room temperature. Then the contents of Tube 1 were mixed with the contents of Tube 2 followed by 20 minutes incubation at room temperature. The complexes were added dropwise to the each well. A mock transfection was also included where no DNA had been added to the Opti-MEM mix. Cells were incubated overnight at 37 °C. Next day the cells were passage in 1:10 dilution, their media was changed to DMEM with 10% FBS and 1μg/mL puromycin was added to it. Cells were grown for three days in this media and only the cells which have integrated the pPUR.EpoE.SV40p.GFP vector were able to survive. FACS analysis (section) was performed to confirm GFP signal. Cells with high GFP signal were FACS sorted as described previously for better selection.

2.24 Oxygen consumption assays

60,000 MCF7 cells were plated on 96 well plates and incubated overnight at 37 ° C. The following day 10 μl MitoXpress-Xtra HS□oxygen probe was added to the

medium. The wells were sealed with mineral oil before measuring fluorescence over time with the FLUOstar OMEGA microplate reader. Data was analyzed with the OMEGA Mars data analysis tool.

2.25 Statistical analyses

Statistical analysis and graphs were performed using GraphPad Prism® v4.0 software (GraphPad). Statistics were carried out using non-paired Student's t-tests and significance is represented by * $p<0.05$, ** $p<0.01$, and *** $p<0.00$

2.26 Buffers and Solutions

For cell culture:

PBS	137mM NaCl 2.7mM KCL 4.3 mM Na_2HPO_4 1.4 mM KH_2PO_4 Ca^{2+} and Mg^{2+} free pH 7.3
Trypsin/EDTA	20 mg/ml Trypsin 1 mM ethylenediaminetetraacetic acid (EDTA) in PBS

For protein extraction from monolayer cell cultures:

Lysis Buffer	10% (v/v) glycerol 10 mM Tris-HCL pH 6.8 5mM dithiothreitol (DTT) 1% (v/v) sodium dodecyl sulphate (SDS) 6.25 M urea 1 protease inhibitor tablet (Roche Diagnostics) per 50 ml

For protein analysis:

1x running buffer	25 mM Tris 250mM glycine 0.1% (v/v) SDS
6x sample buffer	72mM Tris-HCL pH 6.8 20% (v/v) glycerol 4.5% (v/v) SDS

	10% (v/v) β-mercaptoethanol 0.015% (v/v) bromophenol blue
Transfer buffer	25mM Tris 192 mM glycine 15% (v/v) methanol
TBS	50mM Tris-HCl 150mM NaCl pH 7.4
Stripping buffer	62.5 mM Tris-HCl pH 6.8 2% (v/v) SDS 100mM b-mercaptoethanol

For immunohistochemistry:

Citrate Buffer	10mM citric acid pH 6.0
Tris EDTA buffer	50mM Tris 2mM EDTA pH 9.0
EDTA buffer	1mM EDTA pH 8.0

For ChiP:

ChiP Dilution Buffer	0.01% SDS 1.1% Triton X- 100 1.2mM EDTA 16.7mM Tris-HCl pH 8.1 167mM NaCl
Low Salt Immune Complex Wash Buffer	0.1% SDS, 150mM NaCl 1% Triton X-100 2mM EDTA 20mM Tris-HCl, pH 8.1
High Salt Immune Complex Wash Buffer	0.1% SDS

	1% Triton X-100 2mM EDTA 20mM Tris-HCl, pH 8.1 500mM NaCl
LiCi Immune Complex Wash Buffer	0.25M LiCl, 1% IGEPAL CA630 1% deoxycholic acid (sodium salt) 1mM EDTA 10mM Tris, pH 8.1.
TE Buffer	10mM Tris-HCl, pH 8.0 1mM EDTA
SDS Lysis Buffer	1% SDS 10mM EDTA 50mM Tris, pH 8.1
ChiP Locked Protein G Agarose	2.5 mL packed beads 1 mg sonicated salmon sperm DNA 2.5 mg BSA 5 mg recombinant Protein G 10 mM Tris-HCl 1 mM EDTA, pH 8.0

All solutions were made up in distilled water unless otherwise stated.

Chapter Three

Differential expression of CAIX

3.1Introduction

3.1.1 Tumour heterogeneity

Solid tumours are composed of heterogenous cell populations that interact in complex networks. This phenotypic heterogeneity is a result of the interplay between genetic and non-genetic factors that shape cellular phenotypes (Marusyk et al., 2012). Tumour heterogeneity is one of the significant factors of cancer development that most treatments fail to address sufficiently. The cancer stem cell hypothesis, the clonal evolution model and the tumour plasticity model have been proposed as descriptions for the establishment and maintenance of intratumour heterogeneity (Campbell and Polyak, 2007; Hill, 2006; Merlo et al., 2006; Michor and Polyak, 2010). The cancer stem cell hypothesis suggests that the tumour is composed of cells with similar genetic background but with different states of stemness, differentiation and tumourigenic potential. According to this notion, the self-renewing cancer stem cells (CSC) undergo symmetric division to replenish the CSC pool and asymmetric division to produce differentiated cells (non-CSCs) with low tumourigenic potential. The differentiation of stem cells then leads to the production of all cell types (CSC and non-CSC) in the tumour generates intratumour heterogeneity (Al-Hajj and Clarke, 2004; Ichim and Wells, 2006; Michor and Polyak, 2010). The experimental evidence for this comes from certain forms of hematopoietic malignancies in which first cancer stem cells were first described (Lapidot et al., 1994), subsequently followed by identification of stem cells in other tumour types, including breast cancer (Al-Hajj et al., 2003b). Development of cancer drugs targeting CSC may produce effective

treatment that can create a durable clinical response. An example of CSC targeted therapy is the development of a selective (ABL1) kinase inhibitor that is used for the treatment of CML in combination with histone deacetylase inhibitors (Duy et al., 2011).

The clonal evolution theory of cancer proposed by Peter Nowell in 1976, implies an evolutionary process in which a tumour is initiated by normal cells that have accumulated large numbers of genetic mutations and epigenetic changes over time, generating new clonal populations evolutionarily favored to survive and drive tumour development. In the context of this model, the emergence of the new fittest populations in tumour cells give rise to heterogeneity (Michor and Polyak, 2010). Currently three studies have confirmed the clonal heterogeneity of primary tumours and metastases at single-nucleotide level (Gerlinger et al., 2012; Hou et al., 2012; Xu et al., 2012). Identifying key somatic driver mutations may be important from the therapeutic point of view. For example, the identification of breast cancers driven by human epidermal factor receptor 2 (HER2) (Guedj et al., 2012) resulted in the development of Herceptin, a HER2 inhibitor, with a major beneficial impact in the treatment of HER2-positive breast cancers. Likewise, understanding the biological significance of these key mutations can provide useful information on disease course and progression, as it is in the case of patients harboring BRAC1 (breast cancer 1) or BRAC2 (breast cancer 2) germline mutations. Recent evidence indicates that clonal evolution and CSC-directed development may not be mutually exclusive and both mechanisms may cooperate to create tumour cell heterogeneity (Anderson et al.,

2011; Notta et al., 2011).

Cell plasticity is argued to be an alternative model for the establishment of tumour heterogeneity. According to this model the majority of tumour cells can acquire stem-like characteristics, dependent on microenvironmental conditions and/or cell intrinsic variability. As tumours progress they experience hypoxia and other microenvironmental changes that result in the continuous alteration of clonal composition and cellular phenotypes. Concordant with this notion, the increased infiltration of macrophages, the autocrine/ or paracrine release of cytokines, which attract mesenchymal stem cells and initiate the epithelial–mesenchymal transition (EMT), are factors that stimulate or deregulate self-renewal processes. Taken together, hypoxia, cytokine signaling networks, EMT, inflammatory mediators and other microenvironment factors can all promote the dedifferentiation of non-CSCs and increase the overall 'stemness' of the tumour (Tang, 2012). Experimental evidence for the above model comes from recent studies showing that genetic and epigenetic events such as loss of BRCA1 or PTEN, can cause luminal progenitors cells to acquire basal like phenotype (Liu et al., 2008). In addition, it has been shown that overexpressing pluripotency factors (OCT-4, SOX2, TWIST, hTERT, etc) is sufficient to reprogram non-CSC into induced pluripotent stem (iPS) cells (Jeter et al., 2011; Paranjape et al., 2012; Scaffidi and Misteli, 2011; Yamanaka and Blau, 2010). Finally, microenvironmental factors such as hypoxia have been linked to expansion of cancer stem cells, and to the increase in CSC phenotypes (Mathieu et al., 2011; Paranjape et al., 2012). From a therapeutic point of view eradicating only the CSC

may not be sufficient for successful therapy, because of the possible de novo generation of CSCs from non-CSCs within the tumour. Therefore, identifying the interactions of CSC with the rest of the tumour cells (non-CSC) and with their microenvironment could lead to a better understanding of the pathways that promote tumour progression and recurrence, resulting in the development of potential novel targets for therapeutic intervention.

3.1.2 Hypoxic Microenvironmental Heterogeneity

Tumour microenvironment contributes to mutagenesis and to genetic instability leading to the development of heterogeneity in the tumour cell population, their further evolution and progression toward increasingly aggressive phenotypes and ultimately, progression of the malignancy (Reynolds et al., 1996; Yuan and Glazer, 1998; Yuan et al., 2000). Of note, during tumour development, rapid expansion and growth of cancer cells creates poorly vascularized regions, characterized by hypoxia, with irregular blood flow, low pH and nutrient starvation, which can select for a more aggressive tumour phenotype (Heddleston et al., 2010a). The extent of hypoxia also strongly correlates with poor patient survival and therapeutic resistance (Heddleston et al., 2010a).

3.1.3 Changes in gene expression

Cellular responses and adaptation to hypoxia are mediated partly through activation of hypoxia inducible transcription factors (HIFs). The HIFs induce the transcription of many hypoxia-response genes, such as the pro-angiogenic vascular endothelial growth factor (VEGF), Carbonic Anhydrase 9 (CA9) and Lactate Dehydrogenase-A

(LDHA) by binding to hypoxia-response elements (HRE) in their promoters (Forsythe et al., 1996). The activation of hypoxic genes that confer an advantage in survival under stress condition leads to the selection of more aggressive clonal populations, which in turn further upregulate expression of these genes. This contributes to the development of intra- and inter- tumour heterogeneity as revealed by the pronounced but non-uniform expression of hypoxia-driven genes in solid tumours (Diaz-Cano, 2012; Harris, 2002).

3.1.4 Epigenetic regulation of gene expression

Cancer cells also exhibit alterations in global levels of specific chromatin modifications, such as methylation or acetylation, generating an additional layer of epigenetic heterogeneity at the cellular level in tumour tissues. It has been suggested that deregulation of DNA methylation as well as alteration in histone modifications play a central role in cancer development and progression (Esteller, 2008). For example, the DNA of cancer cells is generally hypomethylated, thus driving oncogene activation and chromosomal instability. On the other hand, heterochromatization may lead to transcriptional silencing of specific tumour suppressor genes and in this way contributing to genome instability (Feinberg, 2004). Several studies have reported that inactivation of some DNA repair genes due to hypermethylation of the CpG islands within their promoters contributes to tumourigenesis. For example, the epigenetic silencing of the DNA repair gene MGMT (O6-methylguanine DNA methyltransferase), blocks the repair of a specific type of DNA damage and also correlates with the patients' responsiveness to therapy utilizing alkylating agents

(Esteller et al., 2000). Likewise, silencing of BRAC1 (Chiang et al., 2006) or hMLH1 (Goel et al., 2011) is also associated with poor prognosis in breast cancer patients or early onset of colorectal cancer, respectively. In addition to DNA methylation, histone modifications play a role in epigenetic alterations of tumour cells. In eukaryotes an octamer of histones H2A, H2B, H3 and H4 is wrapped by 147 bp of DNA to form a nucleosome, the fundamental unit of chromatin. Chromatin can be generally divided into two major types: heterochromatin (condensed and transcriptionally silent) or euchromatin (open and transcriptionally active). These two states differ in their degree of DNA compactness, regulated by combinations of histones post-translational modifications, which are involved in regulating chromatin formation. The most common histone modifications occurring in cancer are acetylation at lysine residues (K) and methylation (me) of lysines and arginines (R) as well as phosphorylation, ubiquitination, glycosylation, sumoylation, ADP-ribosylation and carbonylation (Kurdistani, 2007). Histone acetyltransferases (HATs) or deacetylases (HDACs) can acetylate or deacetylate the lysine residues with distinct specificities and ability to distinguish between histone subtypes as well as individual residues within a given histone (Kurdistani, 2007; Peng et al., 2008). For instance, methylation at the H3K9 (di and trimethylation), trimethylation at H3K36, dimethylation at H3K79, as well as a general histone hypoacetylation and the recruitment of the heterochromatin protein 1 (HP1) are all hallmarks of heterochromatin, a transcriptionally inactive and late replicating regions of the genome (Berger, 2007; Portela and Esteller, 2010). This is in contrast to increased histone acetylation and the di- and trimethylation at H3K4, H3K27, and H4K20 that are all associated with euchromatin, a gene rich and

transcriptionally active regions of the genome (Strahl et al., 1999).

Tumour hypoxia is thought to induce chromatin alterations that could enable cells to overcome nutritive deprivation or to escape anti-proliferative signals imposed by a stressful environment. Accordingly, several studies have reported an increase in the H3K9me2/me3 and H3K4me3 and a global decrease in deacetylation at the promoters of hypoxia regulated genes (Johnson et al., 2008). Surprisingly, hypoxia also increases the expression of histone demethylases (Xia et al., 2009a) such as the histone demethylases JMJD1A and JMJD2B. It is believed that their upregulation helps to maintain histone homeostasis during hypoxic tumourigenesis (Ponnaluri et al., 2011; Xia et al., 2009b; Yang et al., 2009). Taken together, the identification of epigenetic regulation of the histone modifying enzymes in response to hypoxia may provide a vital connection between the epigenetic mechanisms that the cells are using under environmental stress and cancer progression. This in turn could lead to the development of novel anti-cancer therapies targeting epigenetic alterations within the tumour.

3.1.5 Mutational load of hypoxic cells

Hypoxia, low extracellular pH, and nutrient deprivation inhibits the activity of many enzymes critical to a balanced DNA metabolism, such as DNA polymerases, topoisomerases, helicases and ligases (Yuan et al., 2000). The decrease ability of cells to repair damaged DNA (Reynolds et al., 1996; Unruh et al., 2003) combined with an increased level of reactive oxygen species (ROS) production (Chandel et al., 2000) contributes to the development of genomic instability in tumour cells. In addition, it

has been shown that hypoxia and reoxygenation induce overreplication of DNA, resulting in the formation of tetraploid subpopulations from original diploid cells (Rofstad et al., 1996) . Further to this, over-replication of DNA is also associated with gene amplification and drug resistance (Rice et al., 1986). For example, it has been reported that over-replication of a large portion of the genome led to the amplification and increased expression of the P-glycoprotein and dihydrofolate reductase genes, which are responsible for the resistance to adriamycin and methotrexate, respectively (Rice et al., 1986). Furthermore, tumour hypoxia has been also shown to favor cells that have lost sensitivity to p53-mediated apoptosis (Sermeus et al., 2008). This results in the formation of subpopulation of cells that are mutated for p53, the so-called guardian of the genome. Taken together hypoxia promotes genetic mutations driving genomic and epigenetic instability thus enhancing the development of intratumoural heterogeneity and the appearance of aggressive and drug resistance subpopulations responsible for the progression of the malignancy.

3.1.6 CAIX as Hypoxic Tumour Biomarker

Tumour heterogeneity is correlated with differential gene expression patterns. The identification and characterization of distinct tumour populations' "signatures" (for example distinct functional signaling profiles) may allow classification of tumours and stratification of patients for better management.

An excellent biomarker of hypoxia is the transmembrane protein CAIX, which is also a potential therapeutic target (Robertson et al., 2004). The majority of studies

investigating CAIX as a tumour biomarker have used immunohistochemistry and/or immunofluorescence techniques. The major drawbacks of these methods are that they are invasive, require tissue samples (biopsy or TMA core) and they show high measurement errors due to the size of tissue sample (Iakovlev et al., 2007). Therefore, more analytical and quantitative methods for the assessment of intratumoural heterogeneity are needed to provide reliable measurements of CAIX expression. Given the above, we utilized the CAIX stability and transmembrane location to employ flow cytometry-based analysis for the assessment of CAIX heterogeneity in cancer cell lines.

3.2 Results

3.3 Carbonic anhydrase expression under hypoxic conditions

Previous studies have shown that CAIX is significantly upregulated under hypoxic conditions. To determine the induction profile of CAIX we performed a 72h time course under 0.1% O_2. The breast cancer cell line MCF7, showed no expression of CAIX in normoxia and an upregulation of CAIX in hypoxia, with higher levels of expression at 72h both at RNA and protein level **(Figure 3.1).** Previous work in our laboratory has shown that CAIX has the same expression pattern in other cancer cell lines such as HCT116 and MDA-MB-231. Interestingly, expression of HIF-1α, which was used as a marker of hypoxia, was lower at 72h, compared to 48h and 24h. The increased expression of CAIX seen at 72h of hypoxia may be explained by the longer time course required for CAIX upregulation compared to that of HIF-1α. Therefore all the subsequent hypoxic (0.1% O_2) experiments in cancer cell lines grown in monolayers were performed at 72 h.

Spheroids are three-dimensional aggregates of tumour cells. This *in vitro* model mimics the tumour microenvironment and its properties such as oxygen, pH, and nutrient gradients and induces an inner necrotic core surrounded by a viable rim of cells. As reported in previous studies, the ability of HCT116 to form spheroids was confirmed (Mueller et al., 2000), and subsequently the effect of the expression of CAIX on HCT116 spheroid growth was assessed using a spheroid growth assay. The

HCT116 spheroids were grown in spinner flask placed on a magnetic stirrer platform for 15d. A day prior harvesting, 100μM pimonidazole was added to the culture media for 16h overnight. The spheroids were harvested, formalin-fixed and paraffin-embedded for immunohistochemical staining for CAIX and pimonidazole. The HCT116 spheroids displayed large necrotic areas, a phenomenon associated with hypoxia, amongst other factors, and binding of the hypoxia marker, pimonidazole (Sminia et al., 2003). A large perinecrotic rim of pimonidazole was observed, which colocalizes with CAIX expression. However CAIX expression was limited mainly to a discrete perinecrotic rim of the spheroids, showing that not all pimonidazole positive cells were expressing CAIX (**Figure 3.2**). This raised the question if there were hypoxic cells that are not upregulating CAIX resulting in the development of hypoxic subpopulations of cancer cells. Thus, HCT116 cell line was confirmed as a suitable cell line in which to assess CAIX expression in spheroid model.

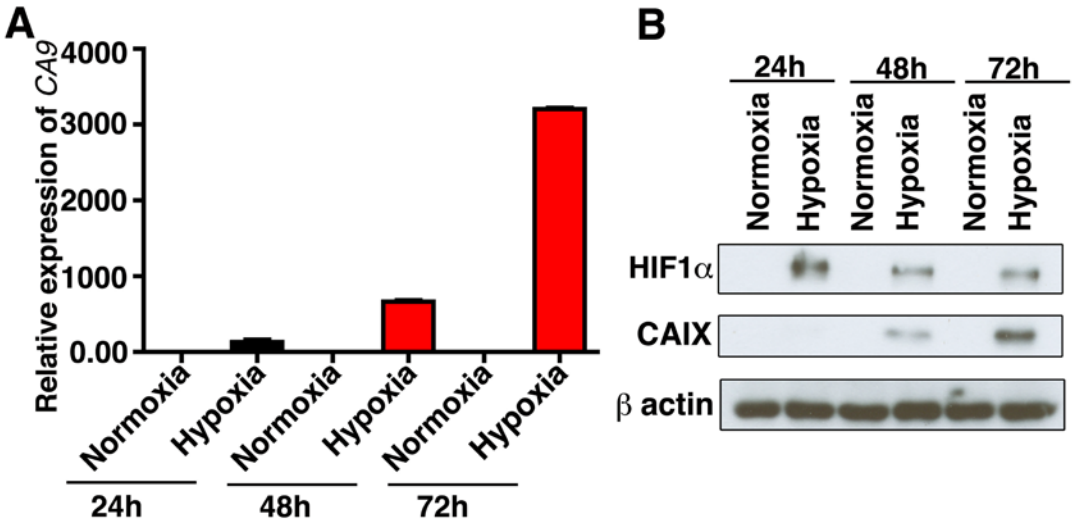


Figure 3.1 Expression of CAIX in MCF7 breast cancer cell line. MCF7 breast cancer cell line shows no expression of CAIX under normal growth condition and an upregulation of CAIX in hypoxia, with higher levels of expression at 72h at both mRNA (A) and protein level (B). Error bars represent SD.

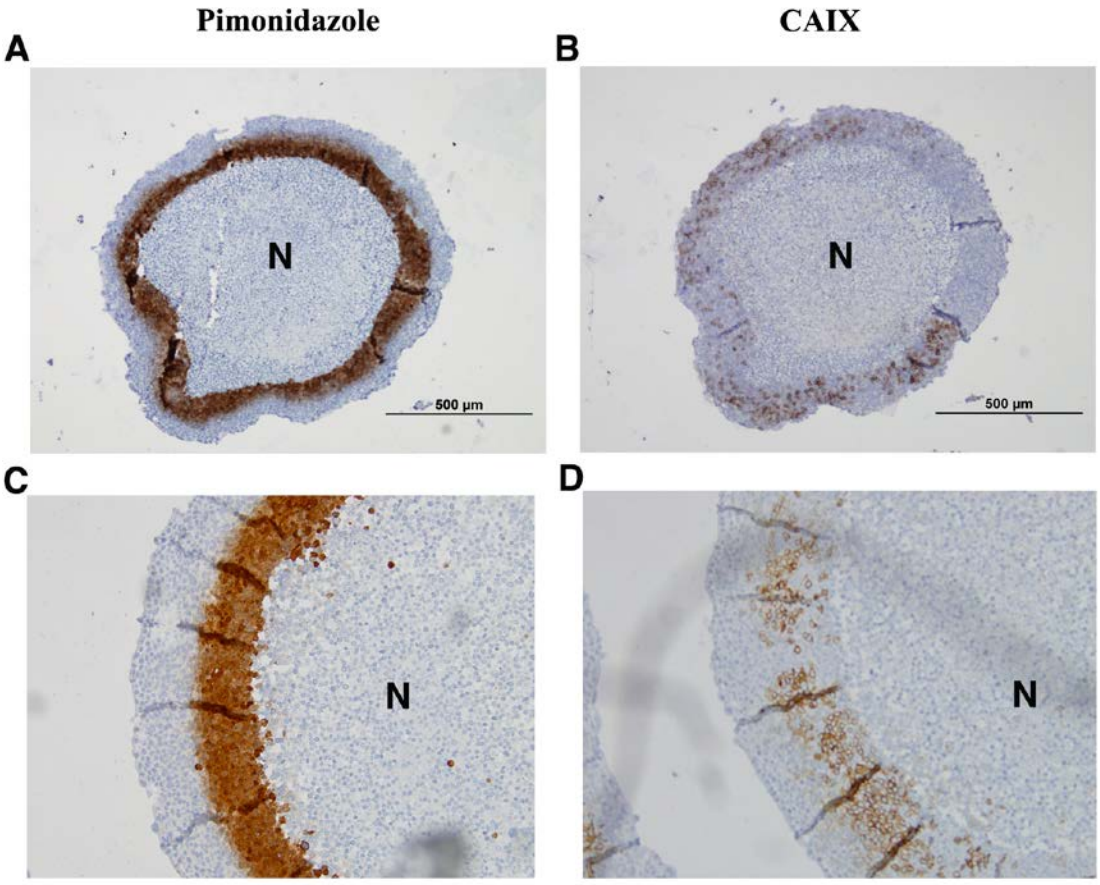


Figure 3.2 Pimonidazole and CAIX expression in HCT116 spheroids (A) and (C) anti-pimonidazole antibody and (B) and (D) anti-CAIX antibody M75. Expression of pimonidazole and CAIX was confirmed to the perinecrotic region. N= necrosis.

3.3.1 Differential expression of CAIX

The detection of hypoxic subpopulations of cancer cells was examined using CAIX as a marker. The majority of studies thus far using CAIX as a tumour biomarker utilized both immunohistochemistry and immunofluorescence techniques, which are prone to inter- and intra observer variability. Here taking advantage of CAIX's transmembrane location its expression was examined by flow cytometry (FACS). The breast cancer cell lines MCF7 and MDA-MD-231, and the colon cancer cell lines SW1222 and HCT116 were tested for CAIX expression using a FITC conjugated anti-CAIX antibody. The FACS analysis showed that under hypoxic (0.1%) conditions there were two populations, which differentially express the hypoxic marker CAIX, in MCF-7, HCT116 and SW1222, but not MDA231 **(Figure 3.3)**. One population shows no expression of CAIX, whereas the second population was positive for CAIX. As a control, normoxic samples of the four cell lines were used. The cells were exposed to 0.1% O_2 because previous experiments from our laboratory have shown that at 1% O_2 the two subpopulations are not existing. In all cells lines the CAIX negative population does not express CAIX, and its expression overlays with the normoxic sample. The percentage of CAIX positive cells ranged from 30% to 50% in the four cell lines tested **(Figure 3.4)**.

Using CAIX as a marker, the CAIX positive (CAIX+ve) (extreme high 10%) population and the CAIX negative (CAIX-ve) population (extreme low 10%) (**Figure 3.5A**) were FACS sorted from the four cell lines. The expression of CAIX in the two sorted populations was tested by western blotting using the mouse monoclonal M75

antibody. In all four cancer cell lines only in the CAIX+ve population CAIX was detected, confirming the results from FACS analysis (**Figure 3.5 B)**.

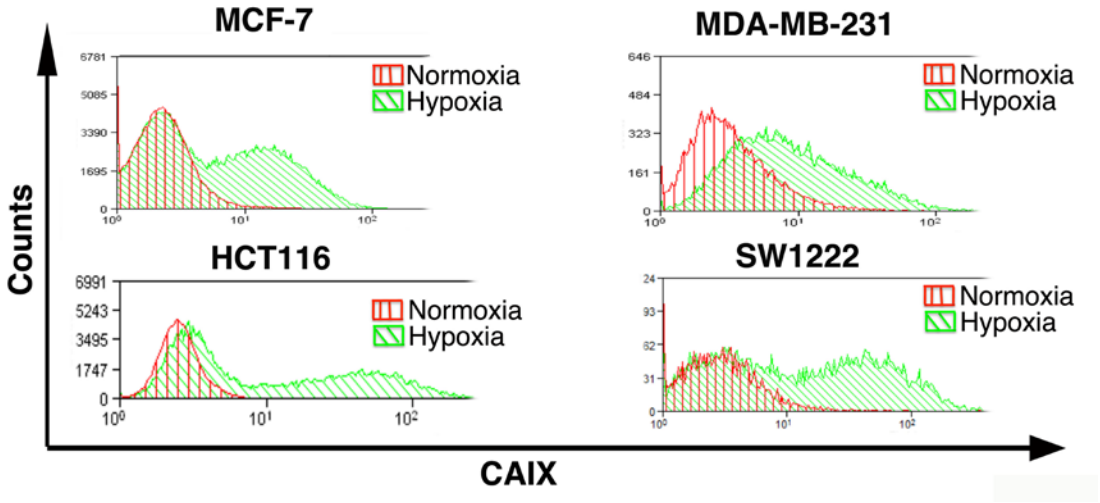


Figure 3.3 Hypoxic subpopulations of CAIX expression. Two distinct subpopulations of CAIX+ve and CAIX-ve cells exist in MCF-7, HCT116 and SW1222 lines stained with CAIX antibody and analysed by FACS.

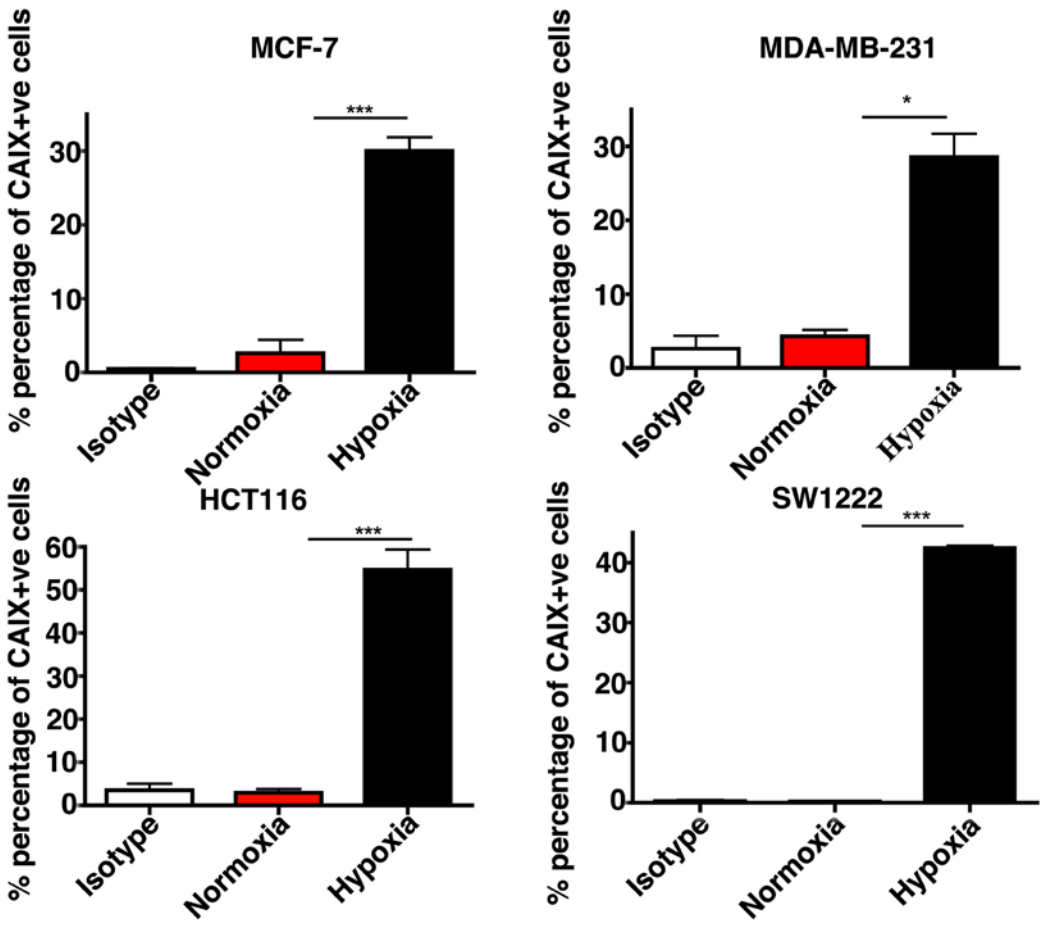


Figure 3.4 The percentage of CAIX+ve cells in breast and colorectal cancer cell lines. Percentage of CAIX+ve cells under hypoxia in MCF-7, MDA-MB-231, HCT116 and SW122 cell lines. *=p<0.05, ***=p<0.001. Error bars represent SD.

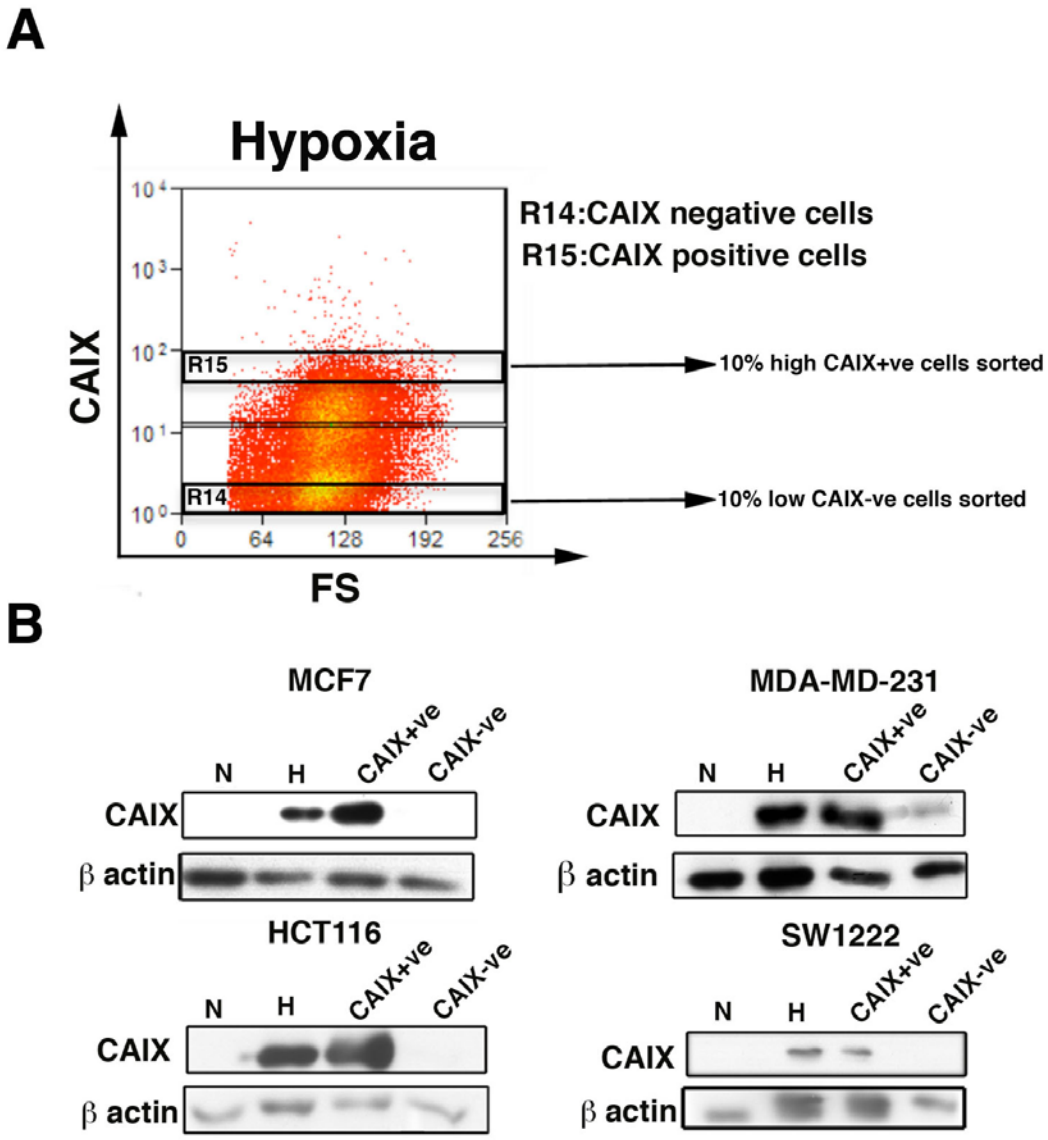
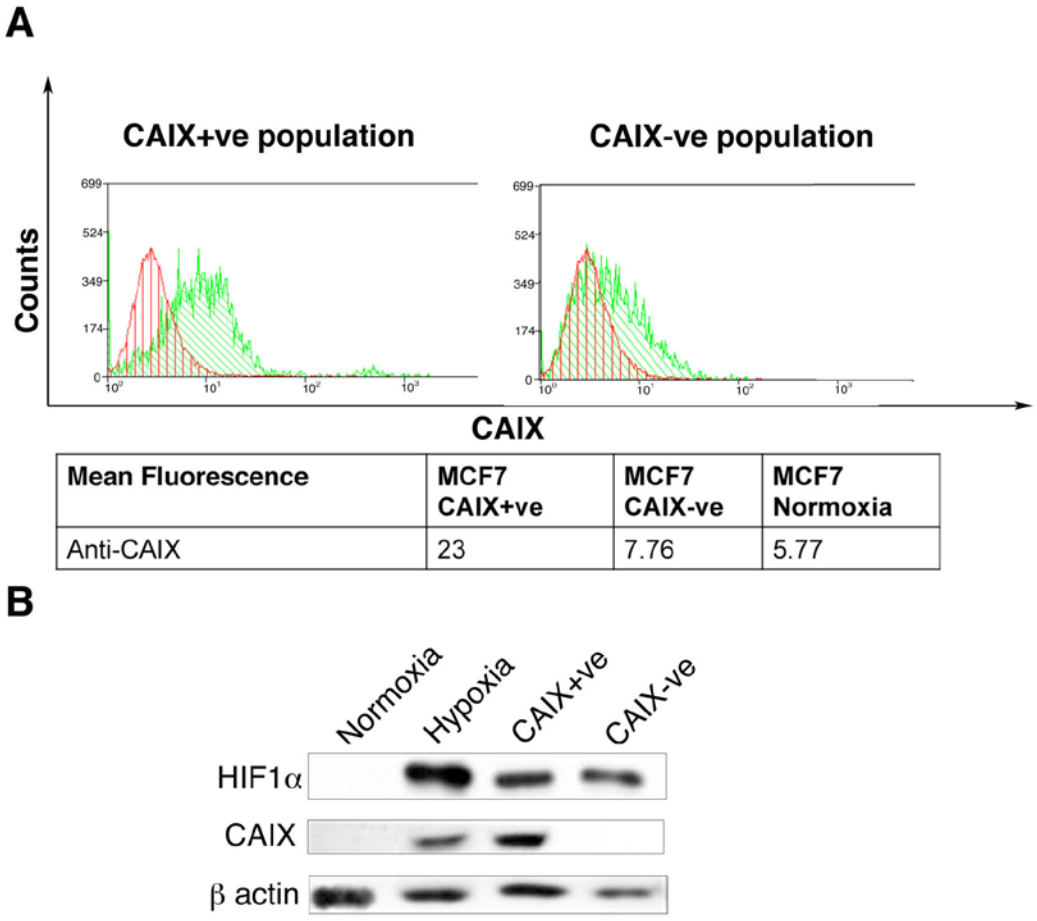


Figure 3.5 Sorted CAIX positive and CAIX negative cells. (A) The top 10% of CAIX+ve cells and the low 10% CAIX-ve cells were sorted for further experiments. (B) The expression levels of CAIX of the sorted cells were confirmed at protein level. FS=Forward Scatter.

3.3.2 Generation of CAIX positive and CAIX negative cell lines

To investigate whether either population of CAIX+ve and CAIX-ve cells could repopulate both CAIX+ve and CAIX-ve cells, I performed two rounds of sorting of hypoxia–induced MCF7 cells into CAIX+ve and CAIX-ve populations. After the first round of sorting both populations were cultured for 4 weeks in normoxic conditions. In the 4 weeks culture period prior to the second round of sorting both populations were tested for CAIX expression. After the first week in culture, the CAIX+ve and CAIX-ve cells were exposed for 72h to hypoxia, in order to evaluate the CAIX expression status of the two populations. The CAIX+ve cells contained both CAIX+ve and CAIX-ve cells, whereas the CAIX-ve cells contained mainly CAIX negative cells **(Figure 3.6A)**. The FACS results were confirmed by western blotting using the mouse monoclonal M75 antibody **(Figure 3.6B)**.

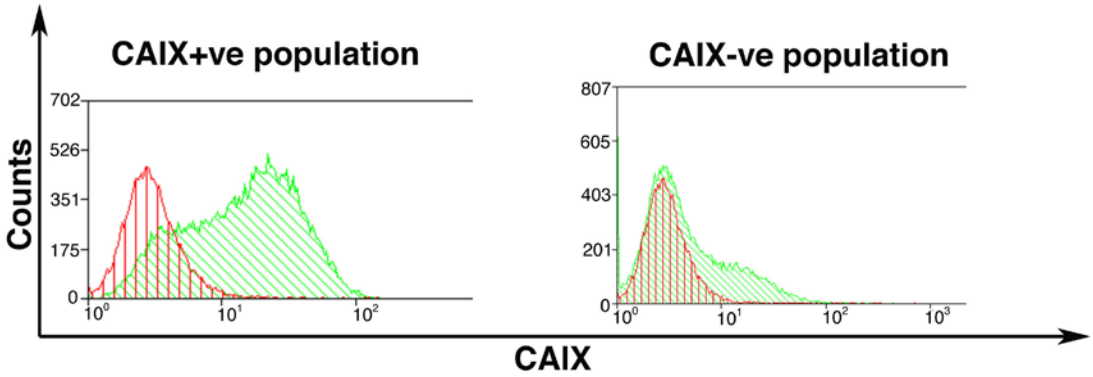


Mean Fluorescence	MCF7 CAIX+ve	MCF7 CAIX-ve	MCF7 Normoxia
Anti-CAIX	23	7.76	5.77

Figure 3.6 FACS analysis of sorted cells in culture (A) FACS analysis of sorted cells cultured for one week shows that the CAIX+ve cells contained both CAIX+ve and CAIX-ve cells, whereas the CAIX-ve cells contained predominantly CAIX negative cells. (B) The expression levels of CAIX of the sorted cells were confirmed at protein level. Red peaks represent cells in normoxia. Green peaks represent cells in hypoxia. Error bars represent SD.

After 3 weeks in culture both cell populations were reexamined for CAIX expression using FACS analysis. The CAIX+ve population had recapitulated the original unsorted phenotype, generating both populations of CAIX+ve and CAIX-ve cells. The CAIX-ve cells were not capable of reforming both populations and they remained mainly negative for CAIX, showing only a very low levels of CAIX expression **(Figure 3.7)**. In order to further enrich for CAIX+ve cells and CAIX-ve cells, a second round of FACS sorting was performed 3 weeks later. The extreme high 10% of CAIX positive cells and the extreme low 10% of CAIX negative cells were sorted and cultured in normoxic conditions for six months. During this long-term culture, the CAIX+ve cells became again heterogeneous, containing both CAIX+ve and CAIX-ve populations when exposed to hypoxia, and thus recapitulated the original unsorted expression pattern, whereas the CAIX-ve cells continued to be homogenous, and negative for CAIX expression after exposure of the cells to 0.1% O_2 hypoxia for up to 72h **(Figure 3.8A)**. With the long-term culture (6 months) of the CAIX+ve and CAIX-ve cells two cell lines were generated, subsequently named CAIX+ve cell line and CAIX-ve cell line. The expression profile of CAIX from FACS analysis was also confirmed at both mRNA **(Figure 3.8B)** and protein level (**Figure 3.8C**) using the mouse monoclonal M75 antibody.

.



Mean Fluorescence	MCF7 CAIX+ve	MCF7 CAIX-ve	MCF7 Normoxia
Anti-CAIX	20.75	7.15	5.48

Figure 3.7 Expression profile of CAIX+ve and CAIX-ve sorted cells cultured for 3 weeks. The CAIX+ve population had recapitulated the original unsorted phenotype, generating both populations of CAIX+ve and CAIX-ve cells. Red peaks represent cells in normoxia. Green peaks represent cells in hypoxia. Error bars represent SD.

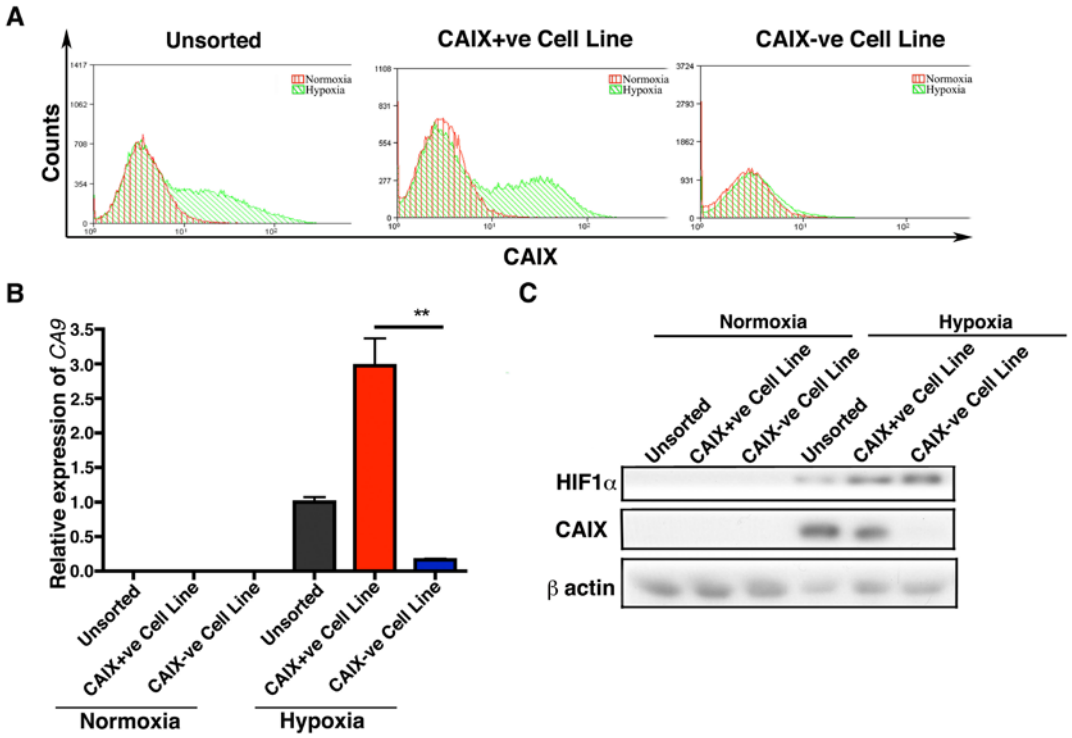


Figure 3.8 Long-term culture of CAIX+ve and CAIX-ve cells. FACS analysis of CAIX shows that only the CAIX+ve population has the ability to recapitulate the original expression pattern and to reform both populations in long term (6 months) culture. (A) The expression levels of CAIX in the long term (6 months) cultures of the sorted cells was confirmed both at RNA (B) and protein level (C). Red peaks represent cells in normoxia. Green peaks represent cells in hypoxia. **=p<0.01. Error bars represent SD.

3.3.3 Molecular Mechanisms of CAIX silencing

3.3.3.1 *CA9* is the only HIF-1α regulated gene that shows differential expression under hypoxia, of those tested

In order to examine if other hypoxia inducible genes also had a differential expression in addition to *CA9*, we tested the RNA and protein levels of well validated hypoxia regulated genes *LDHA*, *PDK1*, and *AK4*. The results showed that under hypoxia in both CAIX+ve and CAIX-ve cell populations *CA9* was the only hypoxia-regulated gene that had differential expression (**Figure 3.9**). The other hypoxia regulated genes tested showed similar expression pattern in both populations. In addition, the protein expression levels of CAIX, LDHA, PDK1 and AK4 showed that only CAIX is differentially expressed, whereas the expression of the rest of the hypoxia proteins tested remained the same in both populations (**Figure 3.10A)**. However, the mRNA levels of PDK1 and AK4 were significantly upregulated in the sorted CAIX+ve and CAIX-ve populations compared to the unsorted hypoxia cells. The cause of this difference requires further study, but it may be related to the effect of FACS sorting in the cells. In order to analyze kinetics of HIF-1α, the major transcriptional activator of *CA9*, the sorted populations were allowed to recover from hypoxia for 1 week, and then re-exposed to 0.1% O_2 hypoxia for 24h. Both populations showed the same levels of HIF-1α induction **(Figure 3.10B)**, suggesting that the differential expression of CAIX was not due to differential regulation of HIF-1α□□□□□□□□□□□ .

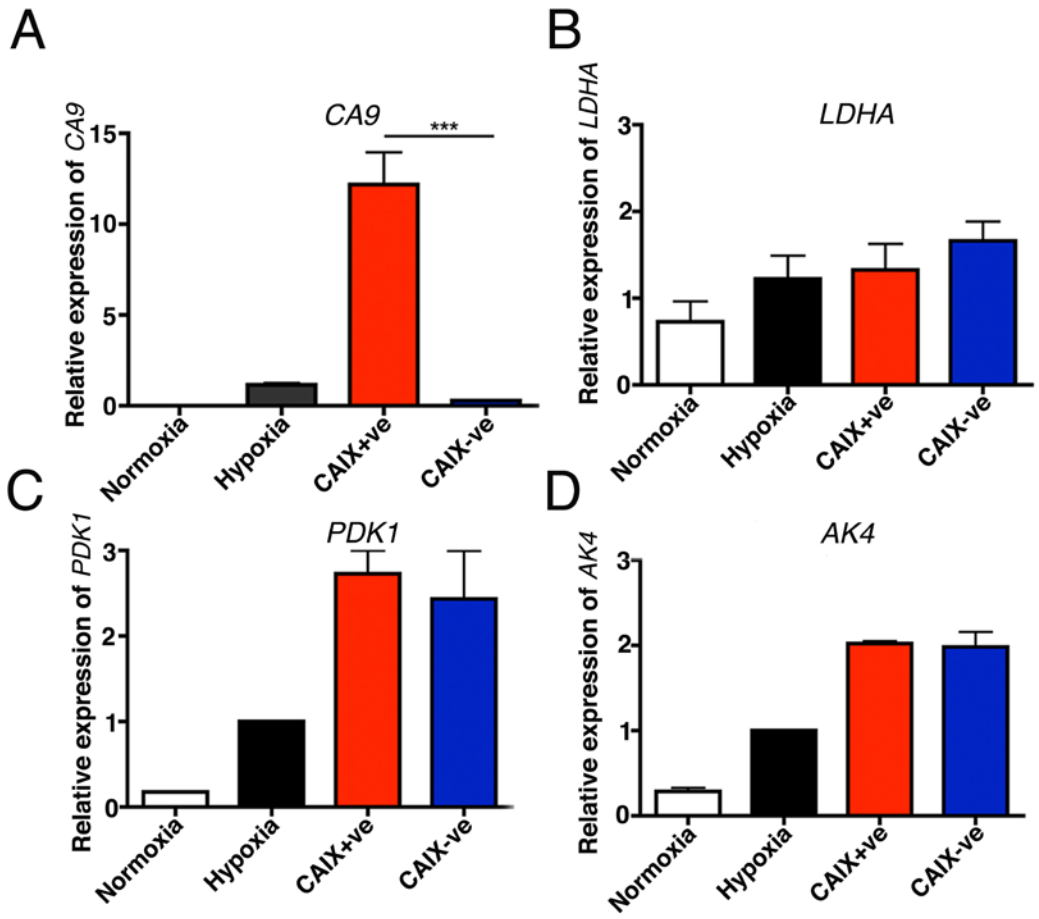


Figure 3.9 Expression of hypoxia inducible genes. CAIX+ve and CAIX-ve sorted MCF-7 cells have the same levels of expression for *LDHA* (B), *PDK1*(C) and *AK4* (D) genes. ***=p<0.001. Error bars represent SD.

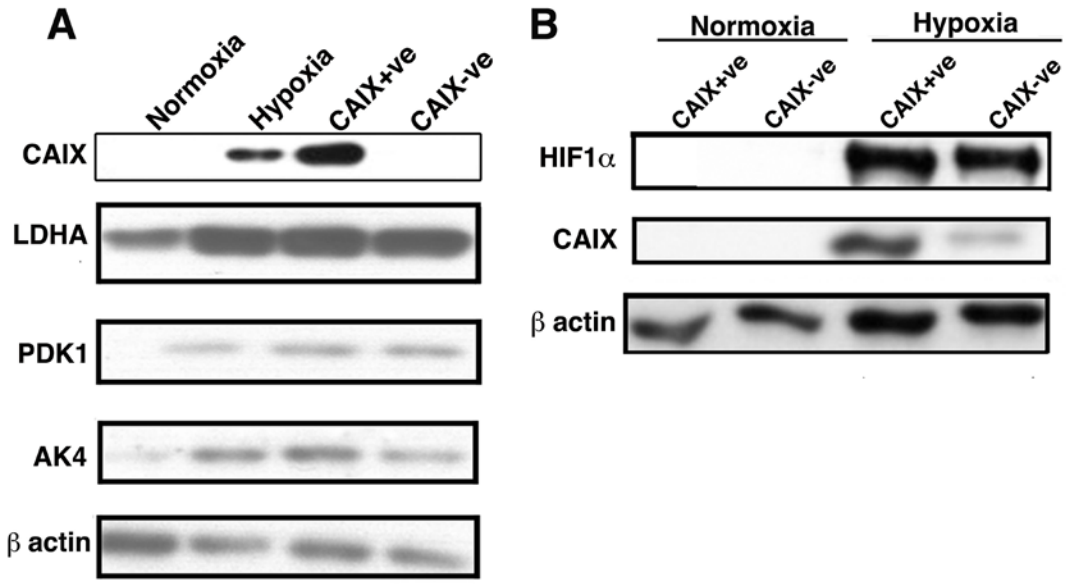


Figure 3.10 Protein expression of hypoxia inducible genes. CAIX+ve and CAIX-ve sorted MCF-7 cells have the same levels of protein expression levels of LDHA, PDK1, AK4 (A) and HIF-1α (B).

3.3.3.2 Generation of HCT116 stable cells expressing Hypoxia Responsive Elements (HREs)

Hypoxic conditions activate the hypoxia inducible factor (HIF), a transcription factor with signaling effects through an intranuclear hypoxia response elements. Stable cell lines with constitutive expression of HREs could be a useful tool for quantifying the degree of tissue hypoxia on the CAIX+ve and CAIX-ve population. To generate stable HREs-expressing cell lines, wild type HCT116, was transfected with the pPur.EpoE.SV40p.GFP vector (GFP-HRE). Transfected cells were selected with 2μg/mL puromycin and resistance clones were picked and screened for the expression of GFP-HRE under normoxic and hypoxic conditions **(Figure3.11A (i) and (ii))**. The HCT116 cell line expressing GFP-HRE was exposed to hypoxia for 72h and then FACS analysis were performed to assess CAIX expression using a PE-conjugated CAIX antibody. The results showed that there were no differences on the expression levels of HREs between the two populations indicating that CAIX+ve and CAIX-ve cells have a similar core hypoxia response **(Figure 3.11C)**.

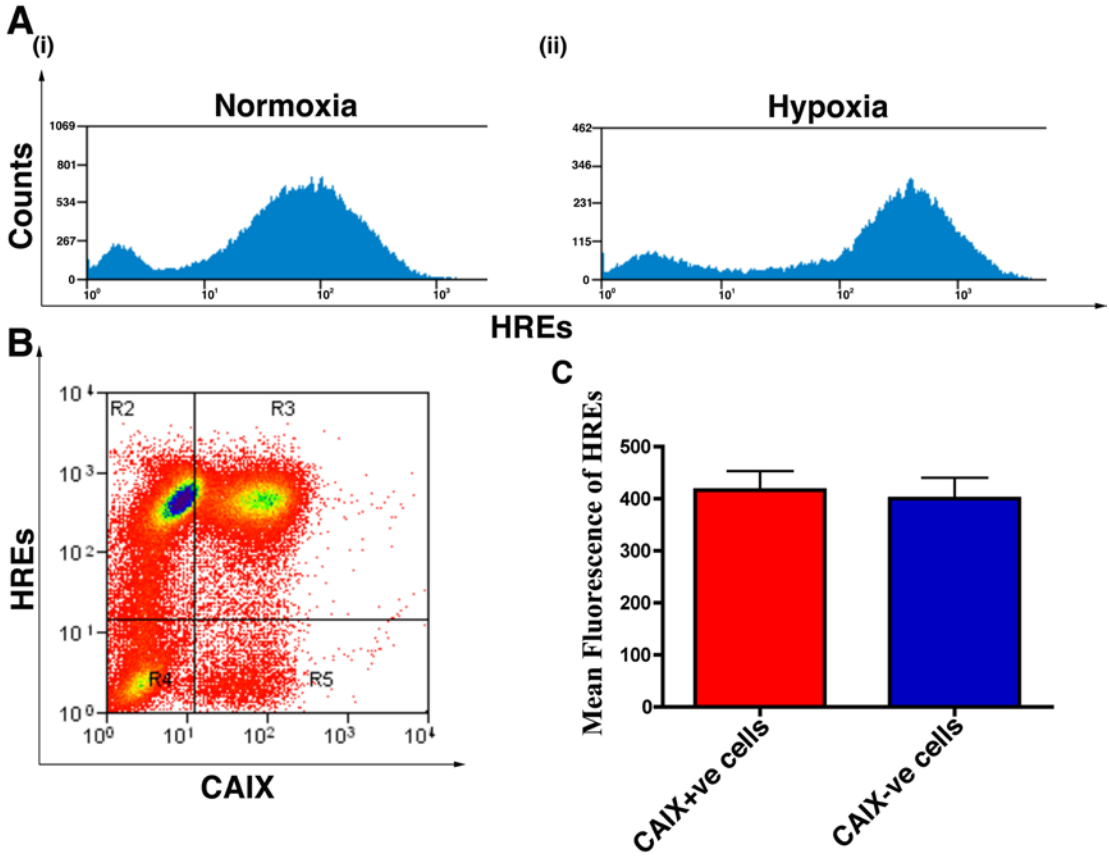


Figure 3.11 Expression of GFP-HREs. Histogram showing GFP fluorescence in HCT116 colon cancer cell line transfected with hypoxia responsive pPur.EpoE.SV40p.GFP vector (A) under normoxic (i) and hypoxic (ii) conditions. The HCT116 GFP-HREs stable expressing were labelled with the PE conjugated anti-CAIX antibody exposed to 0.1% O_2 (B). CAIX+ve and CAIX-ve cells express the same levels of the hypoxia responsive elements (C). Error bars represent SD.

Treatment of CAIX-ve cell line with the demethylating agent, 5-aza-2′-deoxycytidine (5-aza-dC)

It has been shown that expression of *CA9* correlates with hypomethylation of CpG islands of the *CA9* promoter in CAIX positive RCC cell lines, while showing complete methylation of the CpG dinucleotides in CAIX negative cells, including normal kidney tissues (Ashida et al., 2002; Cho et al., 2000; Cho et al., 2001; Grabmaier et al., 2002; Kaluz et al., 2009a). In order to investigate if the lack of CAIX expression was caused by methylation of the CpG islands of *CA9* promoter, the CAIX-ve cell line was treated with the demethylating agent 5-aza-dC. Briefly, the cells were exposed to hypoxia for 72h and treated with 10 μM/L 5-aza-dC. The expression of CAIX was accessed using FACS analysis. The DNA methyltransferase inhibitor 5-aza-2'–deoxycytidin (5-aza-dC) failed to rescue CAIX expression indicating that the silencing of CAIX is not due to DNA-methylation **(Figure 3.12)**. In line with this, a previous study have shown that treatment with 5-aza-dC increased CAIX in gastric cancer cell lines (Jen et al., 2008). These gastric cancer cell lines could be used in this experiment as a positive control in order confirm that the experiment has worked.

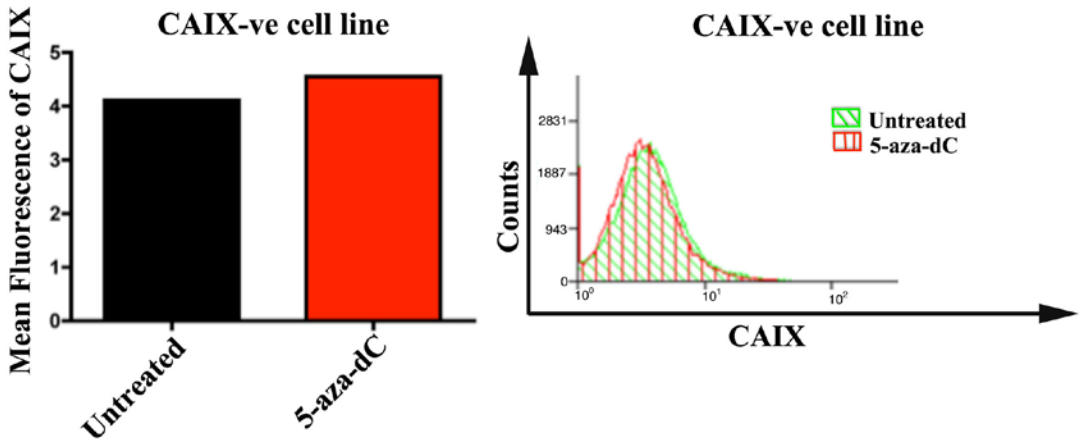


Figure 3.12 Treatment of CAIX-ve cell line with 5aza-dC. CAIX-ve cell line exposed in 0.1% O_2 and treated with the demethylating agent 5-aza-dC. FACS analysis of CAIX shows that treatment with 5-aza-dC does not affect the expression of CAIX.

3.3.3.3 Epigenetic regulation of *CA9* expression

Histone modifications provide an alternative mechanism for regulation of gene expression as they influence chromatin structure and play a crucial role in modulating gene transcription. To investigate if the differential expression of CAIX is due to differences in chromatin organization, the chromatin state of *CA9* promoter in the two populations was analyzed. Using the Epiq chromatin analysis kit the chromatin state of a given locus could be interrogated on the basis of its accessibility to nuclease digestion. The CAIX+ve and CAIX-ve cell line were exposed for 72hrs in 0.1% O_2 or they were maintained under normoxic conditions and then left undigested or were digested with DNase nuclease I for 1 hour. Following extraction and purification of the genomic DNA, the chromatin state of *CA9* promoter was studied by qPCR. The CAIX-ve cells displayed a more "closed" chromatin state as shown by the low accessibility to nuclease digestion, which correlates with low mRNA expression of *CA9,* whereas the CAIX+ve cells under hypoxia adopted a more "open" and accessible *CA9* promoter region which is associated with high expression of *CA9* (**Figure 3.13A**). Interestingly both populations under normoxic condition have a compact "silenced" chromatin. Hypoxia induces epigenetic modifications to chromatin structure resulting in more "open" actively transcribe chromatin within the CAIX+ve population.

We then performed chromatin immunoprecipitation on CAIX+ve and CAIX-ve cell line to evaluate the levels for the tri-methyl H3K9 histone, a well validated marker of heterochromatin, on the *CA9* promoter of both cell lines under normoxic and hypoxic

conditions. The CAIX+ve and CAIX-ve cell lines were either grown in normoxic conditions or they were exposed for 72hrs in 0.1% O_2. Chromatin was immunoprecipitated using the trimethylated H3K9 antibody (EpiQuik Tri-Methyl-Histone H3K9 ChIP Kit). The results showed that under hypoxic conditions the CAIX-ve cell line had significantly ($p<0.05$, n=3, biological replicates) higher levels of tri-methyl H3K9 compared to the CAIX+ve cell line, confirming the compact and transcriptionally silent chromatin structure of *CA9* promoter of the negative cells (**Figure 3.13B**).

3.3.3.4 Reduced HIF binding and silencing of *CA9*

Given that HIF induces the transcription of *CA9* by binding to hypoxia-response elements (HRE) in its promoters we hypothesized that this interaction should be reduced in the CAIX-ve cells. To test this, chromatin immunoprecipitation was performed to examine HIF-1β binding to the *CA9* promoter of both populations. The CAIX+ve and CAIX-ve cell lines were either grown in normoxic conditions or they were exposed for 72hrs in 0.1% O_2. Chromatin was immunoprecipitated using the rabbit polyclonal antisera to HIF-1β. The results showed a significant ($p<0.05$, n=3, biological replicates biological replicates) reduction in binding of HIF-1β to the *CA9* promoter of the negative population (**Figure 3.13C**). Taken together these results show that the heterogeneity of the two populations in respect to CAIX expression is due to hypoxia induced reorganization of chromatin structure.

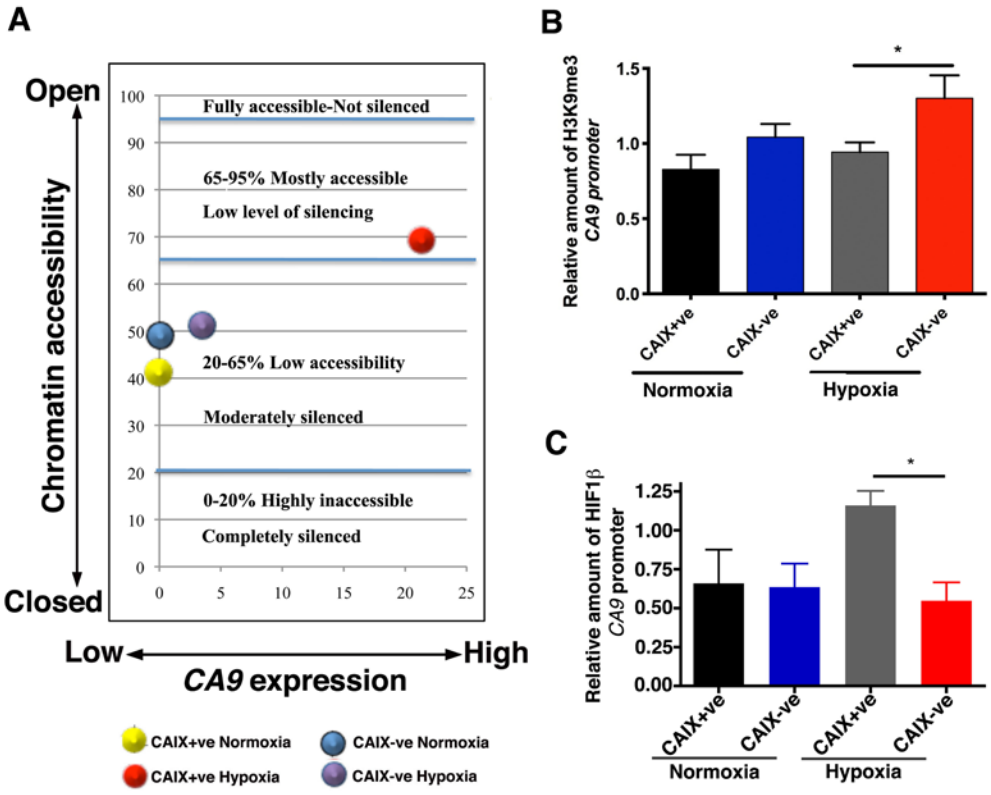


Figure 3.13 Epigenetic regulation of *CA9* expression. **(**A) Effect of CAIX expression on chromatin assembly. Relationship between percentage of chromatin accessibility and levels of silence were defined according to manufacture's protocol. (B) Levels of tri-methyl H3K9 histone modification around the *CA9* promoter region in both the CAIX positive and negative cell lines, in normoxia and hypoxia. (C) Binding of HIF-1β to the *CA9* promoter region in both the CAIX positive and negative cell lines. *=p<0.05. Error bars represent SD.

3.4 Discussion

Cellular markers of hypoxia represent a valuable diagnostic tool and a potential therapeutic target. With this regard, CAIX has emerged as one of the most promising endogenous markers of cellular hypoxia. Its expression is strongly induced by hypoxia and its overexpression is associated with poor therapeutic outcome in cancer (Choschzick et al., 2011; Hussain et al., 2007; Ilie et al., 2010; Klatte et al., 2009; Lou et al., 2011).

In this study, significant heterogeneity in cellular response to hypoxia was shown using CAIX as a marker. Based on the CAIX expression pattern under hypoxic conditions two distinct subpopulations, one that expresses CAIX and the other that does not express CAIX were identified, in three of the four cell lines MCF7, MDA-MB-231, HCT116 and SW1222 lines tested.

In addition the long term culture of the sorted CAIX+ve and CAIX-ve cells showed that only the CAIX+ve cells possess the capacity to recapitulate the original heterogeneous phenotype, consisting of mixed CAIX-ve and CAIX+ve cells in long-term culture. In addition the long-term culture of the sorted cells enabled also the generation of two cell lines, termed CAIX+ve and CAIX-ve, respectively. These were important tools that allowed us to gain insight into the molecular mechanisms of this heterogeneity.

Cellular responses and adaptation to hypoxia are mediated partly through activation of hypoxia inducible transcription factors (HIFs). The HIFs induce transcription of many

hypoxia-response genes involved in various processes, including: angiogenesis e.g. vascular endothelial growth factor (*VEGF*), pH regulation e.g. carbonic anhydrase 9 (*CA9*), and alterations in cellular metabolism e.g. lactate dehydrogenase-A (*LDHA*), by binding to hypoxia-response elements (HRE) in their promoters regions (Forsythe et al., 1996).

In comparison with the other hypoxia genes CAIX is the most highly regulatable gene target of HIF-1α as the HRE/HIF-1 binding site is located at -3/-10 position in the promoter region of this gene (Kaluz et al., 2002). In this study we showed that the differential expression of CAIX is not determined by difference in HIF expression, as both populations stabilize HIF-1α and upregulate other HIF-1α target genes such as LDHA, PDK1 and AK4 similarly. Further to this, both populations showed similar core hypoxia response as indicated by the same activation levels of the transfected hypoxia response elements.

In contrast, the molecular mechanism underlying the heterogeneity of the two populations in respect to CAIX expression is likely due to hypoxia induced reorganization of chromatin structure. The CAIX-ve cell line has a relatively "closed" and transcriptionally silent *CA9* promoter region under hypoxia compared to a transcriptionally active and "open" configuration in the CAIX+ve population. This notion is supported by the following observations: (i) in the CAIX-ve population this region is resistant to nuclease digestion, an indication of a high chromatin compaction and (ii) it has significantly higher levels of the tri-methyl H3K9 histone, a well-validated marker of heterochromatin. It has been demonstrated previously that CAIX

expression is regulated by site-specific CpG hypomethylation at −74 bp in the promoter in renal cell carcinoma and other cancer cell types (Kaluz et al., 2009a). However the differential expression of CAIX observed in this study is unlikely to be an effect of changes in DNA methylation pattern around CAIX promoter. This is based on the fact that the treatment of CAIX-ve cell line with the DNA methyltransferase inhibitor 5-aza-20'–deoxycytidin (5-aza-dC) failed to rescue CAIX expression. In line with this recent studies have also shown that hypoxia can cause chromatin alterations, such as global deacetylation and/or increase in H3K9me3/me2 (Johnson et al., 2008). Furthermore increased H3K4me3 levels and decreased H3K27me3 levels were also observed at promoters of hypoxia-regulated genes (Johnson et al., 2008). Further experiments could be done in order to test the levels of other chromatin marker to validate further these results. The most well-characterized modifications are the methylation of the Lys27 residues of histone H3 (H3K27me3), which repress gene expression, and methylation of H3K4me3 as well as acetylation of H3K4 (H3K4Ac) and H3K9 (H3K9Ac), which are associated with gene activation (Shi, 2007). In line with this, would be important to study if these epigenetic modifications regulate the expression of other differential expressed genes and especially cancer stem cell related genes.

Given that HIF induces the transcription of *CA9* by binding to HRE in its promoter it was hypothesized that this interaction should be reduced in the CAIX-ve cells. In support of this notion, a chromatin immunoprecipitation analysis showed a significant

reduction in binding of HIF to the *CA9* promoter of the negative cells. Overall these results suggest that the genomic locus coding for the *CA9* HIF binding site is heterochromatinised in the CAIX-ve cells under normoxic and hypoxic conditions. In addition, this chromatin state is also present in normoxic CAIX+ve cells and most likely needs to become "open" before *CA9* can be transcribed. The delayed hypoxic expression of CAIX until 48h-72h may be therefore explained by the time needed for chromatin reorganization. Furthermore, these findings suggest that, besides HIF-mediated gene transcription, modulation of histone methylation via an epigenetic mechanism is another mechanisms that cells use to adapt to hypoxia.

Chapter Four

Genes and pathways expressed from RNA-seq analysis

4.1Introduction

4.1.1 CAIX and stem cells

The work presented thus far shows the existence of hypoxic heterogeneity and it was important therefore, to explore the molecular mechanisms that underline this. We hypothesized that this hypoxia-dependent heterogeneity may be associated with an increased proportion of stem cells in the CAIX+ve population. This hypothesis was supported by a previous study showing that CAIX expression in the small and large intestine is very similar to that described for Lgr5, a stem cell biomarker, used to identify the intestinal stem cell niche (Barker et al., 2007; Liao et al., 2009). Further to this, it has been shown that CAIX expression in Mullerian epithelial cells represent the stem cells for endocervical reserve cells and columnar cells (Martens et al., 2007). Interestingly, CAIX expression did not appear to be induced only by hypoxia in these niches, but it seemed to be related to the functional status of and cell origin of the relevant tissue.

Furthermore, recent evidence suggest that CAIX expression is required for the maintenance of cancer stem cells, and plays a role in the invasive potential of breast cancer cells and the production of mammospheres (Lock et al., 2012; Sansone et al., 2007a). Experimental evidence shows that inhibition of CAIX activity with novel small-molecule inhibitors in breast cancer cell lines, or in primary metastatic breast cancer cells, results in the inhibition of breast cancer stem cells expansion in hypoxia (Lock et al., 2012). Further to this, it has been shown that CAIX is upregulated in basal-like breast tumours (Tan et al., 2009), which are characterized by their stem like

phenotype (Kim et al., 2012). Moreover, IL-6 induced Notch-3-dependent upregulation of the CAIX gene, and promoted a hypoxia-resistant/invasive phenotype in the breast cancer cell line MCF7 cells and in mammospheres, which are multicellular structures enriched in stem/progenitor cells of the mammary gland (Sansone et al., 2007b).

Finally, a CAIX knockout mouse has been generated by targeted gene disruption (Leppilampi et al., 2005). These mice developed gastric hyperplasia of the glandular epithelium with disrupted cell lineage differentiation leading to an increased number of surface pit cells and a reduction in the number of glandular chief cells (Leppilampi et al., 2005).

Therefore, we hypothesized that combination studies of currently identified stem cell markers together with analysis of CAIX expression status may give a direct insight into the relationship between tumour heterogeneity in response to hypoxia and the role of stem cells.

4.1.2 RNA sequencing

Microarray technology has been extensively used to study cancer genomes and transcriptomes. In breast cancer the molecular profiling obtained using microarrays has revealed the concept of breast cancer heterogeneity and has helped us to identify distinct molecular pathways that govern each distinct breast cancer subtype.

Although microarrays have been the technology of choice in most gene expression studies, recently researchers have been increasingly turning to a direct high-

throughput sequencing (RNA-seq) technology. In RNA sequencing the starting cDNA material is directly sequenced. Then the transcript sequences are mapped back to a reference genome (Malone and Oliver, 2011). Reads that map back to the reference are then counted to assess the level of gene expression, the number of mapped reads being the measure of expression level for the gene of interest or genomic region (Malone and Oliver, 2011).

In the present study, we used deep sequencing technology to identify differentially expressed transcripts and to explore the pathways that underlie the MCF7 sorted CAIX+ve and CAIX-ve subpopulations.

4.2 Results

4.2.1 Genes upregulated in CAIX positive cells versus CAIX negative cells.

To gain molecular insight into the profile of the CAIX+ve and CAIX-ve cells we determined their gene expression profile. We performed RNA-seq analysis of gene expression patterns within these two cell populations. Cells from the two sorted populations were exposed to hypoxia (0.1% O_2) for 72h, and then trypsinised and stained with the FITC conjugated CAIX antibody on ice for 1h followed by cell sorting. Unsorted normoxic and hypoxic cells were also included in the RNA sequencing. Following the 1h antibody incubation and the 1h cell sorting the RNA was extracted as described in materials and methods, and used for the RNA seq arrays. For this study, one replicate was used for each sorted population. A drawback of the hypoxic exposure is that the cells have to be re-oxygenated for 2 h before RNA extraction as antibody staining and cell sorting it cannot be performed inside the hypoxic chamber. However because of the long half-life of CAIX (72h) its expression levels remains the same after 2 h in normoxia.

The overall analysis of RNA-seq arrays revealed 2670 transcripts showing a greater than 2 fold up-regulation in CAIX+ve with respect to CAIX-ve, and 2093 transcripts showing a greater than 2 fold up-regulation in CAIX-ve with respect to CAIX+ve (**Appendix 1, Table 1 and Table 2**).

4.2.2 The two subpopulations showed similar hypoxia core responses

The genes that were upregulated in the CAIX+ve and CAIX-ve populations were compared to those regulated in response to hypoxia in the unsorted population. The overlap between these genes and genes up-regulated by hypoxia in the unsorted population was very small, and the probability of observing this overlap by chance was p=1 (hypergeometric test, lower tail, i.e negligible) (**Figure 4.1**). The overlap decreased further when increasing the threshold for considering a gene up-regulated, and amongst the top ranked genes there was no overlap. This is expected as the above analysis identifies the differences due to CAIX expression and implicitly removes some of the common hypoxia response by contrasting the two sorted populations directly, rather than simply comparing each one of them to a normoxic control.

However, also the pattern of differentially expressed genes in relation to the unsorted controls was tested. Interestingly, the expression pattern of the CAIX positive cells was significantly different from the one observed in both the CAIX negative and unsorted population (**Figure 4.2(A)**). The expression profile of the CAIX negative was more similar to the unsorted population (**Figure 4.2(B)**), and this may reflect the higher percentage of CAIX negative cells (70%) within the MCF7 unsorted population. Further to this, comparing the genes of the two sub-populations which are under hypoxia and the unsorted population under hypoxia with a common hypoxia signature (Buffa et al., 2010) showed a similar core hypoxia response, with no difference in expression of well established hypoxia genes (**Figure 4.2(C)**). This again suggests that the main, or currently well-characterized, hypoxia response is conserved between the two populations. The genes are ranked based on the fold

change in expression between CAIX+ve versus CAIX-ve (**Figure 4.2(A)**), fold change between CAIX-ve versus CAIX+ve (**Figure 4.2(B)**), and hypoxia signature score (**Figure 4.2(C)**)

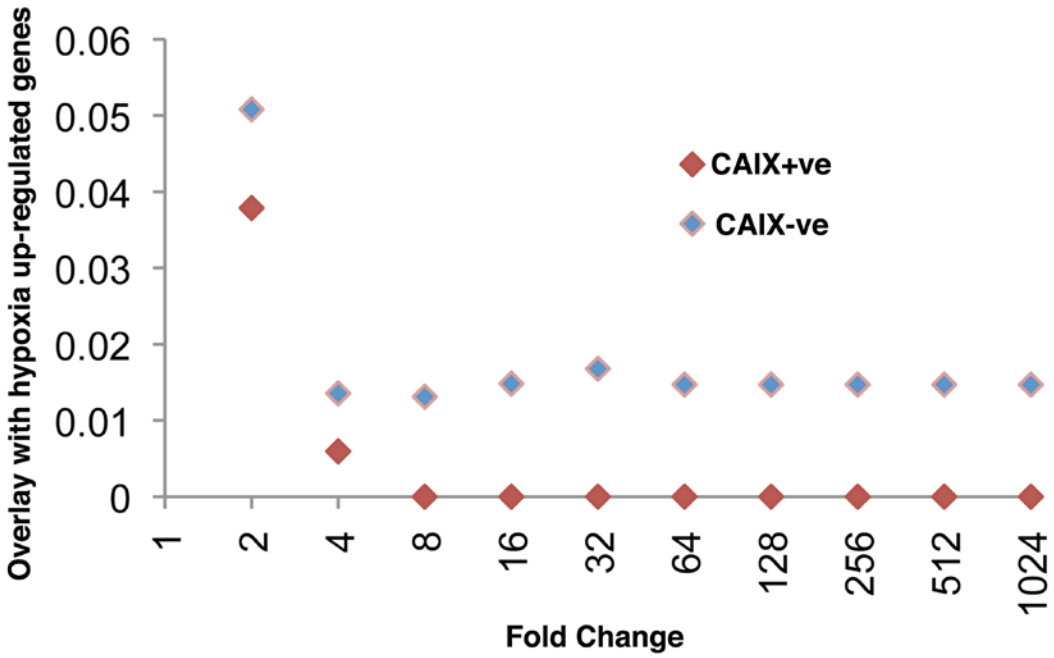


Figure 4.1 Percentage overlap between genes up-regulated under hypoxia in the unsorted population and genes differentially regulated between the two CAIX subpopulations. The normalized overlap is provided for various FC thresholds. The normalized overlap was calculated as the intersection of the gene lists normalized to the dimension of the global list (full overlap would be 1 and no overlap 0). Actual fold change is provided, plotted on a logged base 2 scale.

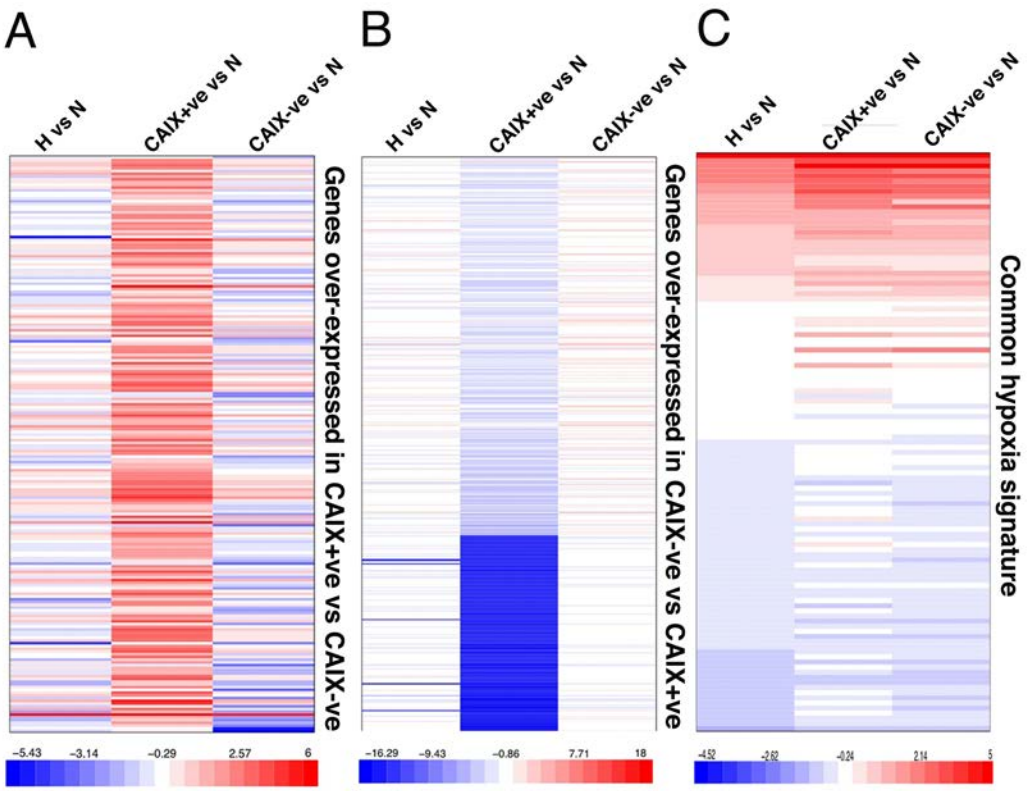


Figure 4.2 Relationship between CAIX transcriptional regulation and hypoxia. Expression of genes over-expressed in CAIX+ve with respect to CAIX-ve (A) and over-expressed in CAIX-ve with respect to CAIX+ve (B) is displayed for the three hypoxia conditions: 1) whole-population (left column), 2) CAIX+ve population (middle column) and 3) CAIX-ve population (right column) versus a normoxia whole-population control. Conversely, the expression of hypoxia related genes are displayed in the same three conditions (C). Fold changes (logged 2) are shown and the scale is provided at the bottom of each heatmap.

4.2.3 KEGG and IPA Pathway Analysis

4.2.3.1 Cancer stem cells pathways are upregulated in CAIX+ve cells

In order to place the two population signature genes into a functional context the CAIX+ve and CAIX-ve transcriptomes were analysed using KEGG and Ingenuity Pathway Analysis (IPA) software.

The KEGG pathway analysis showed that the CAIX+ve signature (i.e. genes up-regulated in CAIX+ve with respect to CAIX-ve) was significantly enriched for pathways involved in stem cell maintenance, such as the ABC transporters, Hedgehog and WNT signaling pathway **(Table 4.1**) and (**Appendix 3, Table 1**). These signaling pathways are implicated in the maintenance of tissue homeostasis by regulating self-renewal of normal stem cells as well as proliferation or differentiation of progenitor (transit-amplifying) cells cells (Katoh, 2007). The ABC transporters signaling pathway which is involved in stem cells survival is known to play a crucial role in the development of the multidrug resistance (MDR) (van de Ven et al., 2009). Increased expression levels of ABC transporters have been shown to correlate with decreases in response to various chemotherapy drugs and a reduction in overall survival (Wind and Holen, 2011). When the threshold for calling gene significantly differentially regulated was moved to a stricker FC>2.5 or >3 no annotation was significantly enriched.

Table 4.1: KEGG pathway analysis for CAIX+ve cells

Genes	Hyp*	Annotations
10	**0.0009**	**ABC transporters**
8	**0.0392**	**Wnt and Hedgehog signaling pathway**
14	0.0013	Dilated cardiomyopathy/tumour migration
12	0.0021	Arrhythmogenic right ventricular cardiomyopathy (ARVC)/ Tumour EMT
11	0.0088	Protein digestion and absorption/ECM components
16	0.0058	Cell adhesion molecules (CAMs)
12	0.0061	Hematopoetic cell lineage
15	0.0057	Glutamatergic synapse
35	<0.0001	Neuroactive ligand-receptor

(Hyp* = Corrected hypergeometric pValue)

Table 4.2: Ingenuity pathway analysis for CAIX+ve cells

Ingenuity Canonical Pathways	-log(p-value)*
Glutamate Receptor Signaling	4.84E00
Neuropathic Pain Signaling In Dorsal Horn Neurons	3.82E00
Xenobiotic Metabolism Signaling	3.57E00
Amyotrophic Lateral Sclerosis Signaling	2.92E00
Cellular Effects of Sildenafil (Viagra)	2.77E00
Synaptic Long Term Potentiation	2.59E00
GABA Receptor Signaling	2.08E00
Basal Cell Carcinoma Signaling	**2.04E00**
Calcium Signaling	2.01E00
Glycerolipid Metabolism	1.99E00
CREB Signaling in Neurons	1.97E00
Human Embryonic Stem Cell Pluripotency	**1.89E00**
Sphingosine-1-phosphate Signaling	1.86E00
Pyruvate Metabolism	1.82E00
LPS/IL-1 Mediated Inhibition of RXR Function	1.73E00
Cysteine Metabolism	1.64E00
FXR/RXR Activation	1.6E00
Synaptic Long Term Depression	1.45E00
TREM1 Signaling	1.44E00
Retinol Metabolism	1.4E00
Altered T Cell and B Cell Signaling in Rheumatoid Arthritis	1.4E00
Communication between Innate and Adaptive Immune Cells	1.34E00
Propanoate Metabolism	1.34E00
β-alanine Metabolism	1.29E00
Wnt/β-catenin Signaling	**1.21E00**

(*Statistical significance was determined by using Fisher's exact test ($P < 0.05$))

Agents commonly associated with this type of resistance include doxorubicin, daunorubicin, vinblastine, vincristine and paclitaxel (Wind and Holen, 2011). Interestingly, treatment of MCF7 unsorted cells with 20 μM and 50 μM verapamil, an ABC transporter inhibitor for 72h under hypoxia (0.1% O_2) resulted in the reduction of CAIX protein levels (**Figure 4.3A**). This reduction was independent of HIF-1α as verapamil did not affect the expression levels HIF-1α **(Figure 4.3A)**. In addition 72h treatment with 20μM verapamil causes a significant decrease in cell growth of MCF7 cells under hypoxic conditions (**Figure 4.3B**). These results suggest that ABC transporters may play an important role in the survival of CAIX+ve cells.

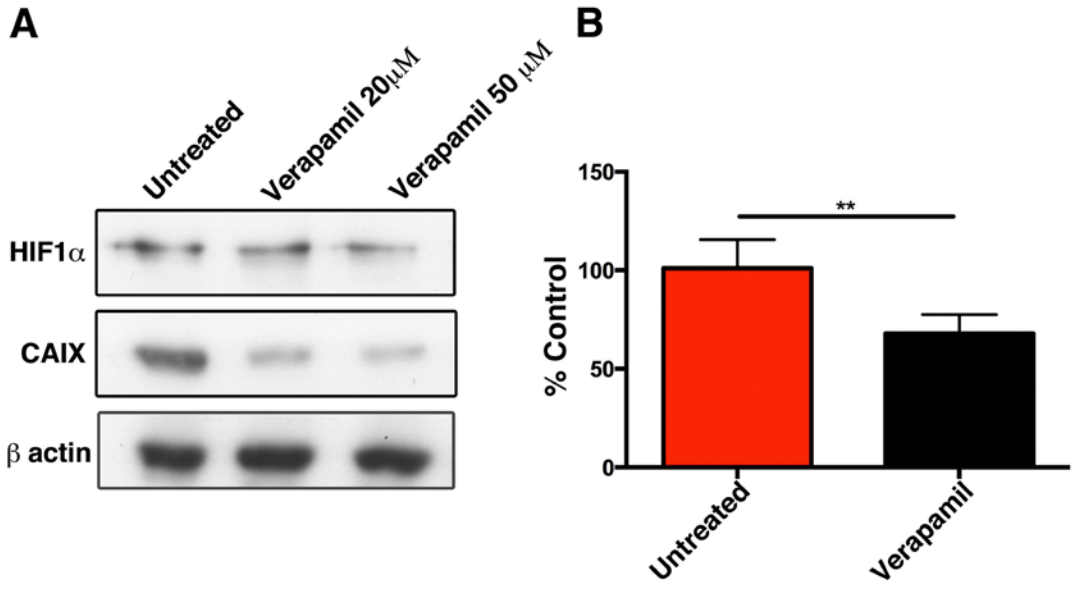


Figure 4.3 Treatment of unsorted MCF7 cells with verapamil. A) Western blot analysis of HIF-1α and CAIX demonstrates the downregulation of CAIX upon verapamil treatment in unsorted MCF7 cells under hypoxic conditions. B) Verapamil treatment causes decrease in cell growth of MCF7 cells.

The Wnt pathway and Hedgehog signaling pathways were also upregulated in the CAIX+ve cells. As described before, both pathways are involved in the stem cell fate and deregulation of the Wnt pathway and can lead to excessive stem cell renewal, proliferation and predisposing of tumourigenesis (Taketo, 2004). It has been implicated in a wide variety of human tumours and early clinical trials, and pathway antagonists have validated Hedgehog signaling as a promising anticancer target (Merchant and Matsui, 2010). Overall, the upregulation of these pathways in the CAIX+ve populations suggests that this population may be enriched with stem-like cells.

The pathway analysis also revealed upregulation of other signaling pathways such as arrhythmogenic right ventricular cardiomyopathy (ARVC), dilated cardiomyopathy, protein digestion and absorption. Genes belonging to these pathways are involved in tumour migration, epithelial-mesenchymal transition (EMT), and are also components of extracellular matrix (ECM). Genes associated with EMT phenotype besides the WNT signaling genes, were N-cadherin and catenin (**Appendix 3, Table 1**). Tumour migration associated genes included the myosin heavy chain 7 and the myosin heavy chain 6. Interestingly, it has been suggested that the non-muscle myosin II is involved in tumour migration by contributing to the contraction of the cell rear (Beach et al., 2011) (**Appendix 3, Table 1**). Overall this could suggest that besides the necessity of the induction of EMT, that allows cancer cells to acquire migratory and invasive properties, tumour migration and invasion may also require cytoskeletal force generation (Beach et al., 2011). However, how cytoskeletal forces drive the mechanical process of invasion is not well understood (Beach et al., 2011).

Our sequencing data also showed that the CAIX+ve populations upregulate genes that are important for their interaction with the ECM (**Appendix 3, Table 1**). Mounting evidence suggests that the ECM is an essential non-cellular component of the adult stem niche. Abnormal changes of the ECM can also disrupt the cellular differentiation process, resulting in the loss of differentiation and an increase of stem/progenitor cell pool (Lu et al., 2012). In addition various collagens, including collagen I, II, III, V and IX show increase deposition during tumour formation (Lu et al., 2012). Interestingly, the CAIX+ve cells have higher expression of collagen IV, IX, XI, XVI and they also express genes coding for calcium channels, which has been showed to lead to an increase turnover of focal adhesions and more effective proteolysis of ECM (Prevarskaya et al., 2011) **(Appendix 3, Table 1).**

Bioinformatics analysis using Ingenuity pathway analysis (IPA) software was also used to interpret the list of the CAIX+ve upregulated genes. The purpose of using two different bioinformatics software was to have a more comprehensive analysis of our results. The major difference in the compatibility of the two softwares are the use of different analysis algorithms to interrogate biological pathway information (Soh et al., 2010). For example, KEGG database is curated independently by a single lab from published literature, whereas Ingenuity is a commercial product (Soh et al., 2010). Extended research and discussion of the differences between different bioinformatics software is beyond the scope of this study.

The IPA database analysis revealed a larger number of biological pathways (**Table 4.2**) and (**Appendix 3, Table 2)**. Among them the stem cells pathways, such as

Human Embryonic Stem Cell Pluripotency, the basal cell carcinoma and the Wnt/β-catenin signaling pathway were consistent between the two databases. In addition, IPA was used to predict transcription factors that regulate the upregulated genes in our dataset. Interestingly, among them, there are transcription factors regulating stem cell genes such as E2F-1, HMGB1, KLF4, Snail, TBX3 and Twist1 **(Appendix 1, Table 3)**. These results strengthen our hypothesis that CAIX+ve cells are enriched with cells expressing stem cell markers.

4.2.4 CAIX positive cells upregulate stem cells genes

Previous studies have shown that CAIX expression in normal tissues may serve as a biomarker of stem cell or transit amplifying cells (Liao et al., 2009). In order to test if the CAIX+ve population is enriched with markers associated with a stem cell phenotype, and to validate the results of the RNA-Seq, I extracted RNA from the freshly sorted MCF7 CAIX+ve and CAIX-ve cells and examined the mRNA expression levels by q-PCR of genes that are implicated in stem cell maintenance, in the epithelial mesenchymal transition (EMT) and multidrug resistance. This analysis showed that significantly upregulation of ALDH1 ($p<0.001$, n=3, biological replicates, biological replicates), WNT2 ($p<0.01$, n=3, biological replicates), TWIST1 ($p<0.001$, n=3, biological replicates), LIN28 ($p<0.001$, n=3, biological replicates), ABCC2 ($p<0.01$, n=3, biological replicates), IGF1 ($p<0.001$, n=3, biological replicates), SOX2 ($p<0.05$, n=3, biological replicates) in CAIX+ve population (**Figure 4.4A**). In addition, the protein expression levels of ALDH1 in the CAIX+ve cells sorted from two different cells lines, MCF7 and HCT116 were also higher compared to the CAIX-ve cells (**Figure 4.4B**).

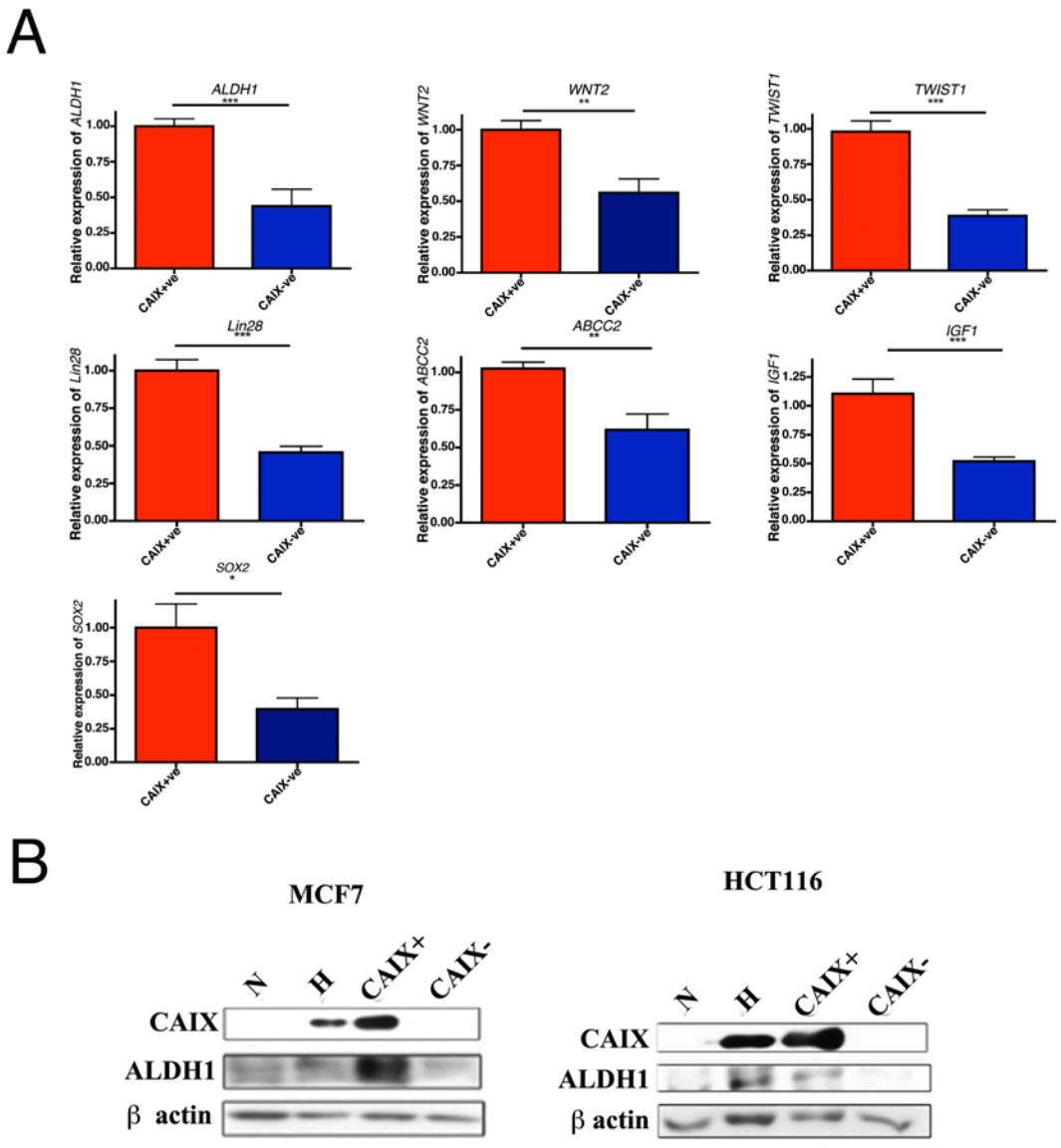


Figure 4.4 mRNA expression profiles of the CAIX+ve and CAIX-ve sorted MCF-7 cells. (A) qPCR analysis of genes implicated in stem cell maintenance in CAIX+ve and CAIX-ve populations in MCF-7 cells. (B) Protein levels of ALDH1 in MCF-7 and HCT116 cell lines. *=p<0.05 **=p<0.01, ***=p<0.001. Error bars represent SD.

In order to understand whether CAIX is causative or correlative with the stem cell phenotype, CAIX was silenced in CAIX+ve cell line and the gene expression of *ALDH1*, *TWIST1* and *ABCC2* was tested. CAIX+ve cells were transfected with *CA9* siRNA or scr siRNA and exposed to 0.1 % O_2 for 72h. RNA was extracted and the gene expression levels of *ALDH1*, *TWIST1* and *ABCC2* were evaluated by q-PCR. The results showed that CAIX siRNA knockdown caused significant reduction in the expression levels of the tested stem cells genes *ALDH1* ($p<0.05$, n=3, biological replicates), *TWIST1* ($p<0.05$, n=3, biological replicates), and *ABCC2* ($p<0.001$, n=3, biological replicates), (**Figure 4.5**).

Additionally, our laboratory have shown that CAIX knockdown in xenograft tumours of MDA-MB-468 (breast cancer) cells using stable shRNA resulted in a significant reduction of the expression of stem cell associated genes. These included homeobox genes and development proteins involved in stem cell maintenance such as OCT4 and NANOG, TWIST1, JAG2 (Ledaki I, McIntyre A, in submission, 2013).

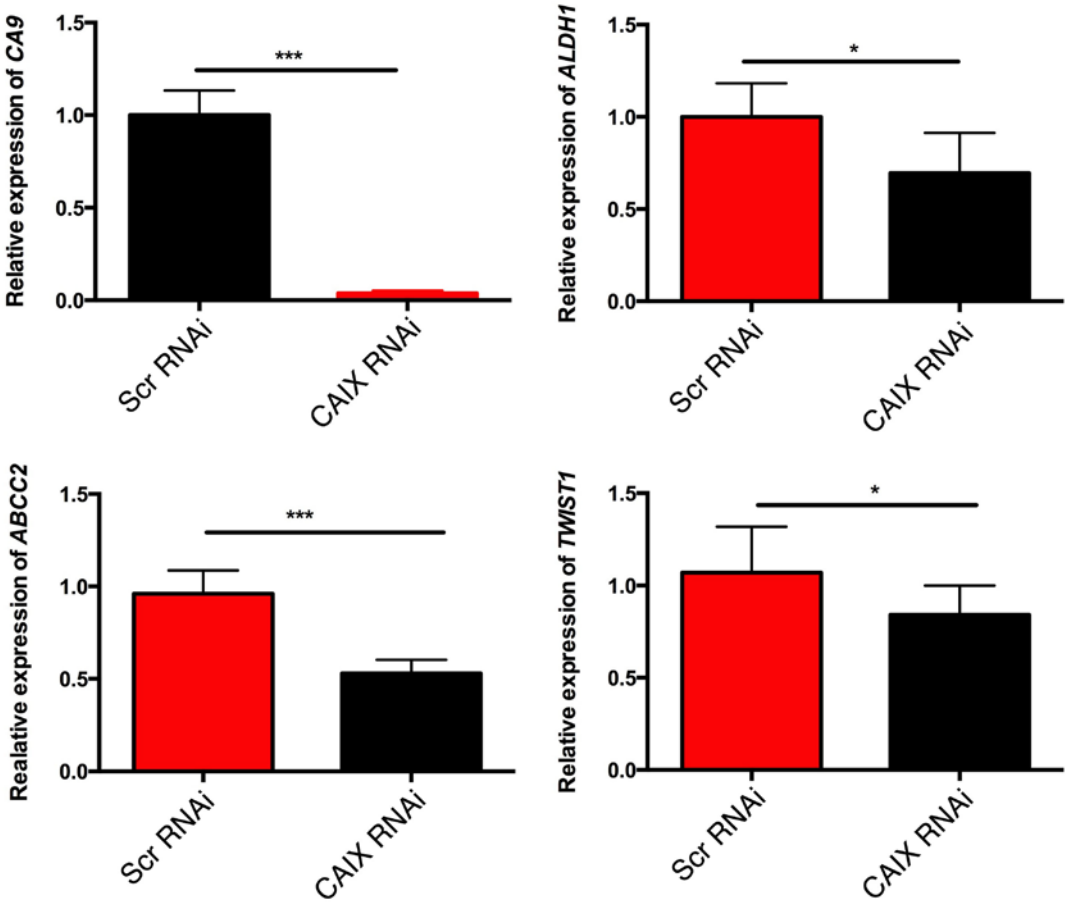


Figure 4.5 q-PCR analysis of genes implicated in stem cell maintenance in CAIX+ve cells transfected with Scr RNAi or CAIX RNAi. The expression of stem cells genes are significantly reduced in CAIX knockdown cells. *=$p<0.05$, ***=$p<0.001$.Error bars represents SD.

4.2.5 CAIX positive cells display an upregulation of mTORC1 pathway.

A recent study has shown that CAIX expression is essential in modulating the activity of mTOR under hypoxic conditions (Lock et al., 2012). Prior to this, the mTOR pathway was reported to be important for the viability and maintenance of breast cancer stem cells (Zhou et al., 2007a).

To examine if there is differential activation of mTOR signaling, I checked by western blot the expression levels of the ribosomal phospho S6 kinase ($pS6K^{SER235/236}$) and 4E-BP1, two downstream targets of mTORC1 component in the CAIX+ve and CAIX-ve cell lines. The results showed that the CAIX+ve cell line display an activation of mTORC1 component, leading to a remarkable upregulation in the phosphorylation of S6 kinase as well as an increased expression of 4EBP1 both, under normoxic and hypoxic conditions (**Figure 4.6A**).

Previous studies have shown that rapamycin inhibits the mTOR signaling to downstream targets, S6K1 and 4E-BP1 (Hidalgo and Rowinsky, 2000). Given the above, I wanted to check the effect of mTOR inhibition on CAIX expression. To this end, CAIX+ve cell line was treated with 20 μM□□□□□□□□□□□□ for 72h and exposed to 0.1% O_2. We performed FACS and western blot based analysis to evaluate the protein levels of CAIX, HIF-1α, LDHA, PDK1 and AK4 upon rapamycin treatment. Also, the mRNA levels of *CA9* were examined by q-PCR analysis. Rapamycin treatment caused a significant reduction of CAIX both at protein ($p<0.01$,

n=3, biological replicates) and RNA levels ($p<0.001$, n=3, biological replicates) (**Figure 4.6B**, **Figure 4.6C(i)** and **Figure 4.6C(ii)**). Rapamycin treatment caused also a reduction in the level of HIF-1α□ although to a lesser extent than CAIX. Interestingly, the expression levels of the other HIF-1α regulated genes LDHA and PDK1 did not change upon rapamycin treatment (**Figure 4.6D**).

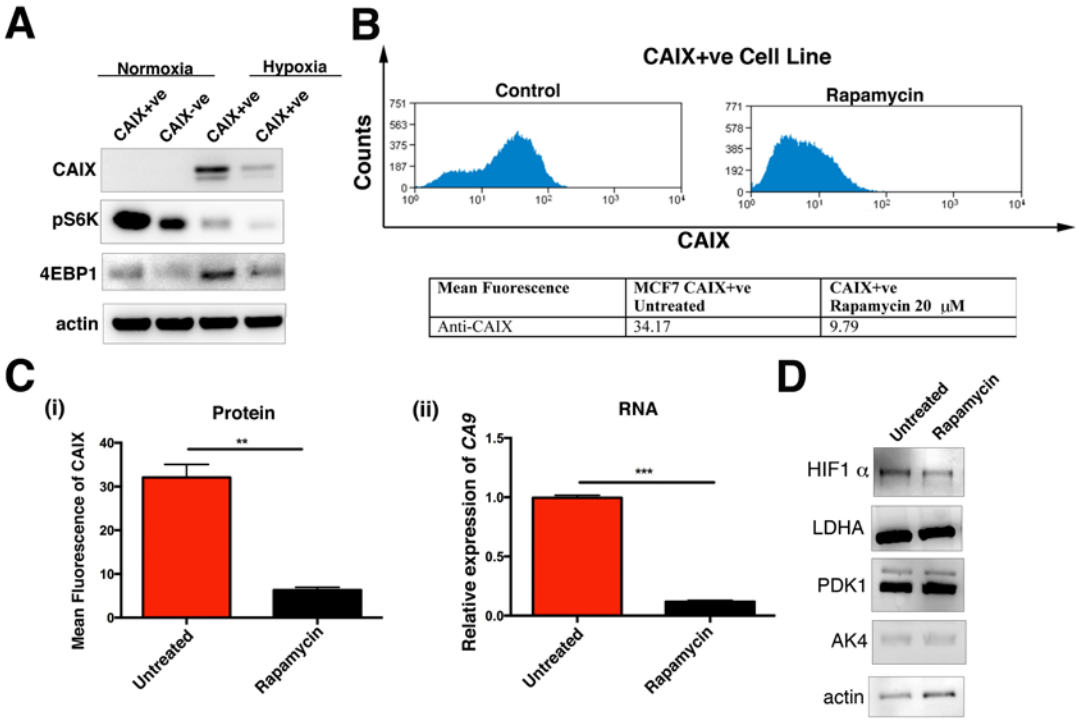


Figure 4.6 Expression of mTORC1 components in CAIX+ve and CAIX-ve cell lines. A) Protein expression levels of pS6K$^{SER235/236}$ and 4EBP1 in CAIX+ve and CAIX-ve cell lines under normoxia and hypoxia. B) Representative FACS analysis of CAIX in untreated and rapamycin treated CAIX+ve cell line under hypoxia. C)(i) Mean fluorescence of CAIX in in untreated and rapamycin treated CAIX+ve cell line under hypoxia. (ii) Relative mRNA expression of *CA9* in untreated and rapamycin treated CAIX+ve cell line under hypoxia. D) Protein expression levels of HIF-1α□, LDHA, PDK1 and AK4 in in untreated and rapamycin treated CAIX+ve cell line under hypoxia. *=p<0.05 **=p<0.01, ***=p<0.001. Error bars represent SD.

4.2.6 Genes and pathways upregulated in CAIX negative cells

The same analysis was performed in order to cluster the CAIX-ve upregulated genes in functional pathways. The KEGG analysis showed that CAIX-ve cells were enriched for cytokine-cytokine receptor interaction, the mitogen-activated protein kinase (MAPK) signaling pathway, osteoblast differentiation and ECM-receptor interaction pathway **(Table 4.3).**

The MAPK kinase pathways transduce a large variety of external signals, leading to a wide range of cellular responses, including growth, differentiation, inflammation and apoptosis. Further to this, the cytokine-cytokine receptor interaction pathway shows that the CAIX-ve cells express high levels of cytokines such as TGF-β, M-CSF, CXCL5 and members of the TNF superfamily (**Appendix 3, Table 3)**.

Given the above, I suggest a mechanism by which these two populations may interact with each other and with their environment; i.e. CAIX-ve secreted cytokines induce paracrine signals that regulate the CAIX+ve cells. Supportive evidence for the above model is a recent study showing that cytokines such as IL-1, IL-6, TNF-α and TGF-β positively influence CAIX expression under both normoxic and hypoxic conditions (Kockar et al., 2012). Further to this, it has been shown that cytokines such as CXCL5, M-CSF-1, CXCL1 as well as TGF-β generated by cells within the tumour stimulate CSC self-renewal, which then promote tumour growth, EMT and metastasis (Adamson et al., 1988; Ginestier et al., 2010a; Korkaya et al., 2011b; Liu et al., 2011b; Place et al., 2011; Sansone et al., 2007a).

The release of cytokines and specific CSF-1 from tumour cells results in the recruitment of the macrophages to the tumour periphery where they secrete motility and angiogenic factors that facilitate tumour cell invasion and metastasis (Korkaya et al., 2011a). Importantly, CSF-1-deficient mice lack macrophages and have significantly lower rates of tumour progression and metastasis formation in models of breast cancer (Scholl et al., 1994). In breast cancer patients, CSF-1 was expressed in 74% of the tumours and associated with poor prognosis (Lin et al., 2001). Thus, recruitment of tumour-associated macrophages (TAMs) to tumour sites via CSF-1 and other chemokines appears to be crucial for tumour progression in many types of cancers (Pollard, 2004). Also our laboratory has previously shown an increase in macrophage infiltration in xenografts tumours from CAIX knockdown HT29 (shCAIX) colon cancer cell line compared to empty vector (EV) controls. In addition to this, xenografts tumours from overexpressed CAIX HCT116 (FLCAIX) colon cancer cells showed a reduction in tumour associated macrophages (**Figure 4.9**).

Consistent with the KEGG pathway results, IPA analysis revealed upregulation of pathways implicating in cytokine signaling such as the IL-17A Signaling in Gastric and fibroblasts cells, the Role of JAK1 and JAK3 in γc Cytokine Signaling, as well as macrophage related pathway like the Role of Macrophages, Fibroblasts and Endothelial Cells in Rheumatoid Arthritis (**Table 4.4**) and (**Appendix 3, Table 4**).

Table 4.3 KEGG pathway analysis for CAIX-ve cells

Genes	Hyp*	Annotations
15	**0.0007**	**Cytokine-cytokine receptor interaction**
13	**0.0072**	**MAPK signaling pathway**
8	0.0203	Osteoclast differentiation
6	0.0341	ECM-receptor interaction
6	**0.0376**	**TGF-beta signaling pathway**

(Hyp* = Corrected hypergeometric pValue)

Table 4.4 Ingenuity pathway analysis for CAIX-ve cells

Ingenuity Canonical Pathways	-log(p-value)
Atherosclerosis Signaling	3.64E00
Primary Immunodeficiency Signaling	3.43E00
LPS/IL-1 Mediated Inhibition of RXR Function	3.28E00
IL-17A Signaling in Gastric Cells	**3.14E00**
TNFR2 Signaling	2.91E00
LXR/RXR Activation	2.58E00
IL-17A Signaling in Fibroblasts	1.72E00
Intrinsic Prothrombin Activation Pathway	1.64E00
MIF Regulation of Innate Immunity	**1.64E00**
Acute Phase Response Signalling	1.58E00
Tryptophan Metabolism	1.56E00
Pathogenesis of Multiple Sclerosis	1.56E00
cAMP-mediated signaling	1.56E00
Antigen Presentation Pathway	1.53E00
Role of Macrophages, Fibroblasts and Endothelial Cells in Rheumatoid Arthritis	**1.52E00**
Dendritic Cell Maturation	1.5E00
Activation of IRF by Cytosolic Pattern Recognition Receptors	1.5E00
Role of JAK1 and JAK3 in γc Cytokine Signaling	**1.5E00**
Role of JAK1 and JAK3 in γc Cytokine Signaling	**1.5E00**
Communication between Innate and Adaptive Immune Cells	1.47E00
TNFR1 Signaling	1.36E00
Retinol Metabolism	1.35E00
Caveolar-mediated Endocytosis Signaling	1.3E00

(*Statistical significance was determined by using Fisher's exact test ($P < 0.05$))

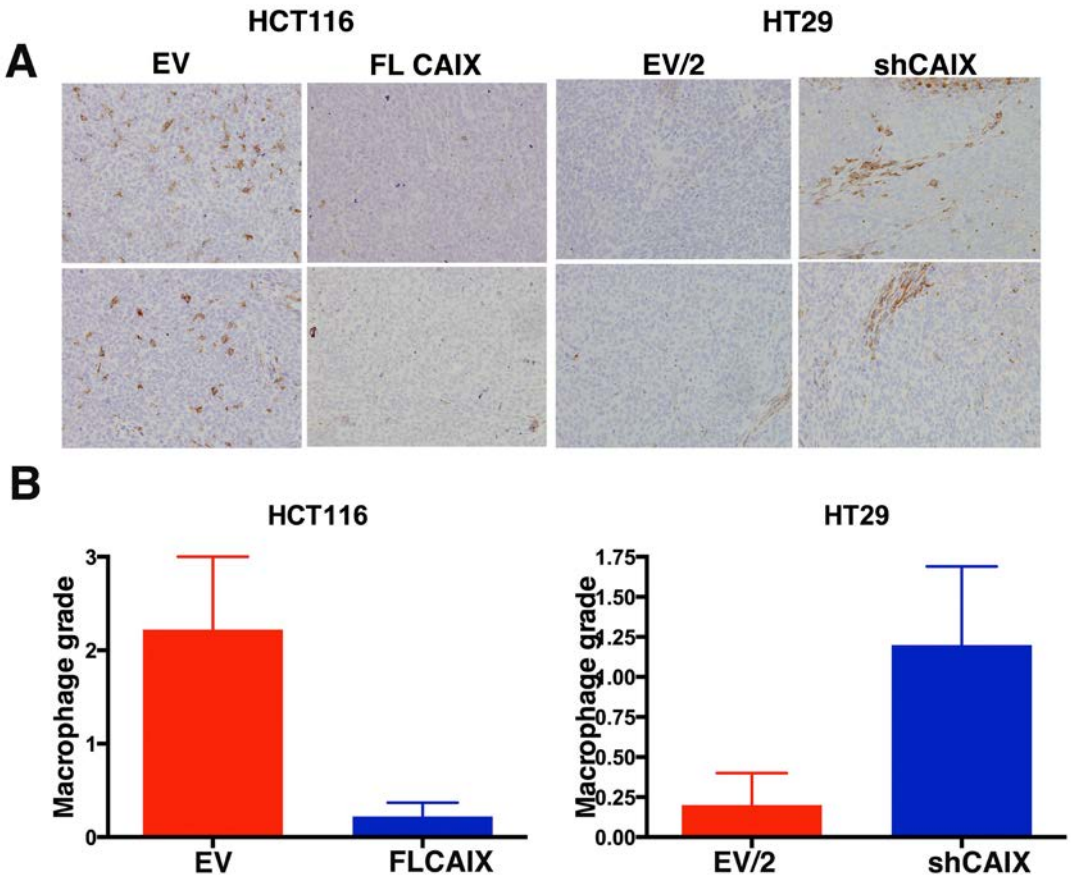


Figure 4.7 Examples of HCT116 EV and FLCA9, HT29 EV and sh CA9 xenografts stained for F4/80 antibody (A). B) Bar scoring of macrophage infiltration in HCT116 transfected with empty vector (EV) and CA9 coding sequence (FLCAIX), and HT29 transfected with empty vector (EV) and an shRNA targeting CA9 (shCAIX). Error bars represent SD.

4.3 Discussion

Recent evidence has expanded on the role of hypoxia by relating it to stem cell niches. The stem cell niche is a distinct microenvironment where stem cells reside in order to control proliferation and apoptosis whilst maintaining a stem-cell like phenotype (Borovski et al., 2011). Evidence for the role of hypoxia in the stem cell niche can be found in bone marrow where hematopoietic stem cells reside in regions regulated by oxygen tension (Heddleston et al., 2010b). In addition, the transcription factors HIF-1α and HIF2α have been linked to the stimulation of cancer stem cells (CSCs) in glioblastoma (Heddleston et al., 2009; Soeda et al., 2009). Further to this, Wicha *et al* has shown that hypoxia increases the population of breast CSCs in xenografts (Wicha et al., 2006). Accordingly, the poor patient survival and therapeutic resistance that is associated with hypoxia may result from increased proportion of CSCs in tumours (Yeung et al., 2011).

We conducted a deep sequencing analysis of the transcriptomes of CAIX+ve and CAIX-ve cells. We show for the first time, that hypoxia promotes tumour heterogeneity through CAIX induction. In addition, we show the CAIX+ve subpopulation is significantly enriched for stem cell related genes.

Among those were WNT, Hedgehog and ATP-binding cassette (ABC) signaling pathways which have been shown to play an important role in the recurrence and maintenance of cancer stem cells (Hu and Fu, 2012) as well as in the regulation of the self-renewal of normal stem cells (Katoh, 2007). In addition to this, CAIX+ve cells

showed significantly higher expression of well validated CSC markers including ALDH1 (Croker et al., 2009), SOX2 (Ben-Porath et al., 2008; Leis et al.), Lin28 (Lv et al., 2012; Peng et al., 2010) and IGF1 (Boiani and Scholer, 2005). The CAIX+ve cell population also showed a higher expression of EMT genes such as WNT2, TWIST1, N-cadherin and BMP6, which are known to be involved in the maintenance of the mesenchymal phenotype, a characteristic of breast CSC (Creighton et al., 2010; Mani et al., 2008). In addition, using the IPA software many transcription factors predicted and among them are regulators of stem cell genes such as E2F-1, HMGB1, KLF4 (Hoffmeyer et al., 2012), Snail (Moody et al., 2005), TBX3 (Fillmore et al., 2010) and Twist1(Vesuna et al., 2009). Future work could answer if these transcription factors regulate CAIX expression and if they play role in maintenance and expansion of stem cells populations under hypoxic conditions.

Our observation of the persistent heterogeneity under hypoxic conditions in the CAIX population and the associated biology support previous studies showing that CAIX expression is associated with stem cell niches in normal tissues (Liao et al., 2009) and provides molecular insight into the mechanisms that could be driving this phenotype. In line with this, it has been shown that CAIX expression is required for the maintenance of CSC, and plays a role in the invasive potential of breast cancer cells and mammospheres (Lock et al., 2012; Sansone et al., 2007a). In addition, a recent study has conducted a gene expression profile of human cervical carcinoma cell line C33A overexpressing exogenous CAIX (Shin et al., 2011). The results of this study have shown CAIX overexpression induces weakening of cell adhesions and augmented cell motility, underlying a mechanism of CAIX-related enhanced

metastatic potential of tumor cells (Shin et al., 2011). The comparison of the upregulated genes of the C33A cells overexpressing exogenous CAIX that have FC>2 (34 in total) with the CAIX+ve and CAIX-ve signatures showed a very small overlap between the gene lists. The common genes with the CAIX+ve signature are the CAIX, GAP43 which is involved in cell growth and cell size, RGS18 involve in signal transduction, NEFH and EPB41L3 involve in the structure contistuent of cytoskeleton. The CAIX-ve signature has only the Apoliprotein E gene in common. The low overlap between the CAIX+ve signature and the C33A overexpressing exogenous CAIX could be due to the different experimental settings and to different cell types. Gene expression arrays in the CAIX+ve and CAIX-ve populations sorted populations of other breast cancer cell lines as well as from other tumour types such as colon cancer would be very important be to be conducted as they will show if these results are cell line specific and also which of the genes are overlapping between different cell lines.

Furthermore, I demonstrated that the functional suppression of CAIX with CAIX siRNA resulted in the downregulation of breast cancer stem cell gene signatures. This suggests that CAIX does not serve only as a marker for the enrichment of hypoxic cancer stem cells, but its expression is causative with the stem cell phenotypes we observed in the CAIX+ve cells. The detailed molecular mechanism through which hypoxia-induced CAIX regulates stemness in the CAIX+ve compartment will need further investigation. One possibility is to create an extensive microenvironment of regulated pH around the much fewer stem cells, a syncytial pH rim, as we showed previously in spheroid models of CAIX expression (Swietach et al., 2008). I would

suggest a term for this population, the hypoxia induced 'stem cell buffer zone' producing a pH protected syncytial zone including a minor stem cell population, but having properties conducive to protect them from environmental stress.

In addition, the 'stem cell buffer zone' may allow the activation of important functional pathways controlling the regulation of EMT and stemness. An example of such a stem cell associated pathway in which activation is controlled by pH is mTOR signaling. The mTORC1 pathway has been reported to be important for the viability and maintenance of breast cancer stem cells (Zhou et al., 2007a). Previous studies have shown that inhibition of mTORC1 signaling *in vitro* disrupts EMT induction and cell invasion and enhances sensitivity to chemotherapeutic agents (Lock et al., 2012). In addition, the mTOR inhibitor rapamycin and its analogs are used in the treatment of cancer, including breast cancer (Lock et al., 2012; Vignot et al., 2005).

Recent studies have suggested that an acidic pH inhibits mTORC1 signaling, resulting in the downregulation of energy-consuming anabolic processes such as protein synthesis as an adaptive response to metabolically stressful conditions (Balgi et al., 2011). Also CAIX expression and activity is an essential regulator for mTORC1 activation and signaling to the cap-dependent translation regulator 4EBP1 (Lock et al., 2012). Given the above, we suggest that the neutral intracellular pH due to CAIX expression in the positive population may be one of the reasons for the upregulation of mTORC1 signaling in these cells. Furthermore, mTORC1 signaling may be the critical regulator by which CAIX regulates stemness and EMT in the CAIX+ve cells.

Over 120 years ago, Paget proposed the “seed and soil” hypothesis of tumour metastasis (Fidler, 2003; Korkaya et al., 2011a). Reframed in modern context, the seeds are the CSCs, and the soil is the rich microenvironment composed of diverse cell types that interact with tumour cells via growth factors and cytokine networks (Fidler, 2003; Korkaya et al., 2011a). Consistent with this notion, our pathway analysis suggests that the two subpopulations interact with each other and with their environment. It has been shown previously that CAIX upregulation by IL-6 in a Notch-3 dependent manner promotes self-renewal, hypoxia survival and the invasive potential of the stem/ progenitor cells in the mammary gland (Sansone et al., 2007a). Although it has been argued that the cytokine may be secreted by cancer cells, it has not yet been determined if IL-6 triggers an autocrine or paracrine loop to boost stem self renewal in the mammary gland (Sansone et al., 2007a). In contrast, our pathway analysis showed that CAIX-ve cells express high levels of cytokines such as TGF-β, M-CSF, CXCL5 and members of the TNF superfamily but not IL-6. Based on this, CAIX-ve cells secreted cytokines may induced paracrine signals that regulate the stem cells of the CAIX+ve cells, and provide a wider hypoxia tolerant microenvironment to protect the stem cell population. This is supported by a recent study showing that cytokines such as IL-1, IL-6, TNFα and TNFβ positively influence CAIX expression under both normoxic and hypoxic conditions (Kockar et al., 2012). Additionally, it has been shown that cytokines generated by cells within the tumour stimulate CSC self-renewal, which then promote tumour growth, EMT and metastasis (Adamson et al., 1988; Ginestier et al., 2010b; Korkaya et al., 2011a; Sansone et al., 2007a).

I suggest that expression of cytokines by CAIX-ve cells result in the recruitment of tumour - associated macrophages. Consistent with this notion, we showed that xenograft tumours from CAIX knockdown HT29 colon cancer cells had an increased macrophage infiltration, whereas xenograft tumours from overexpressing CAIX HCT116 colon cancer cells showed a reduction in the number of the tumour associated macrophages. Interestingly, recent studies have indicated that macrophages promote CSC proliferation and metastasis (Hao et al., 2012; Liu et al., 2011a; Pollard, 2004).

In conclusion, I identified a differential expression of the hypoxia transcriptome that allowed us to define major phenotypic differences in the CAIX+ve and CAIX–ve populations of both breast and colon cancer cell lines. Interestingly, I showed that the CAIX+ve population is enriched with cells expressing cancer stem cell markers. Our findings also suggest that tumours are not homogenous in their response to hypoxia, and distinct signal transduction networks are regulating different populations of cells within the tumour. This highlights the need for the identification of new biomarkers capable of monitoring distinct functional signaling profiles of human cancers, thus permitting the accurate stratification of tumours.

Chapter Five

CAIX+ve cells show functional properties of stem cells and differential sensitivity to HDAC inhibitors

5.1 Introduction

In Chapter Four we showed that the CAIX+ve cells express stem cell markers at a significantly higher level than CAIX-ve cells. It is crucial though to validate if the CAIX+ve sub-population has greater stem cell characteristics. These include extensive self-renewal, generation of a large number of progeny, and multi-lineage differentiation potential as well as the several fold higher *in vivo* capacity to form tumours compared to the control fraction.

5.1.1 *In vitro* stem cells assays: Anchorage independent cell growth and colony forming ability

The two gold standard *in vitro* assays currently used to demonstrate the self renewal property of cancer stem cells are the colony forming assays and the cell culture in non adherent conditions, which results in the propagation of cells as tumourspheres. The colony-forming assay measures the functional capacity of stem cells and has been used recently to study breast and colon cancer stem cells (Asselin-Labat et al., 2011; Yeung et al., 2010). The cell culture in non-adherent conditions was first used in cells isolated from normal breast obtained from mammoplasty (Dontu et al., 2003; Dontu and Wicha, 2005). This assay showed that only the mammary stem cells had the ability to survive in suspension and generate 3D non-adherent colonies called mammospheres. These mammospheres were enriched in mammary stem cells and were able to differentiate into all three mammary epithelial lineages as well as to clonally generate complex functional structures in reconstituted 3D culture systems. Consistent with previous findings, the mammospheres derived from reduction mammoplasties could produce successful outgrowths after transplantation of as few as 500 mammospheres into NOD/SCID mice (Dontu and Wicha, 2005; Rota et al.,

2012). It has been also shown that mammospheres could be formed from a stem cell fraction isolated from the MCF7 breast cancer cell line and this population displays resistance to pro-apoptotic agents and greater tumourigenicity than its parental line in immunodeficient mice (Cariati et al., 2008). In addition to the ability of stem cells to form mammopsheres, investigators have studied the ability of cells to generate secondary and subsequent generation mammospheres as these correlate with greater confidence the number of sphere forming cells with number of multipotential progenitors or stem cells (Rota et al., 2012). This assay is now widely used as a measurement of stemness in normal and cancer stem cells and for the identification of pathways that are implicated in stem/progenitor cells survival (Harrison et al., 2010; Ponti et al., 2005).

5.1.2 *In Vivo* assays: Tumour Xenografts

According to the stem cell theory, only stem cells have the ability to self renew, differentiate and form tumours (Reya et al., 2001). Therefore, the most widely accepted *in vivo* assay to validate the stem cell properties of a candidate cancer stem cell subpopulation is tumour xenografts (Quintana et al., 2008). An advantage of the tumour xenograft experiments compared to the cell line-derived xenograft are that they produce an environment mimicking the original patient environment, in which the tumour grows by maintaining the cell differentiation and morphology, the architecture, and molecular signatures of the original tumours (Boven et al., 1992).

5.1.3 Histone Deacetylases inhibitors

The unique CSCs properties of cell differentiation and somatic cell reprogramming to pluripotency are mainly regulated by epigenetic mechanisms (Hochedlinger and Plath, 2009). These in turn are regulated by enzymatic modifications of histone proteins

such as for example, their acetylation status. In this case the opposing activities of histone acetyltransferases (HAT) and histone deacetylases (HDAC) provide a dynamic mode of regulation (Zhou et al., 2011). Deregulated HDAC activity is commonly found in human cancers (Dokmanovic et al., 2007; Glozak and Seto, 2007; Jones and Baylin, 2007). Inhibition of HDAC function with small molecules inhibitors (HDACi) have been shown to block deacetylation, causing cell cycle arrest, differentiation, and/or apoptosis of tumour cells (Pandolfi, 2001). HDACi are a diverse group of compounds that are divided into classes I-IV. HDAC inhibitors do not act solely as inhibitors of HDACs as a large number of non-histone transcription factors and transcriptional co-regulators are known to be modified by acetylation (Thirlwell et al., 2011). Thus HDCAi have attracted considerable therapeutic attention, and several HDACi's are in various stages of clinical development, with suberoylanilide hydroxamic acid (SAHA) to be the first HDACi approved by the FDA for cancer therapy (Lagger et al., 2002; Wagner et al., 2010).

It has been reported that HDACi downregulates HIF-1α stability in cancer cell lines (Fath et al., 2006). It has been suggested that the transcription complexes of HIF-1α and HIF-2α require modification by type I/II deacetylases in order to become transcriptionally active, it is through this mechanism that HDAC inhibitors are thought to reduce HIF transcription (Fath et al., 2006; Thirlwell et al., 2011). In line with this, it has been shown that sodium butyrate (NaBu) a novel HDACi, downregulates HIF-1 and VEGF expression under hypoxic conditions and it inhibits *in vivo* and *in vitro* angiogenesis (Kim et al., 2007).

Interestingly, the effect of HDAC on chromatin organization is also associated with the regulation and maintenance of stem cell pluripotency in coordination with

numerous signaling pathways (Sun et al., 2011). Supporting evidence for this are findings that show acceleration of the early differentiation steps of embryonic stem cells (ES) upon treatment with TSA, a histone deacetylase inhibitor. Genome-wide analysis revealed two gene groups that are targeted by TSA: the first one contains genes related to pluripotency that are suppressed by TSA (Sall4, Nanog, Klf4, Oct4, and Sox2), the second is required for lineage-specific differentiation and its expression is upregulated by TSA (Karantzali et al., 2008; Kretsovali et al., 2012). In addition to this, treatment with NaBu causes pancreatic and hepatic differentiation of mouse and human ES cells (Rambhatla et al., 2003; Ren et al., 2010; Zhou et al., 2007b). It has been demonstrated also that treatment of HT29 and CaCo2 colon cancer cell lines with NaBu causes a reduction in the expression of the stem cell markers CD133 and CD44 (Haraguchi et al., 2008).

Concordant with this, in this chapter we also investigated the effects of the broad class I and class II HDAC inhibitors (HDACi) SAHA (a hydroxamate-based HDACi) and sodium butyrate (NaBu) on the CAIX+ve and CAIX-ve populations.

5.2 Results

5.2.1 The CAIX+ve cells are ALDH positive and have the ability to recapitulate the original expression pattern of unsorted MCF7 cells.

My previous findings showing an enrichment of CAIX+ve population with cells expressing stem cells markers provide an explanation for the ability of CAIX+ve cells to recapitulate the original phenotype, i.e. generation of both, CAIX+ve and CAIX-ve cells in long term culture **(Figure 3.8)**.

I used the ALDEFLUOR assay in order to assess the presence and size of the population with ALDH enzymatic activity in CAIX+ve and CAIX-ve cell line. The results showed that the CAIX+ve cell line contains a significantly ($p<0.01$, $n=3$, biological replicates) higher percentage of ALDH positive cells compared to CAIX-ve cell line **(Figure 5.1 (A) and (B)).** The enrichment of CAIX+ve cell line with ALDH positive cells is consistence with the observed upregulation of stem cell genes in this population.

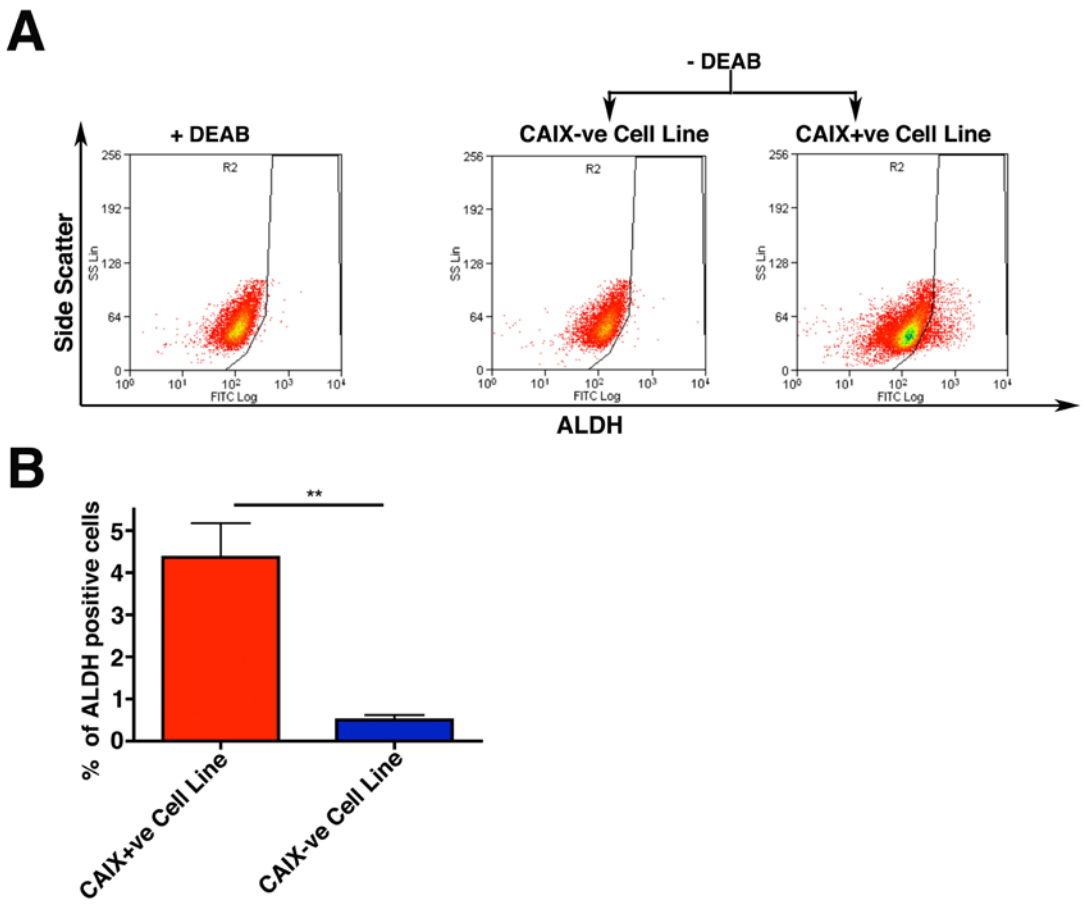


Figure 5.1 Representative FACS analysis of CAIX positive and CAIX negative cell lines for ALDH activity (ALDEFLUOR kit). Left, negative control - cells treated with ALDH inhibitor diethylaminobenzaldehyde (DEAB). Only CAIX+ve cell line contains ALDH positive cells. (A). Percentage of ALDH positive cells in CAIX positive and negative cell lines (B). **=$p<0.01$. Error bar represents SD.

5.2.2 The CAIX+ve cells have stem cell properties and shows increased clonogenic and mammosphere forming activity.

In order to investigate if the CAIX+ve cell line displays functional characteristics of cancer stem cells, I performed a series of *in vitro* assays that are used to analyze functional properties of stem cells. Firstly, I tested the ability of the two cell populations to grow as non-adherent mammospheres, a property associated with mammary stem/progenitor cells. Cells from the CAIX+ve and CAIX-ve cell lines were grown as mammospheres for 7d and then their secondary regeneration mammosphere capacity was tested. The results showed that the CAIX+ve cell line has the capacity to form more second generation mammospheres and significantly ($p<0.01$, n=3, biological replicates) larger mammospheres compared to the CAIX-ve cell line **(Figure 5.2A**), which suggests that the CAIX+ve cell line is enriched with cells that have functional properties of stem cells. These findings are consistent with previous studies showing that mammary epithelial cells that survive and proliferate in anchorage-independent conditions are likely to be breast stem cells with self-renewal capacity (Dontu et al., 2003; Ginestier et al., 2007). Similar results were also obtained with different tissues (Li et al., 2003a).

Secondly, I assessed the ability of the two cell lines to form 3D spheroids. The CAIX+ve cell line formed significantly ($p<0.001$, n=3, biological replicates) larger spheroids (n=10) after 2 weeks compared to the CAIX-ve cell line **(Figure 5.2B).** In addition to this, we observed morphological differences between the two cell lines, with the CAIX-ve spheroids forming spheroids with more circular edges, whereas the CAIX+ve cell line formed spheroids with less uniform edges.

Finally, I used the soft agar assay, a method of assessing the anchorage-independent

growth of the cells, which mimics the tumourigenic ability of the cells in animals. To this end, the CAIX+ve cell line and the CAIX-ve cell line were grown in soft agar for 3 weeks. The results showed that the CAIX+ve cell line formed significantly more colonies than the CAIX-ve cell line ($p<0.001$, $n=3$, biological replicates) **(Figure 5.3)**. Taken together, our results indicate that the CAIX+ve population is significantly enriched with stem-like cells and displays high growth potential *in vitro*.

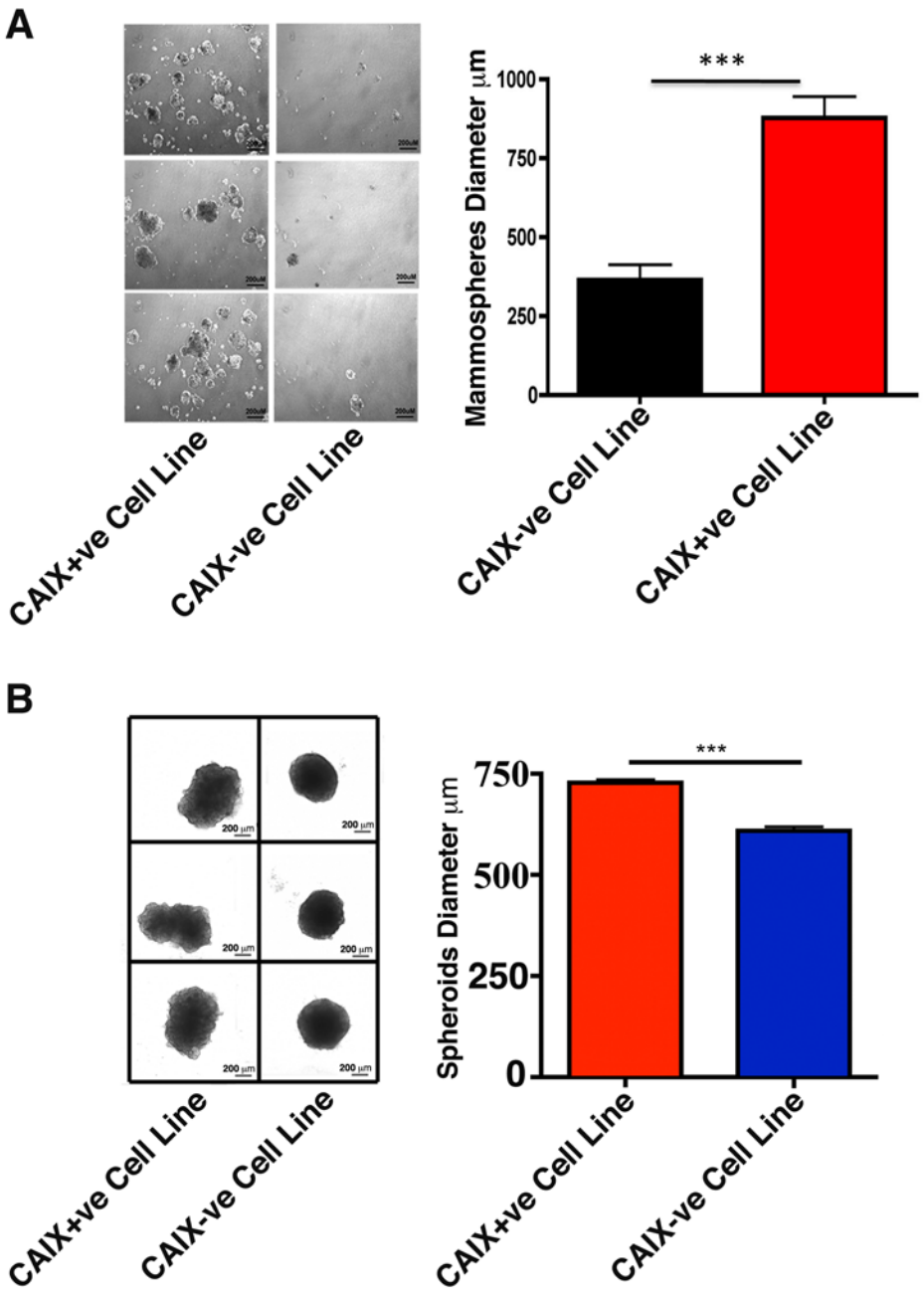


Figure 5.2 Generation of mammospheres and 3D spheroids. (A) The CAIX+ve cell line had the ability to form second generation mammospheres and significantly large compared to CAIX-ve cell line. (B) 3D spheroids growing in matrigel. CAIX+ve cell line formed significantly larger spheroids and morphological different spheroids compared to the CAIX- cell line. ***=$p<0.001$. Error bars represent SD.

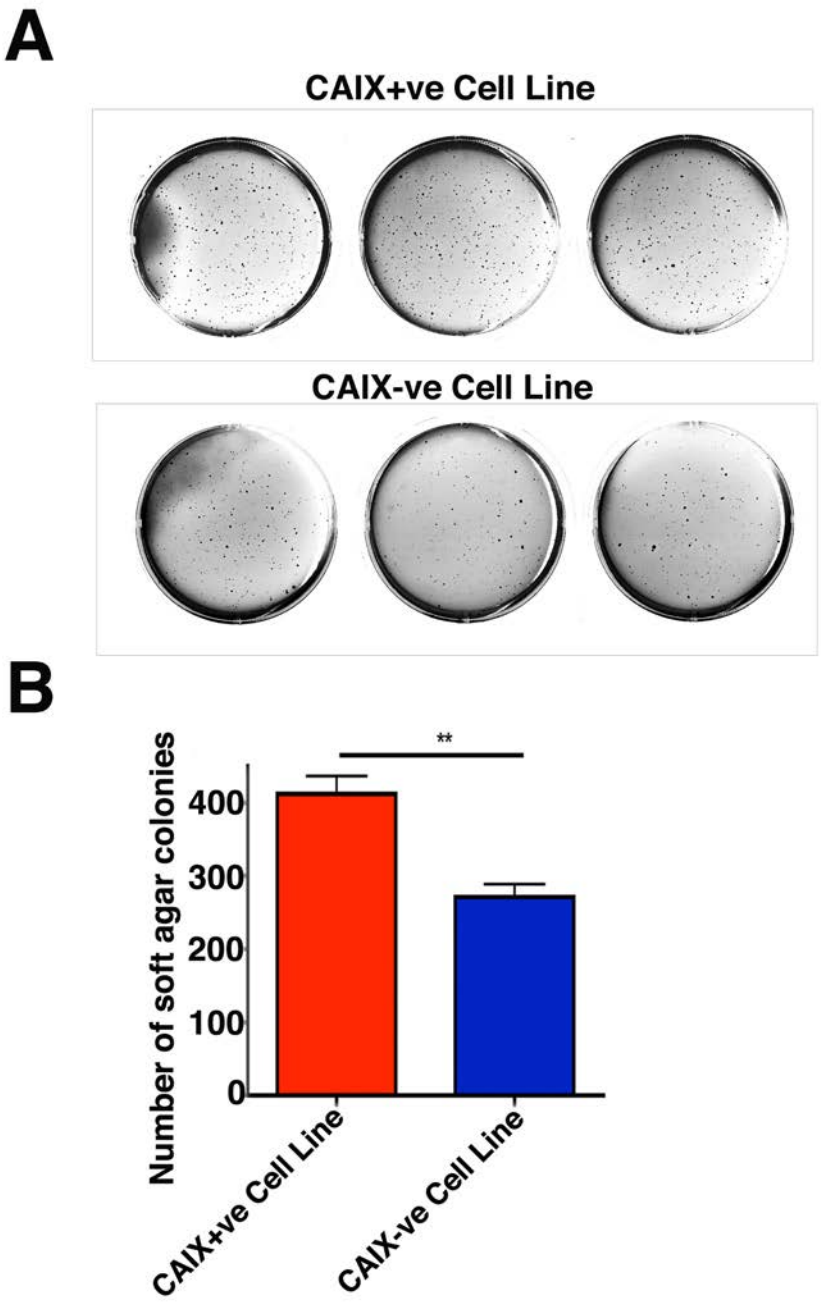


Figure 5.3 Anchorage independent growth of CAIX+ve and CAIX-ve cell lines. (A) To assay anchorage independent growth cells were cultured in soft agar for three weeks and then stained with 0.05% crystal violet. (B) CAIX+ve cell line formed significantly more colonies compared to the CAIX-ve cell line. ***=$p<0.001$. Error bars represent SD.

5.2.3 CAIX+ve cells form faster growing tumours in NSG mice

To investigate the tumourigenicity of the two populations we established xenotransplants from sorted CAIX+ve and CAIX-ve cells derived from the colon cancer cell line SW1222. We showed previously that in the SW1222 cell line under hypoxia there are two populations, which differentially express the hypoxic marker CAIX (**Figure 3.3**). Furthermore we found that only the SW1222 CAIX+ve population expresses the $CD44^{+}CD24^{+}$ markers **(Figure 5.4A)**, previously identified as markers of cancer stem cells (Yeung et al., 2011). We selected the SW1222 colon cancer cells instead of MCF-7 breast cancer cells as an *in vivo* model for our studies in order to avoid potential confounding effects of estrogen supplementation and variable responses. In addition to this, we tried to grow sorted CAIX+ve and CAIX-ve from MCF-7 but the tumours were not formed in neither populations. Sorted SW1222 CAIX+ve and CAIX-ve cells were injected subcutaneously into six to seven-week old male NSG triple negative mice. We used two dilutions (1000 cells and 200 cells) of CAIX+ve and CAIX-ve cells. For both cell dilutions, the SW1222 CAIX+ve cells formed tumours significantly faster ($p<0.05$, $n=5$) than the CAIX-ve population (**Figure 5.4B** and **Figure 5.4C**). The ability of CAIX-ve cells to form tumours suggests that a proportion of these cells retain limited proliferation capacity.

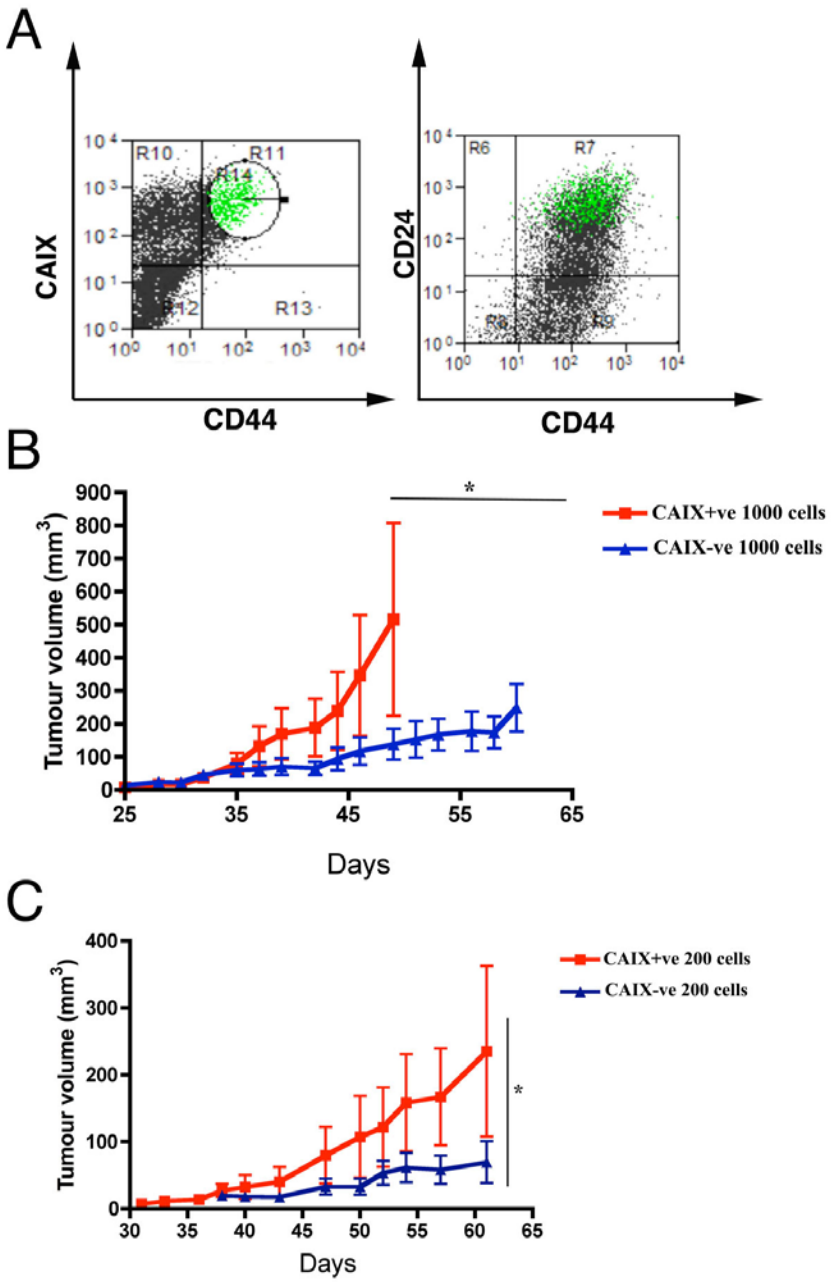


Figure 5.4 Analysis of CAIX positive and CAIX negative cell lines on ability to promote tumour growth in vivo. (A) CAIX+ve SW1222 colon cancer cells express the stem cells markers $CD44^{+HIGH}CD24^{+HIGH}$. CAIX positive and CAIX negative derived from SW1222 cells were seeded with 1000 (B) or 200 cells (C) and growth monitored over time. *=$p<0.05$. Error bars represent SD.

5.2.4 CAIX+ve and CAIX-ve cells show differential sensitivity to HDAC inhibitors

In an effort to determine the cell specific effects of HDACi on hypoxic cells, I have investigated the effects of the broad class I and class II HDAC inhibitors NaBu and SAHA (a hydroxamate-based HDACi). To this end, CAIX+ve and CAIX-ve HCT116 cells were treated for 24h, 48h and 72 h with 5mM NaBu under hypoxic conditions. Then we analyzed by FACS the effect of NaBu on expression of the stem cell marker CD133 as well as on CAIX. I choose CD133 as a marker of colon cancer stem as previous studies have indicated that CD133 is a cell surface marker for the isolation of colon cancer stem cells (Ricci-Vitiani et al., 2007). NaBu treatment caused a significant downregulation in expression of both markers ($p<0.05$, n=3, biological replicates) and (($p<0.01$, n=3, biological replicates) for CD133 and CAIX, respectively (**Figure 5.5A** and **Figure 5.5B (i), (ii)**). In addition, NaBu caused a significant dowregulation of *CA9* at the mRNA level (**Figure 5.5B (iii))**. This is consistent with previous reports showing downregulation of CD133 upon NaBu treatment in HT29 and CaCo2 colon cancer cell lines (Haraguchi et al., 2008). Previous, studies showed that the decrease in CD133 after sodium butyrate treatment was due to post-translational modulation, as there was no change in the CD133 promoter methylation or CD133 mRNA levels (Sgambato et al., 2010).

Further to this I tested the effects of NaBu on the growth of HCT116 3D spheroids. HCT116 spheroids were grown in spinning flasks for 7d followed by treatment with NaBu for 24h, 48h, and 72h. The results showed that exposure to NaBu caused a significant reduction in spheroid growth (n=10 spheroids) **(Figure 5.6).**

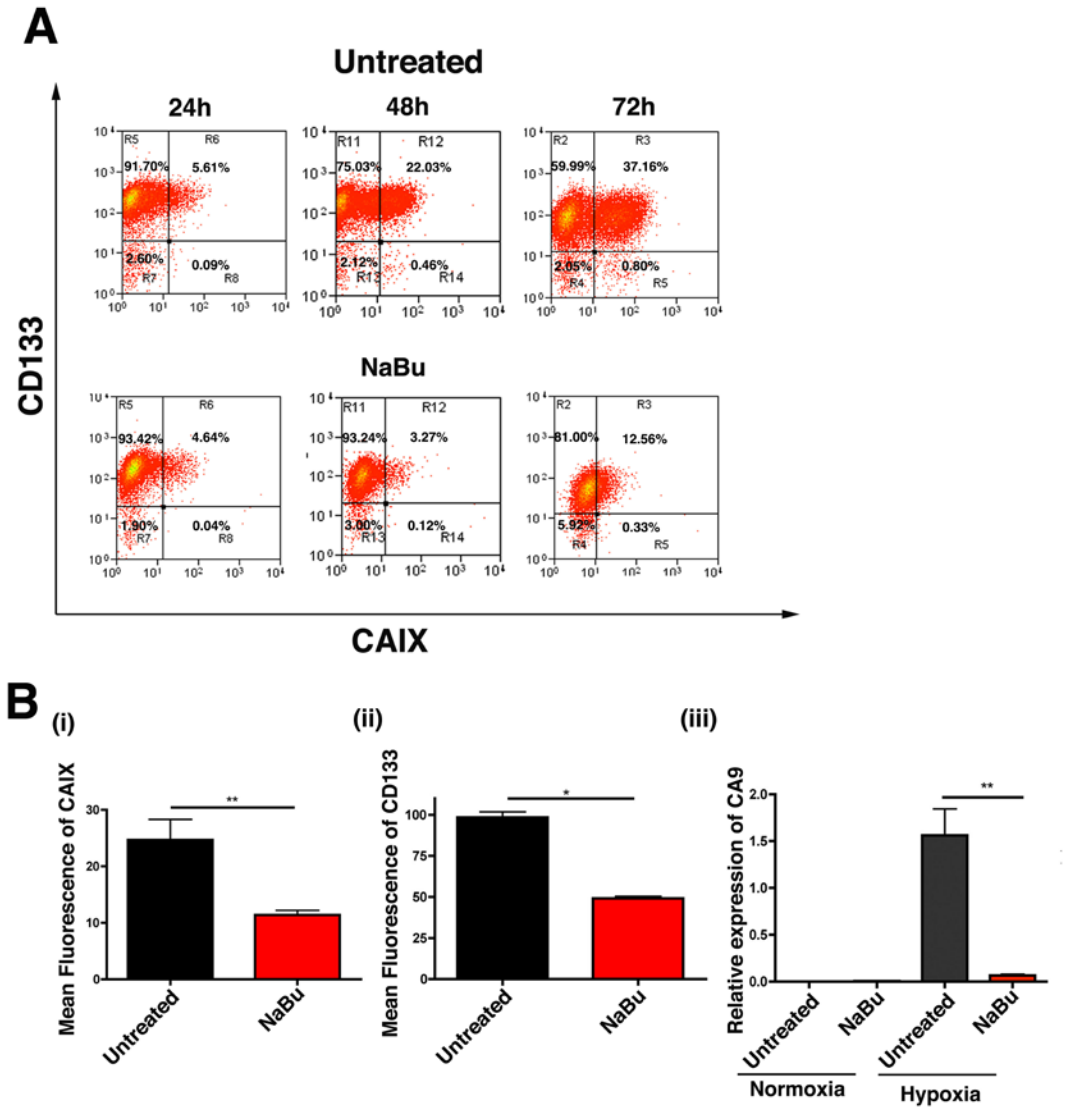


Figure 5.5 Treatment of unsorted HCT116 cells with sodium butyrate. (A) Representative time point of FACS analysis for CAIX and CD133 expression under hypoxia in sodium butyrate (NaBu) treated and untreated HCT116 cells. (B) Mean fluorescence of CAIX (i) and CD133 (ii) in untreated cells and NaBu treated cells. (iii) Relative CAIX mRNA expression of untreated and NaBu treated cells under normoxia and hypoxia. (ii) Mean fluorescence of CAIX in untreated cells and NaBu treated cells. **=p<0.01, ***=p<0.001. Error bars represent SD.

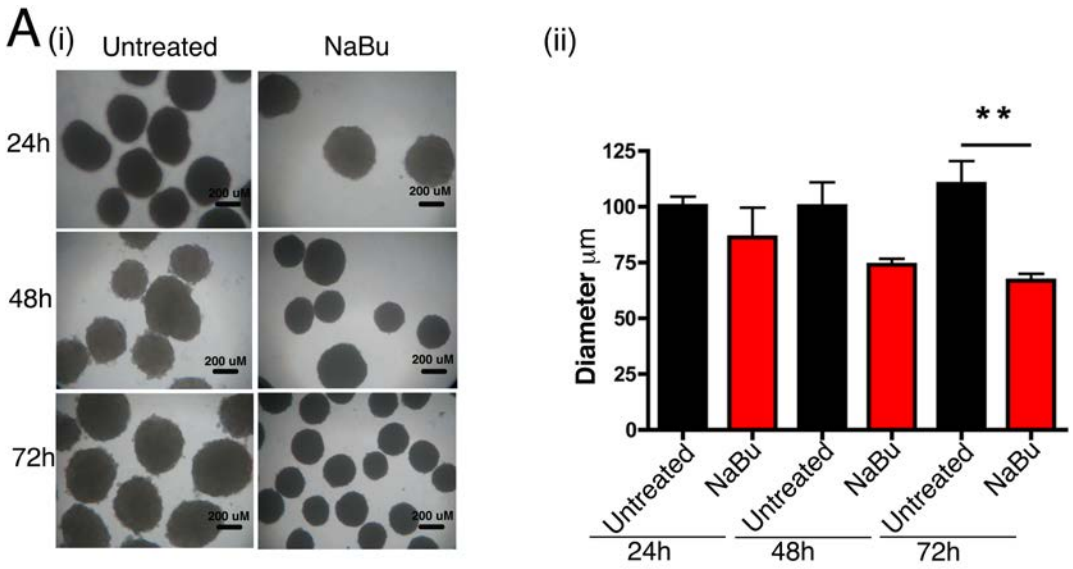


Figure 5.6 Treatment of HCT116 spheroids with sodium butyrate. Representative images of HCT116 spheroids untreated or treated with NaBu for 24h, 48h, and 72h. (ii) Graphical representation of differences in the diameter of the NaBu treated and untreated spheroids. ***=$p<0.001$. Error bars represent SD.

In order to verify this result we also investigated the effect of SAHA on the MCF-7 breast cancer cell line. Cells were treated with 2 μM SAHA for 72 h and exposed under 0.1% O_2. Subsequently, they were stained with antibodies against CD44 and CAIX, followed by FACS analysis. Previous studies have shown that the CD44 positive phenotype is correlated positively with breast cancer stem cells (Al-Hajj et al., 2003a). SAHA significantly reduced the number of cells expressing CAIX ($p<0.05$, n=3, biological replicates) and CD44 ($p<0.05$, n=3, biological replicates) (**Figure 5.7A and Figure 5.7B (i), (ii)**). In addition I tested the protein expression of other hypoxia inducible genes such as HIF-1α, PDK1, and AK4, and we showed that HIF-1α was not downregulated upon SAHA treatment, but PDK1 (44% reduction) and AK4 (80%) were, although to a lesser extent than CAIX (95%) (**Figure 5.7C**). This suggests that there is an effect on HIF-1α efficacy as well as showing target specificity. These results are consistent with the findings of the NaBu treatment, and suggest that SAHA causes elimination of the CAIX+ve population.

A recent study showed that SAHA causes inactivation of mTOR and induction of autophagy (Gammoh et al., 2012). Interestingly, our own data show an upregulation of mTOR in CAIX+ve cells and downregulation of CAIX upon mTOR inhibition. Given the above I hypothesized that SAHA-induced downregulation of CAIX expression could be due to its effect on the mTOR pathway. To test this hypothesis I investigated the effect of SAHA on the expression levels of pS6K, a downstream target of mTOR. Consistent with our hypothesis and previous reports, we showed that treatment with SAHA reduces the expression of pS6K (**Figure 5.7D**). Thus I hypothesized that the molecular mechanism by which SAHA downregulates CAIX is likely to involve mTOR signaling inactivation.

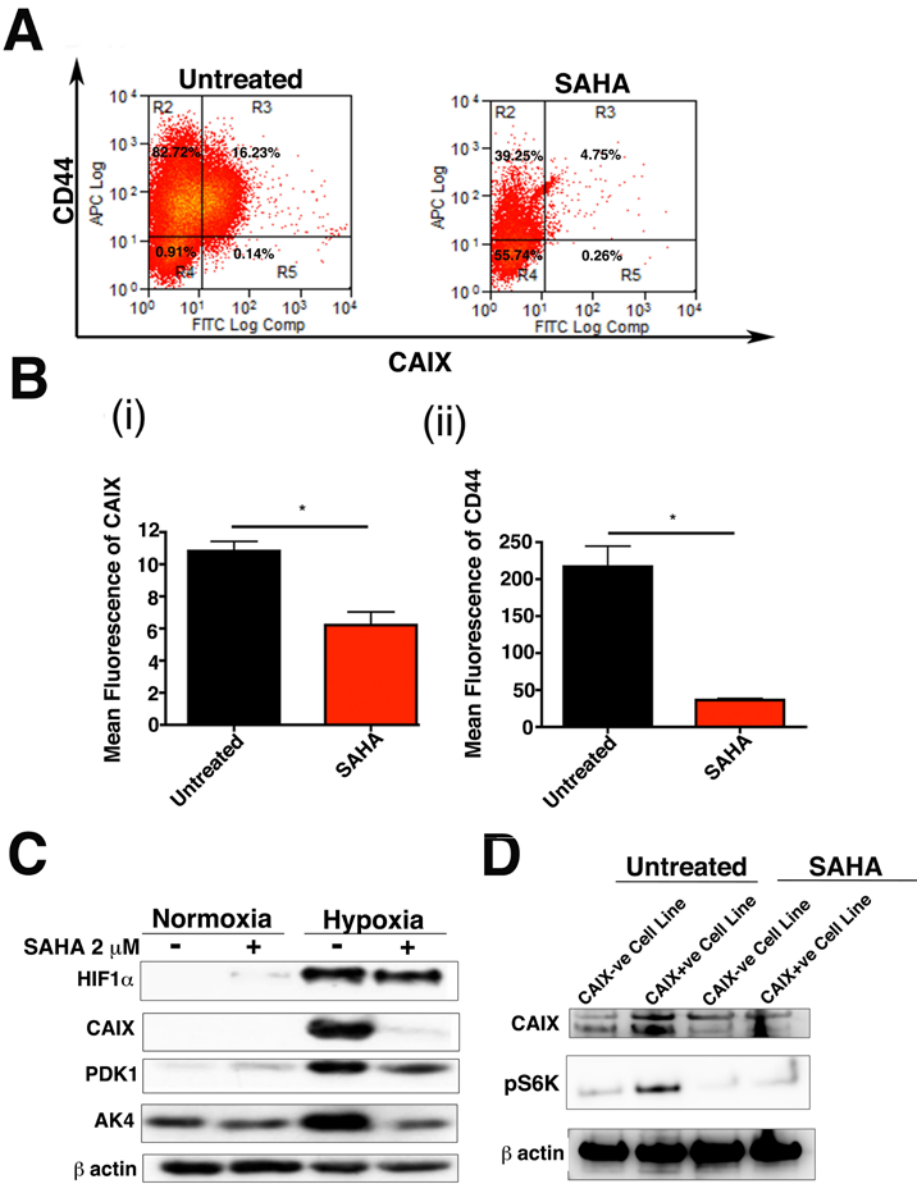


Figure 5.7 Treatment of MCF7 cells with SAHA. (A) Representative histograms of FACS-based analysis of CAIX and CD44 expression in hypoxia upon SAHA treatment of MCF-7 cells. B (i), (ii) Mean fluorescence intensity of CAIX and CD44 (C) Protein expression analysis of HIF-1α, CAIX, PDK1 and AK4 in SAHA treated and untreated cells. (D) Protein expression analysis of pS6K in SAHA treated and untreated cells. . *=$p<0.05$. Error bars represent SD.

5.2.5 Effects of SAHA treatment on survival of CAIX+ve and CAIX-ve cell lines.

Next I investigated whether SAHA induced CAIX downregulation is due to cell differentiation or whether it targets specifically CAIX+ve cells by affecting their cell survival. To test this I performed a colony forming assay. CAIX+ve and CAIX-ve cells were seeded at a density of 1000 cells per 6 cm dish in triplicates and treated with 2 μM SAHA for 72h under hypoxic conditions, untreated control cells were also included in the experiment. After 72h, SAHA was removed from the medium and the cells were recovered for 10d under normoxia. In order to assess cell survival we fixed and counted the colonies. The results showed that SAHA significantly ($p<0.05$, n=3, biological replicates) reduced the number of colonies of the CAIX+ve cell line (**Figure 5.8A**). Additionally, we evaluated the CAIX expression in untreated and SAHA-treated colonies of the CAIX+ve cell line after the 10d recovery. This showed a significant ($p<0.05$, n=3, biological replicates) reduction of expression of CAIX in the SAHA treated colonies as compared to the untreated colonies, even after 10 d of recovery (**Figure 5.8B**). Together, these results suggest that SAHA treatment targets specifically CAIX+ve cells and affects their survival.

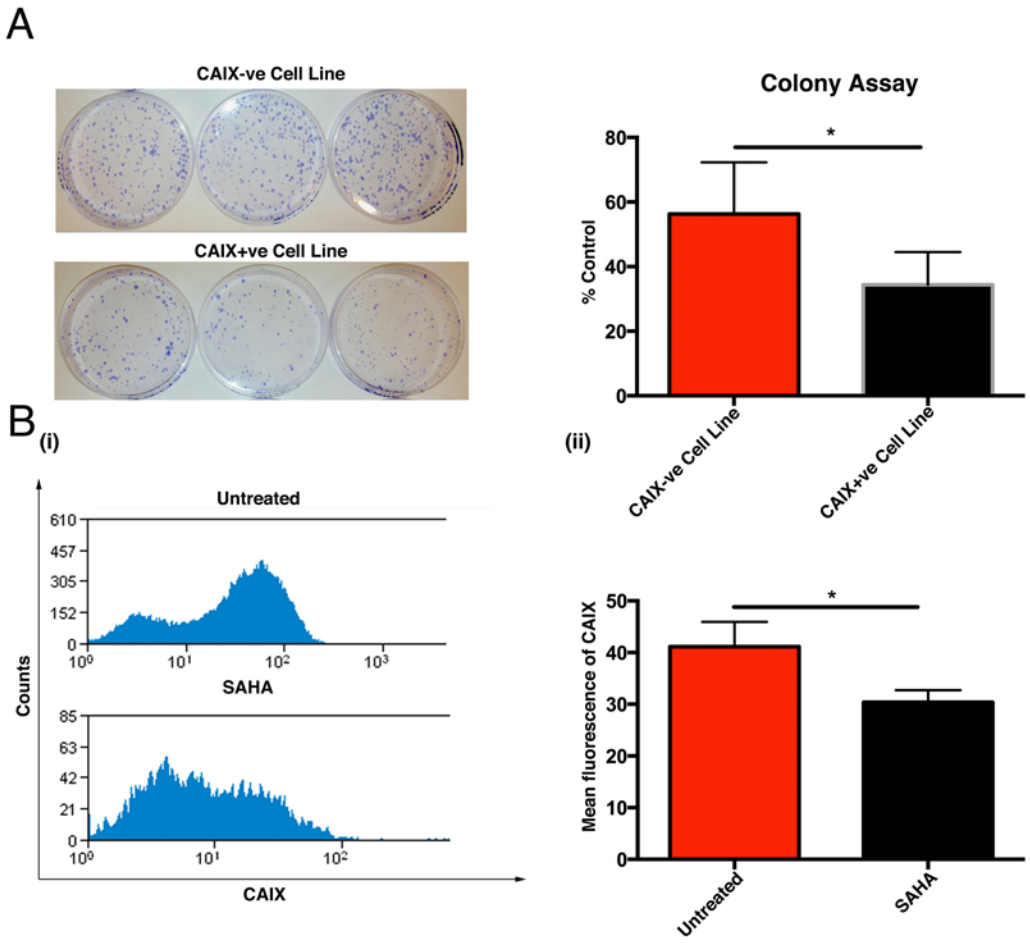


Figure 5.8 Effects of SAHA treatment on colony formation of CAIX+ve and CAIX-ve MCF-7 cell lines (A) A clonogenic survival assay for CAIX+ve and CAIX-ve cell lines treated with SAHA shows that SAHA significantly reduces CAIX+ve cell line colony formation compared to CAIX-ve cells. (B)(i) Representative histograms from FACS-based analysis of CAIX expression in untreated and SAHA treated CAIX+ve colonies after 10d recovery. (ii) Mean fluorescence of CAIX of untreated and SAHA treated CAIX+ve colonies after 10d recovery. *=$p<0.05$. Error bars represent SD.

5.2.6 Effects of SAHA on cell survival are CAIX dependent.

Next, I wanted to understand if sensitivity of CAIX+ve cells to SAHA was dependent on the CAIX status. To investigate this, we transfected the CAIX+ve population with CAIX RNAi or scrambled RNAi (Scr RNAi) and then treated with 2 μM of SAHA for 72h under hypoxic conditions. I also treated the CAIX+ve and CAIX-ve cell line with SAHA for 72h under hypoxic conditions as an additional control. After 72h SAHA was removed from the medium, cells were recovered for another 24h under normoxia and then analyzed for cell growth. Treatment with SAHA significantly reduced cell growth of the CAIX+ve cell line ($p<0.01$, n=3, biological replicates) as well as cells transfected with Scr RNAi ($p<0.05$, n=3, biological replicates) **(Figure 5.9A).** In contrast, CAIX RNAi induced resistance to SAHA in the CAIX+ve cells **(Figure 5.9A).** These results suggest that expression of CAIX confers sensitivity to SAHA treatment in the CAIX+ve population. Given the above it is likely that CAIX could be a valuable biomarker in treatment utilizing HDAC inhibitors.

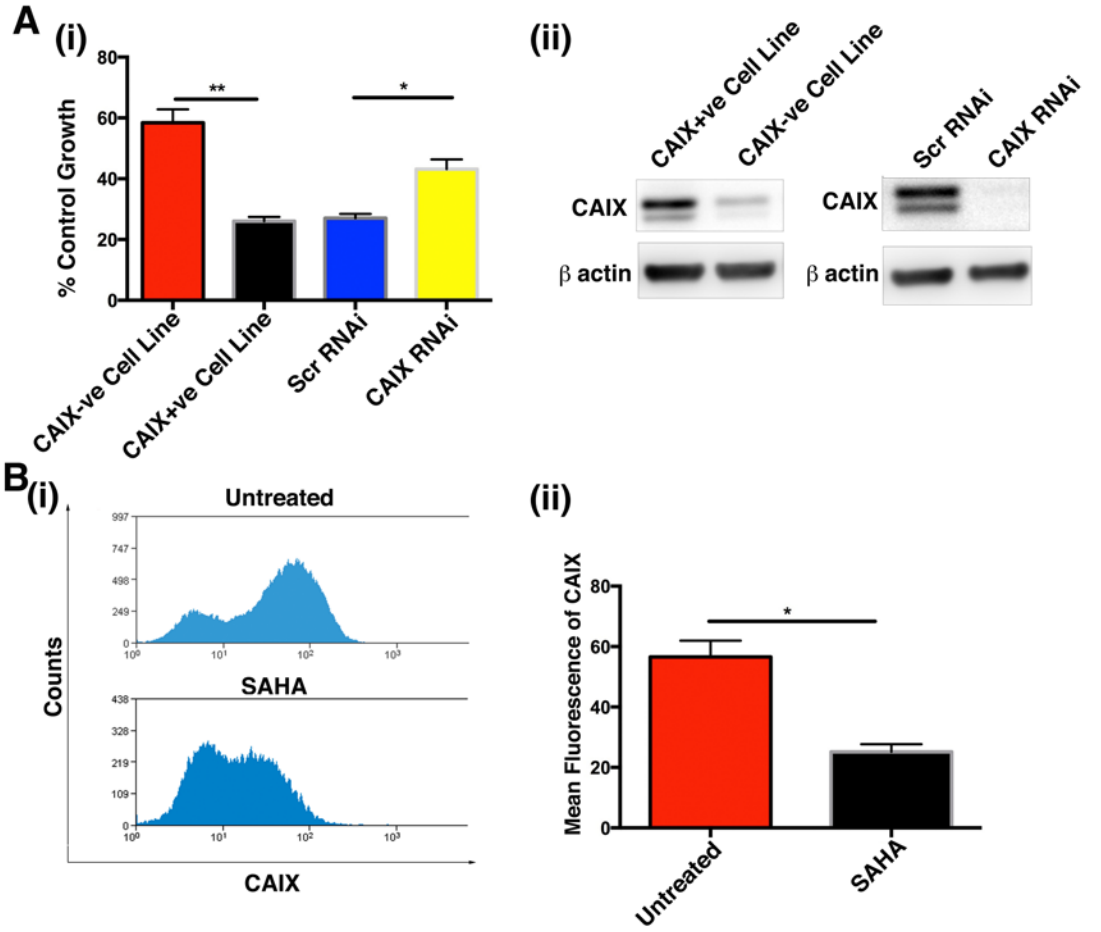


Figure 5.9 Effects of SAHA treatment on cell growth of CAIX+ve, CAIX-ve cells cell lines and CAIX knockdown cells. SAHA significantly downregulates the cell growth of CAIX+ve cells and the control cells transfected with scr RNAi (A)(i). CAIX knockdown was confirmed by western blot analysis (A)(ii). (B)(i) Representative histogram of the FACS-based analysis of CAIX expression in untreated and SAHA treated CAIX+ve cells after 24h of recovery. (ii) Mean fluorescence of CAIX of untreated and SAHA treated CAIX+ve cells after 24h recovery. *=$p<0.05$ **=$p<0.01$. Error bars represent SD.

5.3 Discussion

Like normal stem cells, CSCs display several defining characteristics such as differentiation into multipotent progenitors, self-renewal, and the expression of various molecular markers of stemness. In chapter four we showed that CAIX+ve cells have higher expression of stem cell markers than CAIX-ve cells. Following this notion, in this chapter utilizing *in vitro* and *in vivo* assays we confirmed that CAIX+ve cells indeed contain a subpopulation of cells with functional characteristics of cancer stem cells. I showed that only CAIX+ve cells possess the capacity to drive the original heterogeneous phenotype, consisting of CAIX-ve and CAIX+ve cells in long-term culture, a characteristic property of stemness (Clarke and Fuller, 2006; Dingli et al., 2007). Moreover, CAIX+ve cells show higher ALDH activity compared to CAIX-ve cells. CSCs represent a small subset of cells within a tumour, and the percentage of ALDH positive cells in the CAIX+ve cells is in average 4.5%, which is also consistent with previous reports showing that the cells with high ALDH activity are a small fraction of the total population (an average of 8%) (Ginestier et al., 2007). In line with this, ALDH positive cells represent the tumourigenic cell fraction able to self-renew and to recapitulate the heterogeneity of the parental tumour (Ginestier et al., 2007). Interestingly, basal-like breast cancers, which are associated with stem cell phenotypes and high ALDH1 expression (Ginestier et al., 2007; Nalwoga et al., 2010) also show high CAIX expression (Tan, Yan et al. 2009). Our notion that the CAIX+ve population is enriched with stem-like cells is further supported by the fact that these cell show increased ability to form secondary generation mammospheres, a property known to be associated with mammary stem/progenitor cells (Sansone et al., 2007a) as well as an increased capacity to form colonies in soft agar and a significant increase in growth rate 3 dimensional (3D) spheroids.

Accordingly, our *in vivo* experiments showed that the CAIX+ve cells of SW1222 colon cancer cell line expressing the $CD44^{+}CD24^{+}$ stem cell markers have the ability to form significantly faster growing tumours in NSG mice. Interestingly, the CAIX negative population is also able to replicate itself, though to a lesser extent. This suggests the presence of another class of tumour initiating cell however, without the full range of stem cell functions. In support of this, Barett *et al* showed that glioma tumour cells with high Id1 expression identifies tumour cells with high self renewal capacity, while low Id1 expression identifies tumour cells with proliferative potential but limited self-renewal capacity (Barrett et al., 2012). Although the cancer stem cell concept implies that only the "stem cells" are responsible for the maintenance and initiation of tumours, it is unclear however whether stem-like cells are uniquely qualified in their ability to form tumours in xenograft models or whether other, more differentiated non-self renewing lineages also possess this capacity (Chow et al., 2011; Prestegarden and Enger, 2010; Stiles and Rowitch, 2008). For example, comparisons of the genetic composition of breast cancer $CD44^{+}CD24^{-}$ cells, which are presumed to be "cancer stem cells", versus $CD44^{-}CD24^{+}$ cells, which are considered to be non-stem cells, have revealed that in some cases these subpopulations are genetically divergent, which is inconsistent with a model of simple differentiation (Marusyk and Polyak, 2010; Park et al., 2010; Shipitsin et al., 2007).

Further to this, I demonstrated that the two populations have a differential sensitivity to HDAC inhibitors. I identified that NaBu and SAHA treatment lead to elimination of the CAIX+ve population as well as a significant reduction in the expression of the stem cells associated genes CD44 and CD133. Consistent with this, treatment of HT29 and CaCo2 colon cancer cell lines with NaBu also causes a reduction in the

expression of CD133 and CD44 (Haraguchi et al., 2008). Additionally, it has been shown that HDAC inhibitors induce early differentiation in embryonic stem cells (ES), by reducing the expression of key regulatory stem cell genes such as SOX2, NANOG, and OCT4 (Karantzali et al., 2008; Park et al., 2011). It is important to note that different HDACi have different specificities in different cell lines. Previous work from our laboratory has shown that NaBu did not reduce CAIX expression, and SAHA did not reduce the expression of CAIX in HCT116. The use different cancer cell lines and different HDCAi is giving insights into the differences in drug repsonses in various genetic backgrounds, which is important for cancer therapy.

Interestingly, SAHA treatment did not reduce the levels of HIF-1α, the major transcription activator of CAIX. This suggests that SAHA induced CAIX downregulation is not HIF-1α□dependent. The downregulation of pS6K upon SAHA treatment, which we hypothesize may be a result of mTOR signaling inactivation, could provide a plausible explanation for the observed downregulation of CAIX expression. In support of this, a recent study has shown that SAHA causes inactivation of mTOR and induction of autophagy (Gammoh et al., 2012). Moreover, HDAC inhibitors also disrupt the pH-buffering capacity of cells, significantly lowering the intracellular pH (Chung et al., 2008; Gammoh et al., 2012; McBrian et al., 2013) and mTOR signaling is inhibited by a more acidic intracellular pH (Balgi et al., 2011). Given the above and the fact that CAIX maintains a neutral intracellular pH we postulate that CAIX expression plays an important role in conductive mTOR signaling.

Further to this, I observed that SAHA treatment has a significantly greater effect on survival of CAIX+ve cells than on CAIX-ve cells. Interestingly, this effect is CAIX-

regulated as silencing of CAIX in the positive population increases their survival upon SAHA treatment. This is important from the therapeutic point of view, as it suggest that CAIX could be used as a biomarker in treatments utilizing the use of HDAC inhibitors.

Importantly, this differential sensitivity of the two populations to HDACi implies that one of the reasons for failure of current HDACi-based therapies in solid tumours could be due to a selective targeting of this group of cells. This could lead to a failure in controlling oxygenated proliferating cells. Therefore, eradicating the CAIX-positive cells may provide a more effective therapy due to their stem cell-like potential, which is believed to lie at the root of cancer origin and recurrence. I suggest however, that combinational therapies that target also the CAIX-ve cells, which may provide environmental support for stem-like cells, may further improvement the current treatment strategies.

Chapter Six

Metabolic Heterogeneity revealed by Microarray analysis

6.1Introduction

RNA sequencing (RNA-seq) and microarray are the two major technologies currently used in most gene expression studies. Both methods have contributed a lot in the discovery of the roles played by specific genes in the development of diseases, such as cancer. Microarray are a 2D array on a solid substrate which are using a set of pre defined probes, that are complementary to the various transcripts whose presence is to be investigated (Malone and Oliver, 2011). The isolated transcripts, are labelled with one of two fluorescence dyes following hybridization to the arrays and scanning with a laser (Malone and Oliver, 2011). The light intensity from the fluorescence labelled transcripts is used as measurement of gene expression.

Microarray technology is a well-established way of studying gene expression and it has been the technology of choice in most gene expression studies. There are more than 520,000 individual experiments archived and around 21,000 project submissions, most produced from microarrays (Malone and Oliver, 2011). Because of the relatively long time of use of microarrays as a genomic tool the data analysis and experimental design are very mature.

In contrast, RNA-seq provides a more detailed look at the transcriptome giving higher sensitivity and a more flexible platform. Specifically RNA-seq is not limited by pre-defined probe sets and potential cross-hybridization, as the starting cDNA material is directly sequenced (Malone and Oliver, 2011). This makes RNA-seq more advantageous as it allows the analysis of transciptome without prior knowledge of it. For example, with RNA-seq novel transcripts, splice junctions and noncoding RNAs can be detected. However, despite the advantages of RNA-seq over the microarrays, RNA-seq as a new technology still needs to overcome some challenges. For example,

the cost of RNA-seq is much higher compared to microarrays, which causes some groups to avoid using biological replicates, which can lead to inaccurate estimates of gene expression level and thus false inferences (Auer and Doerge, 2010). Currently, the major problem of RNA-seq is the data analysis. The amount of data generated by RNA-seq is much higher than microarrays, and the analysis of the data requires the knowledge of specific programming languages such as Python, Perl or Unix, with which many biologists are unfamiliar (Malone and Oliver, 2011). In addition, there is no consensus or standardized workflow for filtering, normalizing, alignment, and statistical analysis of these large, and often complex data sets.

Given that both technologies have some limitation, in order to achieve a more comprehensive view, we decided to perform also a microarray analysis on CAIX+ve and CAIX-ve sorted cells. The use of both technologies would also allow us to cross-validate data generated by these two methods.

6.2 Results

6.2.1 Microarray analysis: Genes upregulated in CAIX+ve population versus CAIX negative populations

In order to compare the RNA-seq arrays with the more established technology of microarray, RNA was extracted from the two subpopulations and used for microarray analysis (n=3, biological replicates). It is important to mention that RNA-seq experiment was performed in the beginning of this thesis, while the microarray experiment was performed 2 years later. The overall analysis of microarray data revealed that in the case of CAIX+ve cells ~3,726 genes were upregulated in relationship to CAIX-ve cells using a cut-off of 1.2 for Fold Change (FC), whereas in the case of CAIX-ve cells ~ 3714 genes were upregulated in relationship to CAIX+ve using a cut-off of 0.8 for FC (**Appendix 2, Table 1 and Table 2**). In addition, in microarray analysis we had three biological replicates and we did not use fold change but false discovery rate (FDR) less than 0.05. In RNA-seq we did not have replicates so FDR estimation wouldn't be reliable so we used the fold change. This is not optimal, and more replicates for the RNA-seq experiment would be needed, but this reflects the novelty and cost of RNAseq at the time of the analysis.

Next, I investigated the degree of overlap between the gene lists generated for microarray and RNA-seq. For this reason I compared the microarray's CAIX+ve gene list with the RNA-Seq's CAIX+ve gene list and microarray's CAIX-ve gene list with the RNA's CAIX-ve gene list. The direct comparison between the two CAIX+ve and CAIX-ve gene lists revealed a very small overlap of only 63 genes in the case of CAIX+ve and 65 genes in the case of CAIX-ve (**Figure 6.1**) and (**Appendix 5, Table**

1 and Table 2). In addition, I investigated the degree of overlap between the upregulated genes in CAIX+ve microarray list with the upregulated genes in the CAIX-ve RNA-seq list and the upregulated genes in the CAIX-ve microarray list with the upregulated genes in the CAIX+ve RNA-seq list. The results showed that there are 32 genes in common between the CAIX+ve microarray list and CAIX-ve RNA-seq list (**Figure 6.2A**), and 57 genes in common between the CAIX-ve microarray list and the CAIX+ve RNA-seq list (**Figure 6.2B)**. With regard to this, it is worth noting that previous studies have shown that microarrays and RNA-seq give results that are not completely consistent (Fu et al., 2009; Marioni et al., 2008). These differences may result from many factors, including the fact that the two experiments were performed at different time points. RNA seq was performed at the beginning of the thesis, where the standardization of the workflow for filtering, normalization, alignment, and statistical analysis of these large, and often complex data sets were still at an initial stage.

As in the case of RNA-seq, the genes upregulated in the two subpopulations were compared with a previously published common hypoxia signature (Buffa et al., 2010) and the results showed that both populations have a similar hypoxia core response (**Figure 6.3**). Overall, this analysis showed that although both populations expressed a core set of very well-described inducible genes under hypoxia, the genes distinguishing them were not themselves hypoxia inducible, besides CAIX. Given that HIF-1α is the major mediator of oxygen homeostasis and the activator of the hypoxia inducible genes (Patiar and Harris 2006), the common hypoxia core response of the two populations revealed by the RNA-seq and microarray analysis are in agreement with our previous findings showing that both populations have the same levels of HIF-1α expression.

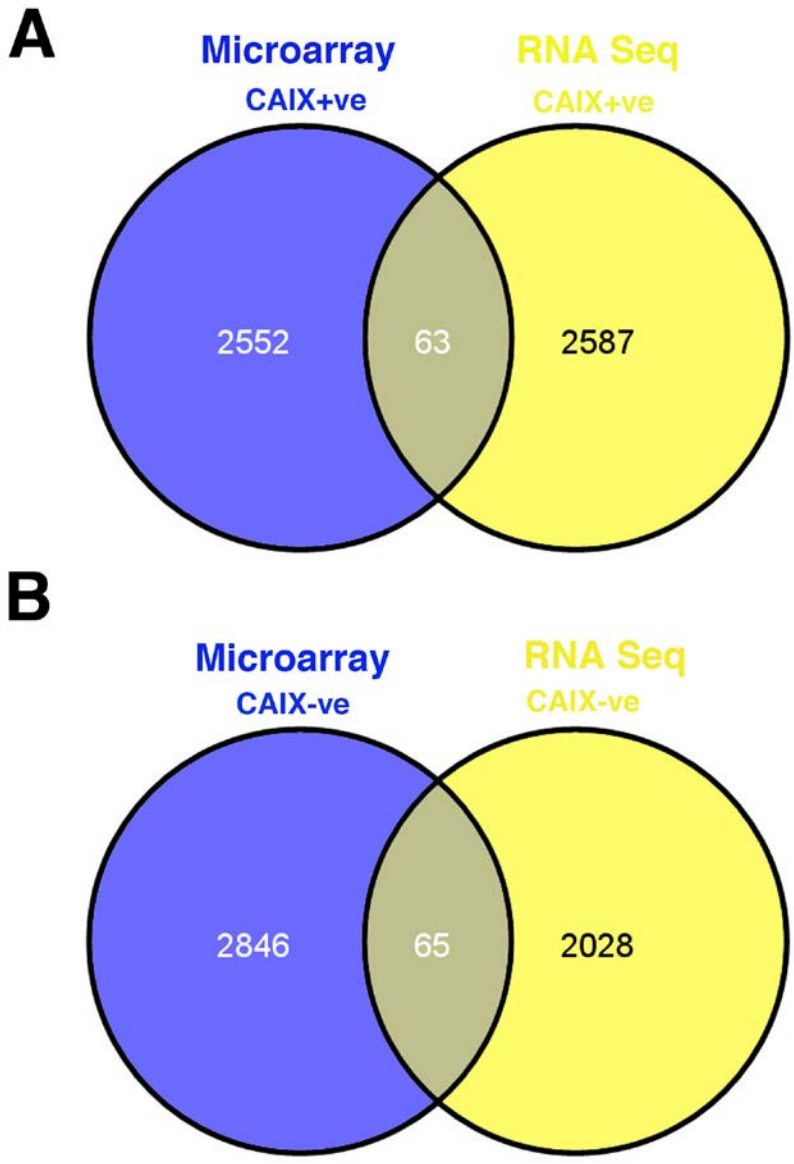


Figure 6.1 Comparison of microarrays and RNA-seq gene lists. (A) The Venn diagram generated by comparing the CAIX+ve microarray gene list with the CAIX+ve RNA-seq gene list. (B) The Venn diagram generated by comparing the CAIX-ve microarray gene list with the CAIX-ve RNA-seq gene list.

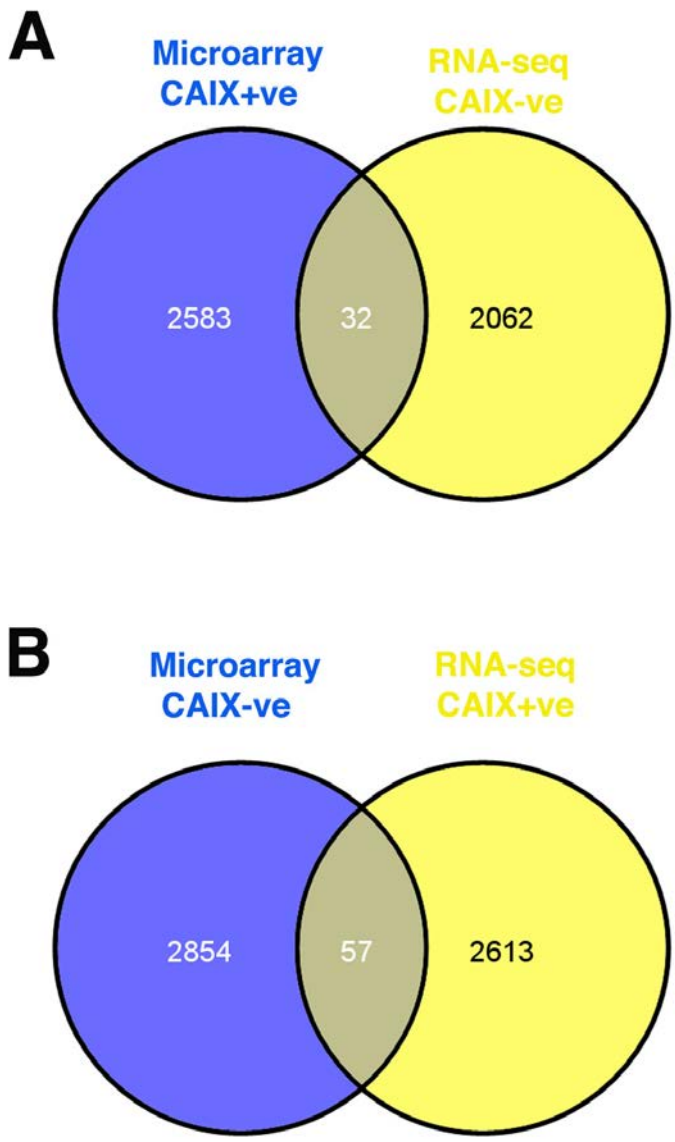


Figure 6.2 Comparison of microarrays and RNA-seq gene lists of upregulated and downregulated genes (A) The Venn diagram generated by comparing the CAIX+ve microarray gene list with the CAIX-ve RNA-seq gene list. (B) The Venn diagram generated by comparing the CAIX-ve microarray gene list with the CAIX+ve RNA-seq gene list.

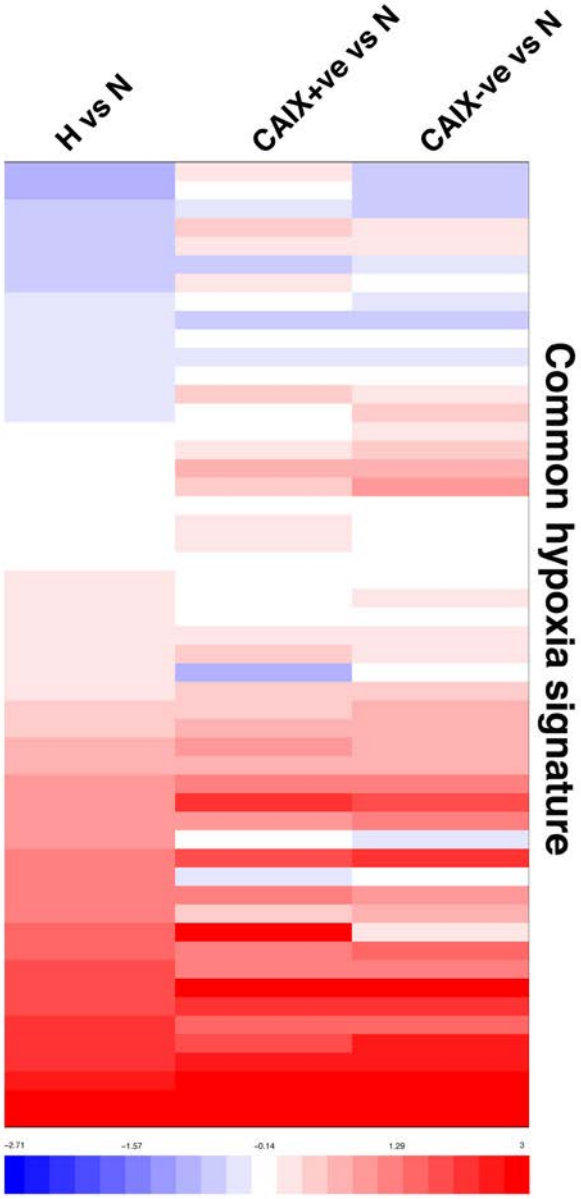


Figure 6.3 Comparison of CAIX+ve and CAIX-ve gene signatures with a conserved core hypoxia signatures. Heatmap showing the conserved core hypoxia signatures common to whole-population (left column), 2) CAIX+ve cells (middle column) and 3) CAIX-ve cells (right column) versus a normoxia whole-population control. Fold changes (log2) are shown and the scale is provided at the bottom of each heatmap.

6.2.2 Pathways and genes upregulated in the CAIX+ve populations

In order to characterize the two populations at the transcription level we performed a similar pathway analysis using KEGG and IPA software. This allowed us to cluster the CAIX+ve upregulated genes revealed from the microarray analysis into biological pathways. Interestingly, the common pathways identified by both software showed an upregulation of key metabolic pathways (**Table 6.1** and **Table 6.2**) and (**Appendix 4, Table 1 and Table 2)**. The majority of the upregulated metabolic pathways are implicated in the production of biomass components that are essential for cell division. These included, Aminoacyl-tRNA biosynthesis, Pyruvate metabolism, Fatty Acid Metabolism, Glycolysis/ Gluconeogenesis, Citrate cycle (TCA cycle), Valine, Leucine and Isoleucine Degradation, Propanoate Metabolism, Oxidative Phosphorylation. This suggests a possible intratumoural metabolic heterogeneity within these two populations.

Table 6.1: KEGG pathway analysis for CAIX+ve cells

Genes	Hyp*	Annotations
21	**2.21E-11**	**Aminoacyl-tRNA biosynthesis**
39	1.16E-10	RNA transport
36	9.47E-08	Protein processing in endoplasmic reticulum
32	9.81E-08	Parkinson's disease
30	1.09E-07	Spliceosome
17	1.19E-07	Tryptophan metabolism
22	3.61E-07	Ribosome biogenesis in eukaryotes
35	3.65E-07	Alzheimer's disease
16	**3.85E-07**	**Pyruvate metabolism**
30	**5.82E-07**	**Oxidative phosphorylation**
23	1.41E-06	Ribosome
16	1.51E-06	Valine, leucine and isoleucine degradation
32	3.59E-06	Purine metabolism
13	5.13E-06	Propanoate metabolism
14	**1.67E-05**	**Fatty acid metabolism**
17	**3.28E-05**	**Glycolysis / Gluconeogenesis**
25	5.29E-05	Cell cycle
21	5.72E-05	Pyrimidine metabolism
11	**9.70E-05**	**Citrate cycle (TCA cycle)**
19	**0.0431344**	**Wnt signaling pathway**

(Hyp* = Corrected hypergeometric pValue)

Table 6.2: Ingenuity pathway analysis for CAIX+ve cells

Ingenuity Canonical Pathways	-log(p-value)*
Lysine Degradation	5.2E00
Butanoate Metabolism	4.89E00
Fatty Acid Metabolism	**4.81E00**
Mitochondrial Dysfunction	4.52E00
Valine, Leucine and Isoleucine Degradation	4.48E00
Propanoate Metabolism	4.18E00
Oxidative Phosphorylation	**3.47E00**
Glycolysis/Gluconeogenesis	**3.35E00**
Pyruvate Metabolism	**3.16E00**
Glyoxylate and Dicarboxylate Metabolism	3.11E00
Tryptophan Metabolism	3.11E00
Purine Metabolism	2.89E00
Phenylalanine, Tyrosine and Tryptophan Biosynthesis	2.86E00
Glycine, Serine and Threonine Metabolism	2.68E00
One Carbon Pool by Folate	2.61E00
Fatty Acid Elongation in Mitochondria	2.45E00
Citrate Cycle	**2.2E00**
ATM Signaling	2.18E00
Valine, Leucine and Isoleucine Biosynthesis	2.15E00
Pyrimidine Metabolism	2.11E00
Role of CHK Proteins in Cell Cycle Checkpoint Control	2.04E00
EIF2 Signaling	1.97E00
Ubiquinone Biosynthesis	1.89E00
Alanine and Aspartate Metabolism	1.85E00
Biosynthesis of Steroids	1.84E00
Protein Ubiquitination Pathway	1.82E00
Urea Cycle and Metabolism of Amino Groups	1.79E00
Fructose and Mannose Metabolism	1.21E00
mTOR Signalling	**6.16E-01**
Wnt/β-catenin Signaling	**5.93E-01** **5.93E-01**

(*Statistical significance was determined by using Fisher's exact test ($P < 0.05$))

In Chapter Four I showed that components of mTOR pathway are upregulated in CAIX+ve cell line. Interestingly, mTOR signaling was among the upregulated pathways observed also from this analysis, further supporting our initial observation. mTOR is another major regulator of metabolism, which itself contributes to the anabolic growth of cancer cells (Wullschleger et al., 2006). Given this, the aminoacyl-tRNA biosynthesis pathway, which is related to protein synthesis and activation of mTORC1 is also upregulated in the CAIX+ve cells (**Appendix 4, Table 1**). The aminoacyl-tRNA biosynthesis pathway consists of 21 tRNA synthetases, the function of aminoacyl tRNA synthetases are to catalyze the ligation of amino acids to their cognate tRNAs (Park et al., 2008). The aminoacylation of transfer RNAs determines the rules of genetic code, and thus plays a central role in the regulation of protein synthesis and cell survival (Park et al., 2008). Dysregulation of aminoacyl tRNA synthetases can lead to the development of cancer, neuronal pathologies, autoimmune disorders, and disrupted metabolic conditions (Park et al., 2008). Intriguingly, among the 21 upregulated tRNA synthetases, leucyl-tRNA synthetase has been recently shown to play a critical role in amino acid-induced mTORC1 activation by sensing intracellular leucine concentration and initiating molecular events leading to mTORC1 activation (Han et al., 2012a).

The upregulation of oxidative phosphorylation and glycolysis is also notable. According to the Warburg effect most cancer cells perform aerobic glycolysis. In this phenomenon, cancer cells metabolize glucose to pyruvate even under normoxic conditions. This metabolic route is thought to be used by the cancer cells that constitute the bulk of the tumour, but it has not yet been specifically described for CSCs. A possible explanation for the upregulation of these metabolic pathways is that CAIX+ve cells use both glycolysis and oxidative phosphorylation to maximize ATP

production. In normal cells the usage of both oxidation phosphorylation and glycolysis it can be seen in cells that required large amounts of energy in order to function. One example is the heart that requires large amounts of ATP for contraction, and uses both glycolysis and oxidative phosphorylation to maximize ATP production (Tennant et al., 2010).

6.2.3 Validation of the expression of genes implicated in Fatty Acid synthesis and pyruvate metabolism in CAIX+ve cells

Moreover the upregulation of TCA cycle and pyruvate metabolism is giving further evidence that the CAIX+ve cells have active mitochondria respiration. During aerobic glycolysis two molecules of pyruvate are produced for every molecule of glucose consumed and using the oxidative potential of NAD^+ another 2 molecules of ATP are generated. In most healthy tissues, pyruvate is then directed into the mitochondrion and decarboxylated into acetyl-CoA, which it enters the TCA cycle. In the TCA cycle acetyl-CoA and NADPH are oxidized generating 34 molecules of ATP per glucose. In addition to this, the intermediates of TCA cycle can be used for lipid biosynthesis. Citrate is one of the TCA intermediates, which ones is exported from the mitochondrion, is converted to cytosolic acetyl-CoA by ATP citrate lyase (Tennant et al., 2010). Acetyl-CoA is then converted to malonyl-CoA, which is a substrate for fatty acid synthase (FASN). FASN is a multi-enzyme that catalyzes the synthesis of long-chain fatty acids (FA) by using acetyl-CoA as a primer, malonyl-CoA as a two-carbon donor, and NADPH as a reducing equivalent (Menendez and Lupu, 2007). FAs are important components of all biological membranes lipids and also they serve as substrates for energy metabolism. Interestingly, FASN and ELOVL6, an enzyme that catalyzes the synthesis of saturated and monounsaturated fatty acids are among

the genes that are upregulated in CAIX+ve cells (**Table 6.4**). To validate this data I performed a q-PCR based analysis of FASN and ELOVL6 expression in CAIX+ve and CAIX-ve cell lines. The results were normalized relative to normoxic CAIX+ve and $p<0.001$, n=3, biological replicates) are significantly upregulated in the CAIX+ve cell line both under normoxic and hypoxic conditions **(Figure 6.4C(i) and (ii))**. Under hypoxic conditions the expression of FASN is reduced in both populations compared to normoxia, but only in CAIX-ve cells is statically significant. In addition the expression of ELOV6 is also significantly reduced under hypoxic conditions in both subpopulations. This suggests that CAIX+ve cells display an increased fatty acid synthesis, a phenomenon observed in many tumours, including breast cancer.

Table 6.3: Upregulated genes in CAIX+ve population

SYMBOL	*Score(d)*	*Numerator(r)*	*Denominator(s+s0)*	*Fold Change*
CA9	**8.07**	**3.40**	**0.42**	**10.59**
NFIA	4.87	2.17	0.45	4.49
RFTN1	5.05	2.14	0.42	4.39
PEG10	2.83	2.03	0.72	4.09
TSKU	2.69	1.88	0.70	3.67
RASD1	2.91	1.75	0.60	3.36
LDHB	**3.62**	**1.69**	**0.47**	**3.23**
GBX2	4.34	1.59	0.37	3.01
PEG10	4.77	1.56	0.33	2.95
LOC100132761	1.74	1.41	0.81	2.67
ALDH3B2	1.44	1.05	0.73	2.08
KIAA0114	2.12	1.05	0.50	2.08
LOC100130624	1.87	1.05	0.56	2.07
KIAA1324	3.10	1.05	0.34	2.06
CYB5D2	2.71	1.04	0.39	2.06
IFI30	2.44	1.04	0.43	2.06
LOC100130332	2.20	1.04	0.47	2.05
FAT1	2.34	1.04	0.44	2.05
SUMF1	2.28	1.03	0.45	2.04
ELOVL6	**1.99**	**1.02**	**0.51**	**2.02**
FASN	**1.86**	**1.01**	**0.54**	**2.02**

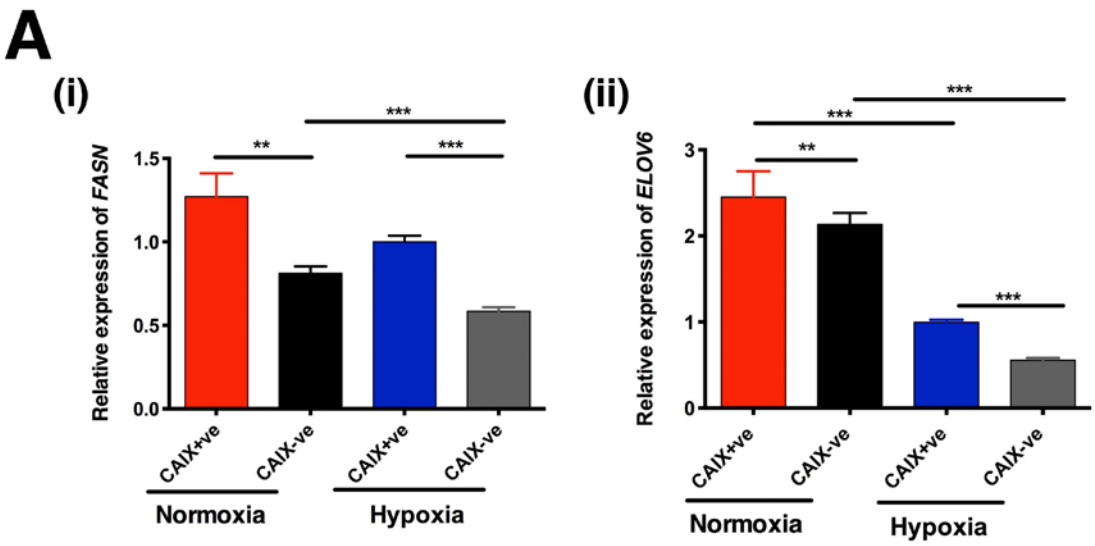


Figure 6.4 Expression of genes implicated in fatty acid synthesis. (A) FASN (i) and ELOVL6 (ii) mRNA expression levels under normoxia and hypoxia in CAIX+ve and CAIX-ve cell lines. FASN and ELOVL6 are significantly upregulated in CAIX+ve cell line. **=p<0.01, ***=p<0.001. Error bars represent SD.

Furthermore, LDHB was another upregulated gene that I selected to validate by q-PCR analysis (**Table 6.4**). LDHB is an enzyme that converts pyruvate, the final product of glycolysis to lactate. To validate this we performed a q-PRC analysis of LDHB in CAIX+ve, CAIX-ve sorted cells and in normoxic and hypoxic unsorted MCF7 cells. The results showed that LDHB is significantly ($p<0.001$, n=3, biological replicates) upregulated in CAIX+ve cells **(Figure 6.5A)**. This is the first study showing differential expression of LDHB between different subpopulations. LDHB is also significantly ($p<0.001$, n=3, biological replicates) downregulated in unsorted hypoxic cells compared with the unsorted cells grown in normoxia, a phenomenon that has been previously described (Zha et al., 2011). Although at this point it remains unclear why LDHB is downregulated under hypoxia, it is worth noting that the expression pattern of LDHB in unsorted hypoxic cells is similar to the expression pattern of LDHB in CAIX-ve cells. This possibly reflects the higher percentage of CAIX-ve cells in the unsorted population.

Mitochondria are the major oxygen consumers in the cell. Quantification of mitochondrial respiration can be detected through measurement of the oxygen consumption rate (OCR). Given the above, I decided to measure the oxygen consumption rate of CAIX+ve and CAIX-ve cell lines under normoxic conditions. The results showed that the oxygen consumption rate of CAIX+ve cells is significantly ($p<0.01$, n=3, biological replicates) higher compared with the CAIX-ve cells **(Figure 6.5B)**. This is in agreement with our previous observations showing a high expression of genes implicated in mitochondria respiration.

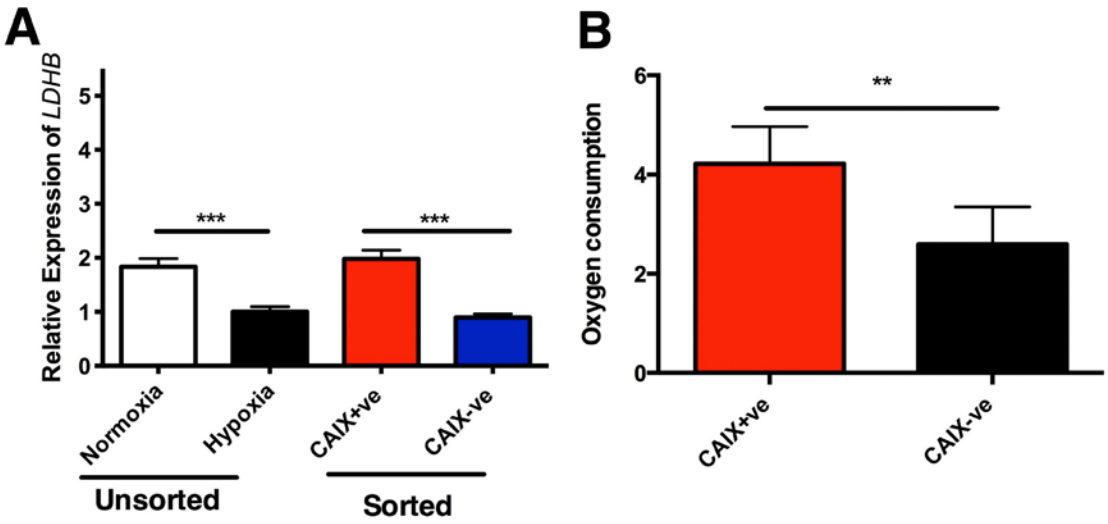


Figure 6.5 LDHB mRNA expression levels in CAIX+ve and CAIX-ve cells and oxygen consumption measurements for CAIX+ve and CAIX-ve cell lines. LDHB is significantly upregulated in CAIX+ve cells (A). (B) Lifetime fluorescence values assessed as an indication of O_2 consumption rate. CAIX+ve cells had significantly higher oxygen consumption than CAIX-ve cells. **=p<0.01, ***=p<0.001. Error bar represent SD.

Interestingly, and consistent with the results obtained from the RNA seq pathway analysis, Wnt and mTOR signaling pathways were also among the upregulated pathways revealed from the microarray pathway analysis. This strengthens my previous findings showing an enrichment for pathways implicated in stem cell maintenance within the CAIX+ve population.

In conclusion, our data show for the first time the existence of metabolic heterogeneity in response to hypoxia. We suggest that the metabolic activities of CAIX+ve cells possibly rely both on glycolysis and oxidative phosphorylation. Thus, it seems likely that CAIX+ve cells have the ability to use multiple metabolic pathways to produce energy. The existence of metabolic heterogeneity within tumours could explain the observed resistance to therapies that target only individual metabolic pathways. For example, inhibition of glycolysis has disappointingly-limited effect on tumourigenesis as monotherapy (Maschek et al., 2004). Given the above, we hypothesize that a new therapeutic avenue targeting different metabolic pathways could be a more effective cancer treatment and may also help to overcome drug resistance.

6.2.4 Pathways and genes upregulated in CAIX-ve cells

The KEGG and IPA pathway analysis showed that signaling pathways implicated in the innate immune responses are upregulated in the CAIX-ve cells (**Table 6.4** and **Table 6.5**). This is in agreement with the results of RNA seq's pathway analysis, which show a high expression levels of cytokines such as TGF-β, M-CSF, CXCL5 and members of the TNF superfamily in the CAIX-ve cells.

Among the upregulated genes in CAIX-ve cells are those implicated in the induction of autophagy **(Table 6.6)**. In order to validate this data I analyzed the expression levels of ULK1 and CHOP, known autophagy markers, using q-PCR and western blot based analysis in CAIX+ve cell line and CAIX-ve cell line under normoxic hypoxic conditions. The results showed that both ULK1 ($p<0.05$, n=3, biological replicates) and CHOP ($p<0.01$, n=3, biological replicates) are significantly upregulated in CAIX-ve cell line at RNA level under hypoxic conditions **(Figure 6.6 (B) and (C)**). In addition the protein levels of ULK1 and CHOP were upregulated in CAIX-ve cells both under normoxic and hypoxic conditions (**Figure 6.6 (D)**).

Table 6.4: KEGG pathway analysis for CAIX-ve cells

Genes	Hyp*	Annotations
4 genes	0.0155	Pentose and glucuronate interconversions Starch and sucrose metabolism
4 genes	0.0202	Metabolism of xenobiotics by cytochrome P450 Steroid hormone biosynthesis
10 genes	0.0285	Regulation of actin cytoskeleton
3 genes	0.0415	Pancreatic secretion Bile secretion Gastric acid secretion
3 genes	0.0453	Rheumatoid arthritis Leishmaniasis

(Hyp* = Corrected hypergeometric pValue)

Table 6.5: Ingenuity pathway analysis for CAIX-ve cells

Ingenuity Canonical Pathways	-log(p-value)
Actin Cytoskeleton Signaling	2.62E00
Pentose and Glucuronate Interconversions	2.06E00
Nucleotide Sugars Metabolism	2.04E00
TNFR2 Signaling	**1.82E00**
TR/RXR Activation	1.76E00
Cardiomyocyte Differentiation via BMP Receptors	1.69E00
IL-1 Signaling	**1.58E00**
C21-Steroid Hormone Metabolism	1.56E00
RAR Activation	1.5E00
MIF Regulation of Innate Immunity	**1.5E00**
Hypoxia Signaling in the Cardiovascular System	1.49E00
IGF-1 Signaling	1.48E00
ILK Signaling	1.48E00
Renal Cell Carcinoma Signaling	1.47E00
April Mediated Signaling	1.47E00
Molecular Mechanisms of Cancer	1.44E00
B Cell Activating Factor Signaling	1.41E00
PDGF Signaling	1.39E00
Signaling by Rho Family GTPases	1.38E00
BMP signaling pathway	1.37E00
Glycosphingolipid Biosynthesis - Neolactoseries	1.31E00
Glucocorticoid Receptor Signaling	1.31E00
TNFR1 Signaling	**1.28E00**
EGF Signaling	1.28E00

(*Statistical significance was determined by using Fisher's exact test ($P < 0.05$))

Table 6.6: Upregulated genes in CAIX-ve population

Symbol	Score(d)	Numerator(r)	Denominator(s+s0)	Fold Change
LOC387820	-2.16	-1.03	0.48	0.49
TCEAL3	-2.04	-1.03	0.50	0.49
LOC730291	-1.09	-1.03	0.94	0.49
SDCBP	-1.69	-1.03	0.61	0.49
HEY1	-1.10	-1.03	0.94	0.49
ULK1	**-1.88**	**-1.03**	**0.55**	**0.49**
SYCP2	-3.27	-1.02	0.31	0.49
NA	-1.94	-1.02	0.53	0.49
FXYD4	-1.31	-1.02	0.78	0.49
DNAJB6	-2.45	-1.02	0.42	0.49
SLC24A3	-1.37	-1.02	0.74	0.49
PIGA	-2.37	-1.01	0.43	0.50
FAM62B	-2.54	-1.01	0.40	0.50
FAM178B	-2.13	-1.01	0.47	0.50
BCAS3	-2.46	-1.01	0.41	0.50
UPLP	-3.26	-1.01	0.31	0.50
FAM83B	-3.13	-1.01	0.32	0.50
CXorf61	-3.05	-1.01	0.33	0.50
DHRS3	-1.53	-1.01	0.66	0.50
LAMP2	**-2.05**	**-1.01**	**0.49**	**0.50**

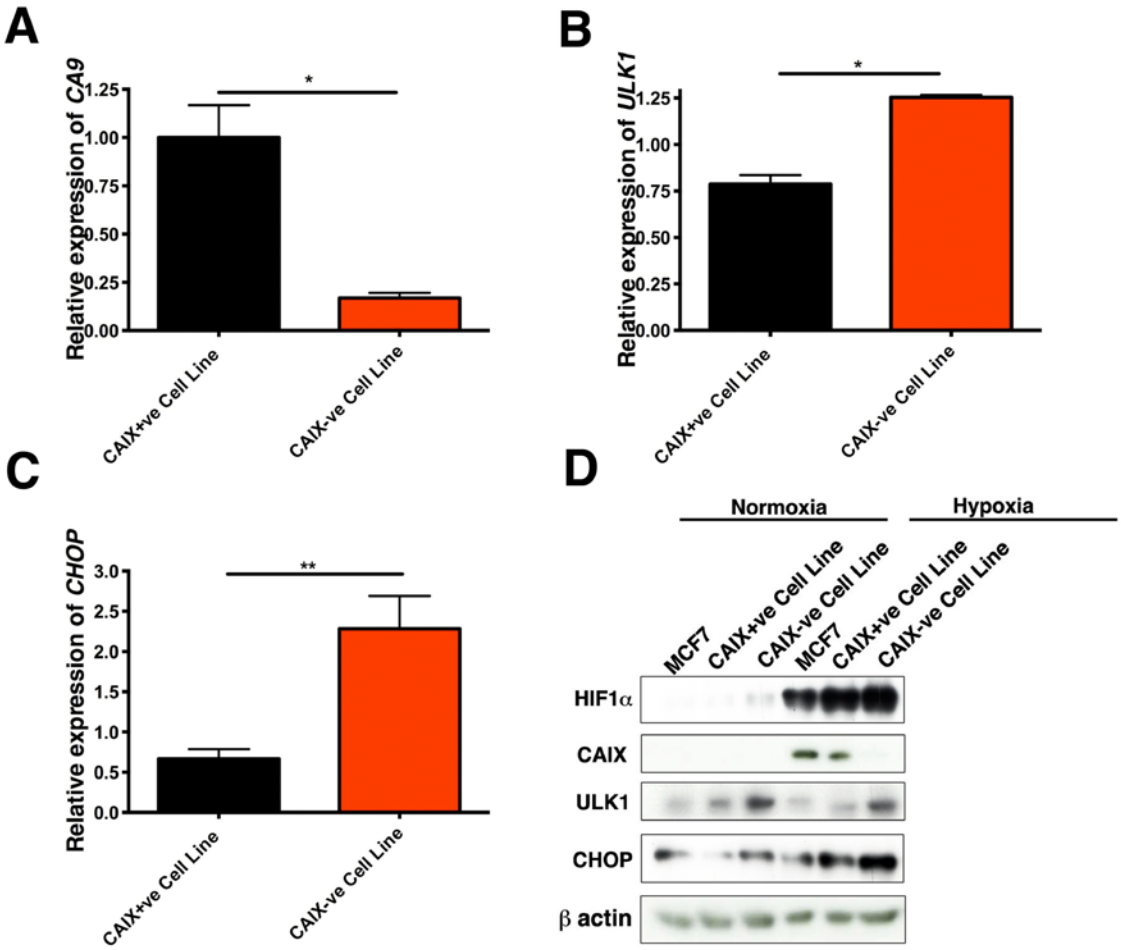


Figure 6.6 Expression of autophagy genes. mRNA and protein expression levels of autophagy related genes, ULK1 (B) and CHOP (C) in CAIX+ve and CAIX-ve cell lines. ULK1 and CHOP are significantly upregulated both at RNA and protein levels (D). *=P<0.05**=P<0.01, ***=p<0.001. Error bars represent SD.

Following this, I checked the mRNA expression levels of an additional three-autophagy marker LC3B, BNIP3 and LAMP1 in CAIX+ve and CAIX-ve cell lines under normoxic and hypoxic conditions. The results showed that LC3B ($p<0.001$, n=3, biological replicates), BNIP3 ($p<0.05$, n=3, biological replicates) and LAMP1 ($p<0.001$, n=3, biological replicates) were significantly upregulated in CAIX-ve cell line compared to CAIX+ve cell line at hypoxic conditions (**Figure 6.7**).

The lack of CAIX expression in the negative population results in the development of an acidic extracellular and intracellular pH. For this reason, the CAIX-ve cells are exposed to acidic stress which may promote the development of inflammatory tumour microenviroment. The high expression of cytokines and the upregulation of innate immune signaling pathways revealed by the RNA sequencing and microarray analysis could be a reflection of this inflammatory tumour microenvironment generated partially by the CAIX-ve cells. In support of this notion, the significant upregulation of autophagy markers in the CAIX-ve cells is in agreement with a recent study showing that acidic stress promotes the induction of autophagy (Hjelmeland et al., 2011).

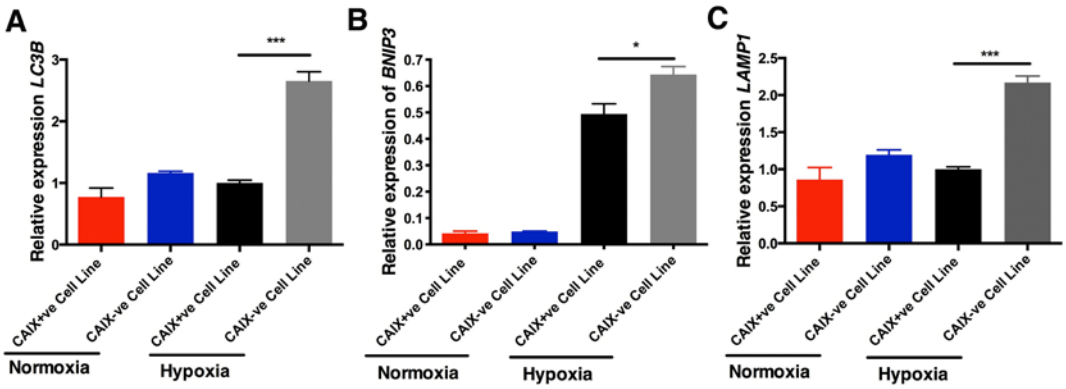


Figure 6.7 mRNA expression levels of LC3B, BNIP3 and LAMP1. LC3B (A)**,** BNIP3 (B) and LAMP1 (C) are significantly upregulated in CAIX-ve cell line both under normoxia and hypoxia. *=p<0.05,***=p<0.001.Error bars represent SD**.**

Discussion

Gene expression analysis using either microarrays or RNA seq technology is an important tool for cancer research as it provides a rich source of quantitative biological informations that allows us to understand and integrate the interactions of multiple components in cancer cells. Previous studies have shown that microarrays and RNA seq give results that are not completely consistence (Fu et al., 2009; Marioni et al., 2008). Although, a previous study have shown that 81% of differentially expressed genes are the same between the two methods (Marioni et al., 2008). Generally these two methods are viewed as complementary rather than competing approaches (Liu et al., 2007; Malone and Oliver, 2011). Accordingly, our results showed a very small overlap between the gene lists obtained from microarrays and RNA seq analysis. Importantly however, our q-PCR results validate both the RNA seq and microarray data. Future experiments looking the expression of genes that do not show the same expression trend between the two methods will be essential. At this stage, I cannot discuss which dataset is the most reliable because the status of development of the two techniques is not comparable nor is the coverage of the genome. In particular, the most comprehensive and potentially sensitive technique in term of coverage had only one replicate and so a limitation on the power due to costs, whilst the most established but less comprehensive or sensitive had three replicates. The pathway analysis results from both gene expression technologies are in agreement with the upregulation of stem cells pathways in the CAIX+ve population. This consistency strengthens our findings, which show stem cell enrichment within the CAIX+ve population. In addition, the pathway analysis from data obtained by both technologies showed an upregulation of pathways involved in inflammatory and

immune responses in the CAIX-ve population. Overall these results suggests that despite the low overlap in the upregulation of genes, both gene expression technologies showed a similar pattern of upregulated signaling pathways. These observations are important, as the main aim of this thesis was to complement the molecular data obtained from the gene expression experiments with phenotypic information in order to further our understanding of the differential molecular pathways that govern the CAIX+ve and CAIX-ve cells.

Further to this, the microarray pathway analysis revealed the existence of metabolic heterogeneity and metabolic coupling between the two CAIX subpopulations. The upregulation of glycolysis, oxidative metabolism, and TCA cycle in the CAIX+ve cells suggest that these cells are capable of utilizing multiple metabolic pathways in order to produce energy. Previous studies have shown that mTORC1 is a key regulator of mitochondria metabolism and biogenesis as well as regulator of oxidative phosphorylation (Chen et al., 2008; Cunningham et al., 2007; Schieke et al., 2006). Having established in the previous chapters that CAIX+ve cells upregulate mTORC1 we postulate that the molecular mechanisms responsible for the upregulation of oxidative metabolism and TCA cycle is driven by mTOR signaling. Given the fact that CAIX+ve cells are enriched with stem cells, these results also suggest that cancer stem cells have a different metabolic status from the differentiated cells that constitute the bulk of the tumour.

Our results are in agreement with the recent study showing that the metabolic state of glioma stem cells (GSC) differ substantially from the metabolic state of differentiated glioma cells (Vlashi et al., 2011). It has been shown that GSCs rely mainly on

oxidative phosphorylation, however if they challenged they can use additional metabolic pathways (Vlashi et al., 2011). This metabolic heterogeneity is correlated with resistance to ionizing radiation (Vlashi et al., 2011). Additionally, it has been shown that in the head and neck cancer the high proliferating cancer stem-like cells have high mitochondrial metabolism, with high lactate and ketone body uptake, compared with the low proliferating non-stem like cells which show low mitochondrial metabolism as well as high lactate and ketone body generation and high oxidative stress (Curry et al., 2013).

The upregulation of oxidative phosphorylation under hypoxia may sound paradoxical, as low oxygen is considered to restrict mitochondrial respiration and oxidative phosphorylation. However it has been shown that even at very low oxygen concentration (0.1% O_2) mitochondria can efficiently respire promoting mitochondrial metabolism (Chance, 1965). Further to this, a recent study revealed the existence of redox state heterogeneity in clinical specimens of breast cancer patients and breast cancer cell lines. Interestingly, a higher oxidized state was observed in the core of the tumour, which is believed to be hypoxic, whereas the tumours peripherals appeared to have more reduced oxidized states (Xu et al., 2013).

Combining the upregulation of oxidative phosphorylation and TCA cycle in the CAIX+ve cells with the upregulation of autophagy genes and immune responses in the CAIX-ve population led us to suggest the existence of metabolic cooperation between these two subpopulations. According to this model, the high mitochondrial respiration of the CAIX+ve cells results in the production of mitochondrial reactive oxygen species (ROS). Given their stem cell-like phenotype, and the fact that cancer

stem cells contain higher levels of antioxidant defense systems (Diehn et al., 2009), it is very likely that CAIX+ve cells can manage their increased oxidative stress. In contrast, the CAIX+ve produced ROS induce oxidative stress in neighboring associated cells such as in CAIX-ve cells. This follows that the oxidative stress induced in the CAIX-ve population leads to upregulation of major transcription factors resulting in the activation of autophagy, mitophagy, aerobic glycolysis and inflammation. Therefore, this catabolic process in the CAIX-ve cells may results in the overproduction of high-energy metabolites such as lactate, glutamine and ketone bodies. Upon secretion, these catabolites can be consumed by CAIX+ve cells to fuel the mitochondrial oxidative metabolism. Our model of metabolic cooperation may also provide explanation for the LDHB upregulation in the CAIX+ve cells, as they need to convert lactate imported from the tumour microenvironment lactate into pyruvate, which can be then directed into the mitochondria and converted to acetyl-CoA. This then could enter the TCA cycle resulting in the production of ATP via mitochondrial oxidative phosphorylation. Overall, we suggest that CAIX+ve cells obtain energy by inducing catabolic processes in the CAIX-ve cells and most likely also in the surrounding host cells such as cancer associated fibroblasts.

The two compartment view of tumour metabolism or “the reverse Warburg effect” model has been described previously between cancer cells and stroma fibroblasts, where aerobic glycolysis and autophagy in host stromal cells fuels anabolic metabolism processes in cancer cells (Ertel et al., 2012; Martinez-Outschoorn et al., 2011a; Martinez-Outschoorn et al., 2012; Pecqueur et al., 2013). Additionally, the lactate shuttle can be found in a variety of tissues including the brain, skeletal and cardiac muscle, where glycolysis generated lactate is consumed from these tissues for

the production of energy (Kennedy and Dewhirst, 2010). Furthermore, our model is also supported by a recent study showing that high uptake of lactate and ketone by the breast cancer cells increases stemness, drives cancer recurrence and metastasis and correlates with poor clinical outcome (Martinez-Outschoorn et al., 2011b). Accordingly, cancer stem cells can be selectively killed by metformin, a standard drug for the treatment of diabetes. Metformin inhibits mitochodrial metabolism and induces aerobic glycolysis, therefore its success in targeting specifically the cancer stem cells may be due to the downregulation of mitochodrial metabolism. In line with our results and recent literature, we postulate that this could represent the "Achilles heel" of cancer stem cells.

mTORC1 is a key regulator of mitochondria metabolism and biogenesis as well as regulator of oxidative phosphorylation (Chen et al., 2008; Cunningham et al., 2007; Schieke et al., 2006). LDHB is a downstream target of mTOR that is critical for oncogenic mTOR-mediated tumourigenesis (Zha et al., 2011). Therefore, the molecular mechanism underlying the metabolic heterogeneity of the two populations is likely due to the differential expression of mTOR signaling. Here we established the upregulation of mTORC1 in CAIX+ve cells, where CAIX-ve cells display an inactive mTORC1 signaling. Previous data have shown that ULK1 inhibits mTORC1 signaling (Dunlop et al., 2011). Given the fact that CAIX-ve cells upregulate ULK1, this study provides an explanation for the mTORC1 inactivation in the CAIX-ve cells. (Dunlop et al., 2011).

In conclusion, our data provide evidence for the existence of metabolic heterogeneity and metabolic cooperativity between the CAIX+ve and CAIX-ve populations. Further

work is needed to provide on in depth-insight into this mechanism.

Chapter Seven

Final Discussion

9.1 CAIX expression and Hypoxic Heterogeneity

During tumour development, rapid expansion and growth of cancer cells creates poorly vascularized regions, characterized by hypoxia, with irregular blood flow, low pH and nutrient starvation. Such a microenvironment makes tumours highly heterogeneous by changing the patterns of gene expression in several ways. This favors the outgrowth of more aggressive survival traits (Heddleston et al., 2010b). In line with this, the extent of hypoxia also strongly correlates with poor patient survival and therapeutic resistance (Heddleston et al., 2010b). For example, it has been shown that hypoxic cells are three-fold more resistance to radiotherapy compared to well oxygenated cells (Vaupel and Harrison, 2004). Currently, pimonidazole, osteopenia, and ^{12}F-fluoromisonidazole are the most commonly used biomarkers of hypoxia. However, they suffer from several limitations. Therefore, identification of novel hypoxic biomarkers is of vital importance from the clinical point of view, as it may help to unravel some of the molecular mechanisms driving the aggressive tumour phenotypes. This knowledge will eventually lead to the development of more effective cancer treatments, and improved patients management.

In recent years, CAIX, a transmembrane protein has been shown to be an excellent biomarker of hypoxia. Moreover, its expression is associated with poor survival in most cancers, such as breast cancer (Chia et al., 2001), non-small cell lung (Giatromanolaki et al., 2001) and head and neck cancer (Jonathan et al., 2006) making CAIX a potential therapeutic target (Robertson et al., 2004).

In this thesis, we demonstrated for the first time that hypoxia promotes tumour heterogeneity through epigenetic regulation of CAIX. We identify, isolate and characterize two distinct populations of tumour cells, one that expresses CAIX and

the other that does not in MCF-7, SW1222, and HCT166, but not MDA-MB-231. The MDA-MB-231 breast cancer cell line displays a more uniform expression of CAIX, with almost all cells expressing CAIX. In line with this, previous studies have shown that CAIX is upregulated in basal-like breast tumours (Tan et al., 2009), which are characterized by their stem like phenotype (Kim et al., 2012). Given the above and the fact that MDA-MB-231 is a basal-like breast cancer cell line, we postulate that the uniform express of CAIX in this cell line is due to the higher proportion of stem like cells in this cell line. Interstingly, previous studies have identified CAXII upregulation in response to CAIX knockdown in 2D culture, in spheroids and in vivo (Chiche et al., 2009; McIntyre et al., 2012). In this study, the analysis of microarray data has shown that the CAIX-ve cells upregulate only CA2 and no other CA.

Importantly, we show that these two hypoxic tumour cell populations are characterized by major genetic and phenotypic differences. This is important from the therapeutic point of view, as this heterogeneity may be also present within the tumour microenvironment.

Moreover recent studies suggest that hypoxia can cause chromatin alterations, such as global deacetylation, and an increase in H3K9me3/me2 (Johnson et al., 2008). Histone methylation is regulated by a group of histone modifying enzymes called histone demethylases and histone methyltransferases. Interestingly, hypoxia induces the expression of the Jumonji C (JmjC) domain-containing histone demethylases JMJD1A and JMJD2B (Pollard et al., 2008; Wellmann et al., 2008; Yang et al., 2009). Moreover, our laboratory has recently shown that $CD133^{+}CA9^{+}$ HCT166 cells express high levels of JMJD1A (Yang et al., 2009) suggesting a differential expression of histone modifying enzymes in response to hypoxia. Thus identifying the

hypoxia-dependent molecular mechanisms driving differential expression of histone methylation and demethylation will provide new insights into specific epigenetic mechanisms that contribute to the generation of tumour heterogeneity. This could be of particular interest from a therapeutic point of view, as it may provide a rationale for the development of novel drugs targeting methyltransferases or histone demethylases.

Overall these results provide clear experimental evidence that tumours are not homogenous. The utilization of CAIX as a biomarker for the identification of hypoxic subpopulations may potentially help classify tumours and stratify patients for a better management. Furthermore, the identification of epigenetic regulation of the histones in response to hypoxia for highly selective gene regulation provides a connection between the epigenetic mechanisms under environmental stress and cancer progression.

9.2 The CAIX positive population is enriched with hypoxic cancer stem cells

The cancer stem cell hypothesis and the clonal evolution model has been proposed to explain the establishment and maintenance of tumour heterogeneity (Campbell and Polyak, 2007). According to this model, only a subpopulation of cells with stem cell properties is able to drive tumour initiation and progression. This is supported by studies showing that only minor fraction of cells, which were isolated using specific stem cell markers, are able to generate serially transplantable tumours in recipient immunodeficient mice (Reya et al., 2001; Visvader, 2009). In contrast, the clonal evolution model states that tumours arise from normal cells that have accumulated various mutations over time that may confer advantages or disadvantages to the cell,

which are then subjected to natural selection (Michor and Polyak, 2010). These mutated cells in turn generate abnormal daughter cells, that are also mutated, generating a genetically heterogenous tumour (Nowell, 1976). However, these two models may not be mutually exclusive (Shackleton et al., 2009). Tumours are composed of different cell lineages, where each of them could originate from either normal stem cell that has undergone oncogenic mutation or from a mutated differentiated progeny through clonal evolution (Greaves and Maley, 2012; Polyak and Weinberg, 2009). In addition to this, cancer stem cells and differentiated progenies may undergo further mutational as well as epigenetic changes, generating additional lineages within the tumour (Polyak and Weinberg, 2009; Shibata and Shen, 2013).

Stem cell maintenance and survival depends upon signals that are generated from the local tissue niche as well as through upregulation of pluripotency transcription factors such as Oct4 and Nanog. The hypoxic microenvironment has been suggested to serve as a stem cell niche. An example of this is the bone marrow, where hematopoietic stem cells reside in regions regulated by oxygen tension (Heddleston et al., 2010b). Additionally, Wicha *et al* has shown that hypoxia increases the population of breast CSCs in xenografts (Wicha et al., 2006). Recent studies have also shown that hypoxia regulates breast cancer stem cells and is associated with metastasis and tumour development (Conley et al., 2012).

Interestingly, in this thesis we showed that the CAIX+ve gene signature was significantly enriched for pathways associated with stemness. Additionally, we also identified that treatment with HDACi led to elimination of the CAIX+ve population without affecting the levels of the HIF-1α, the major transcription activator of CAIX.

This is important as it suggests a HIF-1α-independent CAIX downregulation. Interestingly, SAHA treatment has been shown recently to inactivate mTOR signaling (Gammoh et al., 2012). Given the above and the observed downregulation of pS6K, a downstream target of mTOR, upon SAHA treatment we postulate that mTOR signaling contributes to the expression of CAIX. Since CAIX regulates intracellular pH, this could also provide a plausible explanation for the previously reported effects of HDACi on the acidification of intracellular pH (Chung et al., 2008; Gammoh et al., 2012; McBrian et al., 2013). Thus, considering that rapamycin causes a HIF-1α independent downregulation of CAIX, we postulate a negative feedback loop mechanism involving mTORC1 and CAIX. We hypothesize that the neutral intracellular pH due to CAIX expression in the positive population allows activation of mTORC1 signaling in these cells, which in turn contributes to the to the regulation of CAIX expression. Accordingly, mTORC1 has been recently shown to be a downstream target of CAIX (Lock et al., 2012).

Overall, these results demonstrate that CAIX does not serve only as a pH regulator under hypoxic conditions but its expression is associated with the regulation of stemness. Moreover, our results provide further support to the notion that hypoxic regions serve as stem cell niches, with CAIX being a key stem cell regulator. Therefore, we suggest that expression of CAIX in tumours may play an important role in producing a “a stem cell buffer zone’ producing a pH protected syncytial zone important for the survival and maintenance of cancer stem cells. Lastly, the differential sensitivity of the two populations to HDACi may open a new avenue for the use of HDACi for the treatment of hypoxic tumours.

9.3 A symbiotic relationship between CAIX+ve and CAIX-ve cells

Revisiting the Stephen Paget's "seed and soil" hypothesis of tumour metastasis, the seeds are the CSCs, and the soil is the rich microenvironment composed of diverse cell types which interact with tumour cells via growth factors and cytokine networks (Fidler, 2003; Korkaya et al.; Korkaya et al., 2009). The pathway analysis of RNA sequencing and microarray data revealed genomic heterogeneities and phenotypic variability between the CAIX+ve and CAIX-ve cells. Considering the fact that in tumours these populations are not in isolation from each other and from their microenvironment, we interpreted these results taking in account a possible symbiotic relationship between the CAIX+ve and CAIX-ve cells.

Firstly, we showed that the CAIX-ve cells express high levels of cytokines such as TGF-β, M-F and CXCL5. We suggest that the secreted CAIX-ve cytokines may produce bi-directional paracrine signals that regulate the CAIX+ve cells. Future work using ELISA is needed to be performed in order to confirm the secrection of cytokines formthe CAIX-ve cells. In addition, inhibiton of cytokines such as IL-6 with monoclonal antibodies may show the effect of these to the CAIX expression and how they contribute to the maintainance of a stable mixed population. Secondly, the pathway analysis from the microarray data suggests that each population displays distinct metabolic signatures. Among the upregulated metabolic pathways of CAIX+ve cells were glycolysis, oxidative metabolism, and TCA cycle. This suggests that the CAIX+ve cells are capable of utilizing multiple metabolic pathways in order to produce energy and also implies that stem like cells have a different metabolic status from the differentiated cells that constitute the bulk of the tumour.

The metabolic gene expression of CAIX+ve cells is more likely being driven by the two key signaling pathways HIF and mTORC1. Hypoxia causes increased glycolysis resulting in the production of glycolytic pyruvate which is then converted to lactate for the production of energy (Greer et al., 2012). HIF transcription factor complex is responsible for the upregulation of several genes that supports fermentative glucose metabolism (Cantor and Sabatini, 2012). Among the upregulated genes are lactate dehydrogenase A (LDHA) which is responsible for the conversion of pyruvate to lactate, and pyruvate dehydrogenase kinase-1 (PDK-1) which inhibits the entrance of pyruvate into the mitochondria (Cantor and Sabatini, 2012). Whereas, previous studies have shown that mTORC1 signaling is a key regulator of mitochondrial metabolism and biogenesis as well as a regulator of oxidative phosphorylation (Chen et al., 2008; Cunningham et al., 2007; Schieke et al., 2006).

Further to this, we showed a significantly increased expression of autophagy markers in the CAIX-ve cells. Taking into account the upregulation of oxidative phosphorylation and the TCA cycle in the CAIX+ve cells, we proposed the existence of a metabolic symbiosis between the CAIX+ve and CAIX-ve cells. This model which has been referred as “the reverse Warburg effect” model has been described previously between cancer cells and stroma fibroblasts, where aerobic glycolysis and autophagy in host stromal cells fuels anabolic metabolism processes in cancer cells (Ertel et al., 2012; Martinez-Outschoorn et al., 2011a; Martinez-Outschoorn et al., 2012; Pecqueur et al., 2013). In line with this, we postulate that catabolic processes such as autophagy and mitophagy in the CAIX-ve cells may result in the overproduction of high-energy metabolites such as lactate, glutamine and ketone bodies which in turn are used by CAIX+ve cells to fuel mitochondrial respiration. The

upregulation of LDHB in the CAIX+ve cells further supports this notion, as LDHB may convert imported lactate into pyruvate in order to direct mitochondria to the production of energy.

9.4 Concluding Remarks and Future Prospects

Taken together, the findings presented in this thesis confirm the that hypoxia promotes tumour heterogeneity. In addition it shows clear association between CAIX expression and stemness, and further supports the notion that hypoxia serves as a stem cell niche. Accordingly, the poor patient survival and therapeutic resistance that is associated CAIX expression may be a result of an increased proportion of CSCs in tumours (Yeung et al., 2011).

The differences in the chromatin structure of CAIX promoter between the two populations suggest a differential expression of histone modifying enzymes. Identification of specific histone demethylases or/and methylases that regulate this epigenetic modifications may give new insights of the molecular mechanism that govern the epigenetic changes contributing to the existence of tumour heterogeneity. Recently there is considerable interest in the connection between intermediary metabolism and epigenetic mechanisms of transcriptional regulation (Curry et al., 2013; Galdieri and Vancura, 2012; Rathmell and Newgard, 2009; Wellen et al., 2009). It has been suggested that cancer metabolism plays an important role in promoting stemness by utilization of high energy metabolites (Curry et al., 2013). In line with this, it has been shown that cancer stem cells display high mitochondrial metabolism, with high lactate and ketone body uptake (Curry et al., 2013; Galdieri and Vancura, 2012; Rathmell and Newgard, 2009; Wellen et al., 2009). The

metabolism of these high energy metabolites increases the Acetyl-CoA pool which results in increased histone acetylation (Martinez-Outschoorn et al., 2011b). Histone acetylation increases the gene transcription by neutralizing the positive charge on histones which leads to their dissociation from DNA (Martinez-Outschoorn et al., 2011b). Interestingly, histone acetylation is implicated in the regulation of stemness in ES cells (Markowetz et al., 2010). Given the above together with the stem like phenotype and the high mitochondrial metabolism signature of CAIX+ve cells, we suggest that a future direction would be the investigation of a possible link between mitochondrial metabolism and epigenetic control.

In addition, the imaging of cancer stem cells would provide valuable prognostic and predictive value. The utilization of high energy metabolism such as lactate and ketone by cancer stem cells could be used for the development of new PET tracers. Interestingly, an example of a new imaging agent for PET-scanning is currently being developed for the early detection of tumours in order to trace [^{11}C] Acetoacetate (a ketone body related to 3-hydroxy-butyrate) (Authier et al., 2008; Prenen et al., 1990).

Furthermore, the identification of CAIX as a biomarker of stem like cell populations could drive the development of specific CAIX inhibitors, either in the form of inhibitory antibodies or membrane–impermeable drugs. Additionally, specific inhibitory CAIX antibodies coupled with inhibitors of mitochondrial metabolism or inhibitors of mTOR pathway would increase specificity and decrease their toxicity to normal cells.

The findings of this thesis also highlight the importance of the symbiotic nature of cancer. The cells that represent the bulk of the tumour as well as signals from tumour microenvironment provide environmental support to stem cells. This highlights the

need for the development of combinational therapies that will not only target stem cells but also the more differentiated cells within the tumours.

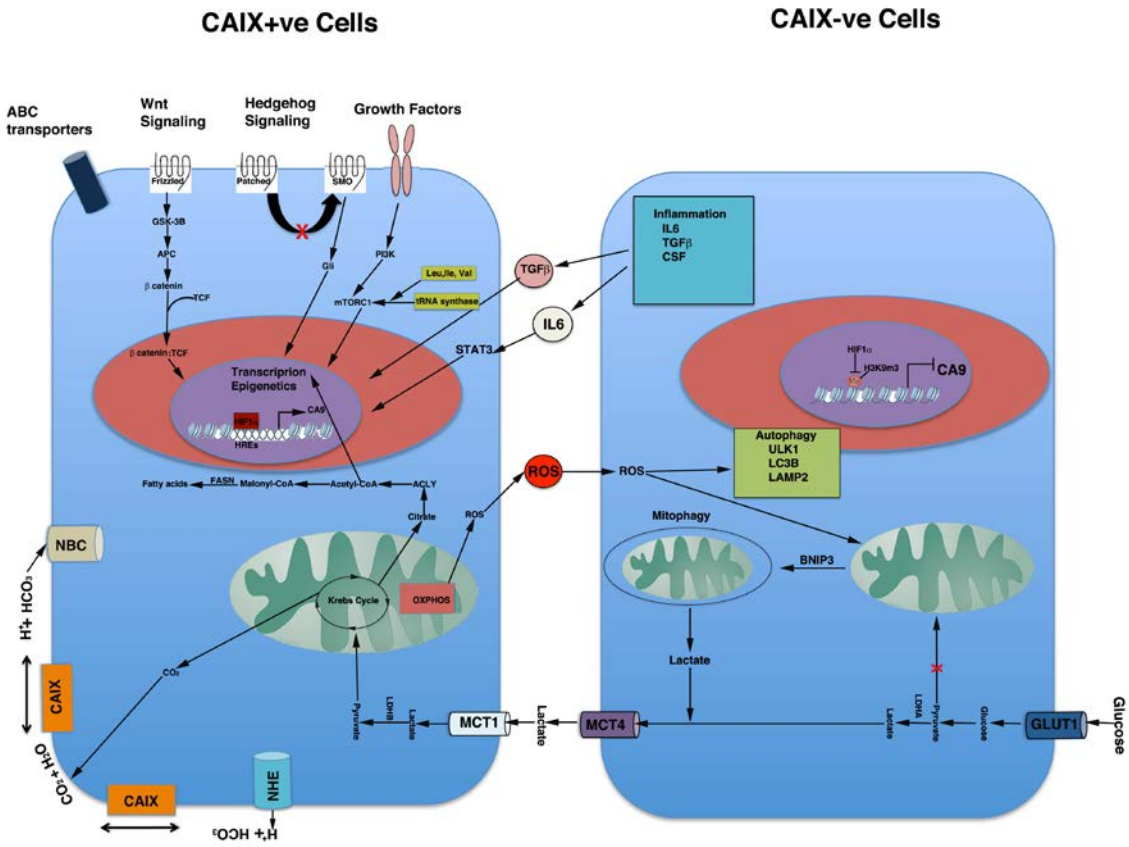


Figure 7.1 Schematic representation of CAIX+ve and CAIX-ve regulation. The genomic locus encoding *CA9* has a more "open" and transcriptionally active chromatin structure in CAIX+ve cells allowing HIF1 to bind to the to hypoxia response elements (HREs) in its promote and induces its transcription. The CAIX+ve cells are significantly enriched for pathways involved in stem cell maintenance, such as the ABC transporters, Hedgehog and WNT signaling pathway. The neutral intracellular pH due to CAIX expression in the positive population allows activation of mTORC1 signaling in these cells, which in turn contributes to the to the regulation of CAIX expression. The CAIX+ve cells show an upregulation of genes implicated in

oxidative phosphorylation, Krebs cycle and fatty acid synthesis. The CO_2 generated from the mitochondria diffuses aout of the cell. In the interstitial space CO_2 is catalytically hydrated by CAIX to HCO_3^- and H^+. A certain fraction of HCO_3^- is recycled into the cell by Na^+- HCO_3^- co-transport (NBC) or Na^+- dependent Cl^- HCO_3^- exchange (NDCBE), thereby maintaining a diffusion gradient of CO_2 and facilitates its diffusion. The high mitochondrial respiration of the CAIX+ve cells results in the production of mitochondrial reactive oxygen species (ROS). The CAIX+ve produced ROS induce oxidative stress in neighboring associated cells such as in CAIX-ve cells. This follows that the oxidative stress induced in the CAIX-ve population leads to upregulation of major transcription factors resulting in the activation of autophagy, mitophagy, aerobic glycolysis and inflammation. Therefore, this catabolic process in the CAIX-ve cells may results in the overproduction of high-energy metabolites such as lactate. In the CAIX-ve the glycolytic metabolism is associated with reduced substrate delivery to the mitochondria (through the action of pyruvate dehydrogenase kinase 1 [PDK1]) and reduced mitochondrial mass (as a result of autophagy triggered by BNIP3). High metabolites such as lactate can be exported from the CAIX-ve cells through MCT4. CAIX+ve cells express proteins that allow them to take up lactate (e.g., MCT1) and use it (e.g., LDHB) as their principal substrate for mitochondrial oxidative phosphorylation. The genomic locus encoding *CA9* has a condense and transcriptionally silent chromatin structure in the CAIX-ve cells and HIF cannot bind to induce its transcription.

9.5 Future Experimental Work

1. Correlation of CAIX staining with stem cells markers in TMAs of breast cancer patients and overlap within samples.
2. Co-culture of CAIX+ve and CAIX-ve population with cancer associated fibroblasts (CAFs) in order to study the interaction of each population with the stroma compartment and its effect in cancer stem cell behaviour.
3. Studying the interaction and the localization of the two subpopulations in 2D and 3D cultures. This can be obtained by mixing CAIX+ve cells transfected with GFP-expressing plasmid and CAIX-ve cells transfected with plasmids expressing the cherry red protein.
4. Functional assays to study the metastatic and migratory capacities of CAIX+ve and CAIX-ve cells.
5. Identification of CAIX as a biomarker of circulating tumour cells (CTCs). The transmembrane location of CAIX enables it to be a valuable circulating cell tumour biomarker. This may give new insights of the nature of the CTSs and may also help to predict outcomes and response to therapies.
6. Evaluation of HDACi *in vivo* in combination with Bevacizum ab (Avastin), an anti-VEGF monoclonal antibody. Correlation of treatment and tumour growth with CAIX expression.
7. Explore in depth the metabolism of each population. Treatment of the two subpopulations with different metabolites such as glucose, pyruvate, lactate, glutamine in order to investigate their metabolic profile and metabolic dependencies.
8. Inhibition of oxidative phosphorylation (OXPHOS) with oligomycin A in the CAIX+ve and CAIX-ve cells in order to study the effects on cell growth.

Additionally, it would be interesting to investigate the effect of OXPHOS inhibition on CAIX expression.

9. Inhibition of mTOR in order to study the metabolic changes in CAIX+ve cells. For example the effects on mitochondria respiration and lipids synthesis.
10. Effects of autophagy inhibition on the cell growth of CAIX+ve and CAIX-ve cells. Additionally, the effects of autophagy inhibition on cell metabolism of the two populations. Also correlation of CAIX staining with autophagy markers in xenograft and patient material.
11. Investigation of differential expression of other genes implicated in tumour metabolism in the two subpopulations. Importantly monocarboxylate transporter 1 (MCT1), which mediates the uptake of lactate, and monocarboxylate transporter 4 (MCT4) which mediates the lactate efflux will provide evidences of the existence metabolic symbiosis between different cancer subpopulations.
12. Investigation of differential expression of histone modifying enzymes such as the histone demethylases JMJD1A and JMJD2B will provide new insight into specific epigenetic mechanisms that contribute to the generation of tumour heterogeneity.

Appendix One

Top 100 genes upregulated in CAIX+ve and

CAIX-ve populations (RNA – Seq analysis)

Table 1: Top 100 genes upregulated in CAIX+ve populations (RNA – Seq)

Fold_change_(log2)	Gene_id	Gene_description
16.871	ENSG00000086991	NOX4, NADPH oxidase 4 - protein_coding
16.5909	ENSG00000154478	GPR26, G protein-coupled receptor 26 - protein_coding
16.4465	ENSG00000086288	TXNDC3, thioredoxin domain containing 3 (spermatozoa) - protein_coding
16.2861	ENSG00000181214	OR8G2, olfactory receptor, family 8, subfamily G, member 2 - pseudogene
16.2861	ENSG00000229254	OR8C1P, olfactory receptor, family 8, subfamily C, member 1 pseudogene - pseudogene
16.1055	ENSG00000237600	Putative uncharacterized protein ENSP00000412947 Fragment - protein_coding
16.1055	ENSG00000148513	ANKRD30A, ankyrin repeat domain 30A - protein_coding
16.006	ENSG00000197632	SERPINB2, serpin peptidase inhibitor, clade B (ovalbumin), member 2 - protein_coding
15.8991	ENSG00000174403	C20orf200, Putative uncharacterized protein C20orf200 - protein_coding
15.8991	ENSG00000149443	C20orf78, Putative uncharacterized protein C20orf78 - protein_coding
15.8991	ENSG00000228868	MYLKP1, myosin light chain kinase pseudogene 1 - pseudogene
15.8425	ENSG00000182816	KRTAP13-2, keratin associated protein 13-2 - protein_coding
15.7837	ENSG00000174946	GPR171, G protein-coupled receptor 171 - protein_coding
15.7837	ENSG00000153822	KCNJ16, potassium inwardly-rectifying channel, subfamily J, member 16 - protein_coding
15.7223	ENSG00000165970	SLC6A5, solute carrier family 6 (neurotransmitter transporter, glycine), member 5 - protein_coding
15.7223	ENSG00000150637	CD226, CD226 molecule - protein_coding
15.6582	ENSG00000150681	RGS18, regulator of G-protein signaling 18 - protein_coding
15.6582	ENSG00000173597	SULT1B1, sulfotransferase family, cytosolic, 1B, member 1 - protein_coding
15.5207	ENSG00000081051	AFP, alpha-fetoprotein - protein_coding
15.5207	ENSG00000197992	CLEC9A, C-type lectin domain family 9, member A - protein_coding
15.5207	ENSG00000180483	DEFB119, defensin, beta 119 - protein_coding
15.5207	ENSG00000105664	COMP, cartilage oligomeric matrix protein - protein_coding
15.4464	ENSG00000236769	unknown - processed_transcript
15.4464	ENSG00000164651	SP8, Sp8 transcription factor - protein_coding
15.3684	ENSG00000145839	IL9, interleukin 9 - protein_coding
15.3684	ENSG00000174407	C20orf166, Uncharacterized protein C20orf166 - protein_coding
15.3684	ENSG00000226684	unknown - processed_transcript
15.3684	ENSG00000184344	GDF3, growth differentiation factor 3 - protein_coding
15.3684	ENSG00000165066	NKX6-3, NK6 homeobox 3 - protein_coding

15.3684	ENSG00000212983	HCG1990367Putative uncharacterized protein DKFZp761K2322
15.3684	ENSG00000213822	CEACAM18, carcinoembryonic antigen-related cell adhesion molecule 18 - protein_coding
15.1984	ENSG00000165471	MBL2, mannose-binding lectin (protein C) 2, soluble (opsonic defect) - protein_coding
15.1984	ENSG00000182477	OR2B8P, olfactory receptor, family 2, subfamily B, member 8 pseudogene - pseudogene
15.1984	ENSG00000183035	CYLC1, cylicin, basic protein of sperm head cytoskeleton 1 - protein_coding
15.1984	ENSG00000106236	NPTX2, neuronal pentraxin II - protein_coding
15.1984	ENSG00000242550	SERPINB10, serpin peptidase inhibitor, clade B (ovalbumin), member 10 - protein_coding
15.1984	ENSG00000205810	KLRC3, killer cell lectin-like receptor subfamily C, member 3 - protein_coding
15.1984	ENSG00000133800	LYVE1, lymphatic vessel endothelial hyaluronan receptor 1 - protein_coding
15.1053	ENSG00000118434	SPACA1, sperm acrosome associated 1 - protein_coding
15.1053	ENSG00000170217	FAM27E3, family with sequence similarity 27, member E3 - pseudogene
6.7636	ENSG00000152214	RIT2, Ras-like without CAAX 2 - protein_coding
6.0438	ENSG00000152578	GRIA4, glutamate receptor, ionotrophic, AMPA 4 - protein_coding
5.562	ENSG00000188487	INSC, inscuteable homolog (Drosophila) - protein_coding
5.488	ENSG00000165805	C12orf50, Uncharacterized protein C12orf50 - protein_coding
5.3694	ENSG00000198542	ITGBL1, integrin, beta-like 1 (with EGF-like repeat domains) - protein_coding
5.3657	ENSG00000206129	HCG2045177cDNA FLJ45743 fis, clone KIDNE2016464 ; - protein_coding
5.2401	ENSG00000070193	FGF10, fibroblast growth factor 10 - protein_coding
5.147	ENSG00000208506	RNU4ATAC, RNA, U4atac small nuclear (U12-dependent splicing) - snRNA
4.7637	ENSG00000134612	FOLH1B, folate hydrolase 1B - protein_coding
4.7188	ENSG00000154262	ABCA6, ATP-binding cassette, sub-family A (ABC1), member 6 - protein_coding
4.6996	ENSG00000158077	NLRP14, NLR family, pyrin domain containing 14 - protein_coding
4.6958	ENSG00000120211	INSL4, insulin-like 4 (placenta) - protein_coding
4.5621	ENSG00000138813	C4orf17, Uncharacterized protein C4orf17 - protein_coding
4.5584	ENSG00000175065	DSG4, desmoglein 4 - protein_coding
4.4098	ENSG00000196578	OR5AC2, olfactory receptor, family 5, subfamily AC, member 2 - protein_coding
4.4064	ENSG00000166342	NETO1, neuropilin (NRP) and tolloid (TLL)-like 1 - protein_coding
4.3274	ENSG00000162618	ELTD1, EGF, latrophilin and seven transmembrane domain containing 1 - protein_coding
4.3239	ENSG00000172020	GAP43, growth associated protein 43 - protein_coding
4.2809	ENSG00000224924	C21orf131, unknown - processed_transcript
4.2399	ENSG00000179676	C18orf20, unknown - processed_transcript
4.2399	ENSG00000147402	GABRQ, gamma-aminobutyric acid (GABA) receptor, theta - protein_coding

4.2365	ENSG00000134827	TCN1, transcobalamin I (vitamin B12 binding protein, R binder family) - protein_coding
4.2072	ENSG00000212997	HCG2009141PRO2397 ; - protein_coding
4.1907	ENSG00000141338	ABCA8, ATP-binding cassette, sub-family A (ABC1), member 8 - protein_coding
4.1762	ENSG00000148948	LRRC4C, leucine rich repeat containing 4C - protein_coding
4.1762	ENSG00000169554	ZEB2, zinc finger E-box binding homeobox 2 - protein_coding
4.1468	ENSG00000204983	PRSS1, protease, serine, 2 (trypsin 2) - protein_coding
4.1434	ENSG00000140067	FAM181A, family with sequence similarity 181, member A - protein_coding
4.1434	ENSG00000140937	CDH11, cadherin 11, type 2, OB-cadherin (osteoblast) - protein_coding
4.0945	ENSG00000151834	GABRA2, gamma-aminobutyric acid (GABA) A receptor, alpha 2 - protein_coding
4.0472	ENSG00000166509	CLEC3A, C-type lectin domain family 3, member A - protein_coding
4.0472	ENSG00000196209	SIRPB2, signal-regulatory protein beta 2 - protein_coding
4.0472	ENSG00000227620	Putative uncharacterized protein ENSP00000407358 Fragment - protein_coding
4.0438	ENSG00000138722	MMRN1, multimerin 1 - protein_coding
4.0102	ENSG00000187498	COL4A1, collagen, type IV, alpha 1 - protein_coding
3.9914	ENSG00000187621	TCL6, T-cell leukemia/lymphoma 6 - protein_coding
3.9746	ENSG00000039537	C6, complement component 6 - protein_coding
3.9381	ENSG00000134538	SLCO1B1, solute carrier organic anion transporter family, member 1B1 - protein_coding
3.9369	ENSG00000148602	LRIT1, leucine-rich repeat, immunoglobulin-like and transmembrane domains 1 - protein_coding
3.9369	ENSG00000236301	C11orf36, unknown - processed_transcript
3.8695	ENSG00000225477	Isocitrate dehydrogenase 3 (NAD+) gamma-like - protein_coding
3.8413	ENSG00000113805	CNTN3, contactin 3 (plasmacytoma associated) - protein_coding
3.8215	ENSG00000229236	TTTY10, testis-specific transcript, Y-linked 10 (non-protein coding) - processed_transcript
3.8215	ENSG00000187151	ANGPTL5, angiopoietin-like 5 - protein_coding
3.8215	ENSG00000242267	Skint-like (pseudogene) (SKINTL), non-coding RNA - processed_transcript
3.8215	ENSG00000008197	TFAP2D, transcription factor AP-2 delta (activating enhancer binding protein 2 delta) - protein_coding
3.7601	ENSG00000207952	MIR624, microRNA 624 - miRNA
3.7601	ENSG00000196800	Putative serine protease inhibitor Kazal-type 5-like 2 Precursor - protein_coding
3.7402	ENSG00000137959	IFI44L, interferon-induced protein 44-like - protein_coding
3.7283	ENSG00000196273	C14orf70, Putative uncharacterized protein C14orf70 - protein_coding
3.7225	ENSG00000165323	FAT3, FAT tumor suppressor homolog 3 (Drosophila) - protein_coding
3.6976	ENSG00000107159	CA9, carbonic anhydrase IX - protein_coding
3.696	ENSG00000137252	HCRTR2, hypocretin (orexin) receptor 2 - protein_coding
3.6627	ENSG00000105967	TFEC, transcription factor EC - protein_coding

3.6527	ENSG00000123892	RAB38, RAB38, member RAS oncogene family - protein_coding
3.6069	ENSG00000186530	XKR5, XK, Kell blood group complex subunit-related family, member 5 - protein_coding
3.594	ENSG00000174740	PABPC5, poly(A) binding protein, cytoplasmic 5 - protein_coding
3.5596	ENSG00000234005	GAPDHP22, glyceraldehyde 3 phosphate dehydrogenase pseudogene 22 - pseudogene
3.5585	ENSG00000105383	CD33, CD33 molecule - protein_coding

Table 2: Top 100 genes upregulated in CAIX-ve populations (RNA – Seq)

Fold_change_ (log2)	***Gene_id***	***Gene_description***
-17.6897	ENSG00000196624	RAB44, RAB44, member RAS oncogene family - protein_coding
-17.6483	ENSG00000232810	Tumor necrosis factor Precursor (TNF-alpha)(Tumor necrosis factor ligand superfamily member 2)(TNF-a)(Cachectin)
-17.4212	ENSG00000169429	IL8, interleukin 8 - protein_coding
-17.1115	ENSG00000090382	LYZ, lysozyme (renal amyloidosis) - protein_coding
-16.9391	ENSG00000241850	GSTTP1, glutathione S-transferase theta pseudogene 1 - pseudogene
-16.9159	ENSG00000185880	TRIM69, tripartite motif-containing 69 - protein_coding
-16.8198	ENSG00000173212	C1orf161, Uncharacterized protein C1orf161 - protein_coding
-16.7167	ENSG00000229645	C14orf139, unknown - processed_transcript
-16.5467	ENSG00000214487	Putative uncharacterized protein ENSP00000391959 - protein_coding
-16.5467	ENSG00000205436	C14orf73, SEC6-like protein C14orf73 - protein_coding
-16.5164	ENSG00000165807	C14orf50, Uncharacterized protein C14orf50 - protein_coding
-16.4853	ENSG00000135346	CGA, glycoprotein hormones, alpha polypeptide - protein_coding
-16.4853	ENSG00000207590	MIR215, microRNA 215 - miRNA
-16.4536	ENSG00000170458	CD14, CD14 molecule - protein_coding
-16.4213	ENSG00000204437	CTSLL6, cathepsin L-like 6 - pseudogene
-16.4213	ENSG00000226979	Lymphotoxin-alpha Precursor (LT-alpha)(TNF-beta)(Tumor necrosis factor ligand superfamily member 1) - protein_coding
-16.3541	ENSG00000166831	RBPMS2, RNA binding protein with multiple splicing 2 - protein_coding
-16.2471	ENSG00000214336	FOXI3, forkhead box I3 - pseudogene
-16.1711	ENSG00000184599	FAM19A3, family with sequence similarity 19 (chemokine (C-C motif)-like), member A3 - protein_coding
-16.1317	ENSG00000111181	SLC6A12, solute carrier family 6 (neurotransmitter transporter, betaine/GABA), member 12 - protein_coding
-16.1317	ENSG00000221062	MIR1292, microRNA 1292 - miRNA
-16.1317	ENSG00000204252	HLA class II histocompatibility antigen, DO alpha chain Precursor (MHC class II antigen DOA)(MHC DZ alpha)(MHC DN-alpha) - protein_coding

-16.0911	ENSG00000214069	Putative uncharacterized protein ENSP00000380580 - protein_coding
-16.0911	ENSG00000188004	C1orf204, unknown - protein_coding
-16.0911	ENSG00000202503	SNORD34, small nucleolar RNA, C/D box 34 - snoRNA
-16.0492	ENSG00000171595	DNAI2, dynein, axonemal, intermediate chain 2 - protein_coding
-16.0062	ENSG00000203412	Lung cancer protooncogene 11 - protein_coding
-16.0062	ENSG00000200354	SNORA71D, small nucleolar RNA, H/ACA box 71D - snoRNA
-16.0062	ENSG00000197046	SIGLEC15, sialic acid binding Ig-like lectin 15 - protein_coding
-15.9617	ENSG00000227263	Putative uncharacterized protein ENSP00000390485 Fragment - protein_coding
-15.9617	ENSG00000207781	MIR625, microRNA 625 - miRNA
-15.9617	ENSG00000180251	SLC9A4, solute carrier family 9 (sodium/hydrogen exchanger), member 4 - protein_coding
-15.916	ENSG00000231818	Putative uncharacterized protein ENSP00000397650 - protein_coding
-15.916	ENSG00000208013	MIR652, microRNA 652 - miRNA
-15.8686	ENSG00000184502	GAST, gastrin - protein_coding
-15.8686	ENSG00000127743	IL17B, interleukin 17B - protein_coding
-15.8198	ENSG00000204086	RPA4, replication protein A4, 34kDa - protein_coding
-15.8198	ENSG00000182963	GJC1, gap junction protein, gamma 1, 45kDa - protein_coding
-15.8198	ENSG00000204241	Putative uncharacterized protein FLJ43312 - protein_coding
-15.8198	ENSG00000211514	MIR454, microRNA 454 - miRNA
-15.769	ENSG00000185668	POU3F1, POU class 3 homeobox 1 - protein_coding
-15.769	ENSG00000167194	C16orf92, Uncharacterized protein C16orf92 - protein_coding
-15.769	ENSG00000221067	MIR1280, microRNA 1280 - miRNA
-15.7167	ENSG00000174992	ZG16, zymogen granule protein 16 homolog (rat) - protein_coding
-15.7167	ENSG00000206612	SNORA2A, small nucleolar RNA, H/ACA box 2A - snoRNA
-15.7167	ENSG00000121690	DEPDC7, DEP domain containing 7 - protein_coding
-15.7167	ENSG00000186150	UBL4B, ubiquitin-like 4B - protein_coding
-15.6623	ENSG00000086159	AQP6, aquaporin 6, kidney specific - protein_coding
-15.6623	ENSG00000205363	C15orf59, UPF0583 protein C15orf59 - protein_coding
-15.6623	ENSG00000163497	FEV, FEV (ETS oncogene family) - protein_coding
-15.6623	ENSG00000217702	Putative uncharacterized protein MGC10955 - protein_coding
-15.6623	ENSG00000207996	MIR301A, microRNA 301a - miRNA
-15.6623	ENSG00000196735	HLA class II histocompatibility antigen, DQ alpha 1 chain precursor - protein_coding
-15.6056	ENSG00000142748	FCN3, ficolin (collagen/fibrinogen domain containing) 3 (Hakata antigen) - protein_coding
-15.5468	ENSG00000096395	MLN, motilin - protein_coding
-15.5468	ENSG00000203871	C6orf164, Putative uncharacterized protein C6orf164 - protein_coding
-15.5468	ENSG00000207688	MIR548D2, microRNA 548d-2 - miRNA
-15.5468	ENSG00000167105	TMEM92, transmembrane protein 92 - protein_coding

-15.5468	ENSG00000177096	FAM109B, family with sequence similarity 109, member B - protein_coding
-15.4853	ENSG00000166592	RRAD, Ras-related associated with diabetes - protein_coding
-15.4853	ENSG00000233186	unknown - pseudogene
-15.4853	ENSG00000180708	OR10K2, olfactory receptor, family 10, subfamily K, member 2 - protein_coding
-15.4853	ENSG00000180616	SSTR2, somatostatin receptor 2 - protein_coding
-15.4213	ENSG00000179520	SLC17A8, solute carrier family 17 (sodium-dependent inorganic phosphate cotransporter), member 8 - protein_coding
-15.4213	ENSG00000109181	UGT2B10, UDP glucuronosyltransferase 2 family, polypeptide B10 - protein_coding
-15.4213	ENSG00000167851	CD300A, CD300a molecule - protein_coding
-15.354	ENSG00000200785	SNORD8, small nucleolar RNA, C/D box 8 - snoRNA
-15.354	ENSG00000205681	PP10513 - protein_coding
-15.354	ENSG00000237452	Putative uncharacterized protein ENSP00000402674 - protein_coding
-15.354	ENSG00000159212	CLIC6, chloride intracellular channel 6 - protein_coding
-15.354	ENSG00000122133	PAEP, progestagen-associated endometrial protein - protein_coding
-15.354	ENSG00000087237	CETP, cholesteryl ester transfer protein, plasma - protein_coding
-15.2837	ENSG00000188771	C11orf34, Placenta-expressed transcript 1 protein Precursor - protein_coding
-15.2837	ENSG00000173714	WFIKKN2, WAP, follistatin/kazal, immunoglobulin, kunitz and netrin domain containing 2 - protein_coding
-15.2837	ENSG00000207973	MIR589, microRNA 589 - miRNA
-15.2837	ENSG00000223730	RPL6, ribosomal protein L6 - processed_transcript
-15.2837	ENSG00000182896	TMEM95, transmembrane protein 95 - protein_coding
-15.2837	ENSG00000206100	cDNA FLJ46459 fis, clone THYMU3020970 - protein_coding
-15.2837	ENSG00000057657	PRDM1, PR domain containing 1, with ZNF domain - protein_coding
-15.2837	ENSG00000128645	HOXD1, homeobox D1 - protein_coding
-15.2837	ENSG00000196611	MMP1, matrix metallopeptidase 1 (interstitial collagenase) - protein_coding
-15.2837	ENSG00000070886	EPHA8, EPH receptor A8 - protein_coding
-15.2837	ENSG00000160801	PTH1R, parathyroid hormone 1 receptor - protein_coding
-15.2837	ENSG00000206532	Putative uncharacterized protein LOC151760 - protein_coding
-15.2837	ENSG00000203985	LDLRAD1, low density lipoprotein receptor class A domain containing 1 - protein_coding
-15.2095	ENSG00000201643	SNORA14A, small nucleolar RNA, H/ACA box 14A - snoRNA
-15.2095	ENSG00000185269	NOTUM, notum pectinacetylesterase homolog (Drosophila) - protein_coding
-15.2095	ENSG00000140287	HDC, histidine decarboxylase - protein_coding
-15.2095	ENSG00000126950	TMEM35, transmembrane protein 35 - protein_coding
-15.2095	ENSG00000066056	TIE1, tyrosine kinase with immunoglobulin-like and EGF-like domains 1 - protein_coding
-15.2095	ENSG00000183801	OLFML1, olfactomedin-like 1 - protein_coding
-15.2095	ENSG00000207966	MIR29C, microRNA 29c - miRNA

-15.2095	ENSG00000110324	IL10RA, interleukin 10 receptor, alpha - protein_coding
-15.2095	ENSG00000198976	MIR429, microRNA 429 - miRNA
-15.2095	ENSG00000103742	IGDCC4, immunoglobulin superfamily, DCC subclass, member 4 - protein_coding
-15.1317	ENSG00000129151	BBOX1, butyrobetaine (gamma), 2-oxoglutarate dioxygenase (gamma-butyrobetaine hydroxylase) 1 - protein_coding
-15.1317	ENSG00000136535	TBR1, T-box, brain, 1 - protein_coding
-15.1317	ENSG00000238300	SNORD121B, small nucleolar RNA, C/D box 121B - snoRNA
-15.1317	ENSG00000134812	GIF, gastric intrinsic factor (vitamin B synthesis) - protein_coding

Table 3: Transcription Regulators

CAIX+ve Transcription Regulators	CAIX-ve Transcription Regulators
PAX6	NFkB (complex)
GSC	NFKB1
ESR1	SMAD3
TWIST1	RELA
REST	SP1
BARX2	ATF2
TSHZ3	SMAD4
NKX2-1	CEBPB (includes EG:1051)
NEUROD2	Ap1
KLF4	ATF3
LHX1	RXRA
Ap1	HDAC1
OTX2	REL
E2F4	BCL3
HNF1B	RUNX1
SNAI1	SIM1 (includes EG:20464)
POU2F1	ARNT2
IRF8	SPI1 (includes EG:20375)
RARG	STAT6
ETS2	STAT1
CTNNB1	FOXO1 (includes EG:2308)
ZFHX3	CEBPA
MZF1	MAGED1
HOXA5	CITED2
SIM1 (includes EG:20464)	VDR
HDAC3	Estrogen Receptor
ARNT2	NR3C1
CEBPB (includes EG:1051)	CREBBP
MYB	RUNX1T1
RARA	ELL2
SMARCA2	EP300
MYC	PRDM1
HMGB1	JUN
TFEC	NCOA2
NR2F2	TP53 (includes EG:22059)
ETS1	POU2AF1
SOX4	CREB1
TBX3	NCOR2
NR5A2	HES1 (includes EG:15205)
E2F1	PML
TBPL2	CTNNB1
THRAP3	EGR1
TAF3 (includes EG:209361)	Nr1h
TCFL5	BCL10
TBX4	RELB
SIX2	Rxr
NRIP2	CEBPE
CUX2	SIRT1
NKX2-8	NR4A1
IRX5	IRF7
PHF5A	NR1H3
CCRN4L	TAF4B
ALX4	HNRNPD
TRIP11	BCL6
	HMGB1

	STAT2
	NR4A2
	TCF7L2
	EPAS1
	JUNB
	Nfat (family)
	SMARCA2
	DACH1
	STAT
	NOTCH1
	VAV1
	Creb
	EZH2
	IRF3
	STAT3
	ESR2
	HTT
	LITAF
	HDAC6
	PAX9
	ELF3
	GATA2
	FOSL1
	STAT5B
	RARB
	NFKB2
	IKZF1
	IRF8
	LDB1
	MYOD1
	GFI1
	HDAC5
	JUND
	KLF4
	ZNF148
	MEF2A
	TCF3
	IRF1 (includes EG:16362)
	STAT4
	GATA3
	NANOG
	RNA polymerase II
	TRIM24
	GATA1
	MYCN
	CIITA
	RARG
	Ikb
	JUN/JUNB/JUND
	DLX2
	FHL2
	EHF
	HIF1A
	HDAC3
	PAX5
	HDAC3
	PAX5

Appendix Two

Top 100 genes upregulated in CAIX+ve and CAIX-ve population (Microarray analysis)

Table 7: Top 100 genes upregulated in CAIX+ve population (Microarray analysis)

PROBE_ID	SYMBOL	Fold Change	q-value(%)	logFC	adj.P.Val
ILMN_1725139	CA9	10.59084673	0	3.404746031	2.10E-07
ILMN_1758049	NFIA	4.490481866	0.873157224	2.166870266	6.46E-06
ILMN_1800787	RFTN1	4.39465603	0.873157224	2.13575025	6.46E-06
ILMN_1763359	PEG10	2.945653958	0.873157224	1.558587959	3.72E-05
ILMN_1680320	GBX2	3.012712033	1.629183601	1.591062781	3.86E-05
ILMN_1728132	LDHB	3.228945202	2.957137942	1.691062958	5.82E-05
ILMN_1700268	QPRT	2.591575376	2.957137942	1.373829355	0.000218594
ILMN_1795026	FAM189B	2.474066862	2.957137942	1.30688449	0.00016549
ILMN_1779213	TFG	2.411408597	2.957137942	1.269876127	0.000149434
ILMN_1782439	CNN3	2.342318806	2.957137942	1.22793745	0.000215343
ILMN_2312194	CYB5A	2.169367704	2.957137942	1.117274608	0.000395859
ILMN_2081335	C7orf44	2.137012374	2.957137942	1.095595262	0.000482655
ILMN_1771482	KIAA1324	2.064249276	2.957137942	1.045617199	0.000781269
ILMN_1804851	MRPS17	1.876436169	2.957137942	0.907995214	0.001750299
ILMN_2297626	PEG10	4.091265913	4.058523198	2.032547309	0.000288663
ILMN_1801443	TSKU	3.671096248	4.058523198	1.876210939	0.0004302
ILMN_1740426	RASD1	3.360120603	4.058523198	1.748513016	0.000224297
ILMN_1699574	NRP1	2.458458622	4.058523198	1.297754074	0.000601407
ILMN_1742547	NRP1	2.432397028	4.058523198	1.282378732	0.000421573
ILMN_1748591	ODC1	2.407627382	4.058523198	1.26761213	0.000408235
ILMN_3277905	LOC645313	2.386120989	4.058523198	1.254667197	0.000341848
ILMN_1730084	COMT	2.372300553	4.058523198	1.2462868	0.000516029
ILMN_1808590	GUCY1A3	2.370647416	4.058523198	1.245281108	0.000357111
ILMN_2349393	MDK	2.258856767	4.058523198	1.175592793	0.000850177
ILMN_1740170	CHCHD10	2.256362109	4.058523198	1.173998615	0.000872573
ILMN_3301740	LOC729887	2.197311722	4.058523198	1.135739552	0.000907735
ILMN_1679041	SLC3A2	2.143784553	4.058523198	1.100159924	0.000658727
ILMN_1696254	CYB5D2	2.061306829	4.058523198	1.043559268	0.001073787
ILMN_1679700	LOC389672	1.919011975	4.058523198	0.940363714	0.001610803
ILMN_2162253	NMU	1.903401187	4.058523198	0.928579676	0.001822132
ILMN_3179620	LOC100129673	1.889314582	4.058523198	0.917862939	0.001664476
ILMN_1678493	CHN1	1.888228404	4.058523198	0.917033287	0.001972291
ILMN_1718972	MFSD3	1.887395584	4.058523198	0.916396832	0.001745378
ILMN_2147114	PSPH	1.87061774	4.058523198	0.903514775	0.001926674
ILMN_1671731	AVPI1	1.862433673	4.058523198	0.897189047	0.001923424
ILMN_1797074	EMG1	1.857548347	4.058523198	0.893399761	0.0019225
ILMN_2414848	TBRG4	1.857113211	4.058523198	0.893061766	0.0019225
ILMN_2143685	CLDN7	1.771482954	4.058523198	0.824957583	0.00330653
ILMN_1693108	RUVBL1	1.747565553	4.058523198	0.805346574	0.003660149

ILMN_1671554	LPIN1	1.734001461	4.058523198	0.794105114	0.004178038
ILMN_1740724	LOC392221	1.6901495	4.058523198	0.757150863	0.005500675
ILMN_1784661	TMEM2	2.307624144	4.616020202	1.206408263	0.001274973
ILMN_1765574	TFAP2A	2.212475592	4.616020202	1.145661539	0.00120139
ILMN_1798270	C11orf75	2.160181055	4.616020202	1.111152237	0.001750299
ILMN_2345872	SUMF2	2.12524784	4.616020202	1.087631094	0.001439743
ILMN_1698766	PYCARD	2.094980181	4.616020202	1.066936596	0.001556908
ILMN_1770206	GEMIN4	2.092571184	4.616020202	1.0652767	0.001262369
ILMN_1807277	IFI30	2.058946112	4.616020202	1.041906071	0.001530047
ILMN_3247578	FAT1	2.051480363	4.616020202	1.036665345	0.00177777
ILMN_1753472	SUMF1	2.042743705	4.616020202	1.030508206	0.001926821
ILMN_1740466	FAM46A	1.992756826	4.616020202	0.994765671	0.001807734
ILMN_1856634	NA	1.918874253	4.616020202	0.940260172	0.002601259
ILMN_1796013	PYCR1	1.898416489	4.616020202	0.924796537	0.002693677
ILMN_1674620	SGCE	1.896279365	4.616020202	0.923171521	0.002580914
ILMN_1684217	AURKB	1.879300912	4.616020202	0.910196088	0.002794918
ILMN_1813938	CHCHD4	1.869793239	4.616020202	0.902878746	0.002516583
ILMN_2357134	SPHK1	1.844626828	4.616020202	0.883328986	0.002698568
ILMN_1792168	GALE	1.840207033	4.616020202	0.879868086	0.002946426
ILMN_1672443	QDPR	1.834042488	4.616020202	0.875027061	0.002867395
ILMN_1714167	CYB5A	1.825529152	4.616020202	0.868314707	0.002946426
ILMN_1805725	B4GALNT1	1.787367372	4.616020202	0.837836194	0.003825897
ILMN_2393169	THOC5	1.769648507	4.616020202	0.823462836	0.003618718
ILMN_1687922	RP9	1.768375558	4.616020202	0.822424699	0.003452269
ILMN_2165867	DHCR7	1.738152361	4.616020202	0.79755455	0.004783351
ILMN_2398489	SIGMAR1	1.736270326	4.616020202	0.795991583	0.004341274
ILMN_1670134	FADS1	1.729348408	4.616020202	0.790228555	0.004383349
ILMN_1781952	MGST1	1.708578356	4.616020202	0.772796411	0.005151084
ILMN_1815626	DHCR7	1.701405569	4.616020202	0.766727081	0.005302876
ILMN_2110252	NPM3	1.697579582	4.616020202	0.763479209	0.005397291
ILMN_1729868	SPRYD4	1.690393763	4.616020202	0.75735935	0.006105064
ILMN_1652163	DVL2	1.658964773	4.616020202	0.730283252	0.007022305
ILMN_1746252	LOC391811	1.644610568	4.616020202	0.717746004	0.007833376
ILMN_1749432	MRPL32	1.641671113	4.616020202	0.715165131	0.007879037
ILMN_2053281	C14orf149	1.631979465	4.616020202	0.706622904	0.008605032
ILMN_1665148	LOC648249	1.59643517	4.616020202	0.674853968	0.010943765
ILMN_2374115	TFAP2A	1.575049956	4.616020202	0.655397587	0.012693532
ILMN_1726456	SLC3A2	2.440334281	5.466164291	1.287078784	0.001610803
ILMN_1787345	FKBP11	2.265466271	5.466164291	1.179808011	0.002601259
ILMN_1746888	PCOLCE2	2.244780651	5.466164291	1.166574479	0.002089325
ILMN_3304555	LOC728324	2.192073287	5.466164291	1.132296032	0.001750299
ILMN_1738578	FILIP1L	2.182531269	5.466164291	1.126002323	0.002786031

ILMN_1801442	KRT81	2.078907148	5.466164291	1.055825324	0.002785259
ILMN_3248882	KIAA0114	2.076304081	5.466164291	1.054017746	0.002680382
ILMN_3273491	LOC100130332	2.052721817	5.466164291	1.037538128	0.002254371
ILMN_1888359	NA	1.938921539	5.466164291	0.955254424	0.002959876
ILMN_3290562	LOC131691	1.928561503	5.466164291	0.947525155	0.003148294
ILMN_2383383	PIR	1.894763123	5.466164291	0.922017499	0.003222823
ILMN_1682717	IER3	1.892522649	5.466164291	0.920310566	0.002918848
ILMN_1734149	LOC388122	1.886413056	5.466164291	0.915645608	0.003799926
ILMN_1789492	ZDHHC8	1.858079488	5.466164291	0.893812221	0.00333522
ILMN_1718997	LOC390956	1.838928365	5.466164291	0.878865281	0.003222823
ILMN_1781983	AP1B1	1.823822292	5.466164291	0.866965165	0.004228401
ILMN_1681437	DCXR	1.810575696	5.466164291	0.856448494	0.003832982
ILMN_1684446	SPAG7	1.784035564	5.466164291	0.835144375	0.004215131
ILMN_3226012	LOC728698	1.770284128	5.466164291	0.823980929	0.004654758
ILMN_1678049	FGB	1.751948703	5.466164291	0.808960533	0.004654758
ILMN_1706301	RET	1.731646834	5.466164291	0.792144725	0.005178895
ILMN_2380588	C6orf108	1.729089035	5.466164291	0.790012158	0.005942833
ILMN_3237562	SNORA76	1.720953557	5.466164291	0.783208164	0.005506783

Table 8: Top 100 genes upregulated in CAIX-ve population (Microarray analysis)

PROBE_ID	SYMBOL	Fold Change	q-value(%)	logFC	adj.P.Val
ILMN_2071809	MGP	0.098764335	4.222768988	-3.339866029	0.006170353
ILMN_1651958	MGP	0.143760913	4.222768988	-2.798256617	0.008465236
ILMN_2412336	AKR1C2	0.165132947	0	-2.598300105	6.46E-06
ILMN_1788874	SERPINA3	0.167745208	4.222768988	-2.575656545	0.0019225
ILMN_1712522	CEACAM6	0.177034332	0	-2.497898932	5.37E-06
ILMN_2218758	EFCBP1	0.183670788	1.649296979	-2.444805907	4.09E-05
ILMN_1721218	KRT13	0.186328378	1.649296979	-2.424080682	0.000144633
ILMN_1762561	PLA2G10	0.192452019	0	-2.377429289	6.46E-06
ILMN_2233319	SPANXA1	0.196187556	1.649296979	-2.34969456	3.21E-05
ILMN_2233314	SPANXA1	0.201815699	0	-2.308889688	5.11E-06
ILMN_1696731	LOC652683	0.208331702	0	-2.263045701	6.46E-06
ILMN_2376313	MSMB	0.224877263	4.222768988	-2.152790295	0.001517248
ILMN_1883745	NA	0.225876202	4.222768988	-2.146395814	0.000791154
ILMN_1728787	AGR3	0.228011344	4.048274402	-2.132822492	0.000482655
ILMN_2150402	TMEM64	0.231830385	4.222768988	-2.108858426	0.000717533
ILMN_1653415	SPANXA2	0.238450656	0	-2.068237341	6.46E-06
ILMN_2050246	AGR3	0.239795848	4.222768988	-2.060121418	0.001258407
ILMN_1790906	MSMB	0.246584888	4.222768988	-2.01984371	0.007576853
ILMN_1669982	CCDC85A	0.24709445	0	-2.016865486	6.46E-06
ILMN_2073289	MTSS1	0.247409045	0	-2.015029848	6.46E-06
ILMN_2199439	CA2	0.248976879	1.649296979	-2.005916323	9.57E-05
ILMN_1749962	NCAM2	0.250973346	1.649296979	-1.994393938	4.51E-05
ILMN_2136147	BCAS1	0.253626595	1.649296979	-1.979222062	3.36E-05
ILMN_3244876	LOC100133171	0.256168171	1.649296979	-1.964836863	8.59E-05
ILMN_1699243	MSMB	0.257150274	4.222768988	-1.959316402	0.008227867
ILMN_1733042	BCAS1	0.258863555	0	-1.949736228	6.46E-06
ILMN_1702487	SGK	0.263607891	4.222768988	-1.923534535	0.002609985
ILMN_1690170	CRABP2	0.267215945	4.222768988	-1.903921995	0.001534846
ILMN_2120247	SLC2A10	0.268498097	0	-1.897016231	6.46E-06
ILMN_1687757	AKR1C4	0.27280227	1.649296979	-1.874072445	0.000183744
ILMN_2137789	KLF4	0.27438167	1.649296979	-1.865743989	0.00016549
ILMN_1736670	PPP1R3C	0.274828585	3.281232936	-1.863396028	0.000255172
ILMN_2384056	GPER	0.276179857	0	-1.856319996	2.69E-05
ILMN_1809639	TMEM26	0.284011997	0	-1.815976224	1.82E-05
ILMN_1811014	PGR	0.284966063	1.649296979	-1.811137976	9.73E-05
ILMN_2337974	PKIA	0.287981549	0	-1.795951714	2.69E-05
ILMN_1731073	CAPN9	0.291348026	0	-1.779184558	2.69E-05
ILMN_1667947	NPY1R	0.295756523	4.222768988	-1.757518106	0.000915539

ILMN_1690923	CAPN9	0.296112637	1.649296979	-1.755782035	9.19E-05
ILMN_1679299	IGSF1	0.297842047	4.048274402	-1.747380657	0.00037916
ILMN_1764861	ISOC1	0.303016978	1.649296979	-1.722529464	0.00016549
ILMN_1669983	RGS22	0.305031285	3.281232936	-1.712970879	0.000306149
ILMN_1748303	MUC5AC	0.30826345	0	-1.697764254	2.71E-05
ILMN_1816342	NA	0.309398579	1.649296979	-1.692461524	0.000186313
ILMN_2230016	HIGD1A	0.312642217	1.649296979	-1.677415493	4.51E-05
ILMN_3236481	LOC100129086	0.316006183	4.222768988	-1.661975309	0.000576307
ILMN_2174189	DKK1	0.318094971	4.222768988	-1.652470531	0.001500559
ILMN_1763196	WDR72	0.320378954	0	-1.642148715	2.69E-05
ILMN_1702835	SH3BGRL	0.320606746	0	-1.641123314	2.69E-05
ILMN_2323007	CDH26	0.32144438	6.472880201	-1.637358968	0.020019042
ILMN_1732781	SPANXE	0.322516622	1.649296979	-1.632554577	6.71E-05
ILMN_1794863	CAMK2N1	0.323848554	4.222768988	-1.626608792	0.005958669
ILMN_1795342	MLPH	0.323902522	1.649296979	-1.626368392	8.62E-05
ILMN_1795298	GPER	0.324874379	1.649296979	-1.622046125	0.000177593
ILMN_1695941	NECAB1	0.328447808	3.281232936	-1.606263956	0.000288972
ILMN_1853876	NA	0.328516037	3.281232936	-1.605964295	0.000315939
ILMN_1773337	DKK1	0.329002594	4.222768988	-1.603829137	0.003264162
ILMN_1785646	PMP22	0.331128925	1.649296979	-1.594535055	0.000186313
ILMN_2131861	SOCS2	0.332413954	0	-1.588947148	3.86E-05
ILMN_1755582	PCSK1N	0.332437188	0	-1.588846317	3.21E-05
ILMN_2261076	NEDD9	0.333583918	0	-1.583878356	3.90E-05
ILMN_1792256	TBX2	0.333953612	1.649296979	-1.582280378	0.000215343
ILMN_2211030	SPANXB1	0.33665381	1.649296979	-1.570662302	5.54E-05
ILMN_1797776	PRSS23	0.33903848	4.222768988	-1.560479068	0.004425132
ILMN_1656171	ADAMTS19	0.341944124	1.649296979	-1.548167496	9.57E-05
ILMN_1814686	BCMO1	0.347658343	4.222768988	-1.524257884	0.001049061
ILMN_2132100	SPANXE	0.34823695	0	-1.521858805	3.90E-05
ILMN_1676980	MTSS1	0.348460643	0	-1.520932376	3.90E-05
ILMN_1695475	SEMA3C	0.350473851	0	-1.512621286	4.51E-05
ILMN_1662795	CA2	0.353588657	4.222768988	-1.499856099	0.002684465
ILMN_1707475	UBE2E2	0.35409086	1.649296979	-1.49780849	6.01E-05
ILMN_1661799	HIGD1A	0.354697499	1.649296979	-1.495338938	0.000101812
ILMN_1744949	RHOBTB3	0.355754816	4.222768988	-1.491044808	0.001326709
ILMN_3305938	SGK1	0.355802259	6.472880201	-1.490852424	0.01750815
ILMN_1743373	DLL1	0.355913773	3.281232936	-1.490400331	0.000255172
ILMN_1762262	PKIA	0.357245088	1.649296979	-1.48501392	0.00016549
ILMN_1748124	TSC22D3	0.357407431	1.649296979	-1.484358466	9.73E-05
ILMN_1674522	HIGD1A	0.359647737	1.649296979	-1.47534357	8.31E-05
ILMN_2054652	TYRP1	0.361098068	1.649296979	-1.469537392	6.01E-05
ILMN_1813572	IL16	0.361190481	0	-1.469168222	5.53E-05
ILMN_1695397	LOC644151	0.361929226	1.649296979	-1.466220484	7.15E-05
ILMN_1718629	NRIP1	0.362164537	1.649296979	-1.465282811	9.24E-05

ILMN_1688780	S100A4	0.362205813	1.649296979	-1.465118395	0.000234299
ILMN_1766054	ABCA1	0.3622885	4.222768988	-1.464789082	0.003852778
ILMN_1684306	S100A4	0.366389755	4.222768988	-1.448548933	0.001817168
ILMN_1787691	CITED4	0.371360353	4.222768988	-1.429108295	0.000788207
ILMN_1709257	DSCR6	0.375475558	1.649296979	-1.413209099	0.000118078
ILMN_1719599	SYTL4	0.378695319	1.649296979	-1.400890506	0.000118078
ILMN_1663351	SLC2A10	0.379874561	1.649296979	-1.396404993	0.000180256
ILMN_1713124	AKR1C3	0.381990519	0	-1.388391265	7.62E-05
ILMN_1704675	IGSF1	0.385138807	1.649296979	-1.376549595	0.000132887
ILMN_1669523	FOS	0.387277176	28.02263464	-1.368561617	0.310038892
ILMN_1738989	GOLSYN	0.388381336	4.222768988	-1.364454223	0.001972291
ILMN_3260026	LOC100130383	0.390776815	1.649296979	-1.355583222	9.73E-05
ILMN_1663080	LFNG	0.391760031	4.222768988	-1.351957881	0.001262369
ILMN_1770505	BIK	0.391827263	1.649296979	-1.351710313	0.000215343
ILMN_1803788	LGALS3	0.392132661	3.281232936	-1.350586284	0.000315939
ILMN_1764522	LMBR1	0.394081668	4.222768988	-1.343433455	0.000811171
ILMN_1738401	FOXC1	0.397758477	4.222768988	-1.330035419	0.001483784

Appendix Three

Genes and pathways upregulated in CAIX+ve and CAIX-ve population (RNA-seq analysis)

Table 1: Pathways and Genes upregulated in CAIX+ve cells

ABC Transporters	Gene Name
ENSG00000154262	ATP-binding cassette, sub-family A (ABC1), member 6
ENSG00000069431	ATP-binding cassette, sub-family C (CFTR/MRP), member 9
ENSG00000023839	ATP-binding cassette, sub-family C (CFTR/MRP), member 2
ENSG00000154263	ATP-binding cassette, sub-family A (ABC1), member 10
ENSG00000004846	ATP-binding cassette, sub-family B (MDR/TAP), member 5
ENSG00000154258	ATP-binding cassette, sub-family A (ABC1), member 9
ENSG00000198691	ATP-binding cassette, sub-family A (ABC1), member 4
ENSG00000172350	ATP-binding cassette, sub-family G (WHITE), member 4
ENSG00000179869	ATP-binding cassette, sub-family A (ABC1), member 13
ENSG00000141338	ATP-binding cassette, sub-family A (ABC1), member 8
Wnt and Hedgehog signaling pathway	Gene Name
ENSG00000085741	wingless-type MMTV integration site family, member 11
ENSG00000154764	wingless-type MMTV integration site family, member 7A
ENSG00000115596	wingless-type MMTV integration site family, member 6
ENSG00000081479	low density lipoprotein receptor-related protein 2
ENSG00000105989	wingless-type MMTV integration site family member 2
ENSG00000164161	hedgehog interacting protein
ENSG00000153162	bone morphogenetic protein 6
ENSG00000061492	wingless-type MMTV integration site family, member 8A
Dilated cardiomyopathy/ Tumour Migration	Gene Name
ENSG00000166862	calcium channel, voltage-dependent, gamma subunit 2
ENSG00000078295	adenylate cyclase 2 (brain)
ENSG00000151067	calcium channel, voltage-dependent, L type, alpha 1C subunit
ENSG00000115232	integrin, alpha 4 (antigen CD49D, alpha 4 subunit of VLA-4 receptor)
ENSG00000017427	insulin-like growth factor 1 (somatomedin C)
ENSG00000092054	myosin, heavy chain 7, cardiac muscle, beta
ENSG00000197616	myosin, heavy chain 6, cardiac muscle, alpha
ENSG00000006116	calcium channel, voltage-dependent, gamma subunit 3
ENSG00000134571	myosin binding protein C, cardiac
ENSG00000144668	integrin, alpha 9
ENSG00000170624	sarcoglycan, delta (35kDa dystrophin-associated glycoprotein)
ENSG00000175084	desmin
ENSG00000137809	integrin, alpha 11
ENSG00000155897	adenylate cyclase 8 (brain)
Arrhythmogenic right ventricular cardiomyopathy (ARVC)/ Tumour EMT	Gene Name
ENSG00000066032	catenin (cadherin-associated protein), alpha 2
ENSG00000077522	actinin, alpha 2
ENSG00000170558	cadherin 2, type 1, N-cadherin (neuronal)
ENSG00000152661	gap junction protein, alpha 1, 43kDa
Protein digestion and absorption/ ECM components	Gene Name
ENSG00000163751	carboxypeptidase A3 (mast cell)
ENSG00000215704	chymotrypsin-like elastase family, member 2B
ENSG00000158516	carboxypeptidase A2 (pancreatic)
ENSG00000065618	collagen, type XVII, alpha 1
ENSG00000088386	solute carrier family 15 (oligopeptide transporter), member 1
ENSG00000049540	elastin
ENSG00000187498	collagen, type IV, alpha 1
ENSG00000204983	protease, serine, 1 (trypsin 1)
ENSG00000112280	collagen, type IX, alpha 1
ENSG00000060718	collagen, type XI, alpha 1
ENSG00000187955	collagen, type XIV, alpha 1

continued of Table 1

Cell adhesion molecules (CAMs)	Gene Name
ENSG00000021645	neurexin 3
ENSG00000169760	neuroligin 1
ENSG00000149294	neural cell adhesion molecule 1
ENSG00000110076	neurexin 2
ENSG00000114013	CD86 molecule
ENSG00000172116	CD8b molecule
ENSG00000018236	contactin 1
ENSG00000066405	claudin 18
ENSG00000134873	claudin 10
ENSG00000163600	inducible T-cell co-stimulator
ENSG00000038427	versican
Hematopoietic cell lineage	Gene Name
ENSG00000125538	interleukin 1, beta
ENSG00000170180	glycophorin A (MNS blood group)
ENSG00000130427	erythropoietin
ENSG00000115008	interleukin 1, alpha
ENSG00000172116	CD8b molecule
ENSG00000185245	glycoprotein Ib (platelet), alpha polypeptide
ENSG00000174059	CD34 molecule
ENSG00000110448	CD5 molecule
ENSG00000113520	interleukin 4
ENSG00000105383	CD33 molecule
Glutamatergic synapse	Gene Name
ENSG00000079215	solute carrier family 1 (glial high affinity glutamate transporter), member 3
Neuroactive ligand-receptor interaction	Gene Name
ENSG00000147402	gamma-aminobutyric acid (GABA) receptor, theta
ENSG00000125675	glutamate receptor, ionotrophic, AMPA 3
ENSG00000151834	gamma-aminobutyric acid (GABA) A receptor, alpha 2
ENSG00000163288	gamma-aminobutyric acid (GABA) A receptor, beta 1
ENSG00000137252	hypocretin (orexin) receptor 2
ENSG00000127533	coagulation factor II (thrombin) receptor-like 3
ENSG00000134489	histamine receptor H4
ENSG00000004948	calcitonin receptor
ENSG00000179603	glutamate receptor, metabotropic 8
ENSG00000116329	opioid receptor, delta 1
ENSG00000182771	glutamate receptor, ionotropic, delta 1
ENSG00000120251	glutamate receptor, ionotropic, AMPA 2
ENSG00000100739	bradykinin receptor B1
ENSG00000122420	prostaglandin F receptor (FP)
ENSG00000168959	glutamate receptor, metabotropic 5
ENSG00000198121	lysophosphatidic acid receptor 1
ENSG00000145864	gamma-aminobutyric acid (GABA) A receptor, beta 2
ENSG00000175344	cholinergic receptor, nicotinic, alpha 7
ENSG00000138039	luteinizing hormone/choriogonadotropin receptor
ENSG00000150086	glutamate receptor, ionotropic, N-methyl D-aspartate 2B
ENSG00000151577	dopamine receptor D3
ENSG00000011677	gamma-aminobutyric acid (GABA) A receptor, alpha 3
ENSG00000155511	glutamate receptor, ionotropic, AMPA 1

Table 2: Ingenuity Canonical Pathways and genes upregulated in CAIX+ve cells

Ingenuity Canonical Pathways	Genes
Glutamate Receptor Signaling	GRM5,GRIN2B,CAMK4,GRID1,GRM8,GRIA1,SLC1A3,GRIA2,GRIA4, GRIA3,GRIK1
Neuropathic Pain Signaling In Dorsal Horn Neurons	GRIN2B,KCNN2,CAMK4,GRM8,GRIA1,GRIA2,PIK3C2G,PLCL2,GRIA 4,GRM5,NTRK2,KCNQ3,PRKD1,GRIA3
Xenobiotic Metabolism Signaling	CYP1A1,IL1A,FMO3,CAMK4,FMO6,LIPC,CYP2C9,FMO2,ABCC2,PIK3 C2G,UGT8,NDST4,HS3ST3A1,MAOB,ALDH1A1,UGT2B4,HS3ST2,CE S5A,IL1B,CHST13,SLCO1B1,NOS2,ALDH3A1,PRKD1
Amyotrophic Lateral Sclerosis Signaling	GRIN2B,GRID1,IGF1,GRIA1,CASP1,PIK3C2G,GRIA2,CACNA1C,NEF H,GRIA4,GRIA3,GRIK1
Cellular Effects of Sildenafil (Viagra)	ADCY2,KCNN2,CAMK4,CACNA1C,PLCL2,PDE4B,PDE1C,CACNG2,M YH2,PDE1B,KCNQ3,ADCY8,MYL10
Synaptic Long Term Potentiation	GRM5,GRIN2B,CAMK4,GRM8,GRIA1,GRIA2,CACNA1C,PPP1R3A,AD CY8,GRIA4,PRKD1,GRIA3
GABA Receptor Signaling	GABRQ,SLC6A11,GABRG3,GABRB1,SLC6A1,GABRA2
Basal Cell Carcinoma Signaling	WNT8A,TCF4,WNT6,HHIP,BMP6,WNT2,WNT11,GLIS1
Calcium Signaling	GRIN2B,CAMK4,GRIA1,RCAN2,GRIA2,HDAC9,TRPC4,TRPC5,GRIA4 ,TRPC7,ATP2B2,MYH2,GRIK1,GRIA3
Glycerolipid Metabolism	PPAPDC1A,ALDH1A1,LIPC,DGKK,ADH1C (includes EG:11522),DGKB,AKR1B1,ALDH3A1,ADH4 (includes EG:127)
CREB Signaling in Neurons	GRIN2B,ADCY2,CAMK4,GRM8,GRIA1,GRIA2,PIK3C2G,PLCL2,GRIA 4,GRM5,GRID1,ADCY8,PRKD1,GRIK1,GRIA3
Human Embryonic Stem Cell Pluripotency	SOX2,WNT8A,TCF4,NTRK2,NTRK3,PDGFRA,PIK3C2G,WNT6,PDGF D,BMP6,WNT2,WNT11
Sphingosine-1-phosphate Signaling	ADCY2,DIRAS3,CASP1,PDGFRA,PIK3C2G,RHOJ,CASP4,PLCL2,AD CY8,PDGFD,CASP5
Pyruvate Metabolism	ALDH1A1,ME3,LDHAL6B,AKR1B1,ALDH3A1,LDHB,ADH4 (includes EG:127)
LPS/IL-1 Mediated Inhibition of RXR Function	FMO3,FMO6,LIPC,CYP2C9,FMO2,ABCC2,NDST4,HS3ST3A1,MAOB, ALDH1A1,HS3ST2,IL1B,LBP,CHST13,ALDH3A1
Cysteine Metabolism	HS3ST2,NDST4,LDHAL6B,CHST13,HS3ST3A1,LDHB
FXR/RXR Activation	IL1A,LIPC,UGT2B4,ABCC2,IL1B,SLC22A7,SLCO1B1,CYP8B1
Synaptic Long Term Depression	GRM5,GRID1,IGF1,GRM8,GRIA1,GRIA2,NOS2,GRIA4,PRKD1,GRIA3
TREM1 Signaling	TLR1,TLR8,CASP1,CD86,IL1B,CASP5
Retinol Metabolism	ALDH1A1,UGT2B4,ADH1C (includes EG:11522),ADH4 (includes EG:127)
Altered T Cell and B Cell Signaling in Rheumatoid Arthritis	TLR1,IL1A,TLR8,CD86,IL1B,IL23A,IL4 (includes EG:16189),TNFRSF17
Communication between Innate and Adaptive Immune Cells	TLR1,IL1A,TLR8,CD86,IL1B,CD8B,IL4 (includes EG:16189),TNFRSF17
Propanoate Metabolism	ACADL,ALDH1A1,LDHAL6B,AGXT2,ALDH3A1,LDHB
β-alanine Metabolism	ACADL,DPYS,ALDH1A1,AGXT2,ALDH3A1
Wnt/β-catenin Signaling	SOX2,WNT8A,CDH2,GJA1,TCF4,SOX6,TGFBR3,WNT6,ACVR1C,WN T2,WNT11,SOX5

Table 3: KEGG pathways and genes upregulated in CAIX-ve cells

Cytokine-cytokine receptor interaction	Gene Name
ENSG00000163083	inhibin, beta B
ENSG00000134470	interleukin 15 receptor, alpha
ENSG00000175189	inhibin, beta C
ENSG00000099985	oncostatin M
ENSG00000163735	chemokine (C-X-C motif) ligand 5
ENSG00000239697	tumor necrosis factor (ligand) superfamily, member 12
ENSG00000117400	myeloproliferative leukemia virus oncogene
ENSG00000160683	chemokine (C-X-C motif) receptor 5
ENSG00000103522	interleukin 21 receptor
ENSG00000184371	colony stimulating factor 1 (macrophage)
ENSG00000092969	transforming growth factor, beta 2
ENSG00000163823	chemokine (C-C motif) receptor 1
ENSG00000139269	inhibin, beta E
ENSG00000161570	chemokine (C-C motif) ligand 5
ENSG00000125657	tumor necrosis factor (ligand) superfamily, member 9
MAPK signaling pathway	**Gene Name**
ENSG00000130829	dual specificity phosphatase 9
ENSG00000185386	mitogen-activated protein kinase 11
ENSG00000116717	growth arrest and DNA-damage-inducible, alpha
ENSG00000126583	protein kinase C, gamma
ENSG00000104856	v-rel reticuloendotheliosis viral oncogene homolog B
ENSG00000175197	DNA-damage-inducible transcript
ENSG00000138166	dual specificity phosphatase 5
ENSG00000130222	growth arrest and DNA-damage-inducible, gamma
ENSG00000177606	jun proto-oncogene
ENSG00000104814	mitogen-activated protein kinase kinase kinase kinase 1
ENSG00000167744	neurotrophin 4
ENSG00000156427	fibroblast growth factor 18
ECM-receptor interaction	**Gene Name**
ENSG00000159164	synaptic vesicle glycoprotein 2A
ENSG00000143127	integrin, alpha 10
ENSG00000050555	laminin, gamma 3
ENSG00000139219	collagen, type II, alpha 1
ENSG00000139626	integrin, beta 7
ENSG00000135424	integrin, alpha 7
Osteoclast differentiation	**Gene Name**
ENSG00000170909	osteoclast associated, immunoglobulin-like receptor
ENSG00000184557	suppressor of cytokine signaling 3
ENSG00000072694	Fc fragment of IgG, low affinity IIb, receptor (CD32)

Table 4: Ingenuity Canonical Pathways and genes upregulated in CAIX-ve cells

Ingenuity Canonical Pathways	Genes 254

Actin Cytoskeleton Signaling	TMSL3,ARHGEF4,TMSB10/TMSB4X,DIAPH3,RDX,DIAPH2,GNA13,GSN,PDGFB,FGF13
Pentose and Glucuronate Interconversions	UGDH,UGP2,GUSB
Nucleotide Sugars Metabolism	UGDH,UGP2
TNFR2 Signaling	FOS,JUN,MAP3K1
TR/RXR Activation	KLF9,AKR1C1/AKR1C2,AKR1C3,BCL3,HIF-1A
Cardiomyocyte Differentiation via BMP Receptors	BMP4,BMPR2
IL-1 Signaling	FOS,JUN,MAP3K1,ADCY1,GNA13
C21-Steroid Hormone Metabolism	AKR1C1/AKR1C2,AKR1C3
RAR Activation	FOS,JUN,CRABP2,MAP3K1,NR2F2,ADCY1,NRIP1
MIF Regulation of Innate Immunity	FOS,JUN,PLA2G10
Hypoxia Signaling in the Cardiovascular System	JUN,UBE2E2,HIF-1A,UBE2F
IGF-1 Signaling	IGFBP4,FOS,JUN,SOCS2,IGF1R
ILK Signaling	TMSL3,FOS,JUN,RHOQ,TMSB10/TMSB4X,HIF-1A,ITGB4
Renal Cell Carcinoma Signaling	FOS,JUN,HIF-1A,PDGFB
Role of Oct4 in Mammalian Embryonic Stem Cell Pluripotency	SOX2,NR2F2,JARID2
April Mediated Signaling	FOS,JUN,MAP3K1
Molecular Mechanisms of Cancer	FOS,PMAIP1,ARHGEF4,JUN,BMP4,RHOQ,RASGRP1,ADCY1,BMPR2,HIF-1A,GNA13
B Cell Activating Factor Signaling	FOS,JUN,MAP3K1
PDGF Signaling	FOS,JUN,MAP3K1,PDGFB
Signaling by Rho Family GTPases	FOS,ARHGEF4,JUN,RHOQ,DIAPH3,RDX,GNA13,SEPT2
BMP signaling pathway	JUN,BMP4,FST,BMPR2
Glycosphingolipid Biosynthesis - Neolactoseries	FUT4,ST3GAL5
Glucocorticoid Receptor Signaling	FOS,JUN,HMGB1,SGK1,ANXA1,MAP3K1,NRIP1,HSPA2,PGR (includes EG:18667)
TNFR1 Signaling	FOS,JUN,MAP3K1
EGF Signaling	FOS,JUN,MAP3K1
Glycosphingolipid Biosynthesis - Globoseries	GLA,FUT4
TGF-β Signaling	FOS,JUN,BMP4,BMPR2
CD28 Signaling in T Helper Cells	FOS,JUN,MAP3K1,HLA-DRB1,HLA-DRB5
PKCθ Signaling in T Lymphocytes	FOS,JUN,MAP3K1,HLA-DRB1,HLA-DRB5
Glycosphingolipid Biosynthesis - Ganglioseries	FUT4,ST3GAL5
Toll-like Receptor Signaling	FOS,JUN,MAP3K1
Starch and Sucrose Metabolism	UGDH,UGP2,GUSB
Eicosanoid Signaling	AKR1C3,PLA2G10,PTGER4
CD27 Signaling in Lymphocytes	FOS,JUN,MAP3K1
Glycosaminoglycan Degradation	IDS,GUSB
RANK Signaling in Osteoclasts	FOS,JUN,MAP3K1,GSN
Cdc42 Signaling	FOS,JUN,DIAPH3,HLA-DRB1,HLA-DRB5
IL-17A Signaling in Gastric Cells	FOS,JUN
Urea Cycle and Metabolism of Amino Groups	CKB,SMS
Estrogen-Dependent Breast Cancer Signaling	FOS,JUN,IGF1R
OX40 Signaling Pathway	JUN,HLA-DRB1,HLA-DRB5
PPAR Signaling	FOS,JUN,NRIP1,PDGFB
HMGB1 Signaling	FOS,JUN,RHOQ,HMGB1
Production of Nitric Oxide and	FOS,JUN,RHOQ,PPP1R3C,MAP3K1,APOD

Reactive Oxygen Species in Macrophages	
Circadian Rhythm Signaling	CRY1,PER2
4-1BB Signaling in T Lymphocytes	JUN,MAP3K1
B Cell Development	HLA-DRB1,HLA-DRB5

Appendix Four

Genes and pathways upregulated in CAIX+ve and CAIX-ve cells (Microarray analysis)

Table 1: KEGG Pathways and Genes upregulated in CAIX+ve cells

Pyruvate metabolism	Genes

ENSG00000120437	acetyl-CoA acetyltransferase 2
ENSG00000137124	aldehyde dehydrogenase 1 family, member B1
ENSG00000132142	acetyl-CoA carboxylase alpha
ENSG00000072210	aldehyde dehydrogenase 3 family, member
ENSG00000150768	dihydrolipoamide S-acetyltransferase
ENSG00000082212	malic enzyme 2, NAD(+)-dependent, mitochondrial
ENSG00000065833	malic enzyme 1, NADP(+)-dependent, cytosolic
ENSG00000075239	acetyl-CoA acetyltransferase 1
ENSG00000168291	pyruvate dehydrogenase
Parkinson's disease	**Genes**
ENSG00000120868	apoptotic peptidase activating factor 1
ENSG00000135390	ATP synthase, H+ transporting, mitochondrial Fo complex, subunit C2 (subunit 9
ENSG00000159199	ATP synthase, H+ transporting, mitochondrial Fo complex, subunit C1 (subunit 9)
ENSG00000185633	NADH dehydrogenase (ubiquinone) 1 alpha subcomplex, 4-like 2
ENSG00000152234	ATP synthase, H+ transporting, mitochondrial F1 complex, alpha subunit 1, cardiac muscle
ENSG00000110717	NADH dehydrogenase (ubiquinone) Fe-S protein 8, 23kDa (NADH-coenzyme Q reductase)
ENSG00000099624	ATP synthase, H+ transporting, mitochondrial F1 complex, delta subunit
ENSG00000171497	peptidylprolyl isomerase D
ENSG00000156587	ubiquitin-conjugating enzyme E2L 6
ENSG00000179091	cytochrome c-1
ENSG00000140990	NADH dehydrogenase (ubiquinone) 1 beta subcomplex, 10, 22kDa
ENSG00000167792	NADH dehydrogenase (ubiquinone) flavoprotein 1, 51kDa
ENSG00000132388	ubiquitin-conjugating enzyme E2G 1
Oxidative phosphorylation	**Genes**
ENSG00000152234	ATP synthase, H+ transporting, mitochondrial F1 complex, alpha subunit 1, cardiac muscle
ENSG00000110717	NADH dehydrogenase (ubiquinone) Fe-S protein 8, 23kDa (NADH-coenzyme Q reductase)
ENSG00000138777	pyrophosphatase (inorganic) 2
ENSG00000006695	COX10 homolog, cytochrome c oxidase assembly protein, heme A: farnesyltransferase (yeast)
ENSG00000179091	cytochrome c-
ENSG00000014919	COX15 homolog, cytochrome c oxidase assembly protein (yeast)
ENSG00000180817	pyrophosphatase (inorganic) 1
ENSG00000184076	ubiquinol-cytochrome c reductase, complex III subunit X

ENSG00000158864	NADH dehydrogenase (ubiquinone) Fe-S protein 2, 49kDa (NADH-coenzyme Q reductase)
ENSG00000173660	ubiquinol-cytochrome c reductase hinge protein
ENSG00000073578	succinate dehydrogenase complex, subunit A, flavoprotein (Fp)
ENSG00000110955	ATP synthase, H+ transporting, mitochondrial F1 complex, beta polypeptide
ENSG00000169021	ubiquinol-cytochrome c reductase, Rieske iron-sulfur polypeptide 1
Aminoacyl-tRNA biosynthesis	**Genes**
ENSG00000196305	isoleucyl-tRNA synthetase
ENSG00000104835	F-box protein 17
ENSG00000140105	tryptophanyl-tRNA synthetase
ENSG00000113407	threonyl-tRNA synthetase
ENSG00000133706	leucyl-tRNA synthetase
ENSG00000179115	phenylalanyl-tRNA synthetase, alpha subunit
ENSG00000106105	glycyl-tRNA synthetase
ENSG00000137513	asparaginyl-tRNA synthetase 2, mitochondrial (putative)
ENSG00000065427	lysyl-tRNA synthetase
ENSG00000103707	mitochondrial methionyl-tRNA formyltransferase
ENSG00000134684	tyrosyl-tRNA synthetase
ENSG00000166986	methionyl-tRNA synthetase
ENSG00000011376	leucyl-tRNA synthetase 2, mitochondrial
ENSG00000116874	tryptophanyl tRNA synthetase 2, mitochondrial
ENSG00000090861	alanyl-tRNA synthetase
ENSG00000134905	cysteinyl-tRNA synthetase 2, mitochondrial (putative)
ENSG00000145982	phenylalanyl-tRNA synthetase 2, mitochondrial
ENSG00000139131	tyrosyl-tRNA synthetase 2, mitochondrial
ENSG00000110619	cysteinyl-tRNA synthetase
ENSG00000170445	histidyl-tRNA synthetase
ENSG00000103356	glutamyl-tRNA synthetase 2, mitochondrial (putative)
RNA transport	**Genes**
ENSG00000184110	eukaryotic translation initiation factor 3, subunit C
ENSG00000082516	gem (nuclear organelle) associated protein 5
ENSG00000179409	gem (nuclear organelle) associated protein 4
ENSG00000163002	nucleoporin 35kDa

ENSG00000170473	within bgcn homolog (Drosophila)
ENSG00000108559	nucleoporin 88kDa
ENSG00000100462	protein arginine methyltransferase 5
ENSG00000111581	nucleoporin 107kDa
ENSG00000205937	RNA binding protein S1, serine-rich domain
ENSG00000006744	elaC homolog 2 (E. coli)
ENSG00000085415	SEH1-like (S. cerevisiae) [Source:HGNC
ENSG00000051596	THO complex 3
ENSG00000106263	eukaryotic translation initiation factor 3, subunit B [
ENSG00000184900	SMT3 suppressor of mif two 3 homolog 3 (S. cerevisiae)
ENSG00000131652	THO complex 6 homolog (Drosophila
ENSG00000172336	processing of precursor 7, ribonuclease P/MRP subunit (S. cerevisiae)
ENSG00000183684	THO complex 4
ENSG00000130811	eukaryotic translation initiation factor 3, subunit G
ENSG00000152464	ribonuclease P/MRP 38kDa subunit
ENSG00000094914	achalasia, adrenocortical insufficiency, alacrimia
ENSG00000167272	processing of precursor 5, ribonuclease P/MRP subunit (S. cerevisiae)
ENSG00000075188	nucleoporin 37kDa
ENSG00000090621	poly(A) binding protein, cytoplasmic 4 (inducible form)
ENSG00000145191	eukaryotic translation initiation factor 2B, subunit 5 epsilon, 82kDa
ENSG00000095319	nucleoporin 188kDa
ENSG00000125450	nucleoporin 85kDa
ENSG00000100296	THO complex 5
ENSG00000169371	snurportin 1
ENSG00000172239	poly(A) binding protein interacting protein 1
ENSG00000058804	transmembrane protein 48
ENSG00000084623	eukaryotic translation initiation factor 3, subunit I
ENSG00000164967	chromosome 9 open reading frame 23
ENSG00000151461	UPF2 regulator of nonsense transcripts homolog (yeast)]
ENSG00000184575	exportin, tRNA (nuclear export receptor for tRNAs)
ENSG00000132182	nucleoporin 210kDa
ENSG00000124571	exportin 5
ENSG00000100401	Ran GTPase activating protein 1

ENSG00000137574	trimethylguanosine synthase 1
ENSG00000188612	SMT3 suppressor of mif two 3 homolog 2 (S. cerevisiae)
Alzheimer's disease	**Genes**
ENSG00000120868	apoptotic peptidase activating factor 1
ENSG00000135390	ATP synthase, H+ transporting, mitochondrial Fo complex, subunit C2 (subunit 9)
ENSG00000100030	mitogen-activated protein kinase 1
ENSG00000159199	ATP synthase, H+ transporting, mitochondrial Fo complex, subunit C1 (subunit 9
ENSG00000185633	NADH dehydrogenase (ubiquinone) 1 alpha subcomplex, 4-like 2
ENSG00000002330	BCL2-associated agonist of cell death [
ENSG00000152234	ATP synthase, H+ transporting, mitochondrial F1 complex, alpha subunit 1, cardiac muscle
ENSG00000165806	caspase 7, apoptosis-related cysteine peptidase
ENSG00000110717	NADH dehydrogenase (ubiquinone) Fe-S protein 8, 23kDa (NADH-coenzyme Q reductase)
ENSG00000099624	ATP synthase, H+ transporting, mitochondrial F1 complex, delta subunit
ENSG00000119912	insulin-degrading enzyme
ENSG00000118217	activating transcription factor 6
ENSG00000179091	cytochrome c-1
ENSG00000140990	NADH dehydrogenase (ubiquinone) 1 beta subcomplex, 10, 22kDa
ENSG00000167792	NADH dehydrogenase (ubiquinone) flavoprotein 1, 51kDa [Source:HGNC Symbol;Acc:7716]
ENSG00000184752	NADH dehydrogenase (ubiquinone) 1 alpha subcomplex, 12
ENSG00000074370	ATPase, Ca++ transporting, ubiquitous
ENSG00000159593	NEDD8 activating enzyme E1 subunit 1
ENSG00000117118	succinate dehydrogenase complex, subunit B, iron sulfur (Ip)
ENSG00000015475	BH3 interacting domain death agonist
ENSG00000143252	succinate dehydrogenase complex, subunit C, integral membrane protein, 15kDa
ENSG00000162736	nicastrin
ENSG00000165264	NADH dehydrogenase (ubiquinone) 1 beta subcomplex, 6, 17kDa
ENSG00000184076	ubiquinol-cytochrome c reductase, complex III subunit X
ENSG00000158864	NADH dehydrogenase (ubiquinone) Fe-S protein 2, 49kDa (NADH-coenzyme Q reductase)
ENSG00000182240	beta-site APP-cleaving enzyme 2
ENSG00000139180	NADH dehydrogenase (ubiquinone) 1 alpha subcomplex, 9, 39kDa [Source:HGNC Symbol;Acc:7693]
ENSG00000176749	cyclin-dependent kinase 5, regulatory subunit 1 (p35)
ENSG00000107758	protein phosphatase 3, catalytic subunit, beta isozyme

ENSG00000173660	ubiquinol-cytochrome c reductase hinge protein
ENSG00000073578	succinate dehydrogenase complex, subunit A, flavoprotein (Fp)
ENSG00000115286	NADH dehydrogenase (ubiquinone) Fe-S protein 7, 20kDa (NADH-coenzyme Q reductase)
ENSG00000166136	NADH dehydrogenase (ubiquinone) 1 beta subcomplex, 8, 19kDa
ENSG00000110955	ATP synthase, H+ transporting, mitochondrial F1 complex, beta polypeptide
ENSG00000169021	ubiquinol-cytochrome c reductase, Rieske iron-sulfur polypeptide
Pyruvate metabolism	**Genes**
ENSG00000120437	acetyl-CoA acetyltransferase 2
ENSG00000164904	aldehyde dehydrogenase 7 family, member A1
ENSG00000137124	aldehyde dehydrogenase 1 family, member B1
ENSG00000132142	acetyl-CoA carboxylase alpha
ENSG00000072210	aldehyde dehydrogenase 3 family, member A2
ENSG00000131069	acyl-CoA synthetase short-chain family member 2
ENSG00000103253	hydroxyacylglutathione hydrolase-like
ENSG00000150768	dihydrolipoamide S-acetyltransferase
ENSG00000111716	lactate dehydrogenase B
ENSG00000170634	acylphosphatase 2, muscle type
ENSG00000137106	glyoxylate reductase/hydroxypyruvate reductase
ENSG00000082212	malic enzyme 2, NAD(+)-dependent, mitochondrial
ENSG00000065833	malic enzyme 1, NADP(+)-dependent, cytosolic [
ENSG00000075239	acetyl-CoA acetyltransferase 1
ENSG00000168291	pyruvate dehydrogenase (lipoamide) beta
ENSG00000166800	lactate dehydrogenase A-like 6A
Oxidative phosphorylation	**Genes**
ENSG00000135390	ATP synthase, H+ transporting, mitochondrial Fo complex, subunit C2 (subunit 9)
ENSG00000159199	ATP synthase, H+ transporting, mitochondrial Fo complex, subunit C1 (subunit 9)
ENSG00000185633	NADH dehydrogenase (ubiquinone) 1 alpha subcomplex, 4-like 2
ENSG00000152234	ATP synthase, H+ transporting, mitochondrial F1 complex, alpha subunit 1, cardiac muscle
ENSG00000110717	NADH dehydrogenase (ubiquinone) Fe-S protein 8, 23kDa (NADH-coenzyme Q reductase)
ENSG00000105929	ATPase, H+ transporting, lysosomal V0 subunit a4
ENSG00000099624	ATP synthase, H+ transporting, mitochondrial F1 complex, delta subunit
ENSG00000006695	COX10 homolog, cytochrome c oxidase assembly protein, heme A: farnesyltransferase (yeast)

ENSG00000179091	cytochrome c-1
ENSG00000140990	NADH dehydrogenase (ubiquinone) 1 beta subcomplex, 10, 22kDa
ENSG00000167792	NADH dehydrogenase (ubiquinone) flavoprotein 1, 51kDa
ENSG00000014919	COX15 homolog, cytochrome c oxidase assembly protein (yeast)
ENSG00000184752	NADH dehydrogenase (ubiquinone) 1 alpha subcomplex, 12
ENSG00000131100	ATPase, H+ transporting, lysosomal 31kDa, V1 subunit E1 [Source:HGNC Symbol;Acc:857]
ENSG00000117118	succinate dehydrogenase complex, subunit B, iron sulfur (Ip)
ENSG00000180817	pyrophosphatase (inorganic) 1
ENSG00000143252	succinate dehydrogenase complex, subunit C, integral membrane protein, 15kDa
ENSG00000165264	NADH dehydrogenase (ubiquinone) 1 beta subcomplex, 6, 17kDa
ENSG00000184076	ubiquinol-cytochrome c reductase, complex III subunit X
ENSG00000158864	NADH dehydrogenase (ubiquinone) Fe-S protein 2, 49kDa (NADH-coenzyme Q reductase)
ENSG00000139180	NADH dehydrogenase (ubiquinone) 1 alpha subcomplex, 9, 39kDa
ENSG00000047249	ATPase, H+ transporting, lysosomal 50/57kDa, V1 subunit H
ENSG00000173660	ubiquinol-cytochrome c reductase hinge protein
ENSG00000073578	succinate dehydrogenase complex, subunit A, flavoprotein (Fp)
ENSG00000115286	NADH dehydrogenase (ubiquinone) Fe-S protein 7, 20kDa (NADH-coenzyme Q reductase)
ENSG00000107902	phospholysine phosphohistidine inorganic pyrophosphate phosphatase
ENSG00000159720	ATPase, H+ transporting, lysosomal 38kDa, V0 subunit d1
ENSG00000166136	NADH dehydrogenase (ubiquinone) 1 beta subcomplex, 8, 19kDa
ENSG00000110955	ATP synthase, H+ transporting, mitochondrial F1 complex, beta polypeptide
ENSG00000169021	ubiquinol-cytochrome c reductase, Rieske iron-sulfur polypeptide 1
Fatty acid metabolism	**Genes**
ENSG00000120437	acetyl-CoA acetyltransferase 2
ENSG00000164904	aldehyde dehydrogenase 7 family, member A1
ENSG00000137124	aldehyde dehydrogenase 1 family, member B1
ENSG00000072210	aldehyde dehydrogenase 3 family, member A2
ENSG00000151726	acyl-CoA synthetase long-chain family member 1
ENSG00000105607	glutaryl-CoA dehydrogenase
ENSG00000167315	acetyl-CoA acyltransferase 2
ENSG00000110090	carnitine palmitoyltransferase 1A (liver)
ENSG00000060971	acetyl-CoA acyltransferase 1

ENSG00000157184	carnitine palmitoyltransferase 2
ENSG00000127884	enoyl CoA hydratase, short chain, 1, mitochondrial
ENSG00000138796	hydroxyacyl-CoA dehydrogenase
ENSG00000072778	acyl-CoA dehydrogenase, very long chain
ENSG00000075239	acetyl-CoA acetyltransferase 1
Glycolysis / Gluconeogenesis	**Genes**
ENSG00000109107	aldolase C, fructose-bisphosphate
ENSG00000164904	aldehyde dehydrogenase 7 family, member A1
ENSG00000137124	aldehyde dehydrogenase 1 family, member B1
ENSG00000072210	aldehyde dehydrogenase 3 family, member A2
ENSG00000131069	acyl-CoA synthetase short-chain family member 2
ENSG00000132746	aldehyde dehydrogenase 3 family, member B2
ENSG00000067057	phosphofructokinase, platelet
ENSG00000108515	enolase 3 (beta, muscle)
ENSG00000150768	dihydrolipoamide S-acetyltransferase
ENSG00000111716	lactate dehydrogenase B
ENSG00000079739	phosphoglucomutase 1
ENSG00000111669	triosephosphate isomerase 1
ENSG00000171314	phosphoglycerate mutase 1 (brain)
ENSG00000168291	pyruvate dehydrogenase (lipoamide) beta
ENSG00000152556	phosphofructokinase, muscle
ENSG00000108602	aldehyde dehydrogenase 3 family, member A1
ENSG00000166800	lactate dehydrogenase A-like 6A
ENSG00000131473	ATP citrate lyase
ENSG00000062485	citrate synthase
ENSG00000101365	isocitrate dehydrogenase 3 (NAD+) beta
ENSG00000150768	dihydrolipoamide S-acetyltransferase
ENSG00000117118	succinate dehydrogenase complex, subunit B, iron sulfur (Ip)
ENSG00000143252	succinate dehydrogenase complex, subunit C, integral membrane protein, 15kDa
ENSG00000166411	isocitrate dehydrogenase 3 (NAD+) alpha
ENSG00000105953	oxoglutarate (alpha-ketoglutarate) dehydrogenase (lipoamide)
ENSG00000163541	succinate-CoA ligase, alpha subunit
ENSG00000073578	succinate dehydrogenase complex, subunit A, flavoprotein (Fp)

ENSG00000168291	pyruvate dehydrogenase (lipoamide) beta
Wnt signaling pathway	**Genes**
ENSG00000004975	dishevelled, dsh homolog 2 (Drosophila)
ENSG00000162337	low density lipoprotein receptor-related protein 5
ENSG00000196470	seven in absentia homolog 1 (Drosophila)
ENSG00000138795	lymphoid enhancer-binding factor 1
ENSG00000058404	calcium/calmodulin-dependent protein kinase II beta
ENSG00000100888	chromodomain helicase DNA binding protein 8
ENSG00000109339	mitogen-activated protein kinase 10
ENSG00000175792	RuvB-like 1 (E. coli)
ENSG00000101266	casein kinase 2, alpha 1 polypeptide
ENSG00000159692	C-terminal binding protein 1
ENSG00000169884	wingless-type MMTV integration site family, member 10B
ENSG00000183943	protein kinase, X-linked
ENSG00000136238	ras-related C3 botulinum toxin substrate 1 (rho family, small GTP binding protein Rac1)
ENSG00000101849	transducin (beta)-like 1X-linked
ENSG00000112576	cyclin D3
ENSG00000107758	protein phosphatase 3, catalytic subunit, beta isozyme
ENSG00000168036	catenin (cadherin-associated protein), beta 1, 88kDa
ENSG00000131196	nuclear factor of activated T-cells, cytoplasmic, calcineurin-dependent 1
ENSG00000113712	casein kinase 1, alpha 1

Table 2: Ingenuity Canonical Pathways and Genes upregulated in CAIX+ve cells

Ingenuity Canonical Pathways	Genes
Aminoacyl-tRNA Biosynthesis	ACAT2,SLC27A2,GCDH,ACAA2,SLC27A5,CYP19A1,ALDH3A2,ECI2,HSD17

	B4,ALDH3A1,ALDH7A1,CYP1A1,CPT1A,ECHS1,ACAA1,ACOX2,ECH1,CYP1B1,ECI1,DHRS9,ACADVL,CYP4B1,AUH,ACAT1,CPT2,CYP2J2,HADH,ACSL1
Lysine Degradation	MAP2K4,SDHB,NDUFA9,COX10 (includes EG:1352),NCSTN,NDUFB8,NDUFA4L2,NDUFB10,UQCRH,PARK7,CYB5R3,NDUFS2,UQCRFS1,NDUFB6,OGDH,AIFM1,SDHA (includes EG:157074),NDUFV1,NDUFAF1,CPT1A,NDUFS7,ATP5A1,SDHC,MAPK12,PRDX3,NDUFS8,ATP5B,NDUFA6,CAT,MAPK10,NDUFA12,CYC1,BACE2,TXNRD2,COX15
Butanoate Metabolism	ECHS1,ACAT2,ACAA1,ECH1,PCCB,ACAA2,ELOVL6,PCCA,ACADVL,HIBADH,ALDH3A2,AUH,ACAT1,DBT,MCCC1,HMGCS1,ALDH3A1,HSD17B4,HADH,ALDH7A1
Fatty Acid Metabolism	AASDH,ECHS1,ACAT2,LDHAL6A,SLC27A2,ECH1,PCCB,LDHB,PCCA,ACADVL,SUCLG1,ALDH3A2,ACSS2,AUH,ACAT1,ACACA,ALDH3A1,ACSL1,ALDH7A1
Mitochondrial Dysfunction	ATP6V0A4,SDHB,NDUFA9,ATP5D,COX10 (includes EG:1352),NDUFB8,ATP5G2,NDUFA4L2,NDUFB10,UQCRH,ATP5G1,NDUFS2,UQCRFS1,NDUFB6,SDHA (includes EG:157074),NDUFV1,LHPP,NDUFS7,ATP5A1,SDHC,PPA1,ATP6V1E1,UQCR10,NDUFS8,ATP6V1H,ATP5B,NDUFA6,ATP5E,ATP6V0D1,NDUFA12,CYC1,COX15
Valine, Leucine and Isoleucine Degradation	LDHAL6A,ENO3,PGM1,TPI1,PGAM4,PFKP,LDHB,G6PC3,PFKM,ALDH3B2,DHRS9,ALDH3A2,DLAT,PGAM1,ACSS2,ALDH3A1,PDHB,ACSL1,ACYP2,ALDH7A1,ALDOC
Propanoate Metabolism	ACAT2,LDHAL6A,HAGHL,ME1,LDHB,GRHPR,ALDH3A2,DLAT,ACSS2,ACAT1,ME2,ACACA,ALDH3A1,PDHB,ACSL1,ACYP2,ALDH7A1
Oxidative Phosphorylation	AFMID,GRHPR,APTX,CS,MTHFD2,MTHFD1,MTHFD1L
Glycolysis/Gluconeogenesis	SIAH1,ACAT2,CCBL2,FTSJ2,GCDH,CYP19A1,ALDH3A2,OGDH,HSD17B4,ALDH3A1,ALDH7A1,NIT1 (includes EG:27045),AFMID,CYP1A1,ECHS1,ECH1,CYP1B1,WARS2,WARS,CYP4B1,CAT,AUH,PRMT5,ACAT1,CYP2J2,HADH
Pyruvate Metabolism	KIF23,CDC20,PTTG1,CCNB3,PPP2R3B,PLK1,CDK1,FZR1,SLK,PLK4,HSP90AB1,PLK2,PKMYT1,PPP2R2C,ANAPC11,CHEK2,CDC25A
Glyoxylate and Dicarboxylate Metabolism	PDE6G,ATP5D,KIF1B,TYMP,ATP5G2,IDE,POLM,APRT,NME6,MPP6 (includes EG:35343),IMPDH2,ATP5G1,ADA,NME4,GUCY1A3,ATP5A1,DGUOK,PDE8A,NME3,NT5C3,POLR3H,MPP3,ATP5B,ERCC3,CHD1L,PFAS,GMPR2,POLD2,NME1 (includes EG:18102),POLQ,ADSL,POLR1C,POLR2L,PRIM1,VCP,ADK,LONP1,ENPP1,DCK,POLR1E,ADCY6,HSPD1,ATIC,NUDT5,PSMC1,PICK1,ITPA,ENTPD2,KIF20B,PAPD5,GMPR
Tryptophan Metabolism	YARS2,YARS,FARS2,ENO3,GOT2,PCBD1,FARSA
Mitotic Roles of Polo-Like Kinase	PSPH,SRR,PEMT,GNA11,GARS,TARS,PISD,ELOVL6,GRHPR,DAO,CHDH,GAMT,GCSH,PHGDH,DBT,SHMT1,SARS2,SHMT2
Purine Metabolism	GCSH,MTHFD2,SHMT1,MTHFD1,MTFMT,ATIC,MTHFD1L,SHMT2
Phenylalanine, Tyrosine and Tryptophan Biosynthesis	M6PR,CASP6,APAF1,DFFB,BID,BAX,CASP7,DFFA,AIFM1
Glycine, Serine and Threonine Metabolism	ECHS1,ACAA1,AUH,ECH1,HSD17B4,ACAA2,HADH
One Carbon Pool by Folate	MSH3 (includes EG:17686),RFC2,PMS2,FEN1,RPA1,MLH1,RFC3
Fatty Acid Elongation in Mitochondria	MAP2K4,CCNB3,MAPK12,CDK1,RAD50,CHEK1,FANCD2,H2AFX,CREB1,MAPK10,BID,CDK2,CHEK2,CDC25A
Citrate Cycle	LARS,LARS2,VARS,PDHB,IARS
ATM Signaling	NME1 (includes EG:18102),POLQ,CTPS2,TYMP,POLM,NME6,POLR1C,POLR2L,PRIM1,NME4,DUT,ENPP1,DCK,POLR1E,DCTD,CTPS,TXNRD1,NUDT5,NT5C3,NME3,POLR3H,ITPA,ENTPD2,PAPD5,CAD,UCK2,TXNRD2,POLD2
Valine, Leucine and Isoleucine Biosynthesis	MAPK1,RPL14,RPL26,EIF3C/EIF3CL,EIF2A,RPL6,EIF3B,RPS9,RPL8,RPL13,EIF2AK1,PIK3C2B,RPL4,NRAS,RPL34,RPL27,RPS2,RPL17,RPL12,EIF2B3,RPL23A,RPL9,RPLP0,EIF3G,RPS29,RPS4X,RPS26,EIF4A1,EIF2B5,EIF3I,RPS15,RPL29 (includes EG:367874),EIF3L,RPL13A,RPSA
Pyrimidine Metabolism	NDUFV1,NDUFA9,NDUFS7,COQ3,NDUFB8,FTSJ2,NDUFA4L2,NDUFB10,NDUFS8,UFSP2,NDUFA6,PRMT5,NDUFS2,NDUFA12,NDUFB6
Role of CHK Proteins in Cell Cycle Checkpoint Control	ADSL,DLAT,ASS1,GAD1 (includes EG:100006588),CAD,AARS,GOT2,ASNS,PDHB,NARS2
EIF2 Signaling	FDPS,FDFT1,DHCR7,VKORC1,COX10 (includes EG:1352),LSS,HMGCR

Ubiquinone Biosynthesis	B2M,DNAJC17,CDC20,USP5,HSPB8,USP2,PSMB6,DNAJB13,UCHL1,PAN2,HSPA4,HSP90AB1,STUB1,USP10,UBE2E3,USP40,ANAPC11,HSPA4L,PSMB4,UCHL3,UBB,PSMB5,DNAJB12,UBE4B,DNAJC9,PSMD13,HSPA9,PSMA1,HSPD1,THOP1,USP33,UBE2L6,FZR1,SKP2 (includes EG:27401),HSPA8,PSMB7,PSMD11,PSMC1,DNAJC5,PSMB2,UBE2G1,UBE2D4,PSMD12,PSMB1,PSMD4,DNAJC7,UBE2C			
Alanine and Aspartate Metabolism	RCC1,CSE1L,TNPO1,RANBP1,IPO5,RANGAP1			
Biosynthesis of Steroids	PRKDC,APAF1,DFFB,BID,LMNB2,DFFA			
Protein Ubiquitination Pathway	SRM,GAMT,ASS1,OAT,CAT,ACY1,ALDH18A1,ODC1			
Urea Cycle and Metabolism of Amino Groups	POLR1C,TAF1A,TAF1C,UBTF			
Cell Cycle: G2/M DNA Damage Checkpoint Regulation	CHST2,SULT1A3/SULT1A4,SRR,CARS,LDHAL6A,UST,CARS2,CHST12,GOT2,LDHB,SULT2A1			
Fructose and Mannose Metabolism	NUDT5,SORD,GMPPA,PFKP,TPI1,PMM2,PFKM,DUSP16,ALDOC			
mTOR Signaling	MAPK1,PPP2R3B,EIF3C/EIF3CL,PD			
Wnt/β-catenin Signaling	LRP5,UBB,WNT10B,CSNK1G1,HDAC1,MARK2,SOX15,CSNK1A1,PPP2R3B,TLE1,SOX11,SOX13,CDH3,GNAO1,CSNK2A1,TGFB3,LEF1,PPP2R2C,RUVBL2,DVL2,CSNK2B,CTNNB1,TAB1,SOX5	5.93E-01	1.57E-01	LRP5,UBB,WN

Table 3: KEGG Pathways and Genes upregulated in CAIX-ve cells

Genes	Pentose and glucuronate interconversions /Starch and sucrose metabolism
ENSG00000167165	UDP glucuronosyltransferase 1 family, polypeptide A6
ENSG00000109814	UDP-glucose 6-dehydrogenase
ENSG00000169764	UDP-glucose pyrophosphorylase 2

ENSG00000169919	glucuronidase, beta
Genes	**Metabolism of xenobiotics by cytochrome P450 /Steroid hormone biosynthesis**
ENSG00000196139	aldo-keto reductase family 1, member C3
ENSG00000167165	UDP glucuronosyltransferase 1 family, polypeptide A6
ENSG00000198610	aldo-keto reductase family 1, member C4 (chlordecone reductase; 3-alpha hydroxysteroid dehydrogenase, type I; dihydrodiol dehydrogenase 4)
ENSG00000151632	aldo-keto reductase family 1, member C2 (dihydrodiol dehydrogenase 2; bile acid binding protein; 3-alpha hydroxysteroid dehydrogenase, type III)
Genes	**Regulation of actin cytoskeleton**
ENSG00000139734	diaphanous homolog 3 (Drosophila)
ENSG00000120063	guanine nucleotide binding protein (G protein), alpha 13
ENSG00000148180	gelsolin
ENSG00000129682	fibroblast growth factor 13
ENSG00000147202	diaphanous homolog 2 (Drosophila)
ENSG00000205542	thymosin beta 4, X-linked
ENSG00000136002	Rho guanine nucleotide exchange factor (GEF) 4
ENSG00000132470	integrin, beta 4
ENSG00000100311	platelet-derived growth factor beta polypeptide
ENSG00000137710	radixin
Genes	**Pancreatic secretion /Bile secretion /Gastric acid secretion**
ENSG00000143153	ATPase, Na+/K+ transporting, beta 1 polypeptide
ENSG00000164742	adenylate cyclase 1 (brain)
ENSG00000104267	carbonic anhydrase II
Genes	**Rheumatoid arthritis / Leishmaniasis**
ENSG00000170345	FBJ murine osteosarcoma viral oncogene homolog
ENSG00000198502	major histocompatibility complex, class II, DR beta 5
ENSG00000177606	jun proto-oncogene

Table 4: Ingenuity Canonical Pathways and Genes upregulated in CAIX-ve cells

Ingenuity Canonical Pathways	Genes
Actin Cytoskeleton Signaling	TMSL3,ARHGEF4,TMSB10/TMSB4X,DIAPH3,RDX,DIAPH2,GNA13,GSN,PDGFB,FGF13
Pentose and Glucuronate Interconversions	UGDH,UGP2,GUSB

Nucleotide Sugars Metabolism	UGDH,UGP2
TNFR2 Signaling	FOS,JUN,MAP3K1
TR/RXR Activation	KLF9,AKR1C1/AKR1C2,AKR1C3,BCL3,HIF-1A
Cardiomyocyte Differentiation via BMP Receptors	BMP4,BMPR2
IL-1 Signaling	FOS,JUN,MAP3K1,ADCY1,GNA13
C21-Steroid Hormone Metabolism	AKR1C1/AKR1C2,AKR1C3
RAR Activation	FOS,JUN,CRABP2,MAP3K1,NR2F2,ADCY1,NRIP1
MIF Regulation of Innate Immunity	FOS,JUN,PLA2G10
Hypoxia Signaling in the Cardiovascular System	JUN,UBE2E2,HIF-1A,UBE2F
IGF-1 Signaling	IGFBP4,FOS,JUN,SOCS2,IGF1R
ILK Signaling	TMSL3,FOS,JUN,RHOQ,TMSB10/TMSB4X,HIF-1A,ITGB4
Renal Cell Carcinoma Signaling	FOS,JUN,HIF-1A,PDGFB
Role of Oct4 in Mammalian Embryonic Stem Cell Pluripotency	SOX2,NR2F2,JARID2
April Mediated Signaling	FOS,JUN,MAP3K1
Molecular Mechanisms of Cancer	FOS,PMAIP1,ARHGEF4,JUN,BMP4,RHOQ,RASGRP1,ADCY1,BMPR2, HIF-1A,GNA13
B Cell Activating Factor Signaling	FOS,JUN,MAP3K1
PDGF Signaling	FOS,JUN,MAP3K1,PDGFB
Signaling by Rho Family GTPases	FOS,ARHGEF4,JUN,RHOQ,DIAPH3,RDX,GNA13,SEPT2
BMP signaling pathway	JUN,BMP4,FST,BMPR2
Glycosphingolipid Biosynthesis - Neolactoseries	FUT4,ST3GAL5
Glucocorticoid Receptor Signaling	FOS,JUN,HMGB1,SGK1,ANXA1,MAP3K1,NRIP1,HSPA2,PGR (includes EG:18667)
TNFR1 Signaling	FOS,JUN,MAP3K1
EGF Signaling	FOS,JUN,MAP3K1

Appendix Five

Common genes between microarray gene lists and RNA-seq gene lists

Table 1: Common upregulated genes between the CAIX+ve microarray gene list and CAIX+ve RNA-seq gene list

ENSG00000115461	IGFBP5, insulin-like growth factor binding protein 5 - protein_coding

ENSG00000107159	CA9, carbonic anhydrase IX - protein_coding
ENSG00000205426	KRT81, keratin 81 - protein_coding
ENSG00000069667	RORA, RAR-related orphan receptor A - protein_coding
ENSG00000185633	NDUFA4L2, NADH dehydrogenase (ubiquinone) 1 alpha subcomplex, 4-like 2 - protein_coding
ENSG00000161671	C19orf63, UPF0510 protein INM02 Precursor (Hematopoietic signal peptide-containing membrane domain-containing protein 1) - protein_coding
ENSG00000140465	CYP1A1, cytochrome P450, family 1, subfamily A, polypeptide 1 - protein_coding
ENSG00000179058	C9orf50, Uncharacterized protein C9orf50 - protein_coding
ENSG00000130226	DPP6, dipeptidyl-peptidase 6 - protein_coding
ENSG00000155849	ELMO1, engulfment and cell motility 1 - protein_coding
ENSG00000176225	RTTN, rotatin - protein_coding
ENSG00000184867	ARMCX2, armadillo repeat containing, X-linked 2 - protein_coding
ENSG00000162599	NFIA, nuclear factor I/A - protein_coding
ENSG00000101265	RASSF2, Ras association (RalGDS/AF-6) domain family member 2 - protein_coding
ENSG00000003436	TFPI, tissue factor pathway inhibitor (lipoprotein-associated coagulation inhibitor) - protein_coding
ENSG00000170954	ZNF415, zinc finger protein 415 - protein_coding
ENSG00000157168	NRG1, neuregulin 1 - protein_coding
ENSG00000021645	NRXN3, neurexin 3 - protein_coding
ENSG00000086289	EPDR1, ependymin related protein 1 (zebrafish) - protein_coding
ENSG00000182771	GRID1, glutamate receptor, ionotropic, delta 1 - protein_coding
ENSG00000172987	HPSE2, heparanase 2 - protein_coding
ENSG00000171124	FUT3, fucosyltransferase 3 (galactoside 3(4)-L-fucosyltransferase, Lewis blood group) - protein_coding
ENSG00000108602	ALDH3A1, aldehyde dehydrogenase 3 family, memberA1 - protein_coding
ENSG00000162676	GFI1, growth factor independent 1 transcription repressor - protein_coding
ENSG00000105427	CNFN, cornifelin - protein_coding
ENSG00000197181	PIWIL2, piwi-like 2 (Drosophila) - protein_coding
ENSG00000134532	SOX5, SRY (sex determining region Y)-box 5 - protein_coding
ENSG00000165300	SLITRK5, SLIT and NTRK-like family, member 5 - protein_coding
ENSG00000198670	LPA, lipoprotein, Lp(a) - protein_coding
ENSG00000118322	ATP10B, ATPase, class V, type 10B - protein_coding
ENSG00000154188	ANGPT1, angiopoietin 1 - protein_coding
ENSG00000147082	CCNB3, cyclin B3 - protein_coding
ENSG00000154027	AK5, adenylate kinase 5 - protein_coding
ENSG00000142530	FAM71E1, family with sequence similarity 71, member E1 - protein_coding
ENSG00000172901	Aminopeptidase Q (AP-Q)(EC 3.4.11.-)(Laeverin)(CHL2 antigen) - protein_coding
ENSG00000181368	C5orf62, putative small membrane protein NID67 - protein_coding
ENSG00000169064	ZBBX, zinc finger, B-box domain containing - protein_coding
ENSG00000111716	LDHB, lactate dehydrogenase B - protein_coding
ENSG00000198658	unknown - pseudogene
ENSG00000105967	TFEC, transcription factor EC - protein_coding
ENSG00000100365	NCF4, neutrophil cytosolic factor 4, 40kDa - protein_coding
ENSG00000038945	MSR1, macrophage scavenger receptor 1 - protein_coding
ENSG00000175315	CST6, cystatin E/M - protein_coding
ENSG00000041982	TNC, tenascin C - protein_coding
ENSG00000197632	SERPINB2, serpin peptidase inhibitor, clade B (ovalbumin), member 2 - protein_coding
ENSG00000104313	EYA1, eyes absent homolog 1 (Drosophila) - protein_coding
ENSG00000146374	RSPO3, R-spondin 3 homolog (Xenopus laevis) - protein_coding
ENSG00000189064	GAGE2A, G antigen 2A - protein_coding
ENSG00000138472	GUCA1C, guanylate cyclase activator 1C - protein_coding
ENSG00000134954	ETS1, v-ets erythroblastosis virus E26 oncogene homolog 1 (avian) - protein_coding
ENSG00000166006	KCNC2, potassium voltage-gated channel, Shaw-related subfamily, member 2 - protein_coding
ENSG00000145839	IL9, interleukin 9 - protein_coding
ENSG00000120280	CXorf21, chromosome X open reading frame 21 - protein_coding
ENSG00000126838	PZP, pregnancy-zone protein - protein_coding

ENSG00000186629	EMR4P, egf-like module containing, mucin-like, hormone receptor-like 4 pseudogene - protein_coding
ENSG00000139797	RNF113B, ring finger protein 113B - protein_coding
ENSG00000164853	UNCX, UNC homeobox - protein_coding
ENSG00000149651	SPINT4, serine peptidase inhibitor, Kunitz type 4 - protein_coding
ENSG00000171916	LGALS9C, lectin, galactoside-binding, soluble, 9C - protein_coding
ENSG00000182667	OPCML, opioid binding protein/cell adhesion molecule-like - protein_coding
ENSG00000198453	ZNF568, zinc finger protein 568 - protein_coding

Table 2: Common upregulated genes between the CAIX-ve microarray gene list and CAIX-ve RNA-seq gene list

ENSG00000138650	PCDH10, protocadherin 10 - protein_coding
ENSG00000201428	unknown - misc_RNA
ENSG00000201428	unknown - misc_RNA

ENSG00000222386	unknown - misc_RNA
ENSG00000202392	unknown - misc_RNA
ENSG00000221399	unknown - misc_RNA
ENSG00000201600	unknown - misc_RNA
ENSG00000182759	MAFA, v-maf musculoaponeurotic fibrosarcoma oncogene homolog A (avian) - protein_coding
ENSG00000107859	PITX3, paired-like homeodomain 3 - protein_coding
ENSG00000182040	USH1G, Usher syndrome 1G (autosomal recessive) - protein_coding
ENSG00000188987	HIST1H4D, histone cluster 1, H4d - protein_coding
ENSG00000196176	HIST1H4A, histone cluster 1, H4a - protein_coding
ENSG00000111348	ARHGDIB, Rho GDP dissociation inhibitor (GDI) beta - protein_coding
ENSG00000140478	GOLGA6D, golgin A6 family, member D - protein_coding
ENSG00000162783	IER5, immediate early response 5 - protein_coding
ENSG00000173805	HAP1, huntingtin-associated protein 1 - protein_coding
ENSG00000143127	ITGA10, integrin, alpha 10 - protein_coding
ENSG00000099984	GSTT2, glutathione S-transferase theta 2 - protein_coding
ENSG00000128596	CCDC136, coiled-coil domain containing 136 - protein_coding
ENSG00000183696	UPP1, uridine phosphorylase 1 - protein_coding
ENSG00000163735	CXCL5, chemokine (C-X-C motif) ligand 5 - protein_coding
ENSG00000162772	ATF3, activating transcription factor 3 - protein_coding
ENSG00000204086	RPA4, replication protein A4, 34kDa - protein_coding
ENSG00000176749	CDK5R1, cyclin-dependent kinase 5, regulatory subunit 1 (p35) - protein_coding
ENSG00000177606	JUN, jun oncogene - protein_coding
ENSG00000188536	HBA2, hemoglobin, alpha 2 - protein_coding
ENSG00000206172	HBA1, hemoglobin, alpha 1 - protein_coding
ENSG00000163132	MSX1, msh homeobox 1 - protein_coding
ENSG00000180616	SSTR2, somatostatin receptor 2 - protein_coding
ENSG00000221970	OR2A1, olfactory receptor, family 2, subfamily A, member 1 - protein_coding
ENSG00000212807	OR2A42, olfactory receptor, family 2, subfamily A, member 42 - protein_coding
ENSG00000106789	CORO2A, coronin, actin binding protein, 2A - protein_coding
ENSG00000125551	PLGLB2, plasminogen-like B2 - protein_coding
ENSG00000116717	GADD45A, growth arrest and DNA-damage-inducible, alpha - protein_coding
ENSG00000215354	FAM90A12, family with sequence similarity 90, member A24 (pseudogene) - protein_coding
ENSG00000166920	C15orf48, microRNA 147b - protein_coding
ENSG00000130222	GADD45G, growth arrest and DNA-damage-inducible, gamma - protein_coding
ENSG00000169429	IL8, interleukin 8 - protein_coding
ENSG00000116652	DLEU2L, deleted in lymphocytic leukemia 2-like - protein_coding
ENSG00000026950	BTN3A1, butyrophilin, subfamily 3, member A1 - protein_coding
ENSG00000005513	SOX8, SRY (sex determining region Y)-box 8 - protein_coding
ENSG00000182866	LCK, lymphocyte-specific protein tyrosine kinase - protein_coding
ENSG00000125775	SDCBP2, syndecan binding protein (syntenin) 2 - protein_coding
ENSG00000124159	MATN4, matrilin 4 - protein_coding
ENSG00000189275	cDNA FLJ46300 fis, clone TESTI4035989 - protein_coding
ENSG00000187848	P2RX2, purinergic receptor P2X, ligand-gated ion channel, 2 - protein_coding
ENSG00000127528	KLF2, Kruppel-like factor 2 (lung) - protein_coding
ENSG00000132031	MATN3, matrilin 3 - protein_coding
ENSG00000143341	HMCN1, hemicentin 1 - protein_coding
ENSG00000023445	BIRC3, baculoviral IAP repeat-containing 3 - protein_coding
ENSG00000197870	PRB3, proline-rich protein BstNI subfamily 3 - protein_coding
ENSG00000181016	C7orf53, Coiled-coil domain-containing transmembrane protein C7orf53 - protein_coding
ENSG00000105697	HAMP, hepcidin antimicrobial peptide - protein_coding
ENSG00000205090	C1orf70, Transmembrane protein C1orf70 - protein_coding
ENSG00000145835	unknown - pseudogene
ENSG00000104808	DHDH, dihydrodiol dehydrogenase (dimeric) - protein_coding
ENSG00000107014	RLN2, relaxin 2 - protein_coding
ENSG00000070985	TRPM5, transient receptor potential cation channel, subfamily M, member 5 -

	protein_coding
ENSG00000006747	SCIN, scinderin - protein_coding
ENSG00000186543	unknown - pseudogene
ENSG00000186594	C17orf91, microRNA 22 - processed_transcript
ENSG00000102032	RENBP, renin binding protein - protein_coding
ENSG00000185022	MAFF, v-maf musculoaponeurotic fibrosarcoma oncogene homolog F (avian) - protein_coding
ENSG00000202058	unknown - misc_RNA
ENSG00000197061	HIST1H4C, histone cluster 1, H4c - protein_coding
ENSG00000087074	PPP1R15A, protein phosphatase 1, regulatory (inhibitor) subunit 15A - protein_coding

Appendix Six

List of publications arising from thesis

The work I did for my PhD contributed to the following publications:

Role of hypoxia-inducible factors in epigenetic regulation via histone demethylases. Yang J, **Ledaki I**, Turley H, Gatter KC, Montero JC, Li JL, Harris AL. Ann N Y Acad Sci. 2009 Oct; 1177.

LC3A-positive light microscopy detected patterns of autophagy and prognosis in operable breast carcinomas. Sivridis E, Koukourakis MI, Zois CE, **Ledaki I**, Ferguson DJ, Harris AL, Gatter KC, Giatromanolaki A.Am J Pathol, 2010 May; 176(5).

Carbonic anhydrase IX promotes tumor growth and necrosis in vivo and inhibition enhances anti-VEGF therapy. McIntyre A, Patiar S, Wigfield S, Li JL**, Ledaki I**, Turley H, Leek R, Snell C, Gatter K, Sly WS, Vaughan-Jones RD, Swietach P, Harris AL.Clin Cancer Res. 2012 Jun 1; 18(11).

Carbonic anhydrase IX induction defines a heterogeneous cancer cell response to hypoxia and mediates stem cell-like properties and sensitivity to HDAC inhibitors. **Ioanna Ledaki**, Alan McIntyre, Simon Wigfield, Francesca Buffa, Simon McGowan, Dilair Baban Ji-liang Li, Helen Turley, Russell Leek, and Adrian L. Harris. (Cell Research, submitted, 2013).

BIBLIOGRAPHY

Adamson, I.Y., Young, L., and Bowden, D.H. (1988). Relationship of alveolar epithelial injury and repair to the induction of pulmonary fibrosis. Am J Pathol *130*, 377-383.

Aharinejad, S., Paulus, P., Sioud, M., Hofmann, M., Zins, K., Schafer, R., Stanley, E.R., and Abraham, D. (2004). Colony-stimulating factor-1 blockade by antisense oligonucleotides and small interfering RNAs suppresses growth of human mammary tumor xenografts in mice. Cancer Res *64*, 5378-5384.

Ahlskog, J.K., Dumelin, C.E., Trussel, S., Marlind, J., and Neri, D. (2009a). In vivo targeting of tumor-associated carbonic anhydrases using acetazolamide derivatives. Bioorg Med Chem Lett *19*, 4851-4856.

Ahlskog, J.K., Schliemann, C., Marlind, J., Qureshi, U., Ammar, A., Pedley, R.B., and Neri, D. (2009b). Human monoclonal antibodies targeting carbonic anhydrase IX for the molecular imaging of hypoxic regions in solid tumours. Br J Cancer *101*, 645-657.

Al-Hajj, M., and Clarke, M.F. (2004). Self-renewal and solid tumor stem cells. Oncogene *23*, 7274-7282.

Al-Hajj, M., Wicha, M.S., Benito-Hernandez, A., Morrison, S.J., and Clarke, M.F. (2003a). Prospective identification of tumorigenic breast cancer cells. Proc Natl Acad Sci U S A *100*, 3983-3988.

Al-Hajj, M., Wicha, M.S., Benito-Hernandez, A., Morrison, S.J., and Clarke, M.F. (2003b). Prospective identification of tumorigenic breast cancer cells. Proc Natl Acad Sci U S A *100*, 3983-3988.

Alterio, V., Hilvo, M., Di Fiore, A., Supuran, C.T., Pan, P., Parkkila, S., Scaloni, A., Pastorek, J., Pastorekova, S., Pedone, C.*, et al.* (2009). Crystal structure of the catalytic domain of the tumor-associated human carbonic anhydrase IX. Proc Natl Acad Sci U S A *106*, 16233-16238.

Anderson, K., Lutz, C., van Delft, F.W., Bateman, C.M., Guo, Y., Colman, S.M., Kempski, H., Moorman, A.V., Titley, I., Swansbury, J.*, et al.* (2011). Genetic variegation of clonal architecture and propagating cells in leukaemia. Nature *469*, 356-361.

Antsiferova, M., and Werner, S. (2012). The bright and the dark sides of activin in wound healing and cancer. Journal of cell science *125*, 3929-3937.

Ashida, S., Nishimori, I., Tanimura, M., Onishi, S., and Shuin, T. (2002). Effects of von Hippel-Lindau gene mutation and methylation status on expression of transmembrane carbonic anhydrases in renal cell carcinoma. J Cancer Res Clin Oncol *128*, 561-568.

Asselin-Labat, M.L., Sutherland, K.D., Vaillant, F., Gyorki, D.E., Wu, D., Holroyd, S., Breslin, K., Ward, T., Shi, W., Bath, M.L.*, et al.* (2011). Gata-3 negatively regulates

the tumor-initiating capacity of mammary luminal progenitor cells and targets the putative tumor suppressor caspase-14. Molecular and cellular biology *31*, 4609-4622.
Auer, P.L., and Doerge, R.W. (2010). Statistical design and analysis of RNA sequencing data. Genetics *185*, 405-416.
Authier, S., Tremblay, S., Dumulon, V., Dubuc, C., Ouellet, R., Lecomte, R., Cunnane, S.C., and Benard, F. (2008). [11C] acetoacetate utilization by breast and prostate tumors: a PET and biodistribution study in mice. Mol Imaging Biol *10*, 217-223.
Avril, N., Menzel, M., Dose, J., Schelling, M., Weber, W., Janicke, F., Nathrath, W., and Schwaiger, M. (2001). Glucose metabolism of breast cancer assessed by 18F-FDG PET: histologic and immunohistochemical tissue analysis. J Nucl Med *42*, 9-16.
Balgi, A.D., Diering, G.H., Donohue, E., Lam, K.K., Fonseca, B.D., Zimmerman, C., Numata, M., and Roberge, M. (2011). Regulation of mTORC1 signaling by pH. PloS one *6*, e21549.
Balic, M., Lin, H., Young, L., Hawes, D., Giuliano, A., McNamara, G., Datar, R.H., and Cote, R.J. (2006). Most early disseminated cancer cells detected in bone marrow of breast cancer patients have a putative breast cancer stem cell phenotype. Clinical cancer research : an official journal of the American Association for Cancer Research *12*, 5615-5621.
Balkwill, F., and Mantovani, A. (2001). Inflammation and cancer: back to Virchow? Lancet *357*, 539-545.
Bando, H., and Toi, M. (2000). Tumor angiogenesis, macrophages, and cytokines. Adv Exp Med Biol *476*, 267-284.
Bar, E.E., Chaudhry, A., Lin, A., Fan, X., Schreck, K., Matsui, W., Piccirillo, S., Vescovi, A.L., DiMeco, F., Olivi, A.*, et al.* (2007). Cyclopamine-mediated hedgehog pathway inhibition depletes stem-like cancer cells in glioblastoma. Stem Cells *25*, 2524-2533.
Bardos, J.I., and Ashcroft, M. (2005). Negative and positive regulation of HIF-1: a complex network. Biochim Biophys Acta *1755*, 107-120.
Barker, H.E., Chang, J., Cox, T.R., Lang, G., Bird, D., Nicolau, M., Evans, H.R., Gartland, A., and Erler, J.T. (2011). LOXL2-mediated matrix remodeling in metastasis and mammary gland involution. Cancer Res *71*, 1561-1572.
Barker, N., van Es, J.H., Kuipers, J., Kujala, P., van den Born, M., Cozijnsen, M., Haegebarth, A., Korving, J., Begthel, H., Peters, P.J.*, et al.* (2007). Identification of stem cells in small intestine and colon by marker gene Lgr5. Nature *449*, 1003-1007.
Barrett, L.E., Granot, Z., Coker, C., Iavarone, A., Hambardzumyan, D., Holland, E.C., Nam, H.S., and Benezra, R. (2012). Self-renewal does not predict tumor growth potential in mouse models of high-grade glioma. Cancer cell *21*, 11-24.
Beach, J.R., Hussey, G.S., Miller, T.E., Chaudhury, A., Patel, P., Monslow, J., Zheng, Q., Keri, R.A., Reizes, O., Bresnick, A.R.*, et al.* (2011). Myosin II isoform switching mediates invasiveness after TGF-beta-induced epithelial-mesenchymal transition. Proc Natl Acad Sci U S A *108*, 17991-17996.
Beasley, N.J., Wykoff, C.C., Watson, P.H., Leek, R., Turley, H., Gatter, K., Pastorek, J., Cox, G.J., Ratcliffe, P., and Harris, A.L. (2001). Carbonic anhydrase IX, an endogenous hypoxia marker, expression in head and neck squamous cell

carcinoma and its relationship to hypoxia, necrosis, and microvessel density. Cancer Res *61*, 5262-5267.
Ben-Porath, I., Thomson, M.W., Carey, V.J., Ge, R., Bell, G.W., Regev, A., and Weinberg, R.A. (2008). An embryonic stem cell-like gene expression signature in poorly differentiated aggressive human tumors. Nat Genet *40*, 499-507.
Berger, S.L. (2007). The complex language of chromatin regulation during transcription. Nature *447*, 407-412.
Bingle, L., Brown, N.J., and Lewis, C.E. (2002). The role of tumour-associated macrophages in tumour progression: implications for new anticancer therapies. J Pathol *196*, 254-265.
Blagosklonny, M.V. (2002). Oncogenic resistance to growth-limiting conditions. Nature reviews. Cancer *2*, 221-225.
Blazek, E.R., Foutch, J.L., and Maki, G. (2007). Daoy medulloblastoma cells that express CD133 are radioresistant relative to CD133- cells, and the CD133+ sector is enlarged by hypoxia. Int J Radiat Oncol Biol Phys *67*, 1-5.
Boiani, M., and Scholer, H.R. (2005). Regulatory networks in embryo-derived pluripotent stem cells. Nat Rev Mol Cell Biol *6*, 872-884.
Bonnet, D., and Dick, J.E. (1997). Human acute myeloid leukemia is organized as a hierarchy that originates from a primitive hematopoietic cell. Nat Med *3*, 730-737.
Borovski, T., De Sousa, E.M.F., Vermeulen, L., and Medema, J.P. (2011). Cancer stem cell niche: the place to be. Cancer Res *71*, 634-639.
Boven, E., Winograd, B., Berger, D.P., Dumont, M.P., Braakhuis, B.J., Fodstad, O., Langdon, S., and Fiebig, H.H. (1992). Phase II preclinical drug screening in human tumor xenografts: a first European multicenter collaborative study. Cancer Res *52*, 5940-5947.
Brabletz, T., Jung, A., Dag, S., Hlubek, F., and Kirchner, T. (1999). beta-catenin regulates the expression of the matrix metalloproteinase-7 in human colorectal cancer. Am J Pathol *155*, 1033-1038.
Bricker, D.K., Taylor, E.B., Schell, J.C., Orsak, T., Boutron, A., Chen, Y.C., Cox, J.E., Cardon, C.M., Van Vranken, J.G., Dephoure, N.*, et al.* (2012). A mitochondrial pyruvate carrier required for pyruvate uptake in yeast, Drosophila, and humans. Science *337*, 96-100.
Brown, J.M., and Giaccia, A.J. (1998). The unique physiology of solid tumors: opportunities (and problems) for cancer therapy. Cancer Res *58*, 1408-1416.
Buffa, F.M., Harris, A.L., West, C.M., and Miller, C.J. (2010). Large meta-analysis of multiple cancers reveals a common, compact and highly prognostic hypoxia metagene. Br J Cancer *102*, 428-435.
Bussard, K.M., and Smith, G.H. (2011). The mammary gland microenvironment directs progenitor cell fate in vivo. Int J Cell Biol *2011*, 451676.
Butcher, D.T., Alliston, T., and Weaver, V.M. (2009). A tense situation: forcing tumour progression. Nature reviews. Cancer *9*, 108-122.
Cammareri, P., Lombardo, Y., Francipane, M.G., Bonventre, S., Todaro, M., and Stassi, G. (2008). Isolation and culture of colon cancer stem cells. Methods Cell Biol *86*, 311-324.
Campbell, L.L., and Polyak, K. (2007). Breast tumor heterogeneity: cancer stem cells or clonal evolution? Cell Cycle *6*, 2332-2338.

Cantor, J.R., and Sabatini, D.M. (2012). Cancer cell metabolism: one hallmark, many faces. Cancer Discov *2*, 881-898.
Capparelli, C., Whitaker-Menezes, D., Guido, C., Balliet, R., Pestell, T.G., Howell, A., Sneddon, S., Pestell, R.G., Martinez-Outschoorn, U., Lisanti, M.P.*, et al.* (2012). CTGF drives autophagy, glycolysis and senescence in cancer-associated fibroblasts via HIF1 activation, metabolically promoting tumor growth. Cell Cycle *11*, 2272-2284.
Cariati, M., Naderi, A., Brown, J.P., Smalley, M.J., Pinder, S.E., Caldas, C., and Purushotham, A.D. (2008). Alpha-6 integrin is necessary for the tumourigenicity of a stem cell-like subpopulation within the MCF7 breast cancer cell line. International journal of cancer. Journal international du cancer *122*, 298-304.
Carmona-Saez, P., Chagoyen, M., Tirado, F., Carazo, J.M., and Pascual-Montano, A. (2007). GENECODIS: a web-based tool for finding significant concurrent annotations in gene lists. Genome Biol *8*, R3.
Carpentino, J.E., Hynes, M.J., Appelman, H.D., Zheng, T., Steindler, D.A., Scott, E.W., and Huang, E.H. (2009). Aldehyde dehydrogenase-expressing colon stem cells contribute to tumorigenesis in the transition from colitis to cancer. Cancer Res *69*, 8208-8215.
Castells, M., Thibault, B., Delord, J.P., and Couderc, B. (2012). Implication of tumor microenvironment in chemoresistance: tumor-associated stromal cells protect tumor cells from cell death. International journal of molecular sciences *13*, 9545-9571.
Cerhan, J.R., Anderson, K.E., Janney, C.A., Vachon, C.M., Witzig, T.E., and Habermann, T.M. (2003). Association of aspirin and other non-steroidal anti-inflammatory drug use with incidence of non-Hodgkin lymphoma. International journal of cancer. Journal international du cancer *106*, 784-788.
Chance, B. (1965). Reaction of oxygen with the respiratory chain in cells and tissues. J Gen Physiol *49*, Suppl:163-195.
Chandel, N.S., McClintock, D.S., Feliciano, C.E., Wood, T.M., Melendez, J.A., Rodriguez, A.M., and Schumacker, P.T. (2000). Reactive oxygen species generated at mitochondrial complex III stabilize hypoxia-inducible factor-1alpha during hypoxia: a mechanism of O2 sensing. The Journal of biological chemistry *275*, 25130-25138.
Chen, C., Liu, Y., Liu, R., Ikenoue, T., Guan, K.L., Liu, Y., and Zheng, P. (2008). TSC-mTOR maintains quiescence and function of hematopoietic stem cells by repressing mitochondrial biogenesis and reactive oxygen species. J Exp Med *205*, 2397-2408.
Chen, C., Pore, N., Behrooz, A., Ismail-Beigi, F., and Maity, A. (2001). Regulation of glut1 mRNA by hypoxia-inducible factor-1. Interaction between H-ras and hypoxia. The Journal of biological chemistry *276*, 9519-9525.
Chen, F.H., and Tuan, R.S. (2008). Mesenchymal stem cells in arthritic diseases. Arthritis Res Ther *10*, 223.
Chen, M.S., Woodward, W.A., Behbod, F., Peddibhotla, S., Alfaro, M.P., Buchholz, T.A., and Rosen, J.M. (2007). Wnt/beta-catenin mediates radiation resistance of Sca1+ progenitors in an immortalized mammary gland cell line. Journal of cell science *120*, 468-477.
Chia, S.K., Wykoff, C.C., Watson, P.H., Han, C., Leek, R.D., Pastorek, J., Gatter, K.C., Ratcliffe, P., and Harris, A.L. (2001). Prognostic significance of a novel hypoxia-

regulated marker, carbonic anhydrase IX, in invasive breast carcinoma. Journal of clinical oncology : official journal of the American Society of Clinical Oncology *19*, 3660-3668.
Chiang, J.W., Karlan, B.Y., Cass, L., and Baldwin, R.L. (2006). BRCA1 promoter methylation predicts adverse ovarian cancer prognosis. Gynecol Oncol *101*, 403-410.
Chiche, J., Brahimi-Horn, M.C., and Pouyssegur, J. (2010). Tumour hypoxia induces a metabolic shift causing acidosis: a common feature in cancer. J Cell Mol Med *14*, 771-794.
Chiche, J., Ilc, K., Laferriere, J., Trottier, E., Dayan, F., Mazure, N.M., Brahimi-Horn, M.C., and Pouyssegur, J. (2009). Hypoxia-inducible carbonic anhydrase IX and XII promote tumor cell growth by counteracting acidosis through the regulation of the intracellular pH. Cancer Res *69*, 358-368.
Cho, M., Grabmaier, K., Kitahori, Y., Hiasa, Y., Nakagawa, Y., Uemura, H., Hirao, Y., Ohnishi, T., Yoshikawa, K., and Ooesterwijk, E. (2000). Activation of the MN/CA9 gene is associated with hypomethylation in human renal cell carcinoma cell lines. Mol Carcinog *27*, 184-189.
Cho, M., Uemura, H., Kim, S.C., Kawada, Y., Yoshida, K., Hirao, Y., Konishi, N., Saga, S., and Yoshikawa, K. (2001). Hypomethylation of the MN/CA9 promoter and upregulated MN/CA9 expression in human renal cell carcinoma. Br J Cancer *85*, 563-567.
Choschzick, M., Oosterwijk, E., Muller, V., Woelber, L., Simon, R., Moch, H., and Tennstedt, P. (2011). Overexpression of carbonic anhydrase IX (CAIX) is an independent unfavorable prognostic marker in endometrioid ovarian cancer. Virchows Archiv : an international journal of pathology *459*, 193-200.
Chow, L.M., Endersby, R., Zhu, X., Rankin, S., Qu, C., Zhang, J., Broniscer, A., Ellison, D.W., and Baker, S.J. (2011). Cooperativity within and among Pten, p53, and Rb pathways induces high-grade astrocytoma in adult brain. Cancer cell *19*, 305-316.
Chrastina, A., Pastorekova, S., and Pastorek, J. (2003a). Immunotargeting of human cervical carcinoma xenograft expressing CA IX tumor-associated antigen by 125I-labeled M75 monoclonal antibody. Neoplasma *50*, 13-21.
Chrastina, A., Zavada, J., Parkkila, S., Kaluz, S., Kaluzova, M., Rajcani, J., Pastorek, J., and Pastorekova, S. (2003b). Biodistribution and pharmacokinetics of 125I-labeled monoclonal antibody M75 specific for carbonic anhydrase IX, an intrinsic marker of hypoxia, in nude mice xenografted with human colorectal carcinoma. International journal of cancer. Journal international du cancer *105*, 873-881.
Chu, E.Y., Hens, J., Andl, T., Kairo, A., Yamaguchi, T.P., Brisken, C., Glick, A., Wysolmerski, J.J., and Millar, S.E. (2004). Canonical WNT signaling promotes mammary placode development and is essential for initiation of mammary gland morphogenesis. Development *131*, 4819-4829.
Chung, Y.L., Troy, H., Kristeleit, R., Aherne, W., Jackson, L.E., Atadja, P., Griffiths, J.R., Judson, I.R., Workman, P., Leach, M.O.*, et al.* (2008). Noninvasive magnetic resonance spectroscopic pharmacodynamic markers of a novel histone deacetylase inhibitor, LAQ824, in human colon carcinoma cells and xenografts. Neoplasia *10*, 303-313.
Chute, J.P., Muramoto, G.G., Whitesides, J., Colvin, M., Safi, R., Chao, N.J., and McDonnell, D.P. (2006). Inhibition of aldehyde dehydrogenase and retinoid

signaling induces the expansion of human hematopoietic stem cells. Proc Natl Acad Sci U S A *103*, 11707-11712.
Cianchi, F., Vinci, M.C., Supuran, C.T., Peruzzi, B., De Giuli, P., Fasolis, G., Perigli, G., Pastorekova, S., Papucci, L., Pini, A.*, et al.* (2010). Selective inhibition of carbonic anhydrase IX decreases cell proliferation and induces ceramide-mediated apoptosis in human cancer cells. J Pharmacol Exp Ther *334*, 710-719.
Clarke, M.F., and Fuller, M. (2006). Stem cells and cancer: two faces of eve. Cell *124*, 1111-1115.
Conley, S.J., Gheordunescu, E., Kakarala, P., Newman, B., Korkaya, H., Heath, A.N., Clouthier, S.G., and Wicha, M.S. (2012). Antiangiogenic agents increase breast cancer stem cells via the generation of tumor hypoxia. Proc Natl Acad Sci U S A *109*, 2784-2789.
Coussens, L.M., Raymond, W.W., Bergers, G., Laig-Webster, M., Behrendtsen, O., Werb, Z., Caughey, G.H., and Hanahan, D. (1999). Inflammatory mast cells up-regulate angiogenesis during squamous epithelial carcinogenesis. Genes & development *13*, 1382-1397.
Coussens, L.M., and Werb, Z. (2002). Inflammation and cancer. Nature *420*, 860-867.
Coussens, L.M., Zitvogel, L., and Palucka, A.K. (2013). Neutralizing tumor-promoting chronic inflammation: a magic bullet? Science *339*, 286-291.
Creighton, C.J., Chang, J.C., and Rosen, J.M. (2010). Epithelial-mesenchymal transition (EMT) in tumor-initiating cells and its clinical implications in breast cancer. J Mammary Gland Biol Neoplasia *15*, 253-260.
Croker, A.K., Goodale, D., Chu, J., Postenka, C., Hedley, B.D., Hess, D.A., and Allan, A.L. (2009). High aldehyde dehydrogenase and expression of cancer stem cell markers selects for breast cancer cells with enhanced malignant and metastatic ability. J Cell Mol Med *13*, 2236-2252.
Cunningham, J.T., Rodgers, J.T., Arlow, D.H., Vazquez, F., Mootha, V.K., and Puigserver, P. (2007). mTOR controls mitochondrial oxidative function through a YY1-PGC-1alpha transcriptional complex. Nature *450*, 736-740.
Curry, J.M., Tuluc, M., Whitaker-Menezes, D., Ames, J.A., Anantharaman, A., Butera, A., Leiby, B., Cognetti, D.M., Sotgia, F., Lisanti, M.P.*, et al.* (2013). Cancer metabolism, stemness and tumor recurrence: MCT1 and MCT4 are functional biomarkers of metabolic symbiosis in head and neck cancer. Cell Cycle *12*, 1371-1384.
Dang, C.V., and Semenza, G.L. (1999). Oncogenic alterations of metabolism. Trends in biochemical sciences *24*, 68-72.
Davis, I.D., Wiseman, G.A., Lee, F.T., Gansen, D.N., Hopkins, W., Papenfuss, A.T., Liu, Z., Moynihan, T.J., Croghan, G.A., Adjei, A.A.*, et al.* (2007). A phase I multiple dose, dose escalation study of cG250 monoclonal antibody in patients with advanced renal cell carcinoma. Cancer Immun *7*, 13.
De Benedetti, A., and Graff, J.R. (2004). eIF-4E expression and its role in malignancies and metastases. Oncogene *23*, 3189-3199.
De Simone, G., and Supuran, C.T. (2010). Carbonic anhydrase IX: Biochemical and crystallographic characterization of a novel antitumor target. Biochim Biophys Acta *1804*, 404-409.

De Wever, O., Demetter, P., Mareel, M., and Bracke, M. (2008). Stromal myofibroblasts are drivers of invasive cancer growth. International journal of cancer. Journal international du cancer *123*, 2229-2238.
Debeb, B.G., Xu, W., and Woodward, W.A. (2009). Radiation resistance of breast cancer stem cells: understanding the clinical framework. J Mammary Gland Biol Neoplasia *14*, 11-17.
DeBerardinis, R.J., Mancuso, A., Daikhin, E., Nissim, I., Yudkoff, M., Wehrli, S., and Thompson, C.B. (2007). Beyond aerobic glycolysis: transformed cells can engage in glutamine metabolism that exceeds the requirement for protein and nucleotide synthesis. Proc Natl Acad Sci U S A *104*, 19345-19350.
Diaz-Cano, S.J. (2012). Tumor heterogeneity: mechanisms and bases for a reliable application of molecular marker design. International journal of molecular sciences *13*, 1951-2011.
Diehn, M., Cho, R.W., Lobo, N.A., Kalisky, T., Dorie, M.J., Kulp, A.N., Qian, D., Lam, J.S., Ailles, L.E., Wong, M.*, et al.* (2009). Association of reactive oxygen species levels and radioresistance in cancer stem cells. Nature *458*, 780-783.
Dierks, C., Beigi, R., Guo, G.R., Zirlik, K., Stegert, M.R., Manley, P., Trussell, C., Schmitt-Graeff, A., Landwerlin, K., Veelken, H.*, et al.* (2008). Expansion of Bcr-Abl-positive leukemic stem cells is dependent on Hedgehog pathway activation. Cancer cell *14*, 238-249.
DiMeo, T.A., Anderson, K., Phadke, P., Fan, C., Perou, C.M., Naber, S., and Kuperwasser, C. (2009). A novel lung metastasis signature links Wnt signaling with cancer cell self-renewal and epithelial-mesenchymal transition in basal-like breast cancer. Cancer Res *69*, 5364-5373.
Dingli, D., Traulsen, A., and Pacheco, J.M. (2007). Stochastic dynamics of hematopoietic tumor stem cells. Cell Cycle *6*, 461-466.
Dokmanovic, M., Clarke, C., and Marks, P.A. (2007). Histone deacetylase inhibitors: overview and perspectives. Mol Cancer Res *5*, 981-989.
Dontu, G., Abdallah, W.M., Foley, J.M., Jackson, K.W., Clarke, M.F., Kawamura, M.J., and Wicha, M.S. (2003). In vitro propagation and transcriptional profiling of human mammary stem/progenitor cells. Genes & development *17*, 1253-1270.
Dontu, G., and Wicha, M.S. (2005). Survival of mammary stem cells in suspension culture: implications for stem cell biology and neoplasia. J Mammary Gland Biol Neoplasia *10*, 75-86.
Dou, J., and Gu, N. (2010). Emerging strategies for the identification and targeting of cancer stem cells. Tumour Biol *31*, 243-253.
Dubois, L., Douma, K., Supuran, C.T., Chiu, R.K., van Zandvoort, M.A., Pastorekova, S., Scozzafava, A., Wouters, B.G., and Lambin, P. (2007). Imaging the hypoxia surrogate marker CA IX requires expression and catalytic activity for binding fluorescent sulfonamide inhibitors. Radiotherapy and oncology : journal of the European Society for Therapeutic Radiology and Oncology *83*, 367-373.
Dubois, L., Peeters, S., Lieuwes, N.G., Geusens, N., Thiry, A., Wigfield, S., Carta, F., McIntyre, A., Scozzafava, A., Dogne, J.M.*, et al.* (2011). Specific inhibition of carbonic anhydrase IX activity enhances the in vivo therapeutic effect of tumor irradiation. Radiotherapy and oncology : journal of the European Society for Therapeutic Radiology and Oncology *99*, 424-431.

Dunlop, E.A., Hunt, D.K., Acosta-Jaquez, H.A., Fingar, D.C., and Tee, A.R. (2011). ULK1 inhibits mTORC1 signaling, promotes multisite Raptor phosphorylation and hinders substrate binding. Autophagy *7*, 737-747.
Duy, C., Hurtz, C., Shojaee, S., Cerchietti, L., Geng, H., Swaminathan, S., Klemm, L., Kweon, S.M., Nahar, R., Braig, M.*, et al.* (2011). BCL6 enables Ph+ acute lymphoblastic leukaemia cells to survive BCR-ABL1 kinase inhibition. Nature *473*, 384-388.
Dylla, S.J., Beviglia, L., Park, I.K., Chartier, C., Raval, J., Ngan, L., Pickell, K., Aguilar, J., Lazetic, S., Smith-Berdan, S.*, et al.* (2008). Colorectal cancer stem cells are enriched in xenogeneic tumors following chemotherapy. PLoS One *3*, e2428.
Egeblad, M., Nakasone, E.S., and Werb, Z. (2010a). Tumors as organs: complex tissues that interface with the entire organism. Dev Cell *18*, 884-901.
Egeblad, M., Rasch, M.G., and Weaver, V.M. (2010b). Dynamic interplay between the collagen scaffold and tumor evolution. Current opinion in cell biology *22*, 697-706.
Elgert, K.D., Alleva, D.G., and Mullins, D.W. (1998). Tumor-induced immune dysfunction: the macrophage connection. J Leukoc Biol *64*, 275-290.
Engelmann, K., Shen, H., and Finn, O.J. (2008). MCF7 side population cells with characteristics of cancer stem/progenitor cells express the tumor antigen MUC1. Cancer Res *68*, 2419-2426.
Engler, A.J., Sen, S., Sweeney, H.L., and Discher, D.E. (2006). Matrix elasticity directs stem cell lineage specification. Cell *126*, 677-689.
Erler, J.T., Bennewith, K.L., Cox, T.R., Lang, G., Bird, D., Koong, A., Le, Q.T., and Giaccia, A.J. (2009). Hypoxia-induced lysyl oxidase is a critical mediator of bone marrow cell recruitment to form the premetastatic niche. Cancer cell *15*, 35-44.
Erler, J.T., Bennewith, K.L., Nicolau, M., Dornhofer, N., Kong, C., Le, Q.T., Chi, J.T., Jeffrey, S.S., and Giaccia, A.J. (2006). Lysyl oxidase is essential for hypoxia-induced metastasis. Nature *440*, 1222-1226.
Ertel, A., Tsirigos, A., Whitaker-Menezes, D., Birbe, R.C., Pavlides, S., Martinez-Outschoorn, U.E., Pestell, R.G., Howell, A., Sotgia, F., and Lisanti, M.P. (2012). Is cancer a metabolic rebellion against host aging? In the quest for immortality, tumor cells try to save themselves by boosting mitochondrial metabolism. Cell Cycle *11*, 253-263.
Esteller, M. (2008). Epigenetics in cancer. N Engl J Med *358*, 1148-1159.
Esteller, M., Toyota, M., Sanchez-Cespedes, M., Capella, G., Peinado, M.A., Watkins, D.N., Issa, J.P., Sidransky, D., Baylin, S.B., and Herman, J.G. (2000). Inactivation of the DNA repair gene O6-methylguanine-DNA methyltransferase by promoter hypermethylation is associated with G to A mutations in K-ras in colorectal tumorigenesis. Cancer Res *60*, 2368-2371.
Fath, D.M., Kong, X., Liang, D., Lin, Z., Chou, A., Jiang, Y., Fang, J., Caro, J., and Sang, N. (2006). Histone deacetylase inhibitors repress the transactivation potential of hypoxia-inducible factors independently of direct acetylation of HIF-alpha. The Journal of biological chemistry *281*, 13612-13619.
Favaro, E., Lord, S., Harris, A.L., and Buffa, F.M. (2011). Gene expression and hypoxia in breast cancer. Genome medicine *3*, 55.
Feinberg, A.P. (2004). The epigenetics of cancer etiology. Semin Cancer Biol *14*, 427-432.

Feki, A., and Irminger-Finger, I. (2004). Mutational spectrum of p53 mutations in primary breast and ovarian tumors. Crit Rev Oncol Hematol *52*, 103-116.
Feldmann, G., Dhara, S., Fendrich, V., Bedja, D., Beaty, R., Mullendore, M., Karikari, C., Alvarez, H., Iacobuzio-Donahue, C., Jimeno, A.*, et al.* (2007). Blockade of hedgehog signaling inhibits pancreatic cancer invasion and metastases: a new paradigm for combination therapy in solid cancers. Cancer Res *67*, 2187-2196.
Ferlay, J., Shin, H.R., Bray, F., Forman, D., Mathers, C., and Parkin, D.M. (2010). Estimates of worldwide burden of cancer in 2008: GLOBOCAN 2008. International journal of cancer. Journal international du cancer *127*, 2893-2917.
Fiaschi, M., Rozell, B., Bergstrom, A., and Toftgard, R. (2009). Development of mammary tumors by conditional expression of GLI1. Cancer Res *69*, 4810-4817.
Fidler, I.J. (2003). The pathogenesis of cancer metastasis: the 'seed and soil' hypothesis revisited. Nature reviews. Cancer *3*, 453-458.
Fillmore, C.M., Gupta, P.B., Rudnick, J.A., Caballero, S., Keller, P.J., Lander, E.S., and Kuperwasser, C. (2010). Estrogen expands breast cancer stem-like cells through paracrine FGF/Tbx3 signaling. Proc Natl Acad Sci U S A *107*, 21737-21742.
Forsythe, J.A., Jiang, B.H., Iyer, N.V., Agani, F., Leung, S.W., Koos, R.D., and Semenza, G.L. (1996). Activation of vascular endothelial growth factor gene transcription by hypoxia-inducible factor 1. Molecular and cellular biology *16*, 4604-4613.
Frantz, C., Stewart, K.M., and Weaver, V.M. (2010). The extracellular matrix at a glance. Journal of cell science *123*, 4195-4200.
Frisch, S.M., and Ruoslahti, E. (1997). Integrins and anoikis. Current opinion in cell biology *9*, 701-706.
Frye, M., Gardner, C., Li, E.R., Arnold, I., and Watt, F.M. (2003). Evidence that Myc activation depletes the epidermal stem cell compartment by modulating adhesive interactions with the local microenvironment. Development *130*, 2793-2808.
Fu, X., Fu, N., Guo, S., Yan, Z., Xu, Y., Hu, H., Menzel, C., Chen, W., Li, Y., Zeng, R.*, et al.* (2009). Estimating accuracy of RNA-Seq and microarrays with proteomics. BMC Genomics *10*, 161.
Fujiwara, S., Kawano, Y., Yuki, H., Okuno, Y., Nosaka, K., Mitsuya, H., and Hata, H. (2013). PDK1 inhibition is a novel therapeutic target in multiple myeloma. Br J Cancer *108*, 170-178.
Galdieri, L., and Vancura, A. (2012). Acetyl-CoA carboxylase regulates global histone acetylation. The Journal of biological chemistry *287*, 23865-23876.
Gammoh, N., Lam, D., Puente, C., Ganley, I., Marks, P.A., and Jiang, X. (2012). Role of autophagy in histone deacetylase inhibitor-induced apoptotic and nonapoptotic cell death. Proc Natl Acad Sci U S A *109*, 6561-6565.
Garber, K. (2010). Oncology's energetic pipeline. Nat Biotechnol *28*, 888-891.
Gerlinger, M., Rowan, A.J., Horswell, S., Larkin, J., Endesfelder, D., Gronroos, E., Martinez, P., Matthews, N., Stewart, A., Tarpey, P.*, et al.* (2012). Intratumor heterogeneity and branched evolution revealed by multiregion sequencing. N Engl J Med *366*, 883-892.
Geyer, F.C., Lacroix-Triki, M., Savage, K., Arnedos, M., Lambros, M.B., MacKay, A., Natrajan, R., and Reis-Filho, J.S. (2011). beta-Catenin pathway activation in breast cancer is associated with triple-negative phenotype but not with CTNNB1 mutation. Mod Pathol *24*, 209-231.

Giatromanolaki, A., Koukourakis, M.I., Sivridis, E., Pastorek, J., Wykoff, C.C., Gatter, K.C., and Harris, A.L. (2001). Expression of hypoxia-inducible carbonic anhydrase-9 relates to angiogenic pathways and independently to poor outcome in non-small cell lung cancer. Cancer Res *61*, 7992-7998.
Gillies, R.J., Raghunand, N., Karczmar, G.S., and Bhujwalla, Z.M. (2002). MRI of the tumor microenvironment. J Magn Reson Imaging *16*, 430-450.
Ginestier, C., Hur, M.H., Charafe-Jauffret, E., Monville, F., Dutcher, J., Brown, M., Jacquemier, J., Viens, P., Kleer, C.G., Liu, S.*, et al.* (2007). ALDH1 is a marker of normal and malignant human mammary stem cells and a predictor of poor clinical outcome. Cell Stem Cell *1*, 555-567.
Ginestier, C., Liu, S., Diebel, M.E., Korkaya, H., Luo, M., Brown, M., Wicinski, J., Cabaud, O., Charafe-Jauffret, E., Birnbaum, D.*, et al.* CXCR1 blockade selectively targets human breast cancer stem cells in vitro and in xenografts. J Clin Invest *120*, 485-497.
Ginestier, C., Liu, S., Diebel, M.E., Korkaya, H., Luo, M., Brown, M., Wicinski, J., Cabaud, O., Charafe-Jauffret, E., Birnbaum, D.*, et al.* (2010a). CXCR1 blockade selectively targets human breast cancer stem cells in vitro and in xenografts. J Clin Invest *120*, 485-497.
Ginestier, C., Liu, S., Diebel, M.E., Korkaya, H., Luo, M., Brown, M., Wicinski, J., Cabaud, O., Charafe-Jauffret, E., Birnbaum, D.*, et al.* (2010b). CXCR1 blockade selectively targets human breast cancer stem cells in vitro and in xenografts. J Clin Invest *120*, 485-497.
Glozak, M.A., and Seto, E. (2007). Histone deacetylases and cancer. Oncogene *26*, 5420-5432.
Goel, A., Nguyen, T.P., Leung, H.C., Nagasaka, T., Rhees, J., Hotchkiss, E., Arnold, M., Banerji, P., Koi, M., Kwok, C.T.*, et al.* (2011). De novo constitutional MLH1 epimutations confer early-onset colorectal cancer in two new sporadic Lynch syndrome cases, with derivation of the epimutation on the paternal allele in one. International journal of cancer. Journal international du cancer *128*, 869-878.
Grabmaier, K., de Weijert, M., Uemura, H., Schalken, J., and Oosterwijk, E. (2002). Renal cell carcinoma-associated G250 methylation and expression: in vivo and in vitro studies. Urology *60*, 357-362.
Greaves, M., and Maley, C.C. (2012). Clonal evolution in cancer. Nature *481*, 306-313.
Greer, S.N., Metcalf, J.L., Wang, Y., and Ohh, M. (2012). The updated biology of hypoxia-inducible factor. EMBO J *31*, 2448-2460.
Guedj, M., Marisa, L., de Reynies, A., Orsetti, B., Schiappa, R., Bibeau, F., MacGrogan, G., Lerebours, F., Finetti, P., Longy, M.*, et al.* (2012). A refined molecular taxonomy of breast cancer. Oncogene *31*, 1196-1206.
Gulhati, P., Bowen, K.A., Liu, J., Stevens, P.D., Rychahou, P.G., Chen, M., Lee, E.Y., Weiss, H.L., O'Connor, K.L., Gao, T.*, et al.* (2011). mTORC1 and mTORC2 regulate EMT, motility, and metastasis of colorectal cancer via RhoA and Rac1 signaling pathways. Cancer Res *71*, 3246-3256.
Guo, J.Y., Chen, H.Y., Mathew, R., Fan, J., Strohecker, A.M., Karsli-Uzunbas, G., Kamphorst, J.J., Chen, G., Lemons, J.M., Karantza, V.*, et al.* (2011a). Activated Ras requires autophagy to maintain oxidative metabolism and tumorigenesis. Genes & development *25*, 460-470.

Guo, W., Schubbert, S., Chen, J.Y., Valamehr, B., Mosessian, S., Shi, H., Dang, N.H., Garcia, C., Theodoro, M.F., Varella-Garcia, M., *et al.* (2011b). Suppression of leukemia development caused by PTEN loss. Proc Natl Acad Sci U S A *108*, 1409-1414.
Gwinn, D.M., Shackelford, D.B., Egan, D.F., Mihaylova, M.M., Mery, A., Vasquez, D.S., Turk, B.E., and Shaw, R.J. (2008). AMPK phosphorylation of raptor mediates a metabolic checkpoint. Mol Cell *30*, 214-226.
Hall, A.P. (2006). Review of the pericyte during angiogenesis and its role in cancer and diabetic retinopathy. Toxicol Pathol *34*, 763-775.
Han, J.M., Jeong, S.J., Park, M.C., Kim, G., Kwon, N.H., Kim, H.K., Ha, S.H., Ryu, S.H., and Kim, S. (2012a). Leucyl-tRNA synthetase is an intracellular leucine sensor for the mTORC1-signaling pathway. Cell *149*, 410-424.
Han, M., Wang, Y., Liu, M., Bi, X., Bao, J., Zeng, N., Zhu, Z., Mo, Z., Wu, C., and Chen, X. (2012b). MiR-21 regulates epithelial-mesenchymal transition phenotype and hypoxia-inducible factor-1alpha expression in third-sphere forming breast cancer stem cell-like cells. Cancer Sci *103*, 1058-1064.
Hao, N.B., Lu, M.H., Fan, Y.H., Cao, Y.L., Zhang, Z.R., and Yang, S.M. (2012). Macrophages in tumor microenvironments and the progression of tumors. Clin Dev Immunol *2012*, 948098.
Hara, K., Yonezawa, K., Weng, Q.P., Kozlowski, M.T., Belham, C., and Avruch, J. (1998). Amino acid sufficiency and mTOR regulate p70 S6 kinase and eIF-4E BP1 through a common effector mechanism. The Journal of biological chemistry *273*, 14484-14494.
Haraguchi, N., Ohkuma, M., Sakashita, H., Matsuzaki, S., Tanaka, F., Mimori, K., Kamohara, Y., Inoue, H., and Mori, M. (2008). CD133+CD44+ population efficiently enriches colon cancer initiating cells. Ann Surg Oncol *15*, 2927-2933.
Harris, A.L. (2002). Hypoxia--a key regulatory factor in tumour growth. Nature reviews. Cancer *2*, 38-47.
Harrison, H., Farnie, G., Howell, S.J., Rock, R.E., Stylianou, S., Brennan, K.R., Bundred, N.J., and Clarke, R.B. (2010). Regulation of breast cancer stem cell activity by signaling through the Notch4 receptor. Cancer Res *70*, 709-718.
Hashemolhosseini, S., Nagamine, Y., Morley, S.J., Desrivieres, S., Mercep, L., and Ferrari, S. (1998). Rapamycin inhibition of the G1 to S transition is mediated by effects on cyclin D1 mRNA and protein stability. The Journal of biological chemistry *273*, 14424-14429.
Hassane, D.C., Sen, S., Minhajuddin, M., Rossi, R.M., Corbett, C.A., Balys, M., Wei, L., Crooks, P.A., Guzman, M.L., and Jordan, C.T. (2010). Chemical genomic screening reveals synergism between parthenolide and inhibitors of the PI-3 kinase and mTOR pathways. Blood *116*, 5983-5990.
He, T.C., Sparks, A.B., Rago, C., Hermeking, H., Zawel, L., da Costa, L.T., Morin, P.J., Vogelstein, B., and Kinzler, K.W. (1998). Identification of c-MYC as a target of the APC pathway. Science *281*, 1509-1512.
Heddleston, J.M., Li, Z., Lathia, J.D., Bao, S., Hjelmeland, A.B., and Rich, J.N. Hypoxia inducible factors in cancer stem cells. Br J Cancer *102*, 789-795.
Heddleston, J.M., Li, Z., Lathia, J.D., Bao, S., Hjelmeland, A.B., and Rich, J.N. (2010a). Hypoxia inducible factors in cancer stem cells. Br J Cancer *102*, 789-795.
Heddleston, J.M., Li, Z., Lathia, J.D., Bao, S., Hjelmeland, A.B., and Rich, J.N. (2010b). Hypoxia inducible factors in cancer stem cells. Br J Cancer *102*, 789-795.

Heddleston, J.M., Li, Z., McLendon, R.E., Hjelmeland, A.B., and Rich, J.N. (2009). The hypoxic microenvironment maintains glioblastoma stem cells and promotes reprogramming towards a cancer stem cell phenotype. Cell Cycle *8*, 3274-3284.
Heinrich, E.L., Walser, T.C., Krysan, K., Liclican, E.L., Grant, J.L., Rodriguez, N.L., and Dubinett, S.M. (2012). The inflammatory tumor microenvironment, epithelial mesenchymal transition and lung carcinogenesis. Cancer Microenviron *5*, 5-18.
Hidalgo, M., and Rowinsky, E.K. (2000). The rapamycin-sensitive signal transduction pathway as a target for cancer therapy. Oncogene *19*, 6680-6686.
Hill, R.P. (2006). Identifying cancer stem cells in solid tumors: case not proven. Cancer Res *66*, 1891-1895; discussion 1890.
Hilvo, M., Baranauskiene, L., Salzano, A.M., Scaloni, A., Matulis, D., Innocenti, A., Scozzafava, A., Monti, S.M., Di Fiore, A., De Simone, G.*, et al.* (2008). Biochemical characterization of CA IX, one of the most active carbonic anhydrase isozymes. The Journal of biological chemistry *283*, 27799-27809.
Hilvo, M., Rafajova, M., Pastorekova, S., Pastorek, J., and Parkkila, S. (2004). Expression of carbonic anhydrase IX in mouse tissues. J Histochem Cytochem *52*, 1313-1322.
Hiratsuka, S., Nakamura, K., Iwai, S., Murakami, M., Itoh, T., Kijima, H., Shipley, J.M., Senior, R.M., and Shibuya, M. (2002). MMP9 induction by vascular endothelial growth factor receptor-1 is involved in lung-specific metastasis. Cancer cell *2*, 289-300.
Hochedlinger, K., and Plath, K. (2009). Epigenetic reprogramming and induced pluripotency. Development *136*, 509-523.
Hoffmeyer, K., Raggioli, A., Rudloff, S., Anton, R., Hierholzer, A., Del Valle, I., Hein, K., Vogt, R., and Kemler, R. (2012). Wnt/beta-catenin signaling regulates telomerase in stem cells and cancer cells. Science *336*, 1549-1554.
Holmgren, L., O'Reilly, M.S., and Folkman, J. (1995). Dormancy of micrometastases: balanced proliferation and apoptosis in the presence of angiogenesis suppression. Nat Med *1*, 149-153.
Hou, Y., Song, L., Zhu, P., Zhang, B., Tao, Y., Xu, X., Li, F., Wu, K., Liang, J., Shao, D.*, et al.* (2012). Single-cell exome sequencing and monoclonal evolution of a JAK2-negative myeloproliferative neoplasm. Cell *148*, 873-885.
Hu, Y., and Fu, L. (2012). Targeting cancer stem cells: a new therapy to cure cancer patients. Am J Cancer Res *2*, 340-356.
Hussain, S.A., Ganesan, R., Reynolds, G., Gross, L., Stevens, A., Pastorek, J., Murray, P.G., Perunovic, B., Anwar, M.S., Billingham, L.*, et al.* (2007). Hypoxia-regulated carbonic anhydrase IX expression is associated with poor survival in patients with invasive breast cancer. Br J Cancer *96*, 104-109.
Iakovlev, V.V., Pintilie, M., Morrison, A., Fyles, A.W., Hill, R.P., and Hedley, D.W. (2007). Effect of distributional heterogeneity on the analysis of tumor hypoxia based on carbonic anhydrase IX. Lab Invest *87*, 1206-1217.
Ichim, C.V., and Wells, R.A. (2006). First among equals: the cancer cell hierarchy. Leuk Lymphoma *47*, 2017-2027.
Ihnatko, R., Kubes, M., Takacova, M., Sedlakova, O., Sedlak, J., Pastorek, J., Kopacek, J., and Pastorekova, S. (2006). Extracellular acidosis elevates carbonic anhydrase IX in human glioblastoma cells via transcriptional modulation that does not depend on hypoxia. Int J Oncol *29*, 1025-1033.

Ilie, M., Mazure, N.M., Hofman, V., Ammadi, R.E., Ortholan, C., Bonnetaud, C., Havet, K., Venissac, N., Mograbi, B., Mouroux, J.*, et al.* (2010). High levels of carbonic anhydrase IX in tumour tissue and plasma are biomarkers of poor prognostic in patients with non-small cell lung cancer. Br J Cancer *102*, 1627-1635.
Iliopoulos, D., Hirsch, H.A., and Struhl, K. (2009). An epigenetic switch involving NF-kappaB, Lin28, Let-7 MicroRNA, and IL6 links inflammation to cell transformation. Cell *139*, 693-706.
Innocenti, A., Pastorekova, S., Pastorek, J., Scozzafava, A., De Simone, G., and Supuran, C.T. (2009). The proteoglycan region of the tumor-associated carbonic anhydrase isoform IX acts as anintrinsic buffer optimizing CO2 hydration at acidic pH values characteristic of solid tumors. Bioorg Med Chem Lett *19*, 5825-5828.
Inoki, K., Ouyang, H., Zhu, T., Lindvall, C., Wang, Y., Zhang, X., Yang, Q., Bennett, C., Harada, Y., Stankunas, K.*, et al.* (2006). TSC2 integrates Wnt and energy signals via a coordinated phosphorylation by AMPK and GSK3 to regulate cell growth. Cell *126*, 955-968.
Inoki, K., Zhu, T., and Guan, K.L. (2003). TSC2 mediates cellular energy response to control cell growth and survival. Cell *115*, 577-590.
Iseri, O.D., Kars, M.D., Arpaci, F., and Gunduz, U. (2010). Gene expression analysis of drug-resistant MCF-7 cells: implications for relation to extracellular matrix proteins. Cancer chemotherapy and pharmacology *65*, 447-455.
Ivascu, A., and Kubbies, M. (2007). Diversity of cell-mediated adhesions in breast cancer spheroids. Int J Oncol *31*, 1403-1413.
Jarvelainen, H., Sainio, A., Koulu, M., Wight, T.N., and Penttinen, R. (2009). Extracellular matrix molecules: potential targets in pharmacotherapy. Pharmacol Rev *61*, 198-223.
Jen, Y.F., Lee, W.M., Lin, C.C., Cheng, Y.H., Wang, J.H., Kuo, T.F., and Chang, M.H. (2008). The expression of carbonic anhydrase in canine mammary gland and mammary gland tumor. The Journal of veterinary medical science / the Japanese Society of Veterinary Science *70*, 437-441.
Jeter, C.R., Liu, B., Liu, X., Chen, X., Liu, C., Calhoun-Davis, T., Repass, J., Zaehres, H., Shen, J.J., and Tang, D.G. (2011). NANOG promotes cancer stem cell characteristics and prostate cancer resistance to androgen deprivation. Oncogene *30*, 3833-3845.
Jiang, B.H., and Liu, L.Z. (2008). PI3K/PTEN signaling in tumorigenesis and angiogenesis. Biochim Biophys Acta *1784*, 150-158.
Jiang, B.H., Rue, E., Wang, G.L., Roe, R., and Semenza, G.L. (1996). Dimerization, DNA binding, and transactivation properties of hypoxia-inducible factor 1. The Journal of biological chemistry *271*, 17771-17778.
Johnson, A.B., Denko, N., and Barton, M.C. (2008). Hypoxia induces a novel signature of chromatin modifications and global repression of transcription. Mutat Res *640*, 174-179.
Jonathan, R.A., Wijffels, K.I., Peeters, W., de Wilde, P.C., Marres, H.A., Merkx, M.A., Oosterwijk, E., van der Kogel, A.J., and Kaanders, J.H. (2006). The prognostic value of endogenous hypoxia-related markers for head and neck squamous cell carcinomas treated with ARCON. Radiother Oncol *79*, 288-297.
Jones, P.A., and Baylin, S.B. (2007). The epigenomics of cancer. Cell *128*, 683-692.

Kaelin, W.G., Jr. (2004). The von Hippel-Lindau tumor suppressor gene and kidney cancer. Clinical cancer research : an official journal of the American Association for Cancer Research *10*, 6290S-6295S.
Kallio, H., Pastorekova, S., Pastorek, J., Waheed, A., Sly, W.S., Mannisto, S., Heikinheimo, M., and Parkkila, S. (2006). Expression of carbonic anhydrases IX and XII during mouse embryonic development. BMC Dev Biol *6*, 22.
Kaluz, S., Kaluzova, M., Chrastina, A., Olive, P.L., Pastorekova, S., Pastorek, J., Lerman, M.I., and Stanbridge, E.J. (2002). Lowered oxygen tension induces expression of the hypoxia marker MN/carbonic anhydrase IX in the absence of hypoxia-inducible factor 1 alpha stabilization: a role for phosphatidylinositol 3'-kinase. Cancer Res *62*, 4469-4477.
Kaluz, S., Kaluzova, M., Liao, S.Y., Lerman, M., and Stanbridge, E.J. (2009a). Transcriptional control of the tumor- and hypoxia-marker carbonic anhydrase 9: A one transcription factor (HIF-1) show? Biochim Biophys Acta *1795*, 162-172.
Kaluz, S., Kaluzova, M., Liao, S.Y., Lerman, M., and Stanbridge, E.J. (2009b). Transcriptional control of the tumor- and hypoxia-marker carbonic anhydrase 9: A one transcription factor (HIF-1) show? Biochim Biophys Acta *1795*, 162-172.
Kaluz, S., Kaluzova, M., Opavsky, R., Pastorekova, S., Gibadulinova, A., Dequiedt, F., Kettmann, R., and Pastorek, J. (1999). Transcriptional regulation of the MN/CA 9 gene coding for the tumor-associated carbonic anhydrase IX. Identification and characterization of a proximal silencer element. The Journal of biological chemistry *274*, 32588-32595.
Kaluz, S., Kaluzova, M., and Stanbridge, E.J. (2006). The role of extracellular signal-regulated protein kinase in transcriptional regulation of the hypoxia marker carbonic anhydrase IX. J Cell Biochem *97*, 207-216.
Kaluzova, M., Pastorekova, S., Svastova, E., Pastorek, J., Stanbridge, E.J., and Kaluz, S. (2001). Characterization of the MN/CA 9 promoter proximal region: a role for specificity protein (SP) and activator protein 1 (AP1) factors. The Biochemical journal *359*, 669-677.
Kamangar, F., Dores, G.M., and Anderson, W.F. (2006). Patterns of cancer incidence, mortality, and prevalence across five continents: defining priorities to reduce cancer disparities in different geographic regions of the world. Journal of clinical oncology : official journal of the American Society of Clinical Oncology *24*, 2137-2150.
Kamp, D.W., Shacter, E., and Weitzman, S.A. (2011). Chronic inflammation and cancer: the role of the mitochondria. Oncology (Williston Park) *25*, 400-410, 413.
Karantzali, E., Schulz, H., Hummel, O., Hubner, N., Hatzopoulos, A., and Kretsovali, A. (2008). Histone deacetylase inhibition accelerates the early events of stem cell differentiation: transcriptomic and epigenetic analysis. Genome Biol *9*, R65.
Kasper, M., Jaks, V., Fiaschi, M., and Toftgard, R. (2009). Hedgehog signalling in breast cancer. Carcinogenesis *30*, 903-911.
Katoh, M. (2007). WNT signaling pathway and stem cell signaling network. Clin Cancer Res *13*, 4042-4045.
Kennedy, K.M., and Dewhirst, M.W. (2010). Tumor metabolism of lactate: the influence and therapeutic potential for MCT and CD147 regulation. Future Oncol *6*, 127-148.
Kim, J., Villadsen, R., Sorlie, T., Fogh, L., Gronlund, S.Z., Fridriksdottir, A.J., Kuhn, I., Rank, F., Wielenga, V.T., Solvang, H.*, et al.* (2012). Tumor initiating but

differentiated luminal-like breast cancer cells are highly invasive in the absence of basal-like activity. Proc Natl Acad Sci U S A *109*, 6124-6129.
Kim, J.B., and Spiegelman, B.M. (1996). ADD1/SREBP1 promotes adipocyte differentiation and gene expression linked to fatty acid metabolism. Genes & development *10*, 1096-1107.
Kim, J.B., Wright, H.M., Wright, M., and Spiegelman, B.M. (1998). ADD1/SREBP1 activates PPARgamma through the production of endogenous ligand. Proc Natl Acad Sci U S A *95*, 4333-4337.
Kim, J.W., and Dang, C.V. (2006). Cancer's molecular sweet tooth and the Warburg effect. Cancer Res *66*, 8927-8930.
Kim, S.H., Kim, K.W., and Jeong, J.W. (2007). Inhibition of hypoxia-induced angiogenesis by sodium butyrate, a histone deacetylase inhibitor, through hypoxia-inducible factor-1alpha suppression. Oncology reports *17*, 793-797.
Kivela, A., Parkkila, S., Saarnio, J., Karttunen, T.J., Kivela, J., Parkkila, A.K., Waheed, A., Sly, W.S., Grubb, J.H., Shah, G.*, et al.* (2000). Expression of a novel transmembrane carbonic anhydrase isozyme XII in normal human gut and colorectal tumors. Am J Pathol *156*, 577-584.
Klatte, T., Seligson, D.B., Rao, J.Y., Yu, H., de Martino, M., Kawaoka, K., Wong, S.G., Belldegrun, A.S., and Pantuck, A.J. (2009). Carbonic anhydrase IX in bladder cancer: a diagnostic, prognostic, and therapeutic molecular marker. Cancer *115*, 1448-1458.
Klezovitch, O., Fernandez, T.E., Tapscott, S.J., and Vasioukhin, V. (2004). Loss of cell polarity causes severe brain dysplasia in Lgl1 knockout mice. Genes & development *18*, 559-571.
Kockar, F., Yildrim, H., Sagkan, R.I., Hagemann, C., Soysal, Y., Anacker, J., Hamza, A.A., Vordermark, D., Flentje, M., and Said, H.M. (2012). Hypoxia and cytokines regulate carbonic anhydrase 9 expression in hepatocellular carcinoma cells in vitro. World J Clin Oncol *3*, 82-91.
Kopacek, J., Barathova, M., Dequiedt, F., Sepelakova, J., Kettmann, R., Pastorek, J., and Pastorekova, S. (2005). MAPK pathway contributes to density- and hypoxia-induced expression of the tumor-associated carbonic anhydrase IX. Biochim Biophys Acta *1729*, 41-49.
Korkaya, H., Liu, S., and Wicha, M.S. Breast cancer stem cells, cytokine networks, and the tumor microenvironment. J Clin Invest *121*, 3804-3809.
Korkaya, H., Liu, S., and Wicha, M.S. (2011a). Breast cancer stem cells, cytokine networks, and the tumor microenvironment. J Clin Invest *121*, 3804-3809.
Korkaya, H., Liu, S., and Wicha, M.S. (2011b). Breast cancer stem cells, cytokine networks, and the tumor microenvironment. J Clin Invest *121*, 3804-3809.
Korkaya, H., Paulson, A., Charafe-Jauffret, E., Ginestier, C., Brown, M., Dutcher, J., Clouthier, S.G., and Wicha, M.S. (2009). Regulation of mammary stem/progenitor cells by PTEN/Akt/beta-catenin signaling. PLoS biology *7*, e1000121.
Kovacina, K.S., Park, G.Y., Bae, S.S., Guzzetta, A.W., Schaefer, E., Birnbaum, M.J., and Roth, R.A. (2003). Identification of a proline-rich Akt substrate as a 14-3-3 binding partner. The Journal of biological chemistry *278*, 10189-10194.
Kretsovali, A., Hadjimichael, C., and Charmpilas, N. (2012). Histone deacetylase inhibitors in cell pluripotency, differentiation, and reprogramming. Stem Cells Int *2012*, 184154.

Kubli, D.A., and Gustafsson, A.B. (2012). Mitochondria and mitophagy: the yin and yang of cell death control. Circ Res *111*, 1208-1221.
Kuper, H., Adami, H.O., and Trichopoulos, D. (2000). Infections as a major preventable cause of human cancer. J Intern Med *248*, 171-183.
Kurdistani, S.K. (2007). Histone modifications as markers of cancer prognosis: a cellular view. Br J Cancer *97*, 1-5.
Lagger, G., O'Carroll, D., Rembold, M., Khier, H., Tischler, J., Weitzer, G., Schuettengruber, B., Hauser, C., Brunmeir, R., Jenuwein, T.*, et al.* (2002). Essential function of histone deacetylase 1 in proliferation control and CDK inhibitor repression. EMBO J *21*, 2672-2681.
Lambert, J.D., and Nagy, L.M. (2002). Asymmetric inheritance of centrosomally localized mRNAs during embryonic cleavages. Nature *420*, 682-686.
Landes, T., Emorine, L.J., Courilleau, D., Rojo, M., Belenguer, P., and Arnaune-Pelloquin, L. (2010). The BH3-only Bnip3 binds to the dynamin Opa1 to promote mitochondrial fragmentation and apoptosis by distinct mechanisms. EMBO Rep *11*, 459-465.
Langmead, B., Trapnell, C., Pop, M., and Salzberg, S.L. (2009). Ultrafast and memory-efficient alignment of short DNA sequences to the human genome. Genome Biol *10*, R25.
Lapidot, T., Sirard, C., Vormoor, J., Murdoch, B., Hoang, T., Caceres-Cortes, J., Minden, M., Paterson, B., Caligiuri, M.A., and Dick, J.E. (1994). A cell initiating human acute myeloid leukaemia after transplantation into SCID mice. Nature *367*, 645-648.
Laplante, M., and Sabatini, D.M. (2009). mTOR signaling at a glance. Journal of cell science *122*, 3589-3594.
Laplante, M., and Sabatini, D.M. (2012). mTOR signaling in growth control and disease. Cell *149*, 274-293.
Laughner, E., Taghavi, P., Chiles, K., Mahon, P.C., and Semenza, G.L. (2001). HER2 (neu) signaling increases the rate of hypoxia-inducible factor 1alpha (HIF-1alpha) synthesis: novel mechanism for HIF-1-mediated vascular endothelial growth factor expression. Molecular and cellular biology *21*, 3995-4004.
Le, Q.T., Harris, J., Magliocco, A.M., Kong, C.S., Diaz, R., Shin, B., Cao, H., Trotti, A., Erler, J.T., Chung, C.H.*, et al.* (2009). Validation of lysyl oxidase as a prognostic marker for metastasis and survival in head and neck squamous cell carcinoma: Radiation Therapy Oncology Group trial 90-03. Journal of clinical oncology : official journal of the American Society of Clinical Oncology *27*, 4281-4286.
Lee, H.H., Tsan, Y.T., Ho, W.C., Lin, M.H., Lee, C.H., Tseng, C.D., Guo, Y.L., Wang, J.D., and Chen, P.C. (2012). Angiotensin-converting enzyme inhibitors enhance the effect of cyclooxygenase inhibitors on breast cancer: a nationwide case-control study. J Hypertens *30*, 2432-2439.
Lee, J.W., and Juliano, R. (2004). Mitogenic signal transduction by integrin- and growth factor receptor-mediated pathways. Molecules and cells *17*, 188-202.
Lee, S., Shin, H.J., Han, I.O., Hong, E.K., Park, S.Y., Roh, J.W., Shin, K.H., Kim, T.H., and Kim, J.Y. (2007). Tumor carbonic anhydrase 9 expression is associated with the presence of lymph node metastases in uterine cervical cancer. Cancer Sci *98*, 329-333.

Leek, R.D., Lewis, C.E., Whitehouse, R., Greenall, M., Clarke, J., and Harris, A.L. (1996). Association of macrophage infiltration with angiogenesis and prognosis in invasive breast carcinoma. Cancer Res *56*, 4625-4629.
Leis, O., Eguiara, A., Lopez-Arribillaga, E., Alberdi, M.J., Hernandez-Garcia, S., Elorriaga, K., Pandiella, A., Rezola, R., and Martin, A.G. Sox2 expression in breast tumours and activation in breast cancer stem cells. Oncogene *31*, 1354-1365.
Leppilampi, M., Karttunen, T.J., Kivela, J., Gut, M.O., Pastorekova, S., Pastorek, J., and Parkkila, S. (2005). Gastric pit cell hyperplasia and glandular atrophy in carbonic anhydrase IX knockout mice: studies on two strains C57/BL6 and BALB/C. Transgenic Res *14*, 655-663.
Levental, K.R., Yu, H., Kass, L., Lakins, J.N., Egeblad, M., Erler, J.T., Fong, S.F., Csiszar, K., Giaccia, A., Weninger, W.*, et al.* (2009). Matrix crosslinking forces tumor progression by enhancing integrin signaling. Cell *139*, 891-906.
Li, H., Liu, H., and Heller, S. (2003a). Pluripotent stem cells from the adult mouse inner ear. Nat Med *9*, 1293-1299.
Li, H.S., Wang, D., Shen, Q., Schonemann, M.D., Gorski, J.A., Jones, K.R., Temple, S., Jan, L.Y., and Jan, Y.N. (2003b). Inactivation of Numb and Numblike in embryonic dorsal forebrain impairs neurogenesis and disrupts cortical morphogenesis. Neuron *40*, 1105-1118.
Li, L., and Xie, T. (2005). Stem cell niche: structure and function. Annu Rev Cell Dev Biol *21*, 605-631.
Li, T., Su, Y., Mei, Y., Leng, Q., Leng, B., Liu, Z., Stass, S.A., and Jiang, F. (2010). ALDH1A1 is a marker for malignant prostate stem cells and predictor of prostate cancer patients' outcome. Lab Invest *90*, 234-244.
Liao, S.Y., Aurelio, O.N., Jan, K., Zavada, J., and Stanbridge, E.J. (1997). Identification of the MN/CA9 protein as a reliable diagnostic biomarker of clear cell carcinoma of the kidney. Cancer Res *57*, 2827-2831.
Liao, S.Y., Brewer, C., Zavada, J., Pastorek, J., Pastorekova, S., Manetta, A., Berman, M.L., DiSaia, P.J., and Stanbridge, E.J. (1994). Identification of the MN antigen as a diagnostic biomarker of cervical intraepithelial squamous and glandular neoplasia and cervical carcinomas. Am J Pathol *145*, 598-609.
Liao, S.Y., Lerman, M.I., and Stanbridge, E.J. (2009). Expression of transmembrane carbonic anhydrases, CAIX and CAXII, in human development. BMC Dev Biol *9*, 22.
Lie, D.C., Colamarino, S.A., Song, H.J., Desire, L., Mira, H., Consiglio, A., Lein, E.S., Jessberger, S., Lansford, H., Dearie, A.R.*, et al.* (2005). Wnt signalling regulates adult hippocampal neurogenesis. Nature *437*, 1370-1375.
Lin, E.Y., Nguyen, A.V., Russell, R.G., and Pollard, J.W. (2001). Colony-stimulating factor 1 promotes progression of mammary tumors to malignancy. J Exp Med *193*, 727-740.
Ling, L., Nurcombe, V., and Cool, S.M. (2009). Wnt signaling controls the fate of mesenchymal stem cells. Gene *433*, 1-7.
Liotta, L.A., and Rao, C.N. (1985). Role of the extracellular matrix in cancer. Ann N Y Acad Sci *460*, 333-344.
Liu, C.C., Prior, J., Piwnica-Worms, D., and Bu, G. (2010a). LRP6 overexpression defines a class of breast cancer subtype and is a target for therapy. Proc Natl Acad Sci U S A *107*, 5136-5141.

Liu, F., Jenssen, T.K., Trimarchi, J., Punzo, C., Cepko, C.L., Ohno-Machado, L., Hovig, E., and Kuo, W.P. (2007). Comparison of hybridization-based and sequencing-based gene expression technologies on biological replicates. BMC Genomics *8*, 153.
Liu, S., Dontu, G., Mantle, I.D., Patel, S., Ahn, N.S., Jackson, K.W., Suri, P., and Wicha, M.S. (2006). Hedgehog signaling and Bmi-1 regulate self-renewal of normal and malignant human mammary stem cells. Cancer Res *66*, 6063-6071.
Liu, S., Ginestier, C., Charafe-Jauffret, E., Foco, H., Kleer, C.G., Merajver, S.D., Dontu, G., and Wicha, M.S. (2008). BRCA1 regulates human mammary stem/progenitor cell fate. Proc Natl Acad Sci U S A *105*, 1680-1685.
Liu, S., Ginestier, C., Ou, S.J., Clouthier, S.G., Patel, S.H., Monville, F., Korkaya, H., Heath, A., Dutcher, J., Kleer, C.G.*, et al.* (2011a). Breast cancer stem cells are regulated by mesenchymal stem cells through cytokine networks. Cancer Res *71*, 614-624.
Liu, S., Ginestier, C., Ou, S.J., Clouthier, S.G., Patel, S.H., Monville, F., Korkaya, H., Heath, A., Dutcher, J., Kleer, C.G.*, et al.* (2011b). Breast cancer stem cells are regulated by mesenchymal stem cells through cytokine networks. Cancer Res *71*, 614-624.
Liu, Y. (2006). Fatty acid oxidation is a dominant bioenergetic pathway in prostate cancer. Prostate Cancer Prostatic Dis *9*, 230-234.
Liu, Y., Zuckier, L.S., and Ghesani, N.V. (2010b). Dominant uptake of fatty acid over glucose by prostate cells: a potential new diagnostic and therapeutic approach. Anticancer Res *30*, 369-374.
Lock, F.E., McDonald, P.C., Lou, Y., Serrano, I., Chafe, S.C., Ostlund, C., Aparicio, S., Winum, J.Y., Supuran, C.T., and Dedhar, S. (2012). Targeting carbonic anhydrase IX depletes breast cancer stem cells within the hypoxic niche. Oncogene.
Lou, Y., McDonald, P.C., Oloumi, A., Chia, S., Ostlund, C., Ahmadi, A., Kyle, A., Auf dem Keller, U., Leung, S., Huntsman, D.*, et al.* (2011). Targeting tumor hypoxia: suppression of breast tumor growth and metastasis by novel carbonic anhydrase IX inhibitors. Cancer Res *71*, 3364-3376.
Louie, E., Nik, S., Chen, J.S., Schmidt, M., Song, B., Pacson, C., Chen, X.F., Park, S., Ju, J., and Chen, E.I. (2010). Identification of a stem-like cell population by exposing metastatic breast cancer cell lines to repetitive cycles of hypoxia and reoxygenation. Breast Cancer Res *12*, R94.
Lu, P., Weaver, V.M., and Werb, Z. (2012). The extracellular matrix: a dynamic niche in cancer progression. The Journal of cell biology *196*, 395-406.
Lv, K., Liu, L., Wang, L., Yu, J., Liu, X., Cheng, Y., Dong, M., Teng, R., Wu, L., Fu, P.*, et al.* (2012). Lin28 mediates paclitaxel resistance by modulating p21, Rb and Let-7a miRNA in breast cancer cells. PLoS One *7*, e40008.
Ma, Y., Liang, D., Liu, J., Axcrona, K., Kvalheim, G., Stokke, T., Nesland, J.M., and Suo, Z. (2011). Prostate cancer cell lines under hypoxia exhibit greater stem-like properties. PloS one *6*, e29170.
Magee, J.A., Ikenoue, T., Nakada, D., Lee, J.Y., Guan, K.L., and Morrison, S.J. (2012). Temporal changes in PTEN and mTORC2 regulation of hematopoietic stem cell self-renewal and leukemia suppression. Cell Stem Cell *11*, 415-428.
Magni, M., Shammah, S., Schiro, R., Mellado, W., Dalla-Favera, R., and Gianni, A.M. (1996). Induction of cyclophosphamide-resistance by aldehyde-dehydrogenase gene transfer. Blood *87*, 1097-1103.

Makino, Y., Cao, R., Svensson, K., Bertilsson, G., Asman, M., Tanaka, H., Cao, Y., Berkenstam, A., and Poellinger, L. (2001). Inhibitory PAS domain protein is a negative regulator of hypoxia-inducible gene expression. Nature *414*, 550-554.
Malladi, P., Xu, Y., Chiou, M., Giaccia, A.J., and Longaker, M.T. (2006). Effect of reduced oxygen tension on chondrogenesis and osteogenesis in adipose-derived mesenchymal cells. Am J Physiol Cell Physiol *290*, C1139-1146.
Malone, J.H., and Oliver, B. (2011). Microarrays, deep sequencing and the true measure of the transcriptome. BMC Biol *9*, 34.
Mani, S.A., Guo, W., Liao, M.J., Eaton, E.N., Ayyanan, A., Zhou, A.Y., Brooks, M., Reinhard, F., Zhang, C.C., Shipitsin, M.*, et al.* (2008). The epithelial-mesenchymal transition generates cells with properties of stem cells. Cell *133*, 704-715.
Mantovani, A., Sozzani, S., Locati, M., Allavena, P., and Sica, A. (2002). Macrophage polarization: tumor-associated macrophages as a paradigm for polarized M2 mononuclear phagocytes. Trends Immunol *23*, 549-555.
Marcato, P., Dean, C.A., Giacomantonio, C.A., and Lee, P.W. (2011a). Aldehyde dehydrogenase: its role as a cancer stem cell marker comes down to the specific isoform. Cell Cycle *10*, 1378-1384.
Marcato, P., Dean, C.A., Pan, D., Araslanova, R., Gillis, M., Joshi, M., Helyer, L., Pan, L., Leidal, A., Gujar, S.*, et al.* (2011b). Aldehyde dehydrogenase activity of breast cancer stem cells is primarily due to isoform ALDH1A3 and its expression is predictive of metastasis. Stem Cells *29*, 32-45.
Marioni, J.C., Mason, C.E., Mane, S.M., Stephens, M., and Gilad, Y. (2008). RNA-seq: an assessment of technical reproducibility and comparison with gene expression arrays. Genome Res *18*, 1509-1517.
Markowetz, F., Mulder, K.W., Airoldi, E.M., Lemischka, I.R., and Troyanskaya, O.G. (2010). Mapping dynamic histone acetylation patterns to gene expression in nanog-depleted murine embryonic stem cells. PLoS Comput Biol *6*, e1001034.
Martens, J.E., Smedts, F., van Muyden, R.C., Schoots, C., Helmerhorst, T.J., Hopman, A., Ramaekers, F.C., and Arends, J.W. (2007). Reserve cells in human uterine cervical epithelium are derived from mullerian epithelium at midgestational age. Int J Gynecol Pathol *26*, 463-468.
Martinez-Outschoorn, U.E., Pavlides, S., Howell, A., Pestell, R.G., Tanowitz, H.B., Sotgia, F., and Lisanti, M.P. (2011a). Stromal-epithelial metabolic coupling in cancer: integrating autophagy and metabolism in the tumor microenvironment. Int J Biochem Cell Biol *43*, 1045-1051.
Martinez-Outschoorn, U.E., Prisco, M., Ertel, A., Tsirigos, A., Lin, Z., Pavlides, S., Wang, C., Flomenberg, N., Knudsen, E.S., Howell, A.*, et al.* (2011b). Ketones and lactate increase cancer cell "stemness," driving recurrence, metastasis, and poor clinical outcome in breast cancer: Achieving personalized medicine via Metabolo-Genomics. Cell Cycle *10*.
Martinez-Outschoorn, U.E., Sotgia, F., and Lisanti, M.P. (2012). Power surge: supporting cells "fuel" cancer cell mitochondria. Cell metabolism *15*, 4-5.
Martinez-Zaguilan, R., Seftor, E.A., Seftor, R.E., Chu, Y.W., Gillies, R.J., and Hendrix, M.J. (1996). Acidic pH enhances the invasive behavior of human melanoma cells. Clin Exp Metastasis *14*, 176-186.
Marusyk, A., Almendro, V., and Polyak, K. (2012). Intra-tumour heterogeneity: a looking glass for cancer? Nature reviews. Cancer *12*, 323-334.

Marusyk, A., and DeGregori, J. (2008). Declining cellular fitness with age promotes cancer initiation by selecting for adaptive oncogenic mutations. Biochim Biophys Acta *1785*, 1-11.
Marusyk, A., and Polyak, K. (2010). Tumor heterogeneity: causes and consequences. Biochim Biophys Acta *1805*, 105-117.
Maschek, G., Savaraj, N., Priebe, W., Braunschweiger, P., Hamilton, K., Tidmarsh, G.F., De Young, L.R., and Lampidis, T.J. (2004). 2-deoxy-D-glucose increases the efficacy of adriamycin and paclitaxel in human osteosarcoma and non-small cell lung cancers in vivo. Cancer Res *64*, 31-34.
Mathieu, J., Zhang, Z., Zhou, W., Wang, A.J., Heddleston, J.M., Pinna, C.M., Hubaud, A., Stadler, B., Choi, M., Bar, M.*, et al.* (2011). HIF induces human embryonic stem cell markers in cancer cells. Cancer Res *71*, 4640-4652.
Maxwell, P.H., Pugh, C.W., and Ratcliffe, P.J. (2001). Activation of the HIF pathway in cancer. Current opinion in genetics & development *11*, 293-299.
Maxwell, P.H., Wiesener, M.S., Chang, G.W., Clifford, S.C., Vaux, E.C., Cockman, M.E., Wykoff, C.C., Pugh, C.W., Maher, E.R., and Ratcliffe, P.J. (1999). The tumour suppressor protein VHL targets hypoxia-inducible factors for oxygen-dependent proteolysis. Nature *399*, 271-275.
Mayer, A., Schneider, F., Vaupel, P., Sommer, C., and Schmidberger, H. (2012). Differential expression of HIF-1 in glioblastoma multiforme and anaplastic astrocytoma. Int J Oncol *41*, 1260-1270.
McBeath, R., Pirone, D.M., Nelson, C.M., Bhadriraju, K., and Chen, C.S. (2004). Cell shape, cytoskeletal tension, and RhoA regulate stem cell lineage commitment. Dev Cell *6*, 483-495.
McBrian, M.A., Behbahan, I.S., Ferrari, R., Su, T., Huang, T.W., Li, K., Hong, C.S., Christofk, H.R., Vogelauer, M., Seligson, D.B.*, et al.* (2013). Histone Acetylation Regulates Intracellular pH. Mol Cell *49*, 310-321.
McDonald, P.C., Winum, J.Y., Supuran, C.T., and Dedhar, S. (2012). Recent developments in targeting carbonic anhydrase IX for cancer therapeutics. Oncotarget *3*, 84-97.
McIntyre, A., Patiar, S., Wigfield, S., Li, J.L., Ledaki, I., Turley, H., Leek, R., Snell, C., Gatter, K., Sly, W.S.*, et al.* (2012). Carbonic anhydrase IX promotes tumor growth and necrosis in vivo and inhibition enhances anti-VEGF therapy. Clinical cancer research : an official journal of the American Association for Cancer Research *18*, 3100-3111.
Menendez, J.A., and Lupu, R. (2007). Fatty acid synthase and the lipogenic phenotype in cancer pathogenesis. Nature reviews. Cancer *7*, 763-777.
Merchant, A.A., and Matsui, W. (2010). Targeting Hedgehog--a cancer stem cell pathway. Clinical cancer research : an official journal of the American Association for Cancer Research *16*, 3130-3140.
Merlo, L.M., Pepper, J.W., Reid, B.J., and Maley, C.C. (2006). Cancer as an evolutionary and ecological process. Nature reviews. Cancer *6*, 924-935.
Michor, F., and Polyak, K. The origins and implications of intratumor heterogeneity. Cancer Prev Res (Phila) *3*, 1361-1364.
Michor, F., and Polyak, K. (2010). The origins and implications of intratumor heterogeneity. Cancer Prev Res (Phila) *3*, 1361-1364.

Mimeault, M., and Batra, S.K. (2006). Concise review: recent advances on the significance of stem cells in tissue regeneration and cancer therapies. Stem Cells *24*, 2319-2345.
Mimeault, M., and Batra, S.K. (2010). New advances on critical implications of tumor- and metastasis-initiating cells in cancer progression, treatment resistance and disease recurrence. Histol Histopathol *25*, 1057-1073.
Mimeault, M., and Batra, S.K. (2013). Hypoxia-inducing factors as master regulators of stemness properties and altered metabolism of cancer- and metastasis-initiating cells. J Cell Mol Med *17*, 30-54.
Mimeault, M., Hauke, R., Mehta, P.P., and Batra, S.K. (2007). Recent advances in cancer stem/progenitor cell research: therapeutic implications for overcoming resistance to the most aggressive cancers. J Cell Mol Med *11*, 981-1011.
Mimeault, M., Johansson, S.L., and Batra, S.K. (2012). Pathobiological implications of the expression of EGFR, pAkt, NF-kappaB and MIC-1 in prostate cancer stem cells and their progenies. PloS one *7*, e31919.
Miron, M., Lasko, P., and Sonenberg, N. (2003). Signaling from Akt to FRAP/TOR targets both 4E-BP and S6K in Drosophila melanogaster. Molecular and cellular biology *23*, 9117-9126.
Molofsky, A.V., Pardal, R., Iwashita, T., Park, I.K., Clarke, M.F., and Morrison, S.J. (2003). Bmi-1 dependence distinguishes neural stem cell self-renewal from progenitor proliferation. Nature *425*, 962-967.
Moody, S.E., Perez, D., Pan, T.C., Sarkisian, C.J., Portocarrero, C.P., Sterner, C.J., Notorfrancesco, K.L., Cardiff, R.D., and Chodosh, L.A. (2005). The transcriptional repressor Snail promotes mammary tumor recurrence. Cancer cell *8*, 197-209.
Moraes, R.C., Zhang, X., Harrington, N., Fung, J.Y., Wu, M.F., Hilsenbeck, S.G., Allred, D.C., and Lewis, M.T. (2007). Constitutive activation of smoothened (SMO) in mammary glands of transgenic mice leads to increased proliferation, altered differentiation and ductal dysplasia. Development *134*, 1231-1242.
Morgan, P.E., Pastorekova, S., Stuart-Tilley, A.K., Alper, S.L., and Casey, J.R. (2007). Interactions of transmembrane carbonic anhydrase, CAIX, with bicarbonate transporters. Am J Physiol Cell Physiol *293*, C738-748.
Morimoto, K., Kim, S.J., Tanei, T., Shimazu, K., Tanji, Y., Taguchi, T., Tamaki, Y., Terada, N., and Noguchi, S. (2009). Stem cell marker aldehyde dehydrogenase 1-positive breast cancers are characterized by negative estrogen receptor, positive human epidermal growth factor receptor type 2, and high Ki67 expression. Cancer Sci *100*, 1062-1068.
Morris, J.C., Chiche, J., Grellier, C., Lopez, M., Bornaghi, L.F., Maresca, A., Supuran, C.T., Pouyssegur, J., and Poulsen, S.A. (2011). Targeting hypoxic tumor cell viability with carbohydrate-based carbonic anhydrase IX and XII inhibitors. J Med Chem *54*, 6905-6918.
Mueller, S., Cadenas, E., and Schonthal, A.H. (2000). p21WAF1 regulates anchorage-independent growth of HCT116 colon carcinoma cells via E-cadherin expression. Cancer Res *60*, 156-163.
Nalwoga, H., Arnes, J.B., Wabinga, H., and Akslen, L.A. Expression of aldehyde dehydrogenase 1 (ALDH1) is associated with basal-like markers and features of aggressive tumours in African breast cancer. Br J Cancer *102*, 369-375.
Nalwoga, H., Arnes, J.B., Wabinga, H., and Akslen, L.A. (2010). Expression of aldehyde dehydrogenase 1 (ALDH1) is associated with basal-like markers and

features of aggressive tumours in African breast cancer. Br J Cancer *102*, 369-375.
Nathke, I. (2006). Cytoskeleton out of the cupboard: colon cancer and cytoskeletal changes induced by loss of APC. Nature reviews. Cancer *6*, 967-974.
Neri, D., and Supuran, C.T. (2011). Interfering with pH regulation in tumours as a therapeutic strategy. Nat Rev Drug Discov *10*, 767-777.
Nogales-Cadenas, R., Carmona-Saez, P., Vazquez, M., Vicente, C., Yang, X., Tirado, F., Carazo, J.M., and Pascual-Montano, A. (2009). GeneCodis: interpreting gene lists through enrichment analysis and integration of diverse biological information. Nucleic Acids Res *37*, W317-322.
Notta, F., Mullighan, C.G., Wang, J.C., Poeppl, A., Doulatov, S., Phillips, L.A., Ma, J., Minden, M.D., Downing, J.R., and Dick, J.E. (2011). Evolution of human BCR-ABL1 lymphoblastic leukaemia-initiating cells. Nature *469*, 362-367.
Nowell, P.C. (1976). The clonal evolution of tumor cell populations. Science *194*, 23-28.
O'Reilly, A.M., Lee, H.H., and Simon, M.A. (2008). Integrins control the positioning and proliferation of follicle stem cells in the Drosophila ovary. The Journal of cell biology *182*, 801-815.
Oliveira-Costa, J.P., Zanetti, J.S., Silveira, G.G., Soave, D.F., Oliveira, L.R., Zorgetto, V.A., Soares, F.A., Zucoloto, S., and Ribeiro-Silva, A. (2011). Differential expression of HIF-1alpha in CD44+CD24-/low breast ductal carcinomas. Diagn Pathol *6*, 73.
Onodera, J., and Ohsumi, Y. (2006). [Physiological role of autophagy for starvation-adaptation in yeast]. Tanpakushitsu Kakusan Koso *51*, 1499-1502.
Opavsky, R., Pastorekova, S., Zelnik, V., Gibadulinova, A., Stanbridge, E.J., Zavada, J., Kettmann, R., and Pastorek, J. (1996). Human MN/CA9 gene, a novel member of the carbonic anhydrase family: structure and exon to protein domain relationships. Genomics *33*, 480-487.
Pandolfi, P.P. (2001). Histone deacetylases and transcriptional therapy with their inhibitors. Cancer Chemother Pharmacol *48 Suppl 1*, S17-19.
Paranjape, A.N., Mandal, T., Mukherjee, G., Kumar, M.V., Sengupta, K., and Rangarajan, A. (2012). Introduction of SV40ER and hTERT into mammospheres generates breast cancer cells with stem cell properties. Oncogene *31*, 1896-1909.
Park, J.A., Kim, Y.E., Seok, H.J., Park, W.Y., Kwon, H.J., and Lee, Y. Differentiation and upregulation of heat shock protein 70 induced by a subset of histone deacetylase inhibitors in mouse and human embryonic stem cells. BMB Rep *44*, 176-181.
Park, J.A., Kim, Y.E., Seok, H.J., Park, W.Y., Kwon, H.J., and Lee, Y. (2011). Differentiation and upregulation of heat shock protein 70 induced by a subset of histone deacetylase inhibitors in mouse and human embryonic stem cells. BMB reports *44*, 176-181.
Park, S.G., Schimmel, P., and Kim, S. (2008). Aminoacyl tRNA synthetases and their connections to disease. Proc Natl Acad Sci U S A *105*, 11043-11049.
Park, S.Y., Gonen, M., Kim, H.J., Michor, F., and Polyak, K. (2010). Cellular and genetic diversity in the progression of in situ human breast carcinomas to an invasive phenotype. J Clin Invest *120*, 636-644.
Parks, S.K., Chiche, J., and Pouyssegur, J. (2011). pH control mechanisms of tumor survival and growth. J Cell Physiol *226*, 299-308.

Pastorek, J., Pastorekova, S., Callebaut, I., Mornon, J.P., Zelnik, V., Opavsky, R., Zat'ovicova, M., Liao, S., Portetelle, D., Stanbridge, E.J.*, et al.* (1994). Cloning and characterization of MN, a human tumor-associated protein with a domain homologous to carbonic anhydrase and a putative helix-loop-helix DNA binding segment. Oncogene *9*, 2877-2888.
Paszek, M.J., Zahir, N., Johnson, K.R., Lakins, J.N., Rozenberg, G.I., Gefen, A., Reinhart-King, C.A., Margulies, S.S., Dembo, M., Boettiger, D.*, et al.* (2005). Tensional homeostasis and the malignant phenotype. Cancer cell *8*, 241-254.
Pearce, D.J., Taussig, D., Simpson, C., Allen, K., Rohatiner, A.Z., Lister, T.A., and Bonnet, D. (2005). Characterization of cells with a high aldehyde dehydrogenase activity from cord blood and acute myeloid leukemia samples. Stem Cells *23*, 752-760.
Pecqueur, C., Oliver, L., Oizel, K., Lalier, L., and Vallette, F.M. (2013). Targeting metabolism to induce cell death in cancer cells and cancer stem cells. Int J Cell Biol *2013*, 805975.
Peng, S., Maihle, N.J., and Huang, Y. (2010). Pluripotency factors Lin28 and Oct4 identify a sub-population of stem cell-like cells in ovarian cancer. Oncogene *29*, 2153-2159.
Peng, W., Togawa, C., Zhang, K., and Kurdistani, S.K. (2008). Regulators of cellular levels of histone acetylation in Saccharomyces cerevisiae. Genetics *179*, 277-289.
Petrul, H.M., Schatz, C.A., Kopitz, C.C., Adnane, L., McCabe, T.J., Trail, P., Ha, S., Chang, Y.S., Voznesensky, A., Ranges, G.*, et al.* (2012). Therapeutic mechanism and efficacy of the antibody-drug conjugate BAY 79-4620 targeting human carbonic anhydrase 9. Mol Cancer Ther *11*, 340-349.
Pfaffl, M.W. (2001). A new mathematical model for relative quantification in real-time RT-PCR. Nucleic acids research *29*, e45.
Philip, M., Rowley, D.A., and Schreiber, H. (2004). Inflammation as a tumor promoter in cancer induction. Semin Cancer Biol *14*, 433-439.
Pike, L.R., Singleton, D.C., Buffa, F., Abramczyk, O., Phadwal, K., Li, J.L., Simon, A.K., Murray, J.T., and Harris, A.L. (2013). Transcriptional up-regulation of ULK1 by ATF4 contributes to cancer cell survival. The Biochemical journal *449*, 389-400.
Place, A.E., Jin Huh, S., and Polyak, K. (2011). The microenvironment in breast cancer progression: biology and implications for treatment. Breast Cancer Res *13*, 227.
Pollard, J.W. (2004). Tumour-educated macrophages promote tumour progression and metastasis. Nature reviews. Cancer *4*, 71-78.
Pollard, P.J., Loenarz, C., Mole, D.R., McDonough, M.A., Gleadle, J.M., Schofield, C.J., and Ratcliffe, P.J. (2008). Regulation of Jumonji-domain-containing histone demethylases by hypoxia-inducible factor (HIF)-1alpha. The Biochemical journal *416*, 387-394.
Polyak, K., Haviv, I., and Campbell, I.G. (2009). Co-evolution of tumor cells and their microenvironment. Trends Genet *25*, 30-38.
Polyak, K., and Weinberg, R.A. (2009). Transitions between epithelial and mesenchymal states: acquisition of malignant and stem cell traits. Nature reviews. Cancer *9*, 265-273.
Ponnaluri, V.K., Vadlapatla, R.K., Vavilala, D.T., Pal, D., Mitra, A.K., and Mukherji, M. (2011). Hypoxia induced expression of histone lysine demethylases:

implications in oxygen-dependent retinal neovascular diseases. Biochemical and biophysical research communications *415*, 373-377.
Ponti, D., Costa, A., Zaffaroni, N., Pratesi, G., Petrangolini, G., Coradini, D., Pilotti, S., Pierotti, M.A., and Daidone, M.G. (2005). Isolation and in vitro propagation of tumorigenic breast cancer cells with stem/progenitor cell properties. Cancer Res *65*, 5506-5511.
Portela, A., and Esteller, M. (2010). Epigenetic modifications and human disease. Nat Biotechnol *28*, 1057-1068.
Prabhakar, N.R. (2001). Oxygen sensing during intermittent hypoxia: cellular and molecular mechanisms. J Appl Physiol *90*, 1986-1994.
Prenen, G.H., Go, K.G., Zuiderveen, F., Paans, A.M., and Vaalburg, W. (1990). An improved synthesis of carbon-11 labeled acetoacetic acid and an evaluation of its potential for the investigation of cerebral pathology by positron emission tomography. Int J Rad Appl Instrum A *41*, 1209-1216.
Prestegarden, L., and Enger, P.O. (2010). Cancer stem cells in the central nervous system--a critical review. Cancer Res *70*, 8255-8258.
Prevarskaya, N., Skryma, R., and Shuba, Y. (2011). Calcium in tumour metastasis: new roles for known actors. Nature reviews. Cancer *11*, 609-618.
Proescholdt, M.A., Mayer, C., Kubitza, M., Schubert, T., Liao, S.Y., Stanbridge, E.J., Ivanov, S., Oldfield, E.H., Brawanski, A., and Merrill, M.J. (2005). Expression of hypoxia-inducible carbonic anhydrases in brain tumors. Neuro-oncology *7*, 465-475.
Pugh, C.W., and Ratcliffe, P.J. (2003). Regulation of angiogenesis by hypoxia: role of the HIF system. Nat Med *9*, 677-684.
Quail, D.F., Taylor, M.J., Walsh, L.A., Dieters-Castator, D., Das, P., Jewer, M., Zhang, G., and Postovit, L.M. (2011). Low oxygen levels induce the expression of the embryonic morphogen Nodal. Mol Biol Cell *22*, 4809-4821.
Quinlan, A.R., and Hall, I.M. (2010). BEDTools: a flexible suite of utilities for comparing genomic features. Bioinformatics *26*, 841-842.
Quintana, E., Shackleton, M., Sabel, M.S., Fullen, D.R., Johnson, T.M., and Morrison, S.J. (2008). Efficient tumour formation by single human melanoma cells. Nature *456*, 593-598.
Rafajova, M., Zatovicova, M., Kettmann, R., Pastorek, J., and Pastorekova, S. (2004). Induction by hypoxia combined with low glucose or low bicarbonate and high posttranslational stability upon reoxygenation contribute to carbonic anhydrase IX expression in cancer cells. Int J Oncol *24*, 995-1004.
Rambhatla, L., Chiu, C.P., Kundu, P., Peng, Y., and Carpenter, M.K. (2003). Generation of hepatocyte-like cells from human embryonic stem cells. Cell Transplant *12*, 1-11.
Ramos-Nino, M.E. (2013). The role of chronic inflammation in obesity-associated cancers. ISRN Oncol *2013*, 697521.
Rathmell, J.C., and Newgard, C.B. (2009). Biochemistry. A glucose-to-gene link. Science *324*, 1021-1022.
Reiserova, L., Kaluzova, M., Kaluz, S., Willis, A.C., Zavada, J., Zavodska, E., Zavadova, Z., Ciampor, F., Pastorek, J., and Pastorekova, S. (1999). Identification of MaTu-MX agent as a new strain of lymphocytic choriomeningitis virus (LCMV) and serological indication of horizontal spread of LCMV in human population. Virology *257*, 73-83.

Ren, M., Yan, L., Shang, C.Z., Cao, J., Lu, L.H., Min, J., and Cheng, H. (2010). Effects of sodium butyrate on the differentiation of pancreatic and hepatic progenitor cells from mouse embryonic stem cells. J Cell Biochem *109*, 236-244.
Reya, T., Morrison, S.J., Clarke, M.F., and Weissman, I.L. (2001). Stem cells, cancer, and cancer stem cells. Nature *414*, 105-111.
Reynolds, T.Y., Rockwell, S., and Glazer, P.M. (1996). Genetic instability induced by the tumor microenvironment. Cancer Res *56*, 5754-5757.
Ricardo, S., Vieira, A.F., Gerhard, R., Leitao, D., Pinto, R., Cameselle-Teijeiro, J.F., Milanezi, F., Schmitt, F., and Paredes, J. (2011). Breast cancer stem cell markers CD44, CD24 and ALDH1: expression distribution within intrinsic molecular subtype. J Clin Pathol *64*, 937-946.
Ricci-Vitiani, L., Lombardi, D.G., Pilozzi, E., Biffoni, M., Todaro, M., Peschle, C., and De Maria, R. (2007). Identification and expansion of human colon-cancer-initiating cells. Nature *445*, 111-115.
Rice, G.C., Hoy, C., and Schimke, R.T. (1986). Transient hypoxia enhances the frequency of dihydrofolate reductase gene amplification in Chinese hamster ovary cells. Proc Natl Acad Sci U S A *83*, 5978-5982.
Richard, D.E., Berra, E., Gothie, E., Roux, D., and Pouyssegur, J. (1999). p42/p44 mitogen-activated protein kinases phosphorylate hypoxia-inducible factor 1alpha (HIF-1alpha) and enhance the transcriptional activity of HIF-1. The Journal of biological chemistry *274*, 32631-32637.
Rikka, S., Quinsay, M.N., Thomas, R.L., Kubli, D.A., Zhang, X., Murphy, A.N., and Gustafsson, A.B. (2011). Bnip3 impairs mitochondrial bioenergetics and stimulates mitochondrial turnover. Cell Death Differ *18*, 721-731.
Robertson, N., Potter, C., and Harris, A.L. (2004). Role of carbonic anhydrase IX in human tumor cell growth, survival, and invasion. Cancer Res *64*, 6160-6165.
Rofstad, E.K., Johnsen, N.M., and Lyng, H. (1996). Hypoxia-induced tetraploidisation of a diploid human melanoma cell line in vitro. Br J Cancer Suppl *27*, S136-139.
Rossignol, R., Gilkerson, R., Aggeler, R., Yamagata, K., Remington, S.J., and Capaldi, R.A. (2004). Energy substrate modulates mitochondrial structure and oxidative capacity in cancer cells. Cancer Res *64*, 985-993.
Rota, L.M., Lazzarino, D.A., Ziegler, A.N., LeRoith, D., and Wood, T.L. (2012). Determining mammosphere-forming potential: application of the limiting dilution analysis. J Mammary Gland Biol Neoplasia *17*, 119-123.
Rouschop, K.M., van den Beucken, T., Dubois, L., Niessen, H., Bussink, J., Savelkouls, K., Keulers, T., Mujcic, H., Landuyt, W., Voncken, J.W.*, et al.* (2010). The unfolded protein response protects human tumor cells during hypoxia through regulation of the autophagy genes MAP1LC3B and ATG5. J Clin Invest *120*, 127-141.
Russell, R.C., Fang, C., and Guan, K.L. (2011). An emerging role for TOR signaling in mammalian tissue and stem cell physiology. Development *138*, 3343-3356.
Rzymski, T., and Harris, A.L. (2007). The unfolded protein response and integrated stress response to anoxia. Clinical cancer research : an official journal of the American Association for Cancer Research *13*, 2537-2540.
Rzymski, T., Milani, M., Pike, L., Buffa, F., Mellor, H.R., Winchester, L., Pires, I., Hammond, E., Ragoussis, I., and Harris, A.L. (2010). Regulation of autophagy by ATF4 in response to severe hypoxia. Oncogene *29*, 4424-4435.

Saarnio, J., Parkkila, S., Parkkila, A.K., Waheed, A., Casey, M.C., Zhou, X.Y., Pastorekova, S., Pastorek, J., Karttunen, T., Haukipuro, K.*, et al.* (1998). Immunohistochemistry of carbonic anhydrase isozyme IX (MN/CA IX) in human gut reveals polarized expression in the epithelial cells with the highest proliferative capacity. J Histochem Cytochem *46*, 497-504.
Salem, A.F., Whitaker-Menezes, D., Lin, Z., Martinez-Outschoorn, U.E., Tanowitz, H.B., Al-Zoubi, M.S., Howell, A., Pestell, R.G., Sotgia, F., and Lisanti, M.P. (2012). Two-compartment tumor metabolism: autophagy in the tumor microenvironment and oxidative mitochondrial metabolism (OXPHOS) in cancer cells. Cell Cycle *11*, 2545-2556.
Samuel, M.S., Lopez, J.I., McGhee, E.J., Croft, D.R., Strachan, D., Timpson, P., Munro, J., Schroder, E., Zhou, J., Brunton, V.G.*, et al.* (2011). Actomyosin-mediated cellular tension drives increased tissue stiffness and beta-catenin activation to induce epidermal hyperplasia and tumor growth. Cancer cell *19*, 776-791.
Sansone, P., Storci, G., Tavolari, S., Guarnieri, T., Giovannini, C., Taffurelli, M., Ceccarelli, C., Santini, D., Paterini, P., Marcu, K.B.*, et al.* (2007a). IL-6 triggers malignant features in mammospheres from human ductal breast carcinoma and normal mammary gland. J Clin Invest *117*, 3988-4002.
Sansone, P., Storci, G., Tavolari, S., Guarnieri, T., Giovannini, C., Taffurelli, M., Ceccarelli, C., Santini, D., Paterini, P., Marcu, K.B.*, et al.* (2007b). IL-6 triggers malignant features in mammospheres from human ductal breast carcinoma and normal mammary gland. J Clin Invest *117*, 3988-4002.
Sasaki, H., Nishizaki, Y., Hui, C., Nakafuku, M., and Kondoh, H. (1999). Regulation of Gli2 and Gli3 activities by an amino-terminal repression domain: implication of Gli2 and Gli3 as primary mediators of Shh signaling. Development *126*, 3915-3924.
Scaffidi, P., and Misteli, T. (2011). In vitro generation of human cells with cancer stem cell properties. Nature cell biology *13*, 1051-1061.
Schaefer, L., and Schaefer, R.M. (2010). Proteoglycans: from structural compounds to signaling molecules. Cell Tissue Res *339*, 237-246.
Schafer, Z.T., and Brugge, J.S. (2007). IL-6 involvement in epithelial cancers. J Clin Invest *117*, 3660-3663.
Scharenberg, C.W., Harkey, M.A., and Torok-Storb, B. (2002). The ABCG2 transporter is an efficient Hoechst 33342 efflux pump and is preferentially expressed by immature human hematopoietic progenitors. Blood *99*, 507-512.
Schieke, S.M., Phillips, D., McCoy, J.P., Jr., Aponte, A.M., Shen, R.F., Balaban, R.S., and Finkel, T. (2006). The mammalian target of rapamycin (mTOR) pathway regulates mitochondrial oxygen consumption and oxidative capacity. The Journal of biological chemistry *281*, 27643-27652.
Schmidt, M., Bollschweiler, E., Dietlein, M., Monig, S.P., Kobe, C., Vallbohmer, D., Eschner, W., Holscher, A., and Schicha, H. (2009). Mean and maximum standardized uptake values in [18F]FDG-PET for assessment of histopathological response in oesophageal squamous cell carcinoma or adenocarcinoma after radiochemotherapy. Eur J Nucl Med Mol Imaging *36*, 735-744.
Scholl, S.M., Pallud, C., Beuvon, F., Hacene, K., Stanley, E.R., Rohrschneider, L., Tang, R., Pouillart, P., and Lidereau, R. (1994). Anti-colony-stimulating factor-1 antibody staining in primary breast adenocarcinomas correlates with marked inflammatory cell infiltrates and prognosis. J Natl Cancer Inst *86*, 120-126.

Seagroves, T.N., Ryan, H.E., Lu, H., Wouters, B.G., Knapp, M., Thibault, P., Laderoute, K., and Johnson, R.S. (2001). Transcription factor HIF-1 is a necessary mediator of the pasteur effect in mammalian cells. Molecular and cellular biology *21*, 3436-3444.
Semenza, G.L. (2003). Targeting HIF-1 for cancer therapy. Nature reviews. Cancer *3*, 721-732.
Sermeus, A., Cosse, J.P., Crespin, M., Mainfroid, V., de Longueville, F., Ninane, N., Raes, M., Remacle, J., and Michiels, C. (2008). Hypoxia induces protection against etoposide-induced apoptosis: molecular profiling of changes in gene expression and transcription factor activity. Mol Cancer *7*, 27.
Sethi, N., Dai, X., Winter, C.G., and Kang, Y. (2011). Tumor-derived JAGGED1 promotes osteolytic bone metastasis of breast cancer by engaging notch signaling in bone cells. Cancer cell *19*, 192-205.
Sgambato, A., Puglisi, M.A., Errico, F., Rafanelli, F., Boninsegna, A., Rettino, A., Genovese, G., Coco, C., Gasbarrini, A., and Cittadini, A. (2010). Post-translational modulation of CD133 expression during sodium butyrate-induced differentiation of HT29 human colon cancer cells: implications for its detection. J Cell Physiol *224*, 234-241.
Shackleton, M., Quintana, E., Fearon, E.R., and Morrison, S.J. (2009). Heterogeneity in cancer: cancer stem cells versus clonal evolution. Cell *138*, 822-829.
Shebl, F.M., Sakoda, L.C., Black, A., Koshiol, J., Andriole, G.L., Grubb, R., Church, T.R., Chia, D., Zhou, C., Chu, L.W.*, et al.* (2012). Aspirin but not ibuprofen use is associated with reduced risk of prostate cancer: a PLCO study. Br J Cancer *107*, 207-214.
Shen, Q., Wang, Y., Kokovay, E., Lin, G., Chuang, S.M., Goderie, S.K., Roysam, B., and Temple, S. (2008). Adult SVZ stem cells lie in a vascular niche: a quantitative analysis of niche cell-cell interactions. Cell Stem Cell *3*, 289-300.
Sheridan, C., Kishimoto, H., Fuchs, R.K., Mehrotra, S., Bhat-Nakshatri, P., Turner, C.H., Goulet, R., Jr., Badve, S., and Nakshatri, H. (2006). CD44+/CD24- breast cancer cells exhibit enhanced invasive properties: an early step necessary for metastasis. Breast Cancer Res *8*, R59.
Sheta, E.A., Trout, H., Gildea, J.J., Harding, M.A., and Theodorescu, D. (2001). Cell density mediated pericellular hypoxia leads to induction of HIF-1alpha via nitric oxide and Ras/MAP kinase mediated signaling pathways. Oncogene *20*, 7624-7634.
Shi, Y. (2007). Histone lysine demethylases: emerging roles in development, physiology and disease. Nature reviews. Genetics *8*, 829-833.
Shibata, M., and Shen, M.M. (2013). The roots of cancer: stem cells and the basis for tumor heterogeneity. Bioessays *35*, 253-260.
Shin, H.J., Rho, S.B., Jung, D.C., Han, I.O., Oh, E.S., and Kim, J.Y. (2011). Carbonic anhydrase IX (CA9) modulates tumor-associated cell migration and invasion. Journal of cell science *124*, 1077-1087.
Shipitsin, M., Campbell, L.L., Argani, P., Weremowicz, S., Bloushtain-Qimron, N., Yao, J., Nikolskaya, T., Serebryiskaya, T., Beroukhim, R., Hu, M.*, et al.* (2007). Molecular definition of breast tumor heterogeneity. Cancer cell *11*, 259-273.

Shulewitz, M., Soloviev, I., Wu, T., Koeppen, H., Polakis, P., and Sakanaka, C. (2006). Repressor roles for TCF-4 and Sfrp1 in Wnt signaling in breast cancer. Oncogene *25*, 4361-4369.
Siebels, M., Rohrmann, K., Oberneder, R., Stahler, M., Haseke, N., Beck, J., Hofmann, R., Kindler, M., Kloepfer, P., and Stief, C. (2011). A clinical phase I/II trial with the monoclonal antibody cG250 (RENCAREX(R)) and interferon-alpha-2a in metastatic renal cell carcinoma patients. World J Urol *29*, 121-126.
Simon, M.C., and Keith, B. (2008). The role of oxygen availability in embryonic development and stem cell function. Nat Rev Mol Cell Biol *9*, 285-296.
Singh, S.K., Clarke, I.D., Terasaki, M., Bonn, V.E., Hawkins, C., Squire, J., and Dirks, P.B. (2003). Identification of a cancer stem cell in human brain tumors. Cancer Res *63*, 5821-5828.
Sminia, P., Acker, H., Eikesdal, H.P., Kaaijk, P., Enger, P., Slotman, B., and Bjerkvig, R. (2003). Oxygenation and response to irradiation of organotypic multicellular spheroids of human glioma. Anticancer Res *23*, 1461-1466.
Society, A.C. (2009). The History of Cance. CancerDecisions.
Soeda, A., Park, M., Lee, D., Mintz, A., Androutsellis-Theotokis, A., McKay, R.D., Engh, J., Iwama, T., Kunisada, T., Kassam, A.B.*, et al.* (2009). Hypoxia promotes expansion of the CD133-positive glioma stem cells through activation of HIF-1alpha. Oncogene *28*, 3949-3959.
Soh, D., Dong, D., Guo, Y., and Wong, L. (2010). Consistency, comprehensiveness, and compatibility of pathway databases. BMC Bioinformatics *11*, 449.
Solinas, G., Germano, G., Mantovani, A., and Allavena, P. (2009). Tumor-associated macrophages (TAM) as major players of the cancer-related inflammation. J Leukoc Biol *86*, 1065-1073.
Song, M.S., Salmena, L., and Pandolfi, P.P. (2012). The functions and regulation of the PTEN tumour suppressor. Nat Rev Mol Cell Biol *13*, 283-296.
Sophos, N.A., and Vasiliou, V. (2003). Aldehyde dehydrogenase gene superfamily: the 2002 update. Chem Biol Interact *143-144*, 5-22.
Steiniger, S.C., Coppinger, J.A., Kruger, J.A., Yates, J., 3rd, and Janda, K.D. (2008). Quantitative mass spectrometry identifies drug targets in cancer stem cell-containing side population. Stem Cells *26*, 3037-3046.
Stiles, C.D., and Rowitch, D.H. (2008). Glioma stem cells: a midterm exam. Neuron *58*, 832-846.
Stoeltzing, O., Liu, W., Reinmuth, N., Fan, F., Parikh, A.A., Bucana, C.D., Evans, D.B., Semenza, G.L., and Ellis, L.M. (2003). Regulation of hypoxia-inducible factor-1alpha, vascular endothelial growth factor, and angiogenesis by an insulin-like growth factor-I receptor autocrine loop in human pancreatic cancer. Am J Pathol *163*, 1001-1011.
Strahl, B.D., Ohba, R., Cook, R.G., and Allis, C.D. (1999). Methylation of histone H3 at lysine 4 is highly conserved and correlates with transcriptionally active nuclei in Tetrahymena. Proc Natl Acad Sci U S A *96*, 14967-14972.
Sun, G., Fu, C., Shen, C., and Shi, Y. (2011). Histone deacetylases in neural stem cells and induced pluripotent stem cells. J Biomed Biotechnol *2011*, 835968.
Supuran, C.T. (2008). Carbonic anhydrases: novel therapeutic applications for inhibitors and activators. Nat Rev Drug Discov *7*, 168-181.
Surfus, J.E., Hank, J.A., Oosterwijk, E., Welt, S., Lindstrom, M.J., Albertini, M.R., Schiller, J.H., and Sondel, P.M. (1996). Anti-renal-cell carcinoma chimeric

antibody G250 facilitates antibody-dependent cellular cytotoxicity with in vitro and in vivo interleukin-2-activated effectors. J Immunother Emphasis Tumor Immunol *19*, 184-191.
Svastova, E., Hulikova, A., Rafajova, M., Zat'ovicova, M., Gibadulinova, A., Casini, A., Cecchi, A., Scozzafava, A., Supuran, C.T., Pastorek, J.*, et al.* (2004). Hypoxia activates the capacity of tumor-associated carbonic anhydrase IX to acidify extracellular pH. FEBS letters *577*, 439-445.
Svastova, E., Zilka, N., Zat'ovicova, M., Gibadulinova, A., Ciampor, F., Pastorek, J., and Pastorekova, S. (2003). Carbonic anhydrase IX reduces E-cadherin-mediated adhesion of MDCK cells via interaction with beta-catenin. Experimental cell research *290*, 332-345.
Swietach, P., Hulikova, A., Vaughan-Jones, R.D., and Harris, A.L. (2010). New insights into the physiological role of carbonic anhydrase IX in tumour pH regulation. Oncogene *29*, 6509-6521.
Swietach, P., Wigfield, S., Cobden, P., Supuran, C.T., Harris, A.L., and Vaughan-Jones, R.D. (2008). Tumor-associated carbonic anhydrase 9 spatially coordinates intracellular pH in three-dimensional multicellular growths. The Journal of biological chemistry *283*, 20473-20483.
Taketo, M.M. (2004). Shutting down Wnt signal-activated cancer. Nat Genet *36*, 320-322.
Tan, E.Y., Yan, M., Campo, L., Han, C., Takano, E., Turley, H., Candiloro, I., Pezzella, F., Gatter, K.C., Millar, E.K.*, et al.* (2009). The key hypoxia regulated gene CAIX is upregulated in basal-like breast tumours and is associated with resistance to chemotherapy. Br J Cancer *100*, 405-411.
Tanentzapf, G., Devenport, D., Godt, D., and Brown, N.H. (2007). Integrin-dependent anchoring of a stem-cell niche. Nature cell biology *9*, 1413-1418.
Tang, D.G. (2012). Understanding cancer stem cell heterogeneity and plasticity. Cell Res *22*, 457-472.
Teissedre, B., Pinderhughes, A., Incassati, A., Hatsell, S.J., Hiremath, M., and Cowin, P. (2009). MMTV-Wnt1 and -DeltaN89beta-catenin induce canonical signaling in distinct progenitors and differentially activate Hedgehog signaling within mammary tumors. PloS one *4*, e4537.
Tennant, D.A., Duran, R.V., and Gottlieb, E. (2010). Targeting metabolic transformation for cancer therapy. Nature reviews. Cancer *10*, 267-277.
Thirlwell, C., Schulz, L., Dibra, H., and Beck, S. (2011). Suffocating cancer: hypoxia-associated epimutations as targets for cancer therapy. Clinical epigenetics *3*, 9.
Thomas, R.L., Kubli, D.A., and Gustafsson, A.B. (2011). Bnip3-mediated defects in oxidative phosphorylation promote mitophagy. Autophagy *7*, 775-777.
Thomlinson, R.H., and Gray, L.H. (1955). The histological structure of some human lung cancers and the possible implications for radiotherapy. Br J Cancer *9*, 539-549.
Touisni, N., Maresca, A., McDonald, P.C., Lou, Y., Scozzafava, A., Dedhar, S., Winum, J.Y., and Supuran, C.T. (2011). Glycosyl coumarin carbonic anhydrase IX and XII inhibitors strongly attenuate the growth of primary breast tumors. J Med Chem *54*, 8271-8277.

Unruh, A., Ressel, A., Mohamed, H.G., Johnson, R.S., Nadrowitz, R., Richter, E., Katschinski, D.M., and Wenger, R.H. (2003). The hypoxia-inducible factor-1 alpha is a negative factor for tumor therapy. Oncogene *22*, 3213-3220.
van de Ven, R., Oerlemans, R., van der Heijden, J.W., Scheffer, G.L., de Gruijl, T.D., Jansen, G., and Scheper, R.J. (2009). ABC drug transporters and immunity: novel therapeutic targets in autoimmunity and cancer. J Leukoc Biol *86*, 1075-1087.
Vander Haar, E., Lee, S.I., Bandhakavi, S., Griffin, T.J., and Kim, D.H. (2007). Insulin signalling to mTOR mediated by the Akt/PKB substrate PRAS40. Nature cell biology *9*, 316-323.
Varnat, F., Duquet, A., Malerba, M., Zbinden, M., Mas, C., Gervaz, P., and Ruiz i Altaba, A. (2009). Human colon cancer epithelial cells harbour active HEDGEHOG-GLI signalling that is essential for tumour growth, recurrence, metastasis and stem cell survival and expansion. EMBO Mol Med *1*, 338-351.
Vaupel, P., and Harrison, L. (2004). Tumor hypoxia: causative factors, compensatory mechanisms, and cellular response. Oncologist *9 Suppl 5*, 4-9.
Vendramini-Costa, D.B., and Carvalho, J.E. (2012). Molecular link mechanisms between inflammation and cancer. Curr Pharm Des *18*, 3831-3852.
Vesuna, F., Lisok, A., Kimble, B., and Raman, V. (2009). Twist modulates breast cancer stem cells by transcriptional regulation of CD24 expression. Neoplasia *11*, 1318-1328.
Vignot, S., Faivre, S., Aguirre, D., and Raymond, E. (2005). mTOR-targeted therapy of cancer with rapamycin derivatives. Ann Oncol *16*, 525-537.
Visvader, J.E. (2009). Keeping abreast of the mammary epithelial hierarchy and breast tumorigenesis. Genes & development *23*, 2563-2577.
Vlashi, E., Lagadec, C., Vergnes, L., Matsutani, T., Masui, K., Poulou, M., Popescu, R., Della Donna, L., Evers, P., Dekmezian, C.*, et al.* (2011). Metabolic state of glioma stem cells and nontumorigenic cells. Proc Natl Acad Sci U S A *108*, 16062-16067.
Wagner, J.M., Hackanson, B., Lubbert, M., and Jung, M. Histone deacetylase (HDAC) inhibitors in recent clinical trials for cancer therapy. Clin Epigenetics *1*, 117-136.
Wagner, J.M., Hackanson, B., Lubbert, M., and Jung, M. (2010). Histone deacetylase (HDAC) inhibitors in recent clinical trials for cancer therapy. Clinical epigenetics *1*, 117-136.
Warburg, O. (1956). On the origin of cancer cells. Science *123*, 309-314.
Wellen, K.E., Hatzivassiliou, G., Sachdeva, U.M., Bui, T.V., Cross, J.R., and Thompson, C.B. (2009). ATP-citrate lyase links cellular metabolism to histone acetylation. Science *324*, 1076-1080.
Wellmann, S., Bettkober, M., Zelmer, A., Seeger, K., Faigle, M., Eltzschig, H.K., and Buhrer, C. (2008). Hypoxia upregulates the histone demethylase JMJD1A via HIF-1. Biochemical and biophysical research communications *372*, 892-897.
West, M.J., Stoneley, M., and Willis, A.E. (1998). Translational induction of the c-myc oncogene via activation of the FRAP/TOR signalling pathway. Oncogene *17*, 769-780.
Wicha, M.S., Liu, S., and Dontu, G. (2006). Cancer stem cells: an old idea--a paradigm shift. Cancer Res *66*, 1883-1890; discussion 1895-1886.
Wiesener, M.S., Jurgensen, J.S., Rosenberger, C., Scholze, C.K., Horstrup, J.H., Warnecke, C., Mandriota, S., Bechmann, I., Frei, U.A., Pugh, C.W.*, et al.* (2003).

Widespread hypoxia-inducible expression of HIF-2alpha in distinct cell populations of different organs. FASEB J *17*, 271-273.
Wilson, D.F., Erecinska, M., Drown, C., and Silver, I.A. (1977). Effect of oxygen tension on cellular energetics. Am J Physiol *233*, C135-140.
Wind, N.S., and Holen, I. (2011). Multidrug resistance in breast cancer: from in vitro models to clinical studies. Int J Breast Cancer *2011*, 967419.
Woelber, L., Kress, K., Kersten, J.F., Choschzick, M., Kilic, E., Herwig, U., Lindner, C., Schwarz, J., Jaenicke, F., Mahner, S*., et al.* (2011). Carbonic anhydrase IX in tumor tissue and sera of patients with primary cervical cancer. BMC cancer *11*, 12.
Woodward, W.A., Chen, M.S., Behbod, F., Alfaro, M.P., Buchholz, T.A., and Rosen, J.M. (2007). WNT/beta-catenin mediates radiation resistance of mouse mammary progenitor cells. Proc Natl Acad Sci U S A *104*, 618-623.
Wozniak, M.A., Desai, R., Solski, P.A., Der, C.J., and Keely, P.J. (2003). ROCK-generated contractility regulates breast epithelial cell differentiation in response to the physical properties of a three-dimensional collagen matrix. The Journal of cell biology *163*, 583-595.
Wullschleger, S., Loewith, R., and Hall, M.N. (2006). TOR signaling in growth and metabolism. Cell *124*, 471-484.
Xia, X., Lemieux, M.E., Li, W., Carroll, J.S., Brown, M., Liu, X.S., and Kung, A.L. (2009a). Integrative analysis of HIF binding and transactivation reveals its role in maintaining histone methylation homeostasis. Proc Natl Acad Sci U S A *106*, 4260-4265.
Xia, X., Lemieux, M.E., Li, W., Carroll, J.S., Brown, M., Liu, X.S., and Kung, A.L. (2009b). Integrative analysis of HIF binding and transactivation reveals its role in maintaining histone methylation homeostasis. Proc Natl Acad Sci U S A *106*, 4260-4265.
Xu, H.N., Zheng, G., Tchou, J., Nioka, S., and Li, L.Z. (2013). Characterizing the metabolic heterogeneity in human breast cancer xenografts by 3D high resolution fluorescence imaging. Springerplus *2*, 73.
Xu, X., Hou, Y., Yin, X., Bao, L., Tang, A., Song, L., Li, F., Tsang, S., Wu, K., Wu, H*., et al.* (2012). Single-cell exome sequencing reveals single-nucleotide mutation characteristics of a kidney tumor. Cell *148*, 886-895.
Yamanaka, S., and Blau, H.M. (2010). Nuclear reprogramming to a pluripotent state by three approaches. Nature *465*, 704-712.
Yamashita, K., Discher, D.J., Hu, J., Bishopric, N.H., and Webster, K.A. (2001). Molecular regulation of the endothelin-1 gene by hypoxia. Contributions of hypoxia-inducible factor-1, activator protein-1, GATA-2, AND p300/CBP. J Biol Chem *276*, 12645-12653.
Yamashita, Y.M., and Fuller, M.T. (2008). Asymmetric centrosome behavior and the mechanisms of stem cell division. The Journal of cell biology *180*, 261-266.
Yang, J., Ledaki, I., Turley, H., Gatter, K.C., Montero, J.C., Li, J.L., and Harris, A.L. (2009). Role of hypoxia-inducible factors in epigenetic regulation via histone demethylases. Ann N Y Acad Sci *1177*, 185-197.
Yang, J., Zhang, L., Erbel, P.J., Gardner, K.H., Ding, K., Garcia, J.A., and Bruick, R.K. (2005). Functions of the Per/ARNT/Sim domains of the hypoxia-inducible factor. The Journal of biological chemistry *280*, 36047-36054.

Yang, S., Wang, X., Contino, G., Liesa, M., Sahin, E., Ying, H., Bause, A., Li, Y., Stommel, J.M., Dell'antonio, G.*, et al.* (2011). Pancreatic cancers require autophagy for tumor growth. Genes & development *25*, 717-729.
Yang, Z., and Klionsky, D.J. (2010). Eaten alive: a history of macroautophagy. Nature cell biology *12*, 814-822.
Yee Koh, M., Spivak-Kroizman, T.R., and Powis, G. (2008). HIF-1 regulation: not so easy come, easy go. Trends Biochem Sci *33*, 526-534.
Yeung, T.M., Gandhi, S.C., and Bodmer, W.F. (2011). Hypoxia and lineage specification of cell line-derived colorectal cancer stem cells. Proc Natl Acad Sci U S A *108*, 4382-4387.
Yeung, T.M., Gandhi, S.C., Wilding, J.L., Muschel, R., and Bodmer, W.F. (2010). Cancer stem cells from colorectal cancer-derived cell lines. Proc Natl Acad Sci U S A *107*, 3722-3727.
Yin, L., Castagnino, P., and Assoian, R.K. (2008). ABCG2 expression and side population abundance regulated by a transforming growth factor beta-directed epithelial-mesenchymal transition. Cancer Res *68*, 800-807.
Yoshida, A., Rzhetsky, A., Hsu, L.C., and Chang, C. (1998). Human aldehyde dehydrogenase gene family. Eur J Biochem *251*, 549-557.
Yu, Q., Toole, B.P., and Stamenkovic, I. (1997). Induction of apoptosis of metastatic mammary carcinoma cells in vivo by disruption of tumor cell surface CD44 function. J Exp Med *186*, 1985-1996.
Yuan, J., and Glazer, P.M. (1998). Mutagenesis induced by the tumor microenvironment. Mutat Res *400*, 439-446.
Yuan, J., Narayanan, L., Rockwell, S., and Glazer, P.M. (2000). Diminished DNA repair and elevated mutagenesis in mammalian cells exposed to hypoxia and low pH. Cancer Res *60*, 4372-4376.
Yun, Z., Lin, Q., and Giaccia, A.J. (2005). Adaptive myogenesis under hypoxia. Molecular and cellular biology *25*, 3040-3055.
Yun, Z., Maecker, H.L., Johnson, R.S., and Giaccia, A.J. (2002). Inhibition of PPAR gamma 2 gene expression by the HIF-1-regulated gene DEC1/Stra13: a mechanism for regulation of adipogenesis by hypoxia. Dev Cell *2*, 331-341.
Zatovicova, M., Jelenska, L., Hulikova, A., Csaderova, L., Ditte, Z., Ditte, P., Goliasova, T., Pastorek, J., and Pastorekova, S. (2010). Carbonic anhydrase IX as an anticancer therapy target: preclinical evaluation of internalizing monoclonal antibody directed to catalytic domain. Curr Pharm Des *16*, 3255-3263.
Zatovicova, M., Sedlakova, O., Svastova, E., Ohradanova, A., Ciampor, F., Arribas, J., Pastorek, J., and Pastorekova, S. (2005). Ectodomain shedding of the hypoxia-induced carbonic anhydrase IX is a metalloprotease-dependent process regulated by TACE/ADAM17. Br J Cancer *93*, 1267-1276.
Zavada, J., Zavadova, Z., Pastorekova, S., Ciampor, F., Pastorek, J., and Zelnik, V. (1993). Expression of MaTu-MN protein in human tumor cultures and in clinical specimens. International journal of cancer. Journal international du cancer *54*, 268-274.
Zavada, J., Zavadova, Z., Zat'ovicova, M., Hyrsl, L., and Kawaciuk, I. (2003). Soluble form of carbonic anhydrase IX (CA IX) in the serum and urine of renal carcinoma patients. Br J Cancer *89*, 1067-1071.

Zha, X., Wang, F., Wang, Y., He, S., Jing, Y., Wu, X., and Zhang, H. (2011). Lactate dehydrogenase B is critical for hyperactive mTOR-mediated tumorigenesis. Cancer Res *71*, 13-18.
Zhang, M., Atkinson, R.L., and Rosen, J.M. (2010). Selective targeting of radiation-resistant tumor-initiating cells. Proc Natl Acad Sci U S A *107*, 3522-3527.
Zhang, Y., Liu, L.M., Ming, J., Yang, G.M., and Chen, W. (2007). [Regulatory role of hypoxia inducible factor-1 alpha in the changes of contraction of vascular smooth muscle cell induced by hypoxia]. Zhongguo Wei Zhong Bing Ji Jiu Yi Xue *19*, 647-651.
Zhong, H., De Marzo, A.M., Laughner, E., Lim, M., Hilton, D.A., Zagzag, D., Buechler, P., Isaacs, W.B., Semenza, G.L., and Simons, J.W. (1999). Overexpression of hypoxia-inducible factor 1alpha in common human cancers and their metastases. Cancer Res *59*, 5830-5835.
Zhou, J., Wulfkuhle, J., Zhang, H., Gu, P., Yang, Y., Deng, J., Margolick, J.B., Liotta, L.A., Petricoin, E., 3rd, and Zhang, Y. (2007a). Activation of the PTEN/mTOR/STAT3 pathway in breast cancer stem-like cells is required for viability and maintenance. Proc Natl Acad Sci U S A *104*, 16158-16163.
Zhou, J., Zhang, H., Gu, P., Margolick, J.B., Yin, D., and Zhang, Y. (2009). Cancer stem/progenitor cell active compound 8-quinolinol in combination with paclitaxel achieves an improved cure of breast cancer in the mouse model. Breast Cancer Res Treat *115*, 269-277.
Zhou, Q., Dalgard, C.L., Wynder, C., and Doughty, M.L. (2011). Histone deacetylase inhibitors SAHA and sodium butyrate block G1-to-S cell cycle progression in neurosphere formation by adult subventricular cells. BMC Neurosci *12*, 50.
Zhou, Q.J., Xiang, L.X., Shao, J.Z., Hu, R.Z., Lu, Y.L., Yao, H., and Dai, L.C. (2007b). In vitro differentiation of hepatic progenitor cells from mouse embryonic stem cells induced by sodium butyrate. J Cell Biochem *100*, 29-42.
Zhou, S., Schuetz, J.D., Bunting, K.D., Colapietro, A.M., Sampath, J., Morris, J.J., Lagutina, I., Grosveld, G.C., Osawa, M., Nakauchi, H.*, et al.* (2001). The ABC transporter Bcrp1/ABCG2 is expressed in a wide variety of stem cells and is a molecular determinant of the side-population phenotype. Nat Med *7*, 1028-1034.
Zhulin, I.B., Taylor, B.L., and Dixon, R. (1997). PAS domain S-boxes in Archaea, Bacteria and sensors for oxygen and redox. Trends in biochemical sciences *22*, 331-333.
Zimmerman, M.R. (1977). An experimental study of mummification pertinent to the antiquity of cancer. Cancer *40*, 1358-1362.
Zundel, W., Schindler, C., Haas-Kogan, D., Koong, A., Kaper, F., Chen, E., Gottschalk, A.R., Ryan, H.E., Johnson, R.S., Jefferson, A.B.*, et al.* (2000). Loss of PTEN facilitates HIF-1-mediated gene expression. Genes & development *14*, 391-396.